

OSTEOCHONDRAL TISSUE ENGINEERING FOR TOTAL JOINT REPAIR
CRITICAL STEPS TOWARDS CELL- BASED CONSTRUCTS

DISSERTATION
by

Doreen Hamann

born on November 27th, 1978

in Parchim, Germany

© 2008, Doreen Hamann

Neither this book nor its parts may be reproduced without written permission of the author.

Table of contents

Abbreviation list	1
Introduction	
1. Osteochondral biology	2
2. Osteochondral tissue regeneration	6
3. Aim and outline of this thesis	14
Chapter 1	
Comparison of seeding methods as the critical factor for cartilage tissue engineering utilizing mesenchymal stem cells on 3D fiber-deposited scaffolds	15
Chapter 2	
Tailored release of TGF β 1 from porous scaffolds for cartilage tissue engineering	30
Chapter 3	
TGF β 1 released from porous scaffolds: influence of delivery rates on cartilage formation	43
Chapter 4	
TGF beta 1 released from porous scaffolds: influence of delivery rates on cartilage formation	59
Chapter 5	
3D fiber deposited electrospun integrated scaffolds enhance cartilage tissue formation	70
Chapter 6	
Osteochondral Tissue Engineering : mechanical characterization and biological performance of triphasic 3D fiber deposited scaffolds utilizing mesenchymal stem cells	70
Chapter 7	
A clinical feasibility study to evaluate the safety and efficacy of PEOT/PBT implants for human donor site filling during mosaicplasty	95
Conclusions and future perspectives	105
References	111
Summary	130
Curriculum Vitae	136

Abbreviation list

3D	three-dimensional
3DF	3D fiber deposition
AGC	aggrecan
BCP	biphasic calcium phosphate
BSA	bovine serum albumine
CaP	calcium phosphate
CM	compression molded
DMEM	Dulbecco's modified Eagle's medium
DMMB	dimethyl methylene blue
DMSO	dimethyl sulfoxide
DNA	deoxyribonucleic acid
ECM	extracellular matrix
ESC	embryonic stem cell
ESP	electrospinning
FBS	fetal bovine serum
GAG	glycosaminoglycan
GMA	Glycol methylacrylate
HA	hydroxyapatite
ITS	insulin, transferrin, selenous acid
MEM	minimal essential medium
MMA	methyl methacrylate
MP	mosaicplasty
MSC	mesenchymal stem cell
PBS	phosphate buffered saline
PBT	polybutylene terephthalate
PEOT	polyethylene oxide terephthalate
SEM	scanning electron microscopy
TE	tissue engineering
TGF	transforming growth factor

Introduction

1. Osteochondral Biology

One of the major factors defining the quality of life is the ability to move. The skeletal system provides the basic tools such as upright posture, and leverage. It is built by 206 bones. Connections between different bones of the skeleton are joints and these are distinguished in different ways. One classification of joints is based on the extent to which movement is allowed and on their anatomical structure. There are (i) diarthroses (freely mobile joints, e.g. knee joint), (ii) amphiarthroses (slight movements are permitted, e.g. intervertebral joints) and (iii) synarthroses (fixed and rigid junctions, e.g. skull sutures). With focus on the diarthroses, Fig. 1 shows an overview of the complex structure which enables mobility. Joints are functional units enclosed in a strong fibrous capsule and strengthened by ligaments and tendons. The inner surface of the joint capsule is lined with a metabolically active tissue, the synovium (*Membrana synovialis*), which secretes the synovia. The synovia provides the nutrients required by the tissue within the joint. At least two bones are required to allow movement.

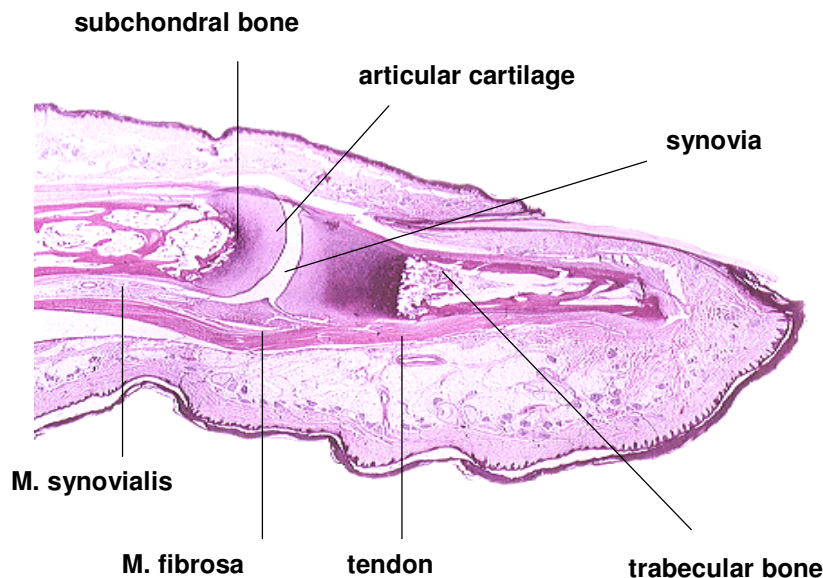


Figure 1: Architecture and cartilaginous surface of joints. Sagittal section of a human finger joint. Haematoxyline & Eosin staining.(modified from [1]).

Bone

Bone is a highly specialized form of connective tissue. Morphologically, there are two forms of bone, cortical bone and trabecular bone. The cortical bone, which forms the dense outer envelope of most bones, plays a crucial role in the mechanical and protective functions. In contrast, the loosely organized porous trabecular bone is metabolically more active and has a higher bone turnover compared to cortical bone due to a higher surface area.

Both types of bone are composed of four main types of cells, depicted in Fig. 2.

(1) Osteoblasts are the cells that are responsible for the production of bone matrix. They originate directly from mesenchymal stem cells (MSCs) in the bone marrow or via osteogenic precursor cells in the periosteum and endosteum. Osteoblasts lie on the

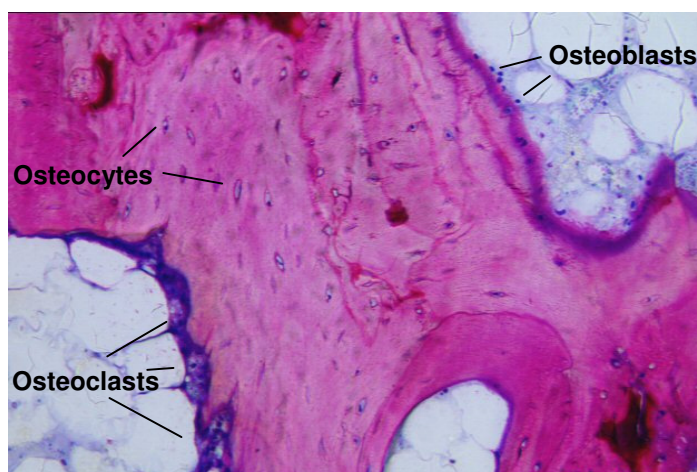


Figure 2: Cellular composition of bone. Sagittal section of the trabecular bone of a goat. Basic fuchsin & Eosin staining. Magnification 10x.

surface of the existing matrix and excrete osteoid, which mainly consists of type I collagen but also contains noncollagenous proteins, such as osteopontin, osteonectin, bone sialoprotein and osteocalcin. After the osteoid is converted into hard matrix by the deposition of hydroxyapatite crystals in a cell-mediated process, the entrapped osteoblasts are referred to as osteocytes.

(2) Osteocytes are completely surrounded by the mineralized matrix and still have the ability to secrete small amounts of matrix, whereas they lost the opportunity to divide. The osteocytes communicate with adjacent osteocytes by tiny canals, called canaliculi, and are suggested to play a role in the inhibition and stimulation of osteoclastic bone resorption [2, 3].

(3) Multinucleated giant cells called osteoclasts carry out the actual bone resorption. Osteoclasts originate from hematopoietic stem cells in the bone marrow. The precursor cells are released as monocytes in the bloodstream and collect at sites of bone resorption, where they fuse to form the active multinucleated osteoclasts. The resorption is carried out by a limited specialized surface of the osteoclast, which is known as the ruffled border. At the edge of the ruffled border, there is a ring-shaped sealing zone, which adheres tightly to the bone and seals the resorption space [4]. In this closed environment lysosomal enzymes are excreted, which degrade the matrix at a pH of approximately 4 [5].

(4) The last main type of cells in bone is the lining cell. Bone lining cells are flat, elongated, inactive cells that cover bone surfaces that are undergoing neither bone formation nor resorption. Although little is known about these cells, it was speculated that lining cells derive from osteoblasts and are capable to re-differentiate into active osteoblasts [6].

Bone is a complex living tissue that combines the elastic properties of collagen fibers with the compressive strength of hydroxyapatite crystals [7]. In order to fulfill its function, bone is a dynamic tissue that undergoes formation and resorption throughout life. To provide optimal mechanical support, bone is continuously rebuilt according to Wolff's law. The principles of Wolff's law are based on the concept that there is a correlation between the architecture of bone and the directions of the principal stresses that occur during normal function [8]. This results in an optimal load bearing structure with a minimal amount of material. Each bone end within the joint is covered by a layer of another connective tissue, the articular cartilage. The function of the joint depends on the

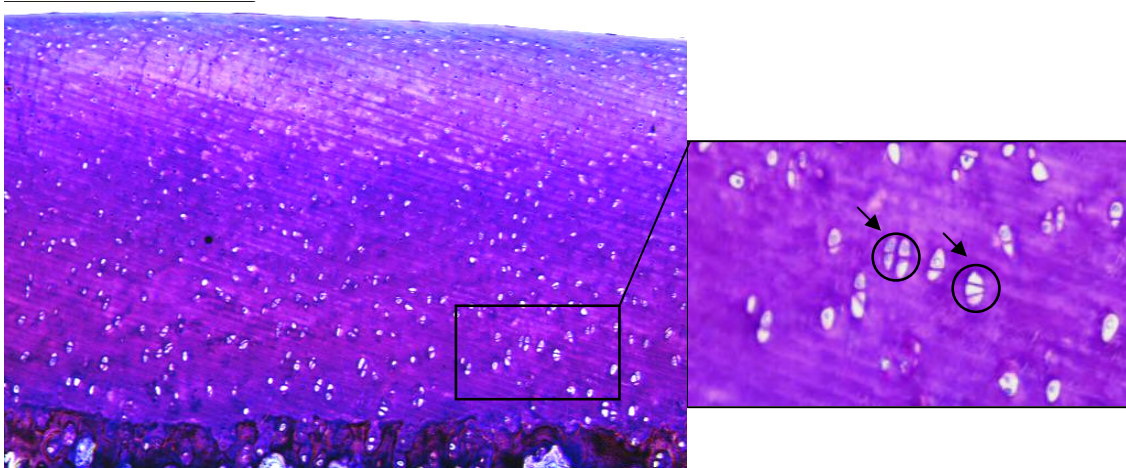


Figure 3: Cellular composition of cartilage. Sagittal section of the articular cartilage of a goat. Insert shows chondrocytes embedded in ECM as single cells or as isogenic groups (arrows). Thionine staining. Magnification 10x (insert 20x).

function of the articular cartilage. The specific biochemical and structural composition of articular cartilage capacitates the joint to compensate strong mechanical forces such as compression, friction and shear.

Cartilage

Articular cartilage is an avascular tissue formed by chondrocytes producing extracellular matrix (ECM). In contrast to bone, cartilage is composed of only one cell type, which is the chondrocyte (Fig. 3). It can be found single or clustered in isogenic groups. Such groups reflect the last mitotic division of a chondrocyte whose progeny have not generated high amounts of ECM around themselves. Lacunae, typical histological appearances in cartilaginous tissue, develop during histological preparation, where chondrocytes shrink or fall out.

The ECM of articular cartilage contains collagen such as type II, VI, IX, X and XI, where type II forms over 90% of the matrix. Other major components are proteoglycans, of which the most abundant is aggrecan. It is a large aggregating proteoglycan composed of a core protein and glycosaminoglycan (GAG) chains, which are covalently linked to the core protein. GAGs generally found in articular cartilage are chondroitin sulfate, keratan sulfate, dermatan sulfate and heparan sulfate. Collagen and aggrecan possess a high amount of bound carbohydrate groups, whereas GAGs are relevant due to their negative charges allowing more interactions with water. Water forms more than 65% of the wet weight of articular cartilage. Furthermore, minor percentages of noncollagen and nonaggrecan molecules like decorin or fibromodulin can be found.

Articular cartilage exhibits a specialized structural organization, in the first place made of collagens [9]. Collagen type II forms a basic fibrillar structure. The different molecules are covalently linked by pyridinium. Type VI forms distinct microfibrils. Type IX collagen is present on the surface of type II collagen fibrils and each molecule of collagen type IX is covalently linked to at least one collagen type II molecule. Together with decorin it might shield the fibril core from bulk proteoglycan and thereby establish a low density, water rich layer around fibrils [10, 11]. The proteoglycan molecules of the cartilage matrix exhibit a tendency to swell and provide the tissue with resistance to compression. In contrast, the collagen network provides the tissue with integrity and stiffness during tensile and shear loading [12]. In this way, articular cartilage guarantees the joint's

properties of withstanding mechanical forces. Beside the avascular nature of cartilage, other differences with bone are the lack of lymphatic drainage and neural elements.

Osteochondral Development

Despite the discrepancies, the development of the skeleton clarifies the close relationship between cartilage and bone. During embryogenesis ossification occurs by two different processes: either intramembranous or intracartilaginous (endochondral) [7]. A stable structure and a well developed vascular supply need to be present at the ossification site to support the generation and mineralization of the extracellular matrix. Furthermore, mobility and low oxygen tension favors differentiation of cells.

Intramembranous ossification is restricted to bones of the cranium, some facial bones, as well as parts of the mandible and clavicle. It occurs by direct transformation of MSCs into osteoblasts; in contrast to endochondral ossification, cartilage is not involved in this process. Therefore, we focus the attention on the endochondral ossification process.

Bones exposed to weight are formed by endochondral ossification, illustrated in Fig. 4. In these bones condensed embryonic mesenchyme transforms into cartilage. In the central part of such a cartilaginous structure, interstitial proliferation of columns of chondrocytes occurs, which further develops into progressive hypertrophy. Hypertrophic chondrocytes mineralize the matrix and subsequently undergo apoptosis, while lining cells from the perichondrium differentiate into osteoblasts to form a periosteal collar.

Empty lacunae from pycnotic chondrocytes are penetrated by blood vessels providing peripheral osteoblasts to the site. Longitudinal bone growth is a precise balance between on the one hand chondrocyte proliferation, cartilage matrix production, and hypertrophy and on the other hand matrix mineralization, vascular invasion, and cell differentiation. Ossification proceeds towards the end of each growing long bone.

As a result, cartilage can be found at the end of these bones, where articulation takes place. The thickness of cartilage varies from joint to joint, from site to site within each joint, and is age related [14]. The thickness in humans ranges from approximately 0.5mm to over 5mm on the patella. Cartilage is firmly fixed to the underlying subchondral bone and is very resistant to shear stress. Cartilage and subchondral bone are both responsible for the normal function of the joint by providing a very low friction articulation and load distribution.

2. Osteochondral Tissue Regeneration

Biological Repair

The highly vascularized bone, built by metabolically active cells, is a dynamic tissue that undergoes formation and resorption throughout life span in response to static conditions. In contrast, the avascular cartilage, built by isolated, metabolically steady cells, has a restricted biological adaptability and a limited regeneration potential. Although the chondrocytes produce extracellular matrix throughout their life span, they can only regenerate very small defects [12, 15, 16]. Besides, whereas during development and growth the collagen content and compressive moduli increase [17, 18], during cartilage repair the proteoglycan and collagen contents [19] as well as the tissue biomechanical properties change [20, 21]. Therefore, repair of chondral lesions are rarely effective. In osteochondral defects, however, macrophages and mesenchymal stem cells (MSCs) from the bone marrow have access to the defect site and provide biological repair. The defect is filled with fibrocartilage of inferior quality regarding biochemical and structural composition and mechanical properties. That is why injuries are maintained for years. In addition, if the loads on the joint, or on a portion of the joint, are extensive, either because of improper alignment, incongruence, excessive weight, extreme activities, or a combination of these factors, it eventually leads to further degeneration like osteoarthritis or to loss of cartilage [22, 23]. In advanced arthritis, the articular cartilage is completely worn, so that the bones of two joints have direct contact (Fig. 5B). This is generally accompanied by excruciating pain, a decrease in motion up to stiffness and muscle weakness.

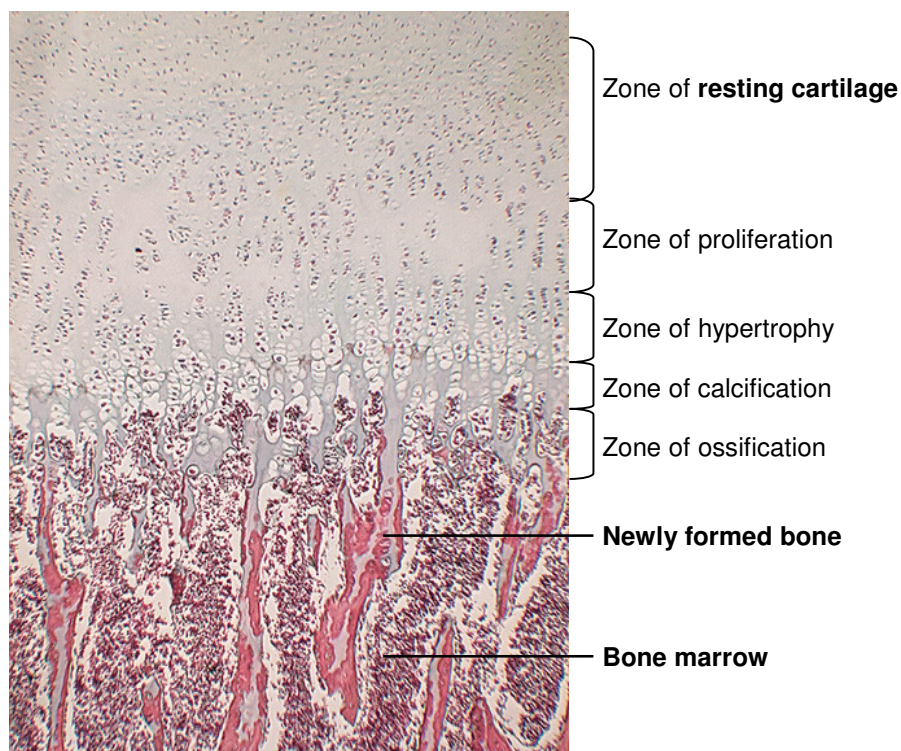


Figure 4: Primary ossification center of a developing finger. Longitudinal section shows five zones characteristic for endochondral ossification. Trichrome staining. (modified from [13]).

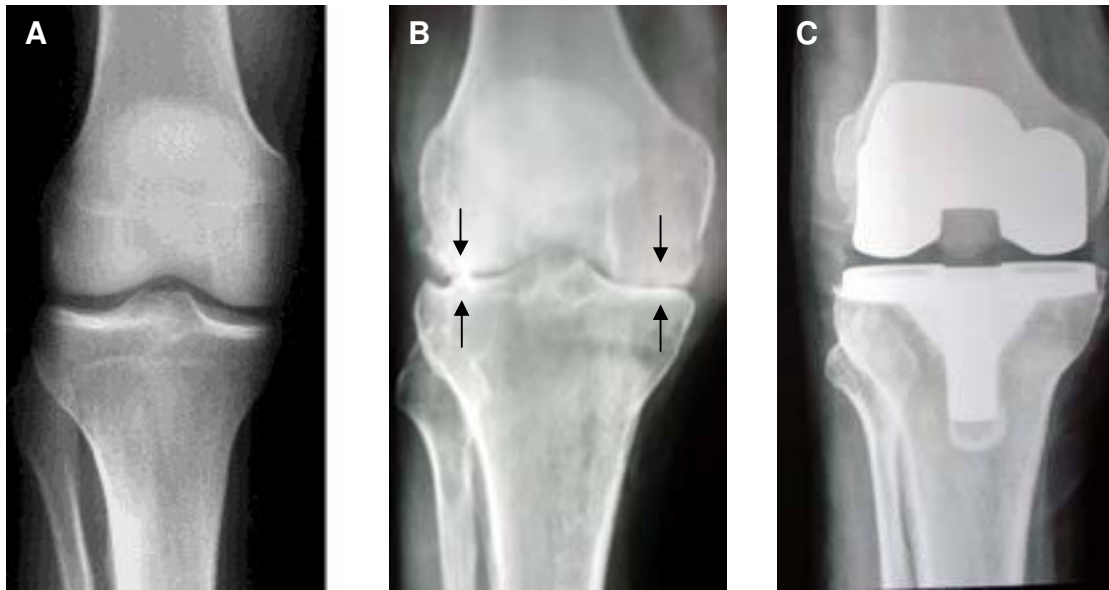


Figure 5: X-ray views of a human knee. (A) A healthy human knee. **(B)** In comparison, in advanced osteoarthritis note the absence of space between the bones as indicated by the arrows. This loss of joint space occurs because the articular cartilage is worn. **(C)** The damaged and worn knee is resurfaced during a total knee replacement to restore function, relieve pain and correct existing leg deformity. (modified from [24, 25]).

Clinical Repair of Osteochondral Lesions

Conventional Treatments

The severe pain due to extensive loss of articular cartilage is the main reason why patients undergo a total joint replacement (Fig. 5C). However, replacements increase the risk of infections and adhesive breakdown at the host-joint interface. To avoid the debilitating consequences of osteochondral degeneration, scientists and clinicians have tried to repair or regenerate injured tissue for decades. Nevertheless, conventional options for surgical treatments are still very limited. Immobilization of injured joints antedates further cartilage degeneration [26]. Restorations like subchondral drilling, abrasion, or production of microfractures which have the aim to recruit MSCs from bone marrow by penetration of the subchondral bone result in repair with qualitatively poor fibrocartilage and could not prove a benefit in relation to large defects or arthritis [27].

Transplantation to restore injured or lost tissue is most promising. Small biopsies of cartilage are taken and cells are isolated, expanded, and returned into the defect. The technique gives stable long-term results with a high percentage of good to excellent results (84%–90%) in patients with different types of single femoral condyle lesions, whereas patients with other types of lesions have a lower degree of success (mean, 74%) [28]. Mosaicplasty (MP) involves the collection of small-sized cylindrical osteochondral grafts ranging from 2.7 to 9mm from the minimal weight-bearing periphery of the femoral condyles, followed by their transplantation to a prepared recipient site. Surface congruence comprised of hyaline cartilage, and progressive fibrocartilaginous sprouting between the grafts resulting in appropriate integration were demonstrated up to 5 years follow up. Multicenter clinical studies revealed superior outcomes of MP in comparison to other restoration methods. As a result, MP has become a valid technique for the treatment of articular cartilage lesions in the knee joint and is one of the major internationally accepted articular cartilage reconstructions in humans [29, 30]. Despite the encouraging results reported, the transplantation of autologous osteochondral grafts

endure several drawbacks such as (i) the limited amount of material available at the donor site, (ii) the donor site morbidity, and (iii) the difficulty to match the topology of the grafts with the injured site. Tissue engineering of osteochondral composites has the potential to overcome the limitations of conventional MP.

Osteochondral Tissue Engineering

Tissue engineering is an interdisciplinary field that applies principles of engineering and life sciences to develop biological substitutes that restore, maintain or improve tissue functions [31]. The strategy of tissue engineering generally involves the following steps: (i) a biocompatible material that can be used as a cell substrate or cell-encapsulation material must be isolated or synthesized and manufactured into the desired shape and dimensions and (ii) an appropriate cell source must be identified, isolated, and produced in sufficient numbers.

Osteochondral tissue engineering offers the possibility to produce sufficient numbers of grafts, tailor-made mechanical properties and topology of the graft essential for regeneration of osteochondral repair. The choice of scaffold material and cell source must be considered carefully when designing a tissue engineering system.

1. Biomaterials in osteochondral tissue engineering

Materials for the chondral compartment have different biological and physical requirements compared to materials for the osseous compartment.

When designing osteochondral constructs, healing of the underlying subchondral area of the defect site is critical to support the overlying regenerating neocartilage. As a result, different implants are designed as such that chondrogenic cells are seeded directly on top of an osteoconductive biomaterials. For bone repair, coated tantalum, bioactive glasses, and ceramics have shown their ability to bond to bone and accelerate bone healing.

In osteochondral TE, Ylaenen *et al.* demonstrated that bioactive glasses restored subchondral bone when implanted into osteochondral defects in a rabbit model [32]. However, in the chondral part they found newly formed tissue of insufficient quality, predominantly composed of fibrocartilage or fibrous tissue. Another study directly compared the applicability of bioactive glass, glass-hydroxyapatite, and hydroxyapatite in osteochondral repair of rabbit femurs [33]. While bioactive glass compositions failed due to brittleness, disturbed bone bonding, and early degradation, hydroxyapatite stimulated the generation of lamellar subchondral bone and restoration of a hyaline-like cartilage surface at 12 weeks. Because of these results and their biodegradability, ceramics are most promising for osteochondral TE. These materials are closely related to the composition of the mineral phase in bone, and as a result, have a high biocompatibility [34]. Another important property of these materials is their bioactivity, which means that bone formation starts at, and proceeds away from the implant surface. Their apatite layer is known to integrate with a calcified layer that is produced by osteogenic cells and is referred to as the cementing substance. This cementing substance is produced at the onset of bone matrix production and comprises fused afibrillar calcium and phosphorous-rich globules to which collagen fibers become anchored [35, 36]. In addition, some ceramics are also known to have osteoinductive properties. Several reports revealed the osteoinductive capacity of CaP ceramics at ectopic sites [37-40]. Osteoinductivity is thought to be induced by the ability of these materials to attract progenitor cells, which is referred to as chemotaxis [41]. It is suggested that the first step of chemotaxis is the adsorption of mediators onto the surface of the ceramics.

Currently, many techniques are focused on resurfacing the osteochondral defect with high-quality neocartilage. However, controversial results were reported when chondrogenic cells were seeded into the bone compartment. Niederauer *et al.* used multiphasic implants where half of the implants were loaded with or without chondrocytes [42]. From the results they concluded that the addition of cells had no effect on cartilage resurfacing, while other studies show a significant advantage of cell-based cartilage restoration compared to cell-free repair [43-45]. Still, numerous approaches fail due to inadequate integration between biomaterial and neocartilage [46] and more advanced biphasic strategies are available to overcome fixation difficulties of the neocartilage and the osseous compartment. A wide range of natural and synthetic materials for cartilage TE were reviewed [47-50]. The major fraction of studies described in literature focuses on the application of poly(hydroxy esters) such as poly(glycolic acid) (PGA), poly(lactic acid) (PLA) and poly(lactide-co-glycolide) (PLGA) and *in vitro* and *in vivo* results are promising.

For osteochondral TE, cartilage and/or bone-like tissues can be engineered separately *in vitro* and combined to a single composite graft. Kreklau *et al.* combined calcium carbonate with PGA/PLLA fleeces using fibrin glue [51]. Chondrocyte-seeded constructs were incubated in perfusion chambers for up to 56 days. Gao *et al.* generated osteochondral grafts from sponges based on hyaluronic acid and porous ceramics [52]. Bone marrow-derived stem cells were differentiated into chondrogenic and osteogenic lineage prior to the seeding into the sponges or porous ceramics. Both compartments were joined using fibrin glue. After 56 days, histological analysis revealed large amounts of lamellar bone in the osseous part, while fibrocartilage and not hyaline cartilage was observed in the chondral part. However, tissue regeneration took place subcutaneously and it remains unclear, if an osteochondral constructs hold by fibrin glue is applicable in a load-bearing environment. A more promising approach to combine chondral and osseous compartments is suturing [53]. *In vitro* generated cartilage sutured on top of an osteoconductive sponge promoted remodeling of large osteochondral defects in adult rabbits [54]. Furthermore, suturing was applied to combine preshaped PGA/PLLA scaffolds seeded with tenocytes and chondrocytes, respectively. Subsequently, scaffolds were wrapped in periosteum to assemble complex structures such as entire phalanges and joints [55].

However, functionality has priority over the assembly of a scaffold. Techniques to precisely control the scaffold architecture enable tissue engineers to improve biological and mechanical properties of the scaffold, and simultaneously to promote osteochondral regeneration. Biphasic scaffolds can be fabricated with distinct regions favoring cartilage and bone growth, respectively.

A human-shaped mandibular condyle was engineered by encapsulating chondrogenic cells in PEG-based hydrogels [56]. The cell-gel suspension was stratified into a hollow bivalved negative mold made of polysiloxane, and photopolymerized. Osteogenic cells were suspended in the PEG hydrogel and loaded into the mold, followed by photopolymerization. 4 weeks after the implantation in immunodeficient mice, most of the differentiated chondrogenic and osteogenic cells had synthesized corresponding cartilaginous and bone-like matrices.

Sintered HA ceramic scaffold bases were fabricated containing a primary and secondary pore network [57]. The primary network was designed for tissue growth into the ceramic while the secondary network served as the PLA mold. Constructs were built by a PLA region seeded with porcine chondrocytes, and human fibroblasts seeded in the HA region. Ectopic implantation in mice enhanced the development of a layer rich in GAG in the cartilage part, whereas the bone layer contained vascularized regions. Furthermore, a mineralized tidemark-like structure was present at the interface of PLA/HA. In another

study, oligo(polyethylene oxide fumarate) hydrogel scaffolds were produced consisting of an upper layer with encapsulated microparticles loaded with a chondrogenic growth factor [58]. When implanted, full-thickness osteochondral defects in rabbits were completely filled with tissue. A Safranin O positive matrix was observed at the surface of this tissue, while newly formed subchondral bone was well integrated into the surrounding bone.

The insertion of the bone part into the cartilage part offers another possibility to create osteochondral scaffolds. A cell-seeded chondral part was press-fitted into a defect filled with injectable calcium phosphate. In the load-bearing environment of rabbit condyles, good integration of the two components could be observed. Furthermore, cartilaginous tissue was found on top of well-integrated newly formed bone [59]. Another approach addressed in the publication of Ito *et al.* is to assemble osteochondral constructs by chondrocytes seeded into collagen sponges, which are surrounded with a PLLA mesh to provide mechanical strength [60]. 12 weeks after insertion of such a construct into the osteochondral part of the rabbit patellar groove, defects were repaired with cartilage-like tissue and subchondral bone formation was observed.

The application of technologies such as three-dimensional printing enables tissue engineers to produce osteochondral scaffolds not only with defined shapes and sizes, but also with variable regions of material compositions, porosity, architecture and mechanical properties. By this, mechanical properties can be changed gradually, preventing discontinuity and delamination of the cartilage and bone region [61].

Our research group extensively investigates biodegradable poly(ether ester) multiblock copolymers as scaffold materials for bone and cartilage TE. Hydrophilic polyethylene oxide terephthalate (PEOT) and hydrophobic polybutylene terephthalate (PBT) blocks are the basis of these copolymers. A major advantage of these PEOT/PBT scaffolds is that by varying the ratio of PEOT and PBT a wide range of polymers can be obtained that are distinguished by different behaviors regarding swelling, degradability, and mechanical strength. Various *in vitro* and *in vivo* studies demonstrated not only biocompatibility, and biodegradability of these polymers [62-65] and attachment, proliferation, and differentiation of chondrocytes [66-70], but also the controlled release of bioactive factors [71-74]. Degradation is realized by both hydrolysis and oxidation, whereby degradation is more rapid for polymer compositions with high PEOT content. On these, hydrophilic, polymers seeded chondrocytes maintained a round morphology and generated cartilaginous matrix rich in collagen type II. In contrast, hydrophobic matrices enhanced cell attachment, spreading, and proliferation, but the matrix generated contained significantly lower amounts of collagen type II, but higher amounts of collagen type I [75, 76]. Therefore, it is crucial for tissue engineers to consider that the tendency of cells to adhere and to spread on a substrate is inversely related to cell differentiation.

2. Cell sources for osteochondral tissue engineering

As diverse as the assembly of different biomaterials is the choice of the appropriate cell source for osteochondral TE.

Chondrocytes are most commonly used in osteochondral TE. It is well known, that articular chondrocytes show the ability to proliferate, when isolated from their extracellular matrix [77]. This makes it possible to start with a relatively small quantity of cartilage as a source of cells. Tissues like periosteum or perichondrium were used as cell source to support cartilage regeneration. *In vitro* studies have shown the chondrogenic potential of those cells, because their generated matrix contained articular cartilage-specific matrix components such as collagen type II, IX and X [78]. In contrast, the composition of the tissue generated after 12 weeks *in vivo* was a mixture of collagen

type I and II, indicating fibrocartilaginous tissue and no articular cartilage [79]. Furthermore, periosteum and perichondrium were combined with *ex vivo* expanded chondrocytes. But despite the supporting effects they did not provide a stable matrix for chondrocytes.

Chondrocytes were also isolated from the nose or from a non load-bearing surface of the joint and combined with matrices like fibrin [80, 81], polylactide [82], collagen and glycosaminoglycans [83], or polysaccharide hydrogel [84]. Although cartilaginous tissue was generated *in vitro* and *in vivo*, there are limitations for such cell sources. Cell isolation from a non load-bearing surface within the joint requires surgery and can result in complications such as postoperative bleeding, donor side morbidity, and the development of painful hemarthroses [85]. Furthermore, it is true that adult nasal chondrocytes are utilizable as articular chondrocytes [86], but it remains to be established whether cartilage engineered from nasal chondrocytes can function effectively when implanted in an articular defect. So the use of undifferentiated cells which have the potential to differentiate in various types of cells might be an improvement.

Pluripotent embryonic stem cells (ESCs) were shown to form differentiated embryonic tumors (teratomas) when injected into the muscle or testis of severe combined immunodeficiency mice [87]. Because they can give rise to many types of cells such as gut, neural epithelium, bone, cartilage, muscle, and even fetal glomeruli, ESCs are very attractive for research. In several studies, ESCs were differentiated *in vitro*, but because the differentiation of human ESCs is spontaneous and uncontrolled [88] growth factors were used to direct the differentiation. Growth factors such as transforming growth factor beta (TGF β) and activin-A appear to inhibit endodermal and ectodermal cells, but allow differentiation into mesodermal cells. Another group of growth factors allow or induce differentiation into ectodermal as well as mesodermal cells (retinoic acid, basic fibroblast growth factor, bone morphogenic protein 4, epidermal growth factor). The third group (nerve growth factor and hepatocyte growth factor) allows differentiation into all three embryonic germ lineages including endoderm [89]. Further studies focused on differentiation of ESCs into cardiomyocytes [90, 91] or neural cells like neurons, astrocytes, and oligodendrocytes [92, 93]. Such potential can be used for tissue repair following trauma, or be of use in various degenerative diseases, for example, Alzheimer or Parkinson diseases, injured spinal cords [94], or for heart muscle regeneration after coronary artery blockage [95]. Tissue engineers consider ESCs also as an appropriate cell source, but ethical issues over the use of embryos have resulted in tight government regulations. Therefore, as long as discordant opinions exist, embryos should be considered as a cell source for tissue engineers with caution.

Fortunately, between the ESC and its terminally differentiated progeny there is an intermediate population of committed progenitors with limited proliferative capacity and restricted differentiation potential. Examples include hematopoietic stem cells which give rise to erythrocytes, granulocytes, and platelets or epithelial stem cells that generate the various types of skin cells [96, 97]. These stem cells are very attractive, since they still can be found in adult tissues to replenish the supply of cells in the body.

In addition to the hematopoietic and epithelial stem cells, fully developed organisms contain several other classes of stem cells. Adult stem cells were isolated from tissue sources including the central nervous system [98, 99], bone marrow [100-102], and even retina [93]. For a long time, adult stem cells were considered to be developmentally committed in such a way that they appear restricted to produce specific cell lineages, namely those from the tissue in which the stem cell resides: neural stem cells are biased to generate neurons and glia, and hematopoietic stem cells to generate blood cells [97]. However, several recent investigations indicate that at least a fraction of stem cells

within these populations can generate cells of a different embryonic lineage (Tab. 1). For example, neural stem cells can give rise to blood [103], and skeletal muscle cells contribute to many embryonic tissues when transplanted into blastocysts [104, 105]. It is well known that bone marrow is the main cell source for hematopoiesis. But early studies of Friedenstein *et al.* indicated first evidence of non-hematopoietic stem cells in the bone marrow [114, 120]. Samples of bone marrow were placed onto plastic dishes and after discarding nonadherent cells (most of the hematopoietic stem cells) a small number of plastic adherent cells remained. These cells were spindle-shaped, and initially formed clusters of two to four cells. After several passages in culture cells differentiated resulting in small deposits of bone or cartilage-like tissue. So the bone marrow of an adult organism is not only the source for blood cells, but also for cells of mesenchymal origin, mesenchymal stem cells (MSCs). Since Friedenstein, abundant studies were performed utilizing MSCs. They showed that MSCs have the ability to regenerate bone or cartilage, as well as differentiate into adipocytes, tendocytes, and stromal cells [100]. But the entire potential of MSCs was revealed by several unexpected findings. MSCs can generate skeletal muscle [118], cardiomyocytes [111], liver [109], and also cells producing neuronal markers in the brain [112, 113, 121]. Because of this multipotency, MSCs are an exciting option for osteochondral TE in comparison to embryonic stem cells and the ethical issues to their use. Given the possibility to produce a wide range of tailor-made biomaterials such as PEOT/PBT copolymer scaffolds in combination with multipotent MSCs, osteochondral TE becomes feasible. However, several essential parameters that affect the successful outcome of the application of MSC in osteochondral TE are neglected in the majority of studies. Considering the inverse relationship between cell attachment and chondrogenic differentiation of MSCs in biocompatible scaffolds as described earlier, the cell loading is the most critical factor for osteochondral TE and therefore extensively addressed in this thesis.

Table 1: Sources of adult stem cells and their differentiating potential

Source	Generated cells	References
brain	neurons, astrocytes, oligodendrocytes	[98, 99, 106]
	blood cells	[103]
	skeletal myocytes	[105]
epithelium	epithelial cells	[96]
	neurons, glia, adipocytes, smooth myocytes	[107]
adipose tissue	myogenic, osteogenic, chondrogenic cells	[108]
bone marrow	hepatic cells	[109]
	adipocytes	[100]
	cardiomyocytes	[110, 111]
	neurons, oligodendrocytes	[112]
	astrocytes	[113]
	osteogenic cells	[114, 100]
	chondrogenic cells	[77, 100, 115, 116]
	myocytes	[117]
	skeletal myocytes	[118]
	blood cells	[97]
stromal cells	[119]	

3. Aim and outline of this thesis

The aim of the research described in this thesis is to develop an osteochondral construct applying cell-based strategies. With respect to the multipotency of adult stem cells, mesenchymal stem cells (MSCs) were used to generate cartilage and bone, respectively. Five critical steps are in the focus: cell seeding, application of growth factors, scaffold design, respective cell seeding and differentiation, and the applicability of osteochondral grafting in the clinic. They are addressed in this thesis by the following questions:

- What is the most suitable polyethylene oxide terephthalate/polybutylene terephthalate (PEOT/PBT) composition and what seeding method needs to be applied to facilitate cell loading on scaffolds and concomitant chondrogenic differentiation?
- Are synthetic PEOT/PBT scaffolds used in cartilage TE suitable for incorporation and controlled release of chondrogenic growth factors and do incorporated growth factors maintain their stability and their biological activity after controlled release?
- How feasible is cell loading and cell differentiation of MSCs in osteochondral scaffolds?
- How can novel scaffold fabrication techniques be applied to support cartilage generation and create integrated three-dimensional osteochondral structures?

The answers to these questions represent critical steps for the development of a cell-based osteochondral construct:

Chapter 1 describes the influence of different PEOT/PBT scaffold compositions on chondrogenic differentiation of MSCs and the consequences of applying different cell seeding methods.

Chapter 2 introduces novel approaches to incorporate and release proteins controlled from porous scaffolds. The application of these approaches in cartilage TE regarding stability and biological performance of released growth factors are addressed in chapter 3.

Chapter 4 points out new insights of growth factor supplementation revealed from previous release studies. Short-term incubation of MSCs with chondrogenic growth factors and its application as a user-friendly method for cell seeding in osteochondral TE was examined.

Chapter 5 presents a method to increase cell seeding efficiency and differentiation of bovine chondrocytes by integrating electrospun fibers into three-dimensional fiber-deposited scaffolds.

Chapter 6 describes advanced scaffold fabrication techniques to create osteochondral scaffolds providing both mechanical properties of cartilage and bone, respectively, and structural niches supporting either chondrogenic or osteogenic cell differentiation. In this study, we explore the feasibility of using MSCs to create osseous and chondrogenic tissue *in vivo*.

Finally, chapter 7 covers a clinical feasibility study to evaluate the safety and efficacy of porous PEOT/PBT implants to fill donor sites during mosaicplasty.

Chapter 1

Comparison of seeding methods as the critical factor for cartilage tissue engineering utilizing mesenchymal stem cells on 3D fiber-deposited scaffolds

Abstract

Adult mesenchymal stem cells (MSCs) isolated from bone marrow are an attractive therapeutic tool in cartilage tissue engineering (TE). The behavior of these cells in TE constructs strongly depends on the seeding protocol, and is poorly controlled to date. In this study, we evaluated different methods to load MSCs into different compositions of a polyethylene oxide terephthalate / polybutylene terephthalate (PEOT/PBT) copolymer efficiently and studied their effect on *in vitro* and *in vivo* cartilage formation.

Expanded goat MSCs were loaded into a hydrophobic (300/55/45) or hydrophilic (1000/70/30) PEOT/PBT copolymer by attachment, detainment, incorporation, and aggregation, respectively. Seeding efficiency, cell viability, and chondrogenic differentiation were assessed *in vitro* and after implantation at the dorsum of nude mice by histochemical and biochemical analyses.

All four methods led to successful cell loading and loaded cells were viable. *In vitro*, only for cells that were incorporated or aggregated significant amounts of glycosaminoglycans and hyaline cartilage-like matrices could be detected. Chondrogenic differentiation could not be detected when MSCs were attached or detained onto the fibers of the scaffolds. *In vivo*, cartilage formation was limited to scaffolds into which cells were loaded by incorporation. We did not detect a significant difference between the two polymer compositions on chondrogenic differentiation neither *in vitro* nor *in vivo*.

We conclude that, rather than cell seeding density or chemical composition of the scaffold, the seeding method is the critical factor influencing chondrogenic differentiation of adult MSCs.

Introduction

Tissue engineering (TE) of cartilage by autologous chondrocyte transplantation has been introduced into clinic with relative success. In this procedure, autologous chondrocytes are expanded in culture, incorporated in a carrier matrix and implanted into the defect side. However, the use of autologous chondrocytes has several disadvantages like the low cell number obtained during harvest, the loss of the cartilage-specific phenotype during culture expansion, as well as donor side morbidity. Hence, there is a need for easy accessible cell populations that can substitute the culture-expanded chondrocytes.

A promising alternative for autologous chondrocytes are mesenchymal stem cells (MSCs) isolated from adipose tissue [108] or bone marrow [100]. These cells are easy to isolate, have a high proliferation capacity, as well as a high regenerative potential due to their plasticity. MSCs are able to differentiate into osteoblasts, chondroblasts, adipocytes, and myoblasts, depending on the culture conditions [101, 122]. Substitution of autologous chondrocytes by MSCs, however, does not result in the formation of hyaline cartilage. Instead, fibrocartilage is formed [123]. This indicates that the cartilaginous environment *in vivo* is inadequate to trigger chondrogenic differentiation of MSCs.

This problem might be circumvented by inducing chondrogenic differentiation of MSCs *in vitro* prior to the implantation. *In vitro* chondrogenic differentiation of MSCs requires serum-free medium containing transforming growth factor beta (TGF β) and an initially high cell density [115, 124]. Wayne *et al.* generated immature tissue on polylactic acid/alginate amalgam constructs *in vivo* when seeded with MSCs stimulated with TGF β *in vitro* [125]. De Bari *et al.* reported the instability of the chondrocyte phenotype of *in vitro* differentiated MSCs after transplantation [126]. In line with this, Pelttari *et al.* described endochondral ossification rather than stable cartilage formation after implantation [127].

Cartilage TE depends not only on the culture conditions, but also on the scaffold materials used. A wide range of synthetic polymers and natural carriers have been tested as scaffolds in cartilage TE. These scaffolds are preferably biocompatible, biodegradable, aim to provide mechanical stability, as well as support tissue regeneration. There is evidence that the production of extracellular matrix by chondrocytes depends on the scaffold type. Results obtained by Grande *et al.* show that the collagen production was enhanced on type I collagen sponges, whereas proteoglycans production was enhanced on polyglycolic acid (PGA) scaffolds [128]. In another study, the rate of chondrocyte proliferation and deposition of cartilage-specific glycosaminoglycans were significantly higher on PGA-based scaffolds when compared to poly(L)lactic acid (PLA)-based scaffolds [129]. Previous studies in our group have focused on architecture and composition of polyethylene oxide terephthalate/polybutylene terephthalate (PEOT/PBT) copolymers. By varying the ratio of hydrophobic PEOT and hydrophilic PBT blocks, properties like swelling, degradability, and mechanical stability can be tailor-made [63, 71, 130]. It has been shown that cell attachment, proliferation, and differentiation clearly respond to different PEOT/PBT compositions [69]. The attachment and proliferation of chondrocytes is significantly higher on hydrophobic compositions [131, 132], whereas differentiation and cartilage-specific matrix production is increased on hydrophilic PEOT/PBT compositions [131, 133]. Despite the application of chondrocytes on PEOT/PBT polymers, the effect of different PEOT/PBT compositions on chondrogenic differentiation of MSCs still remains unknown.

Another challenge is the poor seeding efficiency of MSCs into biomaterials at chondrogenic differentiation conditions. This is due to the serum-free differentiation

medium, in which MSCs tend to detach from surfaces [134]. Generally, two principles of seeding cells into biomaterials are applied in TE: statically and dynamically. The static methods may lead to highly efficient cell seeding and high cell viability. However, due to the serum-free chondrogenic culture conditions, conventional static seeding of MSCs is very time consuming [135]. Furthermore, as soon as scaffold thickness exceeds 2mm, static seeding does not provide a high seeding efficiency or a homogenous cell distribution throughout the scaffolds [136]. Dynamic seeding may provide a tool to achieve a higher seeding efficiency and a more homogeneous distribution of cells [137] using either spinner flasks [138], flow seeding [139], or hydrodynamic loading [140]. Other studies described the encapsulation of MSCs. This resulted in an initially high seeding density, and, moreover, in cartilage tissue formation [141-143]. Conclusively, the encapsulation of MSCs into hydrogels and subsequent incorporation into a stable three-dimensional scaffold is currently seen to be one of the most promising approaches for cartilage TE. We hypothesized that PEOT/PBT polymer scaffolds would be good candidates for cartilage TE using MSCs. In this study we investigated different methods to integrate MSCs and generate cartilage-like tissue in either hydrophobic (300/55/45) or hydrophilic (1000/70/30) PEOT/PBT scaffolds.

Materials & Methods

Scaffold fabrication

The biodegradable PEOT/PBT copolymers were obtained from IsoTis Inc (Irvine, USA) and have been characterized previously [132]. The composition is as a/b/c, where a represents the PEG MW (g/mol), and b and c represent the wt% of the PEOT and PBT blocks, respectively. 300/55/45 is a hydrophobic composition, whereas 1000/70/30 is hydrophilic. Three-dimensional sheets were produced using a Bioplotter device (Envisiontec GmbH, Germany) [144]. To extrude highly viscoelastic fibers, the bioplotter underwent few modifications reported by Moroni *et al.* [145]. For 300/55/45 and 1000/70/30 sheets the space between the fibers was set at 600 μ m and the layer thickness at 150 μ m. The sheets were 4mm thick. From the fabricated sheets scaffolds were punched out using a core with an inner diameter of 4mm resulting in cylindrical scaffolds of \varnothing 4mm. The resulting polymers had an average pore size of 150 μ m and porosity of 98%.

Gas Plasma (GP) treatment

For GP treatment scaffolds were aligned on a needle which was placed into a cylindrical, radiofrequency glow discharge chamber (Harrik Scientific Corp, NY). A vacuum was applied to the chamber (0.01 mbar), which was then four times flushed with argon (purity \geq 99.999%, Hoekloos B.V., The Netherlands). The scaffolds were treated under argon plasma (0.1–0.2mbar) for 30min followed by sterilization using 70% isopropanol. Subsequently, scaffolds were washed twice in phosphate buffered saline (PBS) and incubated in Dulbecco's modified Eagle medium (DMEM) for 24hrs prior to the cell seeding.

Bone marrow isolation and expansion

Caprine mesenchymal stem cells (MSCs) were harvested, isolated and cryopreserved as described previously [146]. For these experiments, MSCs were thawed at 37°C and replated at a density of 1000 cells/cm² in expansion medium containing α -modified Eagle's Medium (α -MEM), supplemented with 15% Fetal Bovine Serum (FBS), 1% Pen/Strep, 0.1mM ascorbate-2-phosphate acid and 2mM L-Glutamine. When 80%

confluent, cells were trypsinized using 0.25% trypsin-EDTA and replated at a density of 1000 cells/cm². When reaching 80% confluence again, cells were trypsinized, washed twice in PBS, counted using a Burker Turk counting chamber and used for experiments.

Tissue engineering

Cells from three different goats were pooled to have sufficient cell amounts at a low passage for the entire experiment, and to reduce individual variations. Four different methods were applied to seed the MSCs into the three-dimensional scaffolds:

Attachment:

Four scaffolds were aligned per sterile needle. Three needles were attached to the lid of a spinner flask. 1.2×10^6 cells were inoculated per flask ($\approx 1 \times 10^6$ cells per scaffold) and incubated in expansion medium at 40rpm for 24hrs at 37°C in a humidified atmosphere of 5% carbon dioxide. After 24hrs, seeded scaffolds were removed from the needles, washed twice in PBS to eliminate FBS, and subsequently placed into bacteriological well plates and statically cultured in chondrogenic differentiation medium (CM) consisting of serum-free DMEM with 4.5g/l glucose, 1% penicillin/streptomycin, 50µg/ml ascorbate-2 phosphate acid, 100µg/ml sodium pyruvate, 40µg/ml proline, 100 nM dexamethasone, 1% ITS¹⁺ and 10ng/ml TGF β1 at 37°C in a humidified atmosphere of 5% carbon dioxide for 21 days.

Detainment:

Cells were seeded into the scaffolds using spinner flasks as aforementioned. After 24hrs, scaffolds were washed twice in PBS, but, prior to the static culture, 50µl growth factor reduced matrigel® (BD Bioscience, later referred to as matrigel) was applied to each scaffold to detain the cells (Fig. 1B). After gelation at 37°C for 30 minutes, constructs were cultured in CM for 21 days as described above.

Incorporation:

1×10^6 cells/50µl CM were mixed with 50µl matrigel, seeded into the scaffold and incubated for 30 minutes at 37°C to allow gelation of the matrigel. Constructs were cultured for 21 days under the same static conditions as abovementioned.

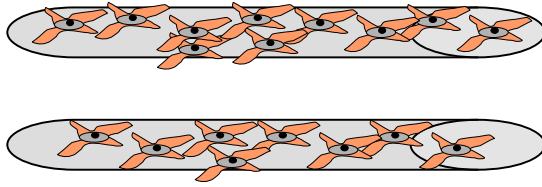
Aggregation:

MSCs were aggregated by inoculating a single cell suspension on an Ultra-Low Attachment Surface (Corning Life Sciences, later referred to as ultra-low attachment plate). 1×10^6 cells/ml CM per well of a 12-well ultra-low attachment plate were incubated for 4hrs at 37°C in a humidified atmosphere of 5% carbon dioxide. Aggregates were collected per well in a separate polystyrene tube, supernatant was removed and aggregates were mixed with 50µl matrigel. Each aggregate-gel mixture was seeded into one scaffold and incubated for 30 minutes at 37°C (Fig. 1C). Constructs were then statically cultured in the same way as stated above earlier for 21 days.

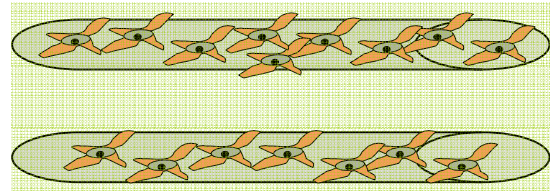
Implantation

The animal experiments were approved by a local Ethics Committee. Tissue engineered constructs were implanted into immunodeficient, six weeks old, male mice (HdCpb:NMRI-nu, Harlan B.V., Horst, The Netherlands). All animals were operated under aseptic conditions. After intraperitoneal injection of 0,05mg/kg Temgesic for analgesia the mice were put under general inhalation anesthesia using isofluran. Four subcutaneous pockets were created at the dorsum of each mouse by blunt dissection. One construct was inserted per pocket. In total 20 mice were used for the implantation.

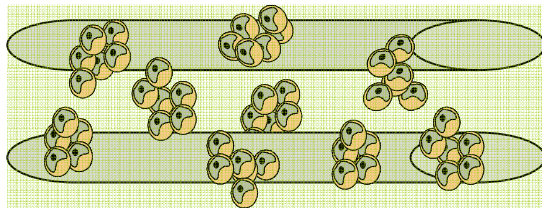
A. Attachment



B. Detainmentment



C. Incorporation



D. Aggregation

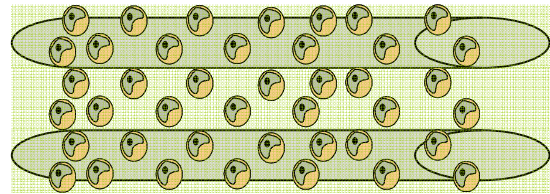


Figure 1: Schematic drawing illustrating the principal differences of four methods to load MSCs into three-dimensional scaffolds. **(A)** Cells are attached onto the fibers (grey). **(B)** Cells are attached onto the fibers followed by detainment with a gel (green). **(C)** Cells are incorporated as single cell suspension into a gel prior to the seeding. **(D)** Cells are aggregated prior to the seeding and subsequently a gel is applied.

Analysis

To evaluate seeding efficiency, samples ($n = 3$ per condition) were harvested after 3 days culture. To qualify and quantify cartilage tissue formation, samples ($n = 3$ per condition) were harvested after 14 and 21 days of culture. To assess the faith of tissue engineered cartilage *in vivo*, samples ($n = 3$) cultured for 14 days *in vitro* were implanted subcutaneously into nude mice and harvested one week later.

Cell viability

Viability was assessed using a live/dead assay which is based on intracellular esterase activity for living cells (green fluorescence) and the DNA-labeling of dead cells (red fluorescence) by ethidium homodimer, which cannot pass the cell membrane.

Histology

Samples were fixed in 1,5% glutaraldehyde in 0,14 M sodium cacodylate buffer at 4°C for 48h. After dehydration by graded ethanol series, specimens were embedded in glycol methylacrylate (GMA). Histological sections of 5 μ m were made and stained with Safranin O/ fast green. Nuclei were stained with hematoxyline.

Biochemical assays

At day 14 and 21, samples were harvested, washed in PBS and frozen at -80°C followed by digestion in 1mg/ml proteinase K, 10 μ g/ml pepstatin A and 180 μ g/ml iodoacetamide at 56°C for 16h. Calculation of total cell numbers was done using the CyQuant dye kit (Invitrogen) to measure DNA content at 520nm with a spectrofluorometer. Glycosaminoglycans (GAGs) were determined by staining GAGs with dimethylene blue and measuring the color intensity at 540nm using a spectrofluorometer. Chondroitin-sulfate served as a standard.

Statistical evaluation

All quantitative data are presented as means \pm standard deviations ($n = 3$). The data obtained were analyzed using SPSS software (version 12.0). Analysis of variance (ANOVA) was used and significant differences were determined by Bonferroni post-hoc test ($p < 0,05$ was considered significantly).

Results

In vitro

Attachment

Equal cell numbers were loaded by attachment into either the hydrophobic or hydrophilic scaffold (Fig. 2A). At day 14, the cells were homogeneously distributed in the construct. Despite the fact that the cells were viable (Fig. 2C) total cell numbers did not increase with time (Fig. 2A). Although low amounts of GAGs were present in either constructs (Fig. 2B), histological Safranin O staining for glycosaminoglycans in the extracellular matrix was negative at day 21. There was no difference between the two different scaffold compositions (Fig. 2D).

Detachment

The detachment of the MSCs onto the scaffold fibers resulted in different success for the two scaffold compositions. In the hydrophobic scaffold loaded cell number was significantly lower as for the hydrophilic scaffold (Fig. 3A). Whereas cells were viable in both materials, differences could be detected in the cell distribution (Fig. 3C). Cells were not homogeneously distributed in hydrophobic scaffolds. The center of the scaffold was empty while cells were loaded only within the first four deposited fiber layers. In contrast, the hydrophilic construct was homogeneously seeded.

After 21 days, hydrophobic scaffolds were empty and only a slight increase in total cell number could be seen in hydrophilic scaffolds (Fig. 3A). No positive Safranin O staining and no GAGs were observed for this composition (Fig. 3B, D).

Incorporation

Significant differences could be found comparing cell numbers of incorporated cells in the two scaffold materials (Fig. 4A). After 3 days, cell number was significantly higher in hydrophilic scaffolds compared to hydrophobic scaffolds. For both compositions, cells remained viable after 14 days, but increased in number only in hydrophobic scaffolds (Fig. 4A, C). These cells were not homogeneously distributed throughout the scaffold. Only the first few deposited layers were covered, while the center remained empty. In contrast, in the hydrophilic scaffold cells had formed aggregates which were homogeneously distributed. However, in both materials cells exhibited a round, chondrocyte-like morphology and their ECM stained very strongly for Safranin O (Fig. 4D).

Biochemical quantification revealed a significantly higher amount of GAGs in hydrophilic constructs at day 14. After 21 days, however, this difference could not be seen anymore (Fig. 4B).

Aggregation

When MSCs were loaded as aggregates, differences in cell number could be detected when both scaffold compositions were compared (Fig. 5A). Significantly higher amounts of DNA were found in the hydrophobic constructs. At day 14, cells were not

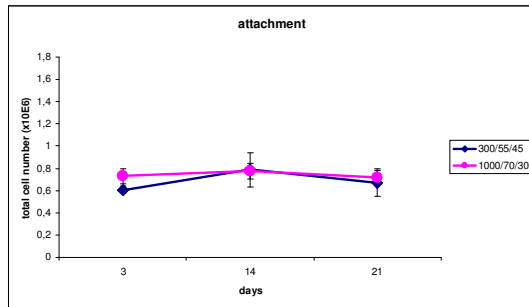
homogeneously distributed and, despite the fact that they were viable in both scaffolds, no increase in cell number could be seen in hydrophobic compositions (Fig. 5A, C). In fact, cell number decreased slightly. Furthermore, similar amounts of GAGs were present and histology revealed cells with a round morphology located in lacunae and surrounded by a strong Safranin O positive ECM in both scaffold compositions (Fig. 5D).

In vivo

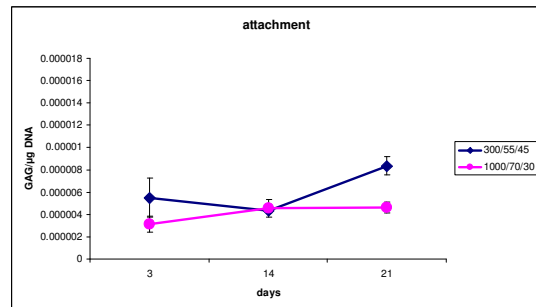
To investigate the stability of the newly formed tissue, after 14 days of *in vitro* culture constructs were implanted subcutaneously into nude mice. After one week, the implants were isolated and processed for histological analyses. All implants were surrounded by a fibrous capsule. In line with the *in vitro* data, no cartilaginous matrix was present in scaffolds loaded with cells by either attachment or detainment. (Fig. 6A, E and B, F). In contrast, small amounts of Safranin O positive areas could be found for the aggregation method (Fig. 6D, H) and strong positive cartilage-like tissue for the incorporation method (Fig. 6C, G). The cartilage was located at the periphery of the scaffolds, while the center remained empty or was only populated with a few single cells. Quantitative analysis of GAGs per construct was in line with the histological staining (data not shown).

Table 1 summarizes the results obtained in this study using a scoring system. Attachment and detainment are the most efficient seeding methods regarding homogeneously cell distribution, whereas chondrogenic differentiation is supported by incorporation and aggregation. However, independently on scaffold composition, incorporation and aggregation revealed the highest total score, indicating that for cartilage TE utilizing MSCs these seeding methods are most suitable on both copolymers.

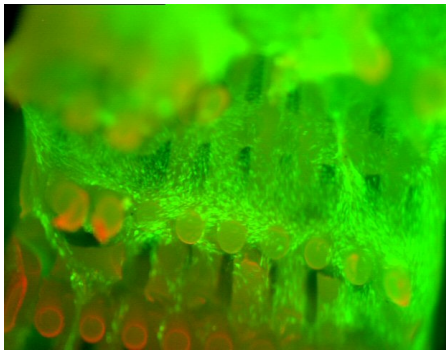
A. Total DNA after 3, 14 and 21 days



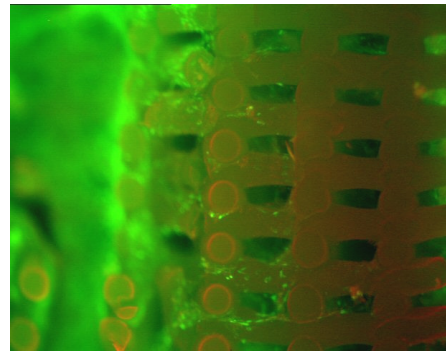
B. GAG/DNA content after 3, 14 and 21 days



C. Cell viability after 14 days

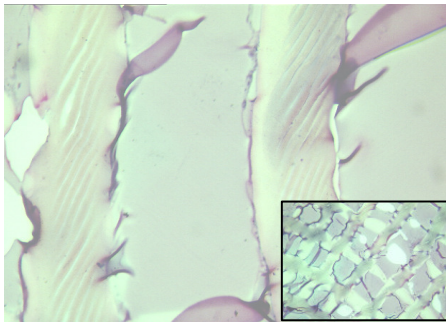


300/55/45

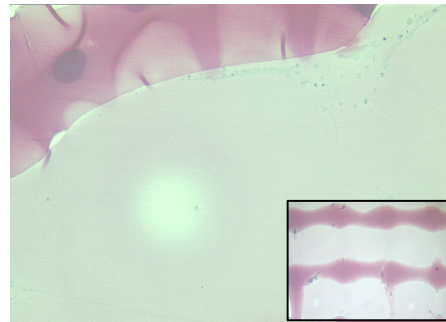


1000/70/30

D. Safranin O staining after 21 days *in vitro*



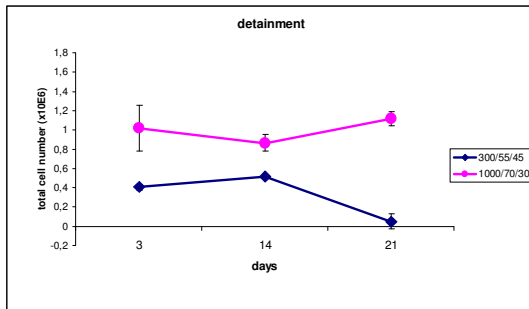
300/55/45



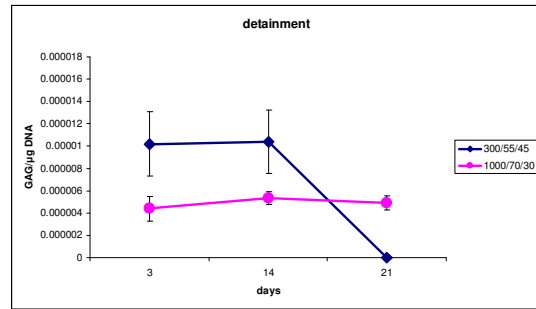
1000/70/30

Figure 2: Attachment: Cells are attached onto the fibers. **(C)** Magnification 10x. **(D)** Magnification 20x (insert 4x).

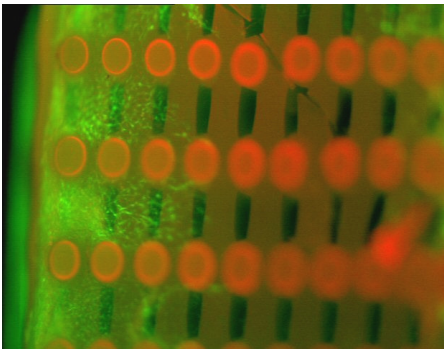
A. Total DNA after 3, 14 and 21 days



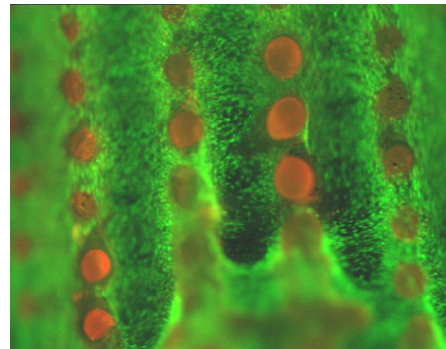
B. GAG/DNA content after 3, 14 and 21 days



C. Cell viability after 14 days

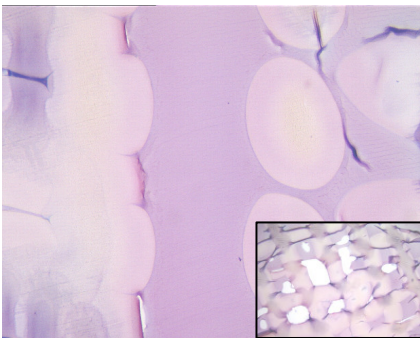


300/55/45

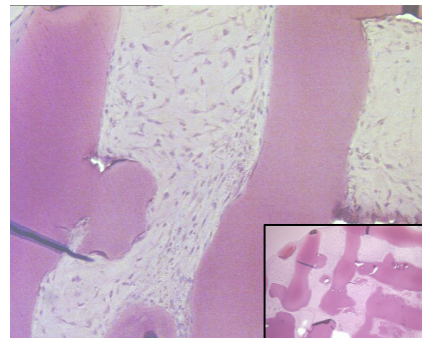


1000/70/30

D. Safranin O staining after 21 days *in vitro*



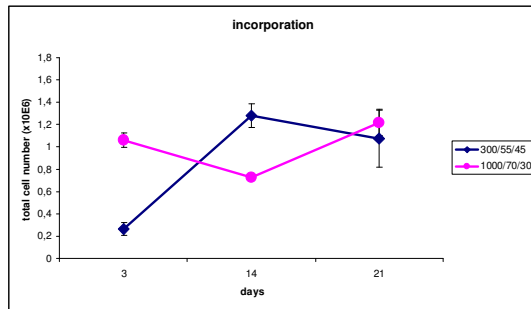
300/55/45



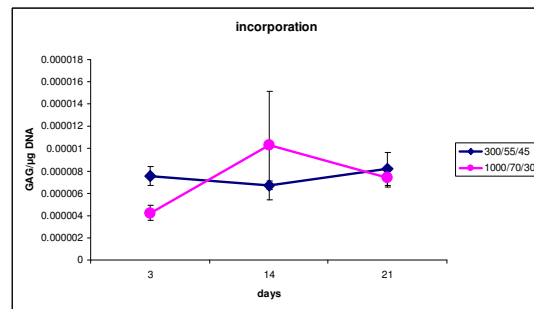
1000/70/30

Figure 3: Detainment: Cells are attached onto the fibers followed by detainment with a gel. **(C)** Magnification 10x. **(D)** Magnification 20x (insert 4x).

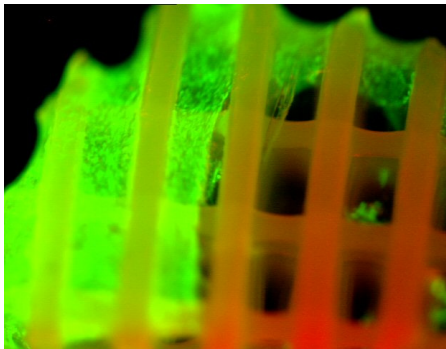
A. Total DNA after 3, 14 and 21 days



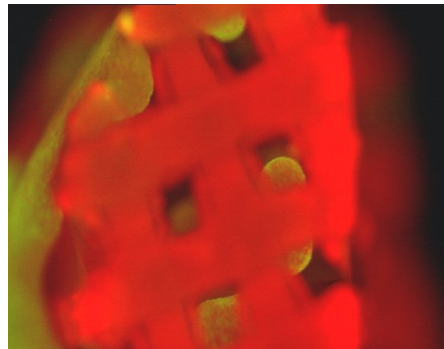
B. GAG/DNA content after 3, 14 and 21 days



C. Cell viability after 14 days

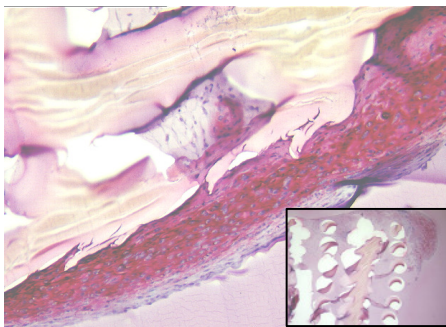


300/55/45

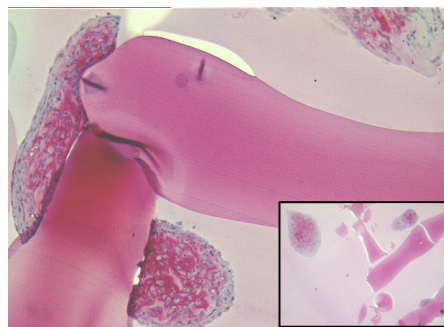


1000/70/30

D. Safranin O staining after 21 days *in vitro*



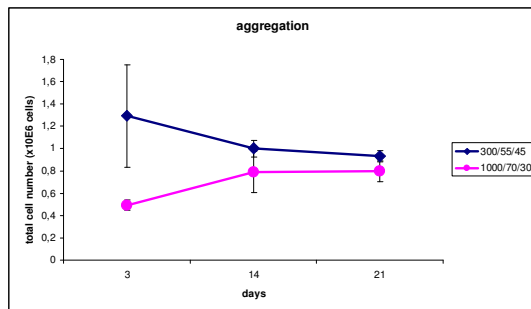
300/55/45



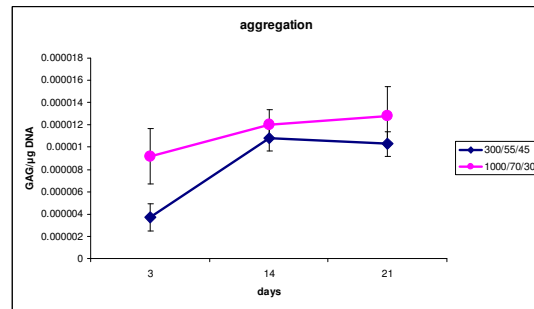
1000/70/30

Figure 4: Incorporation: Cells are incorporated into a gel prior to the seeding. **(C)** Magnification 10x. **(D)** Magnification 20x (insert 4x).

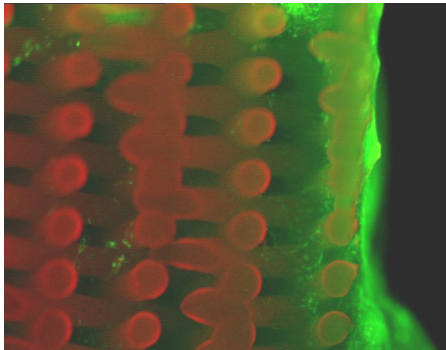
A. Total DNA after 3, 14 and 21 days



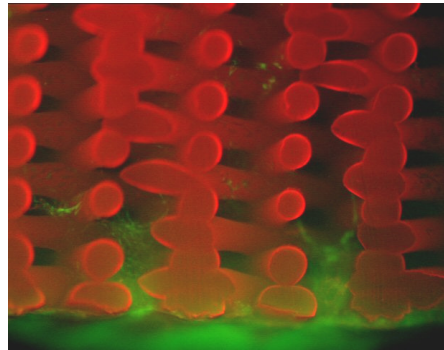
B. GAG/DNA content after 3, 14 and 21



C. Cell viability after 14 days

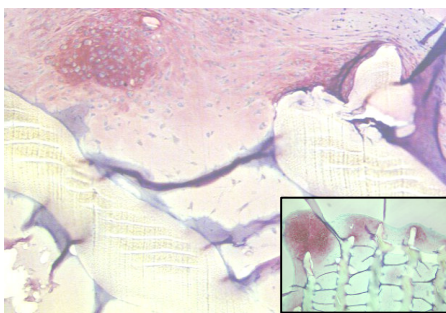


300/55/45

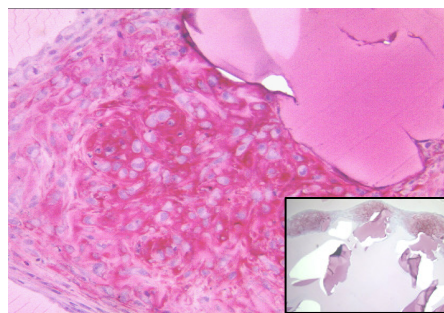


1000/70/30

D. Safranin O staining after 21 days *in vitro*



300/55/45



1000/70/30

Figure 5: Aggregation: Cells are aggregated prior to the seeding and subsequently detained by a gel throughout the fibers. **(C)** Magnification 10x. **(D)** Magnification 20x (insert 4x).

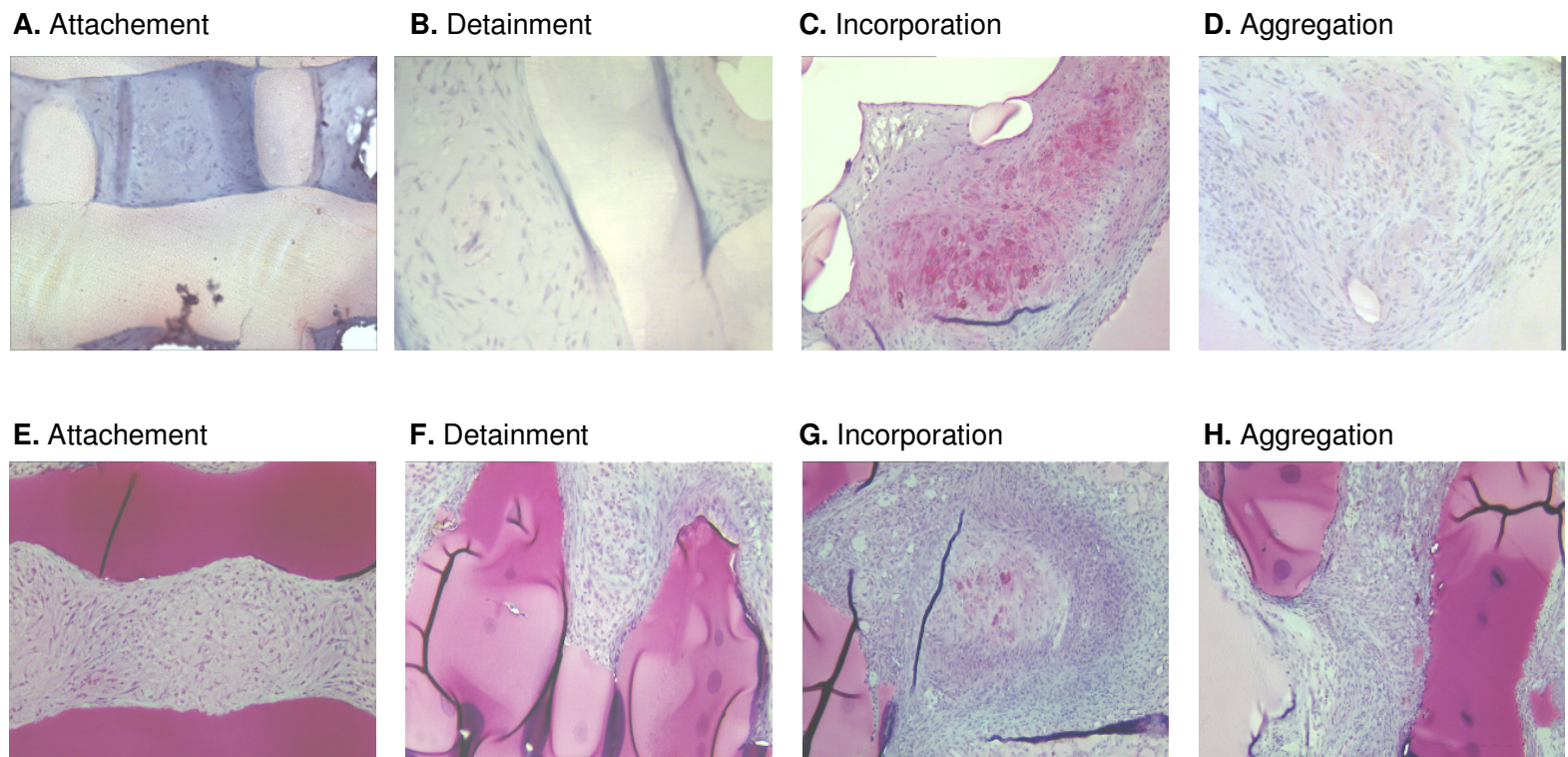


Figure 6. Safranin O staining after 21 days *in vivo* using different seeding methods on two types of scaffolds. 300/55/45 (A - D), 1000/70/30 (E - H). Magnification 20x.

Table 1: Overview of total efficiency of the four seeding methods for PEOT/PBT 300/55/45 and 1000/70/30 regarding seeding efficiency, cell distribution, cell morphology, cell differentiation and stability of newly formed cartilage.

	seeding efficiency ¹	cell distribution ²	cell morphology ³	Safranin O staining ⁴	stability <i>in vivo</i> ⁵	total
300/55/45						
attachment	0	2	0	0	0	2
detainment	0	0	0	0	0	0
incorporation	0	0	2	2	2	6
aggregation	2	0	2	2	1	7
1000/70/30						
attachment	0	2	0	0	0	2
detainment	1	2	0	0	0	3
incorporation	1	1	2	2	2	8
aggregation	0	0	2	2	1	5

¹ 0 low

1 good

2 high

² 0 not homogeneously

1 homogeneously as aggregates

2 homogeneously

³ 0 elongated, fibroblast like

2 round, chondrocyte like

⁴ 0 not positive

1 weak positive

2 strong positive

⁵ 0 no cartilage found

1 cartilage found on few spots

2 cartilage filling the entire scaffold

Discussion

The majority of studies showing successful seeding of mesenchymal stem cells (MSCs) into supportive structures handle scaffolds limited to a thickness of $\leq 2\text{mm}$ [42, 51, 53, 55, 59, 135, 147]. However, clinically relevant dimensions (thickness of $> 2\text{mm}$) are challenging regarding cell seeding efficiency, homogeneous cell distribution, and chondrogenic differentiation. This study shows how critical it is to develop standardized and optimized protocols for efficient seeding and chondrogenic differentiation of MSCs to be applied in cartilage tissue engineering (TE). To be successful, at least two important parameters need to be taken into consideration: the scaffold material and the seeding method.

The chondrogenic differentiation medium for MSCs is chemically defined, no serum is used [115]. As a result, the medium lacks factors mediating cell attachment and cell proliferation. Under these serum-free conditions the challenge for tissue engineers, besides the homogeneous distribution, is the maintenance of the cells in the scaffolds; in particular delicate in highly porous materials such as three-dimensional fiber-deposited scaffolds preferable used in cartilage TE [68, 132, 148].

PEOT/PBT copolymers have been applied to a wide range of tissue engineered structures. Here, we studied the effect of different polymer compositions (hydrophilic 1000/70/30 vs. hydrophobic 300/55/45) on seeding efficiency and chondrogenic differentiation of MSCs. It is known that anchorage-dependent cells prefer to attach on more hydrophobic surfaces [149, 150]. However, there are studies demonstrating different adhesion behavior on hydrophobic 300/55/45 and hydrophilic 1000/70/30. Whereas skeletal muscle cells showed significantly higher cell adhesion on 300/55/45 [69], hepatocytes prefer to attach on hydrophilic surfaces as demonstrated by de Bartolo *et al.* [151].

In our study, we could not observe a significant influence of chemical characteristic on seeding efficiency of MSCs. These findings are in consistency with others [136] and similar to results from studies, where chondrocytes were attached to 300/55/45 and 1000/70/30, respectively [69, 132], suggesting comparable cell-biomaterial interactions. Cells demonstrated a spread, flat morphology on 300/55/45 compositions, in contrast, the round, polygonal shape on 1000/70/30 [131]. Studies have suggested that this round morphology improves chondrocyte re-differentiation and decreases chondrocyte de-differentiation [133, 152]. The influence of polymer compositions on chondrogenic differentiation of MSCs was expected to be similar since MSCs undergo analogous morphological changes during chondrogenic differentiation as re-differentiating chondrocytes [77]. However, our results did not show a significant effect. Neither on 300/55/45 nor on 1000/70/30 cells showed morphological changes. The cells were spread and well attached to the fibers, and no chondrogenic differentiation could be observed by histology or biochemical analysis. Next to attachment, we studied detainment as a method to improve cell seeding efficiency and to support chondrogenesis. Although we were able to increase the seeding efficiency, differentiation was not enhanced. In conclusion, while attachment and detainment are efficient methods to load MSCs into three-dimensional fiber-deposited scaffolds, these methods are not applied to support chondrogenic differentiation.

To accomplish tissue engineered cartilage using MSCs, a different strategy is to integrate the cells into a gel. The advantageous application of a gel has been previously demonstrated by Williams *et al.* [143]. Next to gel incorporation, aggregation of single cells prior to integration is another approach. It is known for embryonic stem cells that aggregation through embryonic body formation is essential for cell survival but also beneficial for chondrogenic differentiation [153]. Furthermore, the publication by

Hendriks *et al.* shows the advantageous effect of fibronectin-mediated aggregation of chondrocytes indicated by significantly higher seeding efficiency and proteoglycan production [133].

We hypothesized that by gel incorporation or aggregation cells are hindered to attach and spread onto the scaffold fibers, and therefore preferably undergo chondrogenesis. Our results show that after 14 days cartilaginous tissue could be detected within the constructs for both methods. Cells showed a round morphology, were located in lacunae and surrounded by a proteoglycan-rich matrix. Surprisingly, we could not detect significant differences in the quality and quantity of cartilage-like tissue when both scaffold compositions were compared. But, the intensity of labor during the cell loading procedure was much higher for the hydrophobic scaffold. In our experimental set up, the gel remained at the surface of the hydrophobic copolymer. Time-consuming soaking and turning of the scaffold resulted in extensive cell loss prior to the actual cell loading. In contrast, the loading of cells into hydrophilic scaffolds was straightforward and not that laborious. This explains the high cell numbers incorporated into the hydrophilic 1000/70/30 scaffolds. Solchaga *et al.* reported that, when an alginate gel on hydrophobic polymer sponges was applied, the addition of vacuum was required to obtain a homogeneous cell distribution throughout the 3 to 5mm thick scaffolds [142].

The findings illustrate the importance of selection of appropriate scaffold materials in combination with a hydrogel and should not be underestimated.

Since we have successfully generated cartilage *in vitro*, we wanted to test its stability in an *in vivo* environment. We implanted *in vitro* tissue engineered constructs subcutaneously in the back of nude mice. For scaffolds loaded by incorporation and aggregation, the presence of GAGs was confirmed prior to the implantation. However, after one week *in vivo* Safranin O staining of the implants was negative. These results suggest the inability of *in vitro* generated cartilage to be stable in a non-cartilaginous environment, and question the subcutaneous implantation of MSC-derived tissue engineered cartilage as a prediction of its faith when implanted into a cartilage defect. The data are supported by previous studies. De Bari *et al.* found that differentiated MSCs with a stable chondrogenic phenotype did not preserve differentiation stage *in vivo*. Micro mass cultures staining strongly positive for Safranin O did not reveal cartilage-specific markers after subcutaneous implantation. Furthermore, when implanted intramuscularly, cells expressed myogenic markers. Another study by Pelttari *et al.* describes calcification of extracellular matrix of engineered cartilage and vascular invasion after ectopic implantation into SCID mice [127]. Although we explanted already after one week and did not perform histology specifying calcified tissue, we cannot exclude its presence.

In conclusion, the results of this study show that cartilage tissue engineering using mesenchymal stem cells is not dependent on an initial high cell density or the chemical composition of the scaffold material. The outcome clearly shows that it is the manner, how cells are seeded into the scaffold. Preferable, they should not attach and spread on the material.

Chapter 2

Tailored release of TGF β 1 from porous scaffolds for cartilage tissue engineering

Abstract

In view of cartilage tissue engineering, the possibility to prepare porous scaffolds releasing transforming growth factor β 1 (TGF β 1) in a well controlled fashion was investigated by means of an emulsion-coating method. Poly(ether ester) multiblock copolymers were used to prepare emulsions containing TGF β 1 which were subsequently applied onto prefabricated scaffolds. This approach resulted in defined porous structures (66%) with interconnected porosity, suitable to allow tissue ingrowth. The scaffolds were effectively associated with TGF β 1 and allowed to tailor precisely the release of the growth factor from 12 to more than 50 days by varying the copolymer composition of the coating. An incomplete release was measured by elisa, possibly linked to the rapid concentration decrease of the protein in solution. The released growth factor retained its biological activity as was assessed by a cell proliferation assay and by the ability of the released protein to induce chondrogenic differentiation of bone marrow-derived mesenchymal stem cells. However, exact bioactivity quantification was rendered difficult by the protein concentration decrease during storage. Therefore, this study confirms the interest of poly(ether ester) multiblock copolymers for controlled release of growth factors, and indicates that emulsion coated scaffolds are promising candidates for cartilage tissue engineering applications requiring precise TGF β 1 release rates.

Introduction

In tissue engineering approaches, the possibility to create new tissues or functional organs usually requires the use of three-dimensional scaffolds as guide and support structures [154]. In addition to the classical requirement such as high porosity and inter-pore connection, specific mechanical properties and degradation rates [48, 155], the scaffolds should have the potency to support, enhance or even induce the growth and differentiation of cells or tissue towards the desired lineage. To do so, porous scaffolds could act as a release matrix for bioactive molecules such as growth and differentiation factors or cytokines. Different molecules can be considered that showed their interest for cartilage and bone applications (insulin-like growth factor 1 and 2, basic fibroblast growth factor, transforming growth factors, and bone morphogenetic proteins) [156, 157].

Promising data were previously reported showing the relevance of local release of various growth factors from scaffolds for bone, cartilage, and angiogenesis [158-161]. However, the well-timed delivery and suitable dosing of the compounds appears to be of high importance to achieve an optimal tissue induction while avoiding adversary or inhibitory effects [162-167]. Therefore, methods must be investigated to achieve a precise control of the release kinetics of selected compounds from porous scaffolds.

Transforming growth factor β 1 (TGF β 1) is a pleiotropic growth factor which has regulatory effects on many different cell types. For instance, it plays an important role in cell proliferation and differentiation, bone formation [168-170], angiogenesis [171, 172], neuroprotection [173] and wound repair [174-176]. It controls the production of extracellular matrices by stimulating the synthesis of collagens, fibronectin and proteoglycans [177, 178]. It also appeared to have positive effects on cartilage differentiation and repair [147, 179-181]. Nevertheless, this multi-potency induces drawbacks linked to the dependency of the tissue responses towards its dose and length of exposure. For instance, a long exposure of high doses of TGF β 1 results in fibrosis and hypertrophic scars [182], while a too high dosage in cartilaginous sites results in osteophytes formation [180]. Therefore, the ability to release TGF β 1 in a controlled fashion is of high importance to use this protein in the most optimal way for cartilage applications. Hence, the opportunity to create scaffolds allowing a wide range of TGF β 1 release periods (from days to months) was here investigated.

A potential approach to create TGF β 1 releasing scaffolds is based on the coating of prefabricated porous polymeric scaffolds with protein-containing emulsions. This method has been successfully applied to control the release of a model protein (lysozyme) [183]. Nevertheless, lysozyme is a relatively stable molecule while TGF β 1 is extremely labile. Therefore, in addition to the ability of the method to produce scaffolds with broad release rates, the activity of the released TGF β 1 was investigated. Poly(ether ester) multiblock hydrogel copolymers were selected as matrix for prefabricated scaffolds and emulsions. These biodegradable hydrogels, based on poly(ethylene oxide)-terephthalate and polybutylene terephthalate (PEOT/PBT), and poly(ethylene oxide)-succinate and polybutylene succinate (PEG(T/S)PB(T/S)), are successfully used as protein release system as they allow to tailor release rates easily by varying the copolymer composition [184, 185]. It was demonstrated that the protein release was controlled by a combination of diffusion and degradation of the polymeric matrix [71, 186].

The resulting scaffolds were evaluated with regard to their structure, TGF β 1 release ability, stability of the released protein, and their potential interest for cartilage tissue engineering.

Materials

Polyethylene oxide terephthalate/polybutylene terephthalate (PEOT/PBT) and polyethylene glycol succinate/polybutylene succinate) (PEGS/PBS) multiblock copolymers were obtained from OctoPlus, Leiden, The Netherlands, and were used as received. Polymers are indicated as **a**PEOT**b**PBT**c** or **a**PEG(T/S)**b**PB(T/S)**c** (**d**/**e**S) in which **a** is the PEO molecular weight, **b** the weight percentage (weight%) of PEOT or the combined weight% of PEOT and PEGS, and **c** (=100-**b**) the weight% of PBT or the combined weight% of PBT and PBS. **d/e** is the molar T/S ratio in the copolymer. Vitamin B₁₂, bovine serum albumin (BSA), dimethyl sulfoxide (DMSO), L-ascorbic acid-2-phosphate, proline, insulin-transferrin-selenium (ITS+1), and dexamethasone were purchased from Sigma Chem. corp. (St. Louis, USA). Recombinant human transforming growth factor beta1 (rhTGF β1 later referred as TGF β1) and enzyme-linked immunosorbent Assay (ELISA) kit were purchased from R&D Systems Inc. (Minneapolis, USA). Dulbecco and alpha modified eagle medium (DMEM and α-MEM), pyruvate, L-glutamine, penicillin and streptomycin were obtained from Gibco (Invitrogen, Carlsbad, USA). Roswell park memorial institute medium (RPMI 1640) and foetal bovine serum (FBS) were purchased from Cambrex (East Rutherford, USA). Glycol methacrylate embedding solutions (GMA) were purchased from Technovit (Heraeus Kulzer, Germany). Beta-fibroblast growth factor (bFGF) was obtained from VWR international (Roden, The Netherlands). Chloroform, obtained from Fluka chemica (Buchs, Switzerland), was of analytical grade.

Methods

Preparation of TGF β1-loaded polymeric scaffolds

Emulsion

The protein was associated to the porous scaffolds by means of a water-in-oil (w/o) emulsion method. An aqueous solution of TGF β1 in a 4 mM HCL solution (with 1 mg/ml BSA, according to the supplier's protocol) was emulsified with a PEOT/PBT or PEG(T/S)PB(T/S) copolymer solution in chloroform, using an Ultra-Turrax (T25 Janke & Kunkel, IKA-Labortechnik) for 30 s at 19 krpm. The TGF β1 concentration of the aqueous solution was set at 1 μg/ml for release and bioactivity experiments, and 20 μg/ml for cell culture and *in vivo* experiments. The volume of the aqueous phase was set to 1 ml per gram of copolymer (water/polymer ratio = 1 ml/g). The copolymer solution was obtained by dissolving 0.5 gram of copolymer in 3 ml of chloroform. Three PEOT/PBT and two PEG(T/S)PB(T/S) copolymer compositions were used in which the PEOT content was of 70 or 80 weight%, the PEG MW of 600, 1000 or 2000 g/mol, and the T/S molar ratio varied between 0 and 100%.

Emulsion coating method

The emulsion coated scaffolds were obtained as described elsewhere [183]. Briefly, compression molded/salt leached scaffolds were obtained by applying pressure (10000 PSI during 10 minutes) and heat (240 °C) to a homogeneous mix of NaCl salt crystals and copolymer powder in a mold. The volume fraction of salt in the mixture was adjusted to 75%. After cooling of the resultant dense block, the salt was extracted by successive immersions in RX-water (water conductivity less than 25 μS). Subsequently, the porous blocks were dried in ambient air for at least 24hrs, and then placed in a vacuum oven (50 °C) for a minimum of 12hrs. The PEOT/PBT copolymer used to prepare the scaffold had

a PEOT content of 55 weight% and a PEG molecular weight of 300 g/mol. The salt crystals were sieved between 400 and 600 μm .

Coated scaffolds were prepared by forcing a TGF β 1 containing emulsion through a prefabricated porous scaffold with the use of vacuum (300 mBars) [183]. This vacuum was applied for at least 5 minutes, in order to evaporate chloroform as much as possible from the emulsion, thereby creating a polymeric coating on the scaffold. The resulting coated scaffolds were frozen in liquid nitrogen and freeze-dried at room temperature for 24hrs.

Blank scaffolds were prepared by using a TGF β 1-free 4 mM HCL solution (with 1 mg/ml BSA) in the same conditions as TGF β 1 containing scaffolds.

Scanning Electron Microscopy

A Philips XL 30 ESEM-FEG was used to evaluate the internal morphology of the scaffolds. The internal porous structure was observed by cutting the scaffolds in the longitudinal axis with a razor blade. All samples were gold sputter-coated using a Cressington 108 auto apparatus before analysis.

Characterization of scaffold porosity

The average porosity (%) of the scaffolds was evaluated from their dry weight, dry volume and density of the PEOT/PBT copolymer (density = 1.2 g/ml) according to the following equation:

$$p = 1 - \frac{\text{sample weight}}{\text{sample volume} \times 1.2} \quad (1)$$

Three scaffold pieces were used to determine the porosity of a specific emulsion coated scaffold.

The scaffold pore interconnection before and after coating treatment was quantified using a method that applies Darcy's law, as described elsewhere [183, 187-189]. In brief, water is forced through the porous samples by applying a constant pressure and the flow rate is measured, from which the sample permeability (κ , μm^2) can be calculated. This parameter reflects the sample porosity and pore interconnection and can therefore be used to compare different scaffolds.

In vitro protein release

TGF β 1 loaded scaffolds (around 100 mg) were incubated in 1 ml RPMI 1640 medium at 37 $^{\circ}\text{C}$ in polypropylene tubes. All samples were kept under constant agitation (25 rpm). The release medium was entirely refreshed at various time points, immediately frozen in liquid nitrogen and conserved at -20 $^{\circ}\text{C}$ until quantification. TGF β 1 concentrations were quantified using an ELISA kit obtained from R&D Systems (Quantikine human TGF β 1 immunoassay). The TGF β 1 used for the standards and the preparation of the releasing scaffolds originated from the same batch. Aliquots of different volumes were frozen in liquid nitrogen immediately after reconstituting the protein solution and stored at -20 $^{\circ}\text{C}$. They were thawed immediately prior to use for scaffold preparation or as standards.

To determine the quantity of emulsion effectively coated on the porous scaffold and establish the amount of protein present, coated scaffolds were prepared in the same conditions using polymer emulsions containing 10 mg of vitamin B₁₂ per gram of polymer, for each copolymer composition used. The size of this molecule allows a complete release within three days when entrapped in the copolymers used in this study. The quantity of vitamin released is correlated to the amount of polymer coated onto a given scaffold, as the vitamin is homogeneously distributed through the emulsion. The amount

of polymer coated can then be related to the amount of protein associated with the scaffold. This indirect detection method was proven to be accurate for other proteins [183]. The amount of vitamin released was calculated using a standard curve of vitamin B₁₂ in phosphate buffered saline and a spectrophotometer (EI 312e, BioTek instruments) at 380 nm.

TGF β1 stability in solution

The stability of TGF β1 in the release or culture medium was assessed by measuring the protein concentration with ELISA as a function of time (from 20 minutes to 6 days). For absolute concentration decrease, fresh TGF β1 was added at a concentration of 5 and 10ng/ml to the release or culture medium (1 ml) containing unloaded scaffolds (1000PEG(T/S)70PB(T/S)30 (0T/100S)) and 2000PEOT80PBT20. At each time interval, the medium was collected in triplicate and assayed for concentration. The unloaded scaffolds were then discarded.

TGF β1 bioactivity assay

The activity of released TGF β1 was determined using a modified cell growth inhibition assay based on Mv 1 Lu mink lung fibroblast (ATCC# CCL64) [190]. CCL64 cells were cultured in DMEM, supplemented with 10 volume% FBS, 100 UI/ml penicillin and 100µg/ml streptomycin. The cells were always kept sub-confluent. For the growth inhibition assay, CCL64 cells were seeded at a density of 1 x 10⁴ cells/well in 48-well plates and subsequently let to attach for 3hrs at 37°C in a 5% CO₂ humidified atmosphere. The cell culture was performed with 1ml of RPMI 1640, supplemented with 10% v/v FBS, 100 UI/ml penicillin and 100µg/ml streptomycin. After 3hrs, releasing scaffolds (100 mg) or standards of known TGF β1 concentration were added in single or multiple boluses to the wells containing cells, in duplicate on the same plate. A schematic drawing of the different conditions assayed is presented in Fig. 1.

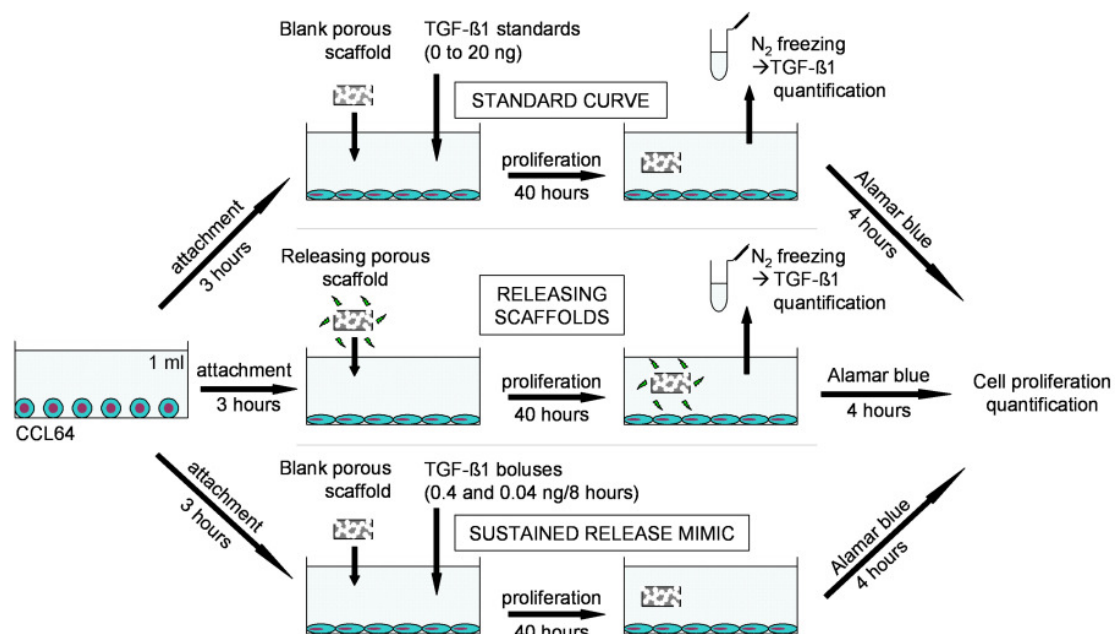


Figure 1: Schematic representation of the different conditions used to evaluate the bioactivity of the released TGF β1 in a CCL64 growth inhibition assay.

Each culture well contained porous scaffolds (100 mg) of similar coating composition for a given plate, either loaded with TGF β 1 (releasing) or unloaded. The plates were then incubated for 40hrs and the relative amount of cells was evaluated using an alamar blue assay (200 μ l added per well and incubated for 4hrs prior reading). The linearity of the alamar blue response towards cell number was assessed for the range of the bioassay, by incubating cell dilutions from 0 to 0.8×10^6 cells/well over 40hrs. Each assay was performed with a standard curve of fresh TGF β 1 comprised between 0 and 20ng/ml. The activity of the protein was defined as the ratio between concentrations obtained from the standards and concentration released from the scaffolds. The same batch of TGF β 1 was used for the standards and the preparation of the releasing scaffolds. Aliquots of different volumes were frozen in liquid nitrogen immediately after reconstituting the protein solution and stored at -20°C . They were thawed immediately prior to use for scaffold preparation or as standards.

Goat mesenchymal stem cell pellet culture

The animal experiments were approved by a local Ethics Committee. Goat mesenchymal stem cells (MSCs) were harvested from the iliac crest of 4 years old female Dutch milk goats under general inhalation anaesthesia. The bone marrow aspirate was collected in heparin tubes. The nucleated cells were plated at a density of 0.5×10^6 cells/cm² in α -MEM, supplemented with 12% FBS, 100 UI/ml penicillin, 100 μ g/ml streptomycin, 0.1 mM L-ascorbic acid-2-phosphate, 1ng/ml bFGF and 2mM L-glutamine. The medium was refreshed first after 3 days and then twice a week until confluency (8 to 10 days). Cells were passaged with 0.05% trypsin to obtain the primary cells, and replated at 5000 cells/cm². Passage 1 cells were cryopreserved in 50% supplemented α -MEM, 40% FBS, 10% DMSO. When needed, cells were thawed, plated and grown until confluent in α -MEM, supplemented with 15% FBS, 100 UI/ml penicillin, 100 μ g/ml streptomycin, 0.1 mM L-ascorbic acid-2-phosphate, and 2mM L-glutamine (expansion medium).

Passage 3 cells were used to prepare the pellets. After trypsinization, 0.5×10^6 cells were spun down at 500 g for 2 minutes in 10 ml polystyrene conical tubes. The expansion medium was then replaced by serum-free medium consisting of 1ml of DMEM with 100UI/ml penicillin, 100 μ g/ml streptomycin, 100 μ g/ml pyruvate, 40 μ g/ml proline, 50 μ g/ml L-ascorbic acid-2-phosphate, 1% ITS+1 and 100nM dexamethasone.

One TGF β 1 loaded or blank scaffold (100mg) was added to the culture tube, directly in the medium. The culture tubes containing pelleted cells were incubated at 37°C , in a 5% CO₂ humidified atmosphere. Three pellets were cultured for each scaffold condition. After 24hrs of incubation, the cells formed round aggregate, not adhering to the tube walls. Medium changes were carried out every 3 days.

Pellets (n=3) were harvested after 15 and 21 days and fixed overnight in 0.14M cacodylate buffer (pH=7.2–7.4) containing 0.25% glutaraldehyde (Merck, Darmstadt, Germany). They were subsequently dehydrated in a graded ethanol series and embedded in GMA. 5 μ m thick cross-sections were made by using a Microm microtome (HM 355 S). The sections were stained with hematoxylin (Sigma) and fast green (Merck) for cells and with Safranin O (Sigma) for glycosaminoglycans (GAGs).

Results and discussion

1. Scaffold characterization

In view of cartilage tissue engineering applications, the possibility to prepare porous polymeric scaffolds containing and releasing TGF β 1 was here investigated. An emulsion-coating method [191] was used for this purpose with the objective to obtain a wide range of release profiles (from days to months) without TGF β 1 loss of activity.

The morphology of the emulsion coated scaffolds, as evaluated by Scanning Electron Microscopy (SEM), is presented in Fig. 2. The pores size was ranging from 100 to 650 μ m while the pores appeared visually interconnected. The porosity of the scaffolds was decreased by the coating application from 77% to $66 \pm 3\%$. As was previously reported for emulsion coated scaffolds, the coated layers partly filled the pores and consequently decreased porosity [183]. In parallel, the permeability of the scaffolds toward water was modified by the coatings. κ increased from 18 to 82 μ m² after coating application. Increasing κ values indicate a higher inter-pore connection of the scaffolds [189]. As can be visually assessed by comparing the scaffolds before and after coating (Fig. 2A and B respectively), the increase of permeability is due to the dissolution of the thin polymeric membranes present between pores of the prefabricated compression molded-salt leached scaffolds by the applied emulsion.

The scaffolds porosity and pore interconnection are suitable to allow tissue ingrowth and integration as was shown by a preliminary *in vivo* study, performed with similar scaffolds implanted in rabbit knee osteochondral defects [192]. After three weeks of implantation, the scaffolds were filled with a tissue consisting of undifferentiated mesenchymal cells, histiocytotic cells and new bone. The pore interconnection was sufficient to allow progenitor cells present in the bone marrow to reach the cartilage zone.

The effectiveness of the coating process during the application of the emulsion was evaluated. About half of the emulsion prepared was effectively coated on the porous scaffolds ($49 \pm 1\%$).

2. Protein release kinetics

The ability of the coated porous scaffolds was first determined for copolymers of fixed PEOT weight percentage (80 wt-%) and of varying PEG segment length. As presented in Fig. 3, the PEG molecular weight (MW) of the coated copolymer appeared of high influence on the growth factor release rate. A MW of 600g/mol resulted in a very slow

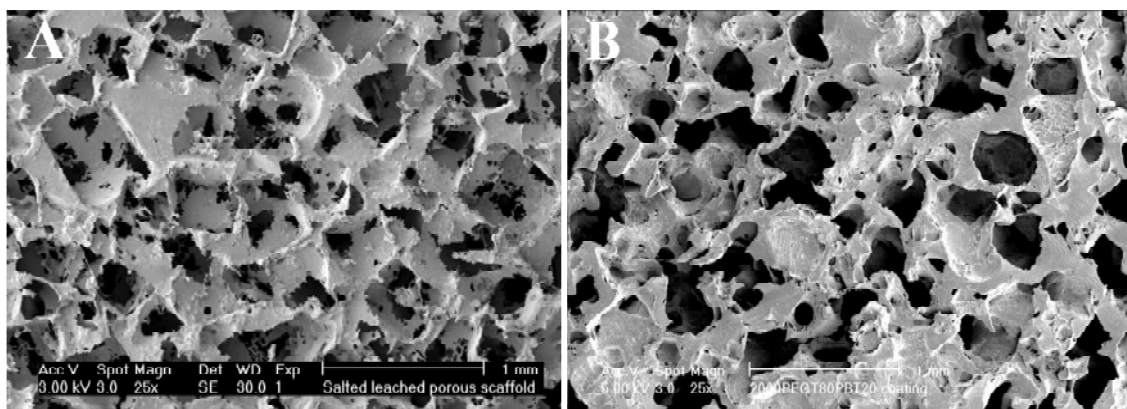


Figure 2: Cross sections of a porous scaffold obtained before (A) and after application of a TGF β 1 containing emulsion (B), examined by scanning electron microscopy. Scale bar 1mm.

release after a small burst, while a MW of 1000 showed a first order release completed within 10 to 20 days. Interestingly, further increase of the MW from 1000 to 2000 resulted only in a slightly faster release. The modulation of proteins release rates by varying the PEOT/PBT copolymers composition is a well described phenomenon [74, 183, 184, 193, 194]. Increasing values of PEG MW are related to an increase of matrix degradation rate, higher swelling and subsequent larger hydrogel mesh size, resulting in a faster diffusion of the incorporated proteins through the polymeric matrix [195]. The important difference in release rate obtained by a small variation of the PEG MW (from 600 to 1000) suggests that a threshold of hydrogel mesh size has been reached for the 600 PEG MW composition, below which the protein cannot diffuse through the coated copolymer. To fine tune the release, the copolymer composition could be further adjusted with regard to the PEOT weight percentage (wt-%), which has a similar effect on the hydrogel mesh size as the PEG MW [195]. To investigate this possibility, scaffolds were prepared with a 1000PEOT70PBT30 coating. In addition, varying the degradation behavior of the copolymers could allow further fine-tuning of the release. Therefore, coated scaffolds succinated copolymers are based on the same degradation and diffusion mechanism [186]. The substitution of aromatic groups (terephthalate) by aliphatic moieties (succinate) results in higher swelling of the copolymer and higher degradation rates of the copolymer due to the higher accessibility of the ester bond for hydrolysis. As a consequence, the protein diffusion coefficients are increased by the degree of substitution [185]. As presented in Fig. 4, the use of 1000PEOT70PBT30 or PEG(T/S)PB(T/S) copolymers resulted indeed in intermediate release profiles.

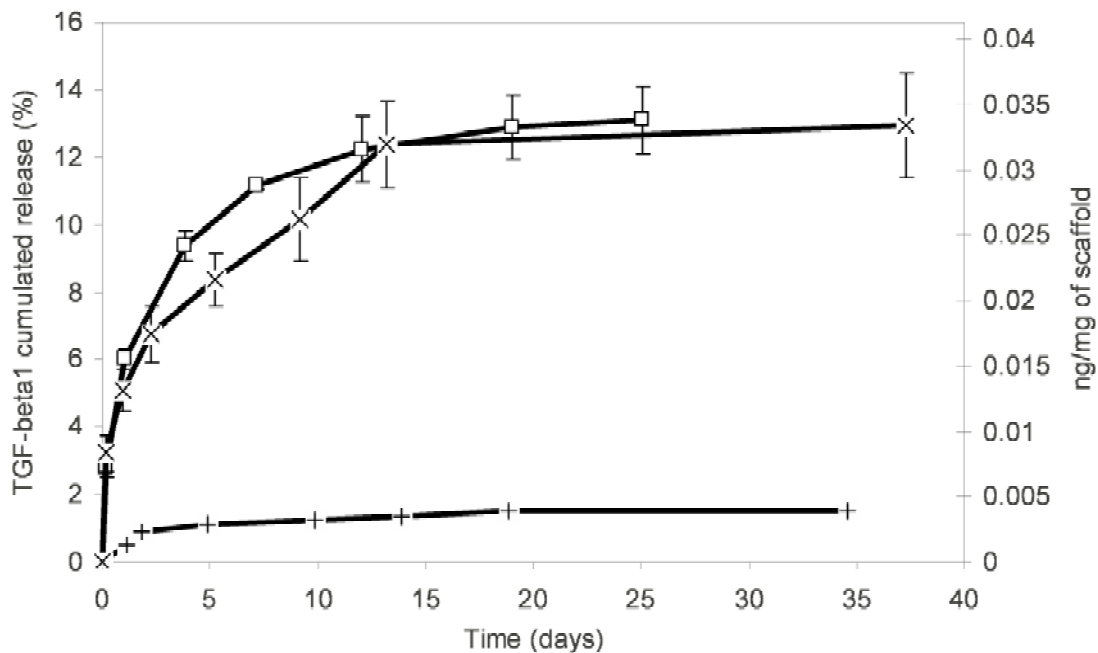


Figure 3: Cumulated release of TGF β 1 from porous polymeric scaffolds coated with water-in-oil emulsions of different copolymeric compositions: 2000PEOT80PBT20 (\square), 1000PEOT80PBT20 (\times), 1000PEOT70PBT30 (\circ) and 600PEOT80PBT20 (+). ($n=3 \pm$ s.d.).

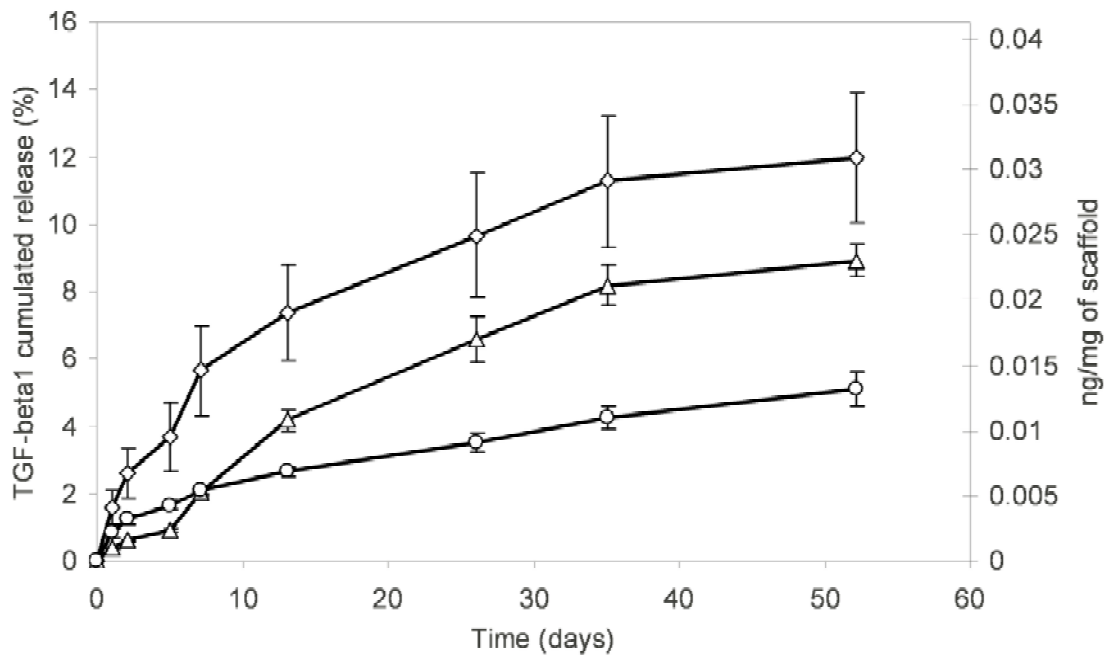


Figure 4: Cumulated release of TGF β 1 from porous polymeric scaffolds coated with water-in-oil emulsions of different copolymeric compositions: 1000PEG(0T/100S)70PB(0T/100S) (\diamond), 1000PEG(50T/50S)70PB(50T/50S) (\triangle) and 1000PEOT70PBT30 (\circ). (n=3 \pm s.d.).

A 1000PEOT70PBT30 coated copolymer showed a zero order release still on going after 50 days, while 1000PEG(T/S)70PB(T/S)30 (50T/50S) and 1000PEG(T/S)70PB(T/S)30 (0T/100S) copolymers presented a release completed within 40 days. The effect of the PEOT wt-% on the release rate was clear as a 10 wt-% decrease of PEOT (from 1000PEOT80PBT20 to 1000PEOT70PBT30) resulted in an important decrease of the protein release rate. The substitution of terephthalate groups by succinate groups increased the release rate of TGF β 1 from the coated scaffolds, as expected.

Noticeably, the total amount of TGF β 1 released (as measured by ELISA) never exceeded 14% of the total amount entrapped in the scaffolds (24ng). This low recovery during release is surprising and could be due to an extensive denaturation of the protein by the coating process or during the release period. Nevertheless, previous release experiments using the emulsion coating method and a model protein (lysozyme) indicated no degradation of the protein during either scaffolds preparation or release [191]. This discrepancy could be linked to the intrinsic stability of TGF β 1 in solution. The half-life of TGF β 1 *in vivo* is less than 30 minutes [171, 182] when in its active form. In addition, due to its high hydrophobicity, TGF β 1 tends to adsorb quickly to plastic surface, reducing so the concentration of the protein in solution [190]. To assess the effective degradation of the protein in our release experiment condition, the concentration decrease of two TGF β 1 standards was measured over time. As can be seen in Fig. 5, the amount of TGF β 1 left in the release medium was decreasing rapidly to reach a stable value close to 2.5% after 12hrs. Within 20 minutes, 60% of the protein amount could not be measured anymore in the solution. This fast decrease of concentration contributes to the low recovery obtained from the releasing scaffolds, as the amount of protein measured by ELISA at each medium refreshment corresponds to a small fraction of the amount effectively released.

The rapid protein depletion renders the release measurement less accurate and hampers the determination of the release completeness. However, the release profile can still be considered to be valid as the protein concentration decrease reached a plateau in 12hrs and as each sampling time was separated by more than 24hrs.

To determine if the growth factor depletion is linked to adsorption phenomena (as the release medium does not contain proteins), the release of TGF β 1 from 1000PEOT80PBT20 coated scaffolds was measured in a release medium, supplemented with BSA (1mg/ml). The resulting release profiles were not significantly different in the presence of BSA (data not shown) suggesting that the protein disappearance cannot be entirely related to adsorption. Additionally, the freezing and thawing of the samples prior to quantification could have played a role in the protein depletion. However, the TGF β 1 concentrations of release samples measured after one and two cycles of freezing and thawing were similar.

In summary, the release rate and profile of TGF β 1 from porous scaffolds could be effectively tailored by the copolymer composition of the coating. The release of the growth factor was varied from 10 to more than 50 days. The incomplete release detected for all coating composition is most likely caused by the intrinsic instability of the protein in solution. Besides the completeness of the release, the activity of the released protein is an important factor in view of cartilage application. Therefore, the activity of the released protein was evaluated.

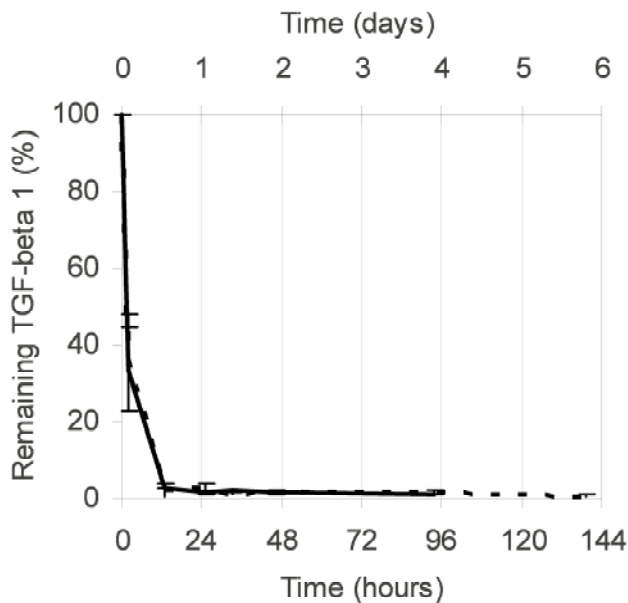


Figure 5: Concentration decrease of TGF β 1 in release medium. Two different concentrations were supplemented as a bolus: 5ng/ml (full line) and 10ng/ml (dotted line). (n=3 \pm s.d.).

3. Activity of released TGF β 1

To confirm that the released protein is not denatured by the emulsion-coating method, the activity of the released protein was measured in a cell growth inhibition assay based on CCL64 cells. A schematic drawing of the different conditions assayed is presented in Fig. 1. The activity of TGF β 1 directly released from emulsion coated scaffolds was assessed during the length of the growth inhibition assay (40hrs). Releasing scaffolds (coated with 2000PEOT80PBT20 and 1000PEG(T/S)70PB(T/S)30 (50T/50S) copolymer)

were placed in the culture medium and the amount of TGF β 1 released was measured by ELISA. The resulting cell growth inhibition of the released TGF β 1 appeared higher than the one obtained from similar TGF β 1 concentrations used as standards (Fig. 6). The protein activity, calculated by comparing the concentrations deduced from the TGF β 1 standard curve and the ELISA, was of respectively $472 \pm 140\%$ and $1500 \pm 63\%$ for 2000PEOT80PBT20 and 1000PEG(T/S)70PB(T/S)30 (50T/50S) coatings. This apparent high activity is surprising and might be linked to the sensitivity of the CCL4 cells towards the sustained delivery of the protein. It is possible that the continuous presence of TGF β 1 in the culture medium, when released from the scaffolds, induce a higher inhibition of the cell growth compare to a single supplementation (standards). To assess if the growth of the cells was reduced by a sustained delivery of the protein, two different TGF β 1 concentrations (0.04 and 0.4ng/ml) were added sequentially to the medium every 8hrs (5 times). As can be seen in Fig. 6A, the total cumulated amount of TGF β 1 (0.2 and 2ng/ml) resulted in a cell inhibition similar to the one obtained with the standards. This indicates that the delivery rate had no effect the cell growth. Another potential cause of the high activity can be found in the detection of the released protein in the culture medium. As stated above, the protein concentration measured by ELISA most likely only reflects a part of the amount effectively released. Therefore, the level of decrease of the protein in the cell culture medium was measured for each type of releasing coated scaffold assayed over 40hrs. Subsequently, the total amount of released protein measured by ELISA was corrected for the protein depletion. A 2000PEOT80PBT20 and 1000PEG(T/S)70PB(T/S)30 (50T/50S) coating respectively showed a protein loss of 86 and 87%. As a result, the corrected activity of the released protein was $85 \pm 25\%$ for scaffolds coated with a 2000PEOT80PBT20 copolymer and $200 \pm 8\%$ for 1000PEG(T/S)70PB(T/S)30 (50T/50S) coated scaffolds. Although these activity values can only be considered as indicative due to the growth factor depletion that prohibited accurate concentration measurements and rendered a quantitative interpretation difficult, they tend to indicate that the bioactivity of the TGF β 1 was at least partly preserved during preparation of the scaffolds.

4. Effect of control released TGF β 1 on cartilage formation in vitro

To confirm the activity of the released protein and the potential benefit of the controlled release of TGF β 1 from porous scaffolds, the ability of the releasing scaffolds to induce cartilage formation in cell pellets was investigated. Bone marrow derived MSCs were selected as they are able to differentiate into the cartilage lineage when exposed to appropriate signals. For instance, goat and rabbit bone marrow cell pellets successfully produced cartilage like matrix when subjected to TGF β 1 [115, 143]. The releasing scaffolds (80mg) were placed directly in the pellet culture medium, but not directly in contact with the cells. A pellet culture was preferred to avoid any potential effects related to seeding efficiency on the scaffold or cellular differentiation due to the cell contact with the copolymer used as coating. Scaffolds coated with a 1000PEG(T/S)70PB(T/S)30 (0T/100S) copolymer which showed a slow delivery over 40 days were selected. Considering the fast degradation of TGF β 1 *in vitro*, scaffolds of higher protein content (360ng/scaffold) were prepared in order to obtain a growth factor release potentially inducing the chondrogenic differentiation of the cells. As negative control, unloaded coated scaffolds were included in the study as well.

The effect of the released TGF β 1 on cell differentiation after 15 and 21 days was assessed histologically. Fig. 7 depicts histological sections of the cell pellets after 21 days, stained with Safranin O/ fast green, which stains cytoplasm green and negatively

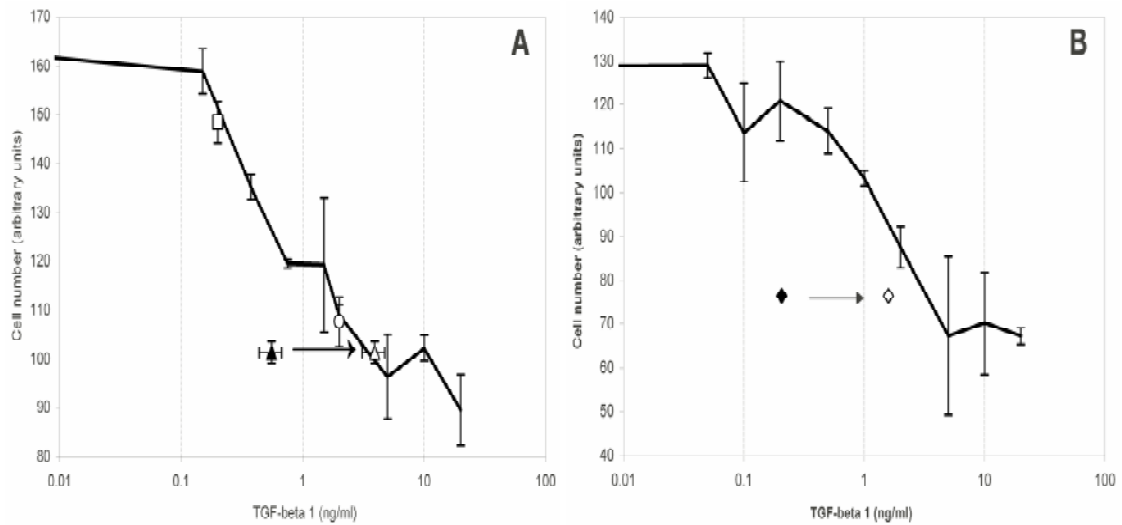


Figure 6: Activity of TGF β 1 releasing scaffolds and samples mimicking a sustained release system. Increasing values of TGF β 1 result in a lower number of cells after 40hrs of culture (standard curve). The releasing scaffold were coated with a 2000PEOT80PBT20 (A) or 1000PEG(T/S)70PB(T/S)30 (50T/50S) (B) copolymer. The cumulated released concentrations mentioned were obtained by ELISA, before (\blacktriangle , \blacklozenge) and after correction for the protein depletion in the medium (\triangle , \diamond). The samples mimicking a sustained delivery of TGF β 1 were of cumulated concentrations of 0.2 (\square) and 2ng/ml (\circ) and were supplemented in the culture medium in 5 regular time intervals (8hrs).

charged glycosaminoglycans (GAGs) red. The positive effect of the releasing scaffolds on cartilage formation was clearly visible after 15 days and was further demonstrated after 21 days. While the negative control, not subjected to TGF β 1, presented no sign of GAG formation, the group containing releasing scaffolds showed an intense Safranin O positive staining. This staining was more intense at the periphery of the pellets which also contained more cells. The cell morphology displayed similarities with hyaline cartilage, including round cells surrounded by large lacunae, creating chondron-like structures. The pellet core was characterized by a low number of cells and the presence of cell debris. Nevertheless, it was positively stained, indicating a strong formation of GAGs. The lower cell density and cellular debris might have been caused by a limitation of nutrient diffusion to the pellet core.

The ability of the TGF β 1 releasing scaffolds to induce cartilage in this cell pellet model confirms qualitatively the activity of the released protein.

Conclusions

To associate TGF β 1 to porous polymeric scaffolds and release it in a controlled fashion, an emulsion-coating method was investigated. This approach resulted in scaffolds of defined porosity and pore interconnection which were shown suitable for tissue ingrowth and migration of progenitor cells in osteochondral defects. The growth factor was effectively released from the scaffolds. By varying the copolymer composition used as coating, the release rate of TGF β 1 could be precisely tailored from 12 to more than 50days. The apparent incompleteness of the release was possibly linked to the

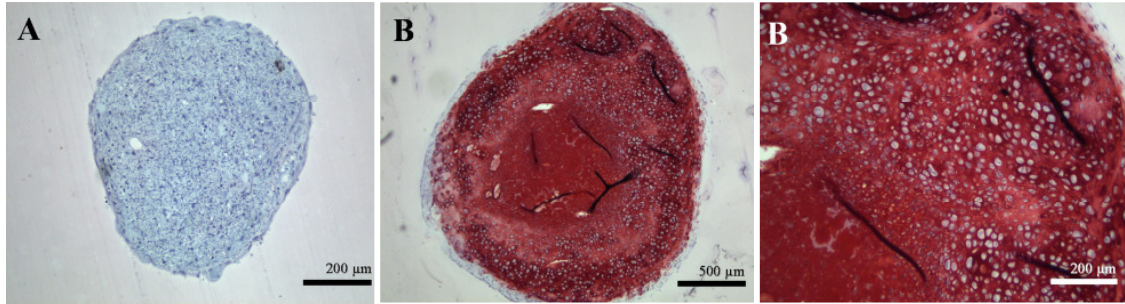


Figure 7: Histological sections of the bone marrow derived MSC pellets cultures for 21 days in the presence of emulsion coated porous scaffolds. The cross sections were stained with Safranin O/fast green. **(A)** Pellets are cultured in the presence of an unloaded emulsion coated scaffold. **(B)** Pellets are cultured in the presence of a releasing TGF β 1 loaded scaffold. **(A, C)** Scale bar 200 μ m **(B)** Scale bar 500 μ m.

instability of the protein in solution combined with the detection method employed (elisa) that did not allow a denaturing independent measurement. The released protein appeared not to be fully denaturated by the emulsion coating process and was shown to retain its bioactivity in a cell inhibition assay, although no exact quantification could be performed due to the inaccurate concentration measurements. This however indicates the safety of the emulsion-coating method and poly(ether ester) multiblock copolymers regarding sensitive proteins. This was further confirmed by the ability of the released protein to induce chondrogenic differentiation of bone marrow-derived mesenchymal stem cells. Therefore, emulsion coated scaffolds appear as potential candidates for cartilage tissue engineering as they release TGF β 1 in a biologically active form and allow a broad control on the growth factor release rates. This last property would be useful to investigate the relative effect of TGF β 1 release rate on cartilage formation and determine the most optimal release profile *in vivo*.

Chapter 3

TGF β 1 released from porous scaffolds: influence of delivery rates on cartilage formation

Abstract

In the perspective of repairing deficient cartilage, an increasing interest is given to the controlled release of TGF β 1 from porous supportive structures to enhance the differentiation of cells. Although the sustained release of growth factors is generally considered beneficial due to their native instability and high potency, the most ideal delivery profile is not known for a given amount of TGF β 1. The present study investigates the effect of different TGF β 1 release profiles from copolymeric porous scaffolds and different supplementation rates on the chondrogenic differentiation of goat mesenchymal stem cells pellets. A similar cumulated dose of growth factor was either released over 12 and 40 days from scaffolds, or supplemented in the culture medium at once (bolus) or every 3 days (positive control). After 21 days, the pellets were evaluated by histology, glycosaminoglycans (GAG) quantification and gene expression of cartilage markers (collagen type 1, 2 and aggrecan). The bolus supplementation of the growth factor was the most effective approach to induce the cells towards the chondrogenic phenotype. It induced a GAG production twice as important as the positive control and a 200 and 100-fold upregulation of respectively collagen type 2 and aggrecan gene expression. In general, the quality of the formed cartilage was increased with increasing delivery rates of the growth factor. The scaffold copolymer composition influenced the cartilage formation in parallel to the TGF β 1 supplementation conditions. The demonstration that mesenchymal stem cell are induced in a better way to the chondrogenic pathway by instantaneous or fast supplementations or releases has important implication for the use of these cells in cartilage tissue engineering applications and for the use of TGF β 1 releasing scaffolds in clinical applications.

Introduction

Among the potential targets of tissue engineering, cartilage is of special importance as this avascularized tissue has poor regeneration capabilities [22]. Concomitantly, an increasing interest is given to the controlled release of growth factors from porous polymeric scaffolds to achieve a better tissue formation [49, 182, 196]. Consequently, the current research to improve cartilage regeneration or formation in engineered constructs tends to focus on the controlled release of TGF β 1 [180, 197]. TGF β 1 is a pleiotropic growth factor which has regulatory effects on many different cell types. For instance, it plays an important role in cell proliferation and differentiation, bone formation [170], angiogenesis [172], neuroprotection [173] and wound repair [176]. More importantly, it controls the production of extracellular matrices by stimulating the synthesis of collagens, fibronectin and proteoglycans [177, 178] and has positive effects on cartilage differentiation and repair [179]. Additionally, TGF β 1 seems the ideal candidate to benefit from a sustained delivery due to its rapid denaturation and high potency.

Controlled release of TGF β 1 from porous scaffolds has been shown to enhance cartilage formation [159, 198]. However, the underlying assumption that sustained release is the optimum way to induce or enhance cartilage formation is seldom questioned and has not been verified. In addition, considering the cost of commercially available growth factors, it is of interest to determine the most effective way to employ a given dose. Therefore, the aim of this study was to investigate the effect of TGF β 1 release profiles from scaffolds on cartilage formation and to evaluate the potential beneficial effect of long term delivery over bolus supplementation.

To address this, a recently developed method based on the coating of porous scaffolds with poly(ether-ester) copolymeric emulsions was used [191]. This biodegradable multiblock copolymer, based on polyethylene oxide terephthalate and polybutylene terephthalate (PEOT/PBT) or polyethylene glycol succinate and polybutylene succinate) (PEGS/PBS), is successfully used as protein release system [117, 185] and as scaffold matrix for tissue engineering applications [63, 132, 148, 199, 200]. The emulsion-coating method allows the associate TGF β 1 with porous scaffolds and to adjust its release kinetics, ranging from release within 12 days up to more than 50 days [201]. Control of the release rate can be obtained by varying the coating copolymer composition.

To investigate the effect of supplementation rates of TGF β 1 on cartilage formation, three different delivery profiles (bolus supplementation, release completed in 12 days and completed in 40 days), a negative (without TGF β 1) and a positive control (regular refreshment of TGF β 1 every 3 days) were compared with respect to the cartilage formation observed in goat mesenchymal stem cells (gMSC) pellets over 21 days of culture *in vitro*. MSC were chosen as they undergo chondrogenic differentiation when exposed to TGF β 1, which makes them attractive candidates for cartilage tissue engineering applications [115, 116, 143, 202]. The use of pellets as a model system for chondrogenesis was preferred as it allows cell-cell interactions analogous to those occurring in precartilaginous condensation during embryonic development [115]. Moreover, this system avoids any effect of seeding efficiency on the scaffolds and minimizes the potential cellular differentiation due to the cell contact with the different copolymers used as coating.

Beside the effect of the supplementation rates, and as the copolymer compositions used as coating were varied to tailor the release rate of the growth factor, the effect of the coating copolymer compositions on cartilage formation was investigated as well.

Materials

Polyethylene oxide terephthalate/polybutylene terephthalate (PEOT/PBT) and polyethylene glycol succinate/polybutylene succinate) (PEGS/PBS) multiblock copolymers were obtained from OctoPlus, Leiden, The Netherlands, and were used as received. Polymers are indicated as **aPEOTbPBTc** or **aPEGSbPBSc** in which **a** is the PEO molecular weight, **b** the weight percentage (weight%) of polyethylene oxide terephthalate (PEOT) or polyethylene glycol succinate) (PEGS), and **c** (=100-**b**) the weight% of PBT or PBS. Vitamin B₁₂, Bovine Serum Albumin (BSA), Dimethyl Sulfoxide (DMSO), L-ascorbic acid-2-phosphate, proline, Insulin-Transferrin-Selenium (ITS+1), dexamethasone, proteinase K, pepstatin A and iodoacetamide were purchased from Sigma Chem. corp. (St. Louis, USA). Recombinant human transforming growth factor beta1 (rhTGF β 1, later referred as TGF β 1) and ELISA kit were purchased from R&D Systems Inc. (Minneapolis, USA). Dubbelco (DMEM), alpha Modified Eagle Medium (α -MEM), pyruvate, L-glutamine, penicillin and streptomycin were obtained from Gibco (Invitrogen, Carlsbad, USA). Foetal Bovine Serum (FBS) was purchased from Cambrex (East Rutherford, USA). Glycol MethAcrylate embedding solutions (GMA) were purchased from Technovit (Heraeus Kulzer, Germany). Beta-Fibroblast Growth Factor (bFGF) was obtained from VWR international (Roden, The Netherlands). Chloroform, obtained from Fluka chemica (Buchs, Switzerland), was of analytical grade.

Methods

Preparation of TGF β 1-loaded polymeric scaffolds.

Emulsion

The protein was associated to the porous scaffolds by mean of a water-in-oil (w/o) emulsion method. An aqueous solution of TGF β 1 in a 4 mM HCL solution (containing 1mg/ml BSA, according to the supplier recommendation) was emulsified with a PEOT/PBT or PEGS/PBS copolymer solution in chloroform, using an Ultra-Turrax (T25 Janke & Kunkel, IKA-Labortechnik) for 30s at 19krpm. The TGF β 1 concentration of the aqueous solution was set at 3.3 μ g/ml. The volume of the aqueous phase was set to 1 ml per gram of copolymer (water/polymer ratio = 1ml/g). The copolymer solution was obtained by dissolving 0.5gram of copolymer in 3ml of chloroform. Two different copolymers were used: 2000PEOT80PBT20 and 1000PEGS70PBS30.

Emulsion-coating method

The emulsion coated scaffolds were obtained as described elsewhere [191]. Briefly, compression molded/salt leached scaffolds were prepared from 300PEOT55PBT45 granules and 400-600 μ m salt crystals (75 volume%). Coated scaffolds were prepared by forcing a TGF β 1 containing emulsion through a prefabricated porous scaffold with the use of vacuum (300mBars). This vacuum was applied for at least 5 minutes in order to evaporate chloroform as much as possible from the emulsion, thereby creating a polymeric coating on the scaffold. The resulting coated scaffolds were frozen in liquid nitrogen and freeze-dried for 24hrs.

Blank scaffolds were prepared by using a TGF β 1-free 4mM HCL solution (with 1mg/ml BSA) in the same conditions as TGF β 1 containing scaffolds.

The quantity of emulsion effectively coated on the porous scaffold and the resulting amount of TGF β 1 present was determined by an indirect method which was proven to be accurate for other proteins [191]. Briefly, emulsion coated scaffolds containing vitamin

B₁₂ were prepared for each copolymer composition used and the fast release of the small molecule was measured. The quantity of vitamin released is correlated to the amount of polymer coated onto a given scaffold. In turn, the amount of polymer coated can be related to the amount of protein associated with the scaffold. The amount of TGF β1 incorporated in a scaffold piece of 100mg was about 70ng.

The copolymer compositions used in the coating were selected considering their ability to release TGF β1 from the scaffolds in a controlled way. A scaffold coated with a 2000PEOT80PBT20 copolymer results in a release of the protein completed within 12 days while a 1000PEGS70PBS30 coating shows a similar amount of protein gradually released over 40 days. In addition, the protein released from the scaffolds was not denaturated during the coating process and retained its bioactivity. A complete characterisation of the scaffolds has been reported previously [201].

TGF β1 concentration decrease in culture medium

TGF β1 concentrations in the culture medium were assessed by ELISA. To determine the absolute concentration decrease over 3 days, triplicates of the bolus and positive control medium (containing originally 70ng/ml and 10ng/ml) were collected and assayed for TGF β1 remaining concentration. To determine the concentration equilibrium over 21 days, the medium of three pellets from the positive control group (containing originally 10ng/ml) was collected every 3 days for TGF β1 quantification. The different groups evaluated in this study are summarized in Fig. 1.

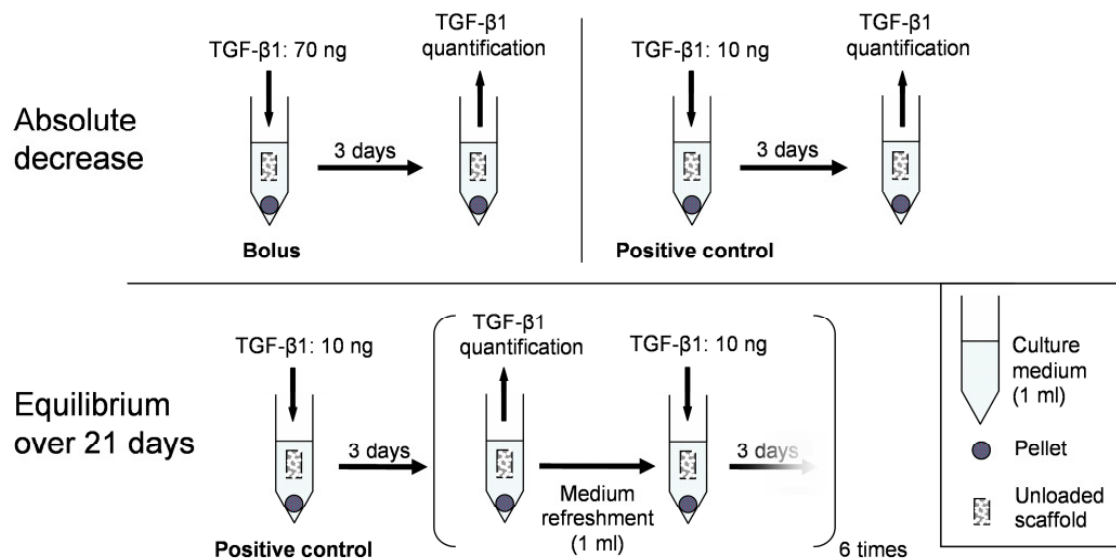


Figure 1: Different experimental conditions used to investigate the TGF β1 concentration decrease in the pellet culture medium. Each condition was performed twice, with two different unloaded scaffolds coated with two different copolymer compositions (2000PEOT80PBT20 and 1000PEGS70PBS30).

Goat mesenchymal stem cell pellet culture

Goat mesenchymal stem cells (MSCs) were harvested from the iliac crest of 4 years old female Dutch milk goats, under general inhalation anaesthesia. The bone marrow aspirate was collected in heparin tubes. The nucleated cells were plated at a density of 0.5×10^6 cells/cm² in α-MEM, supplemented with 12 v/v% FBS, 100 UI/ml penicillin, 100µg/ml streptomycin, 0.1 mM L-ascorbic acid-2-phosphate, 1ng/ml bFGF and 2mM L-

glutamine. The medium was refreshed after 3 days and then twice a week until confluency (8 to 10 days). Cells were passaged with 0.05% trypsin and replated at 5000 cells/cm². Passage 1 cells were cryo-preserved in 50% supplemented α -MEM, 40% FBS, 10% DMSO. When needed, cells were thawed, plated and grown until confluent in α -MEM, supplemented with 12 v/v% FBS, 100UI/ml penicillin, 100 μ g/ml streptomycin, 0.1mM L-ascorbic acid-2-phosphate, and 2mM L-glutamine (expansion medium).

Passage 3 cells were used to prepare the pellets. After trypsinization, 0.5 x 10⁶ cells were centrifuged at 500g for 2 minutes in 10ml polystyrene conical tubes. The expansion medium was then replaced by serum-free medium, consisting of 1ml of DMEM with 100UI/ml penicillin, 100 μ g/ml streptomycin, 100 μ g/ml pyruvate, 40 μ g/ml proline, 50 μ g/ml L-ascorbic acid-2-phosphate, 1% ITS+1, and 100nM dexamethasone.

To study the effect of the TGF β 1 released from the scaffolds, one TGF β 1 loaded scaffold (100mg) was added to the culture tube containing one pellet, directly in the medium. Pellets exposed to TGF β 1 freshly supplemented in the culture medium (70ng/ml as a bolus or 10ng/ml repeated every 3 days) were incubated with 1000PEGS70PBS30-coated blank scaffold unless indicated otherwise. The culture tubes were incubated at 37 °C, in a 5% CO₂ humidified atmosphere. After 24hrs of incubation, the cells formed round aggregates, non-adhering to the tube walls. The medium was refreshed every 3 days, and pellets were harvested after 3, 12 and 21 days.

The different conditions evaluated in this study are summarized in Table 1.

The effect of the TGF β 1 release profile on articular cartilage marker-genes expression was analyzed from the cultured pellets. Primers for all genes were designed using sequences published on the NCBI website. Because the caprine complete gene sequences are not available, we designed primers based on bovine and mouse cDNA information. The genes examined in this study were collagen type 1 and 2 (coll 1 and 2) and aggrecan (AGC), with glyceraldehyde-3-phosphate dehydrogenase (GAPDH) as house keeping gene. The sequence, accession number and product size of each primer are listed hereafter. GAPDH (forward sequence (5'-3'): AACGACCCCTTCATTGAC,

Table 1: Overview of the different experimental groups evaluated. The delivery of TGF β 1 to the pelleted cells was either obtained from releasing scaffolds of different release rate or by supplementing the medium with the growth factor in different pattern. Each pellet was cultured in the same conditions, in the presence of a similar emulsion coated scaffold (100 mg), either containing and releasing TGF β 1 or unloaded.

Experimental group	Coating copolymer composition	Delivery rate (days)	TGF β 1 amount incorporated in scaffold	TGF β 1 amount supplemented in medium
Negative control	1000PEGS70PBS30	0	0	0
	2000PEOT70PB20			
Slow release	1000PEGS70PBS30	40	70ng	0
Fast release	2000PEOT70PB20	12	70ng	0
Bolus	1000PEGS70PBS30	instantaneous	0	70ng once
	2000PEOT70PB20			
Positive control	1000PEGS70PBS30	21	0	7x 10ng (every 3 days)
	2000PEOT70PB20			

reverse sequence (5'-3'): TCCACGACATACTCAGCAC), M32599, 191 bp; coll 1 (forward sequence (5'-3'): GCATGGCCAAGAAGACATCC, reverse sequence (5'-3'): CCTCGGGTTTCCACGTCTC), NM_007742, 82 bp; coll 2 (forward sequence (5'-3'): CAAGGCCCCCGAGGTGACAAA, reverse sequence (5'-3'): GGGGCCAGGATTCCATTAGAG), NM_031163, 216 bp; aggrecan (forward sequence (5'-3'): AAGGGCGGGTGCGGGTCAACAG, reverse sequence (5'-3'): CGCGAAGCAGTACACGTCATAGG), U76615, 473 bp. The amplified product sizes were confirmed by gel electrophoresis and sequencing to eliminate the possibility of cross contamination by mouse or bovine sources.

Total RNA was isolated by crushing the pellets and using a RNeasy kit (Qiagen, Hilden, Germany) and on-column DNase treated with 10U RNase free DNase I (Gibco) at 37°C for 30 minutes. DNase was inactivated at 72°C for 15 minutes. The quality and quantity of RNA was analyzed by gel electrophoresis and spectrophotometry. 1µg of RNA was used for first strand cDNA synthesis using Superscript II (Invitrogen) according to the manufacturer's protocol. 2µl of 100x diluted cDNA was used for GAPDH amplification, 2µl of 50x diluted cDNA for aggrecan, and 2µl of undiluted cDNA for collagen type 1 and 2. PCR was performed on a Light Cycler real time PCR machine (Roche, Basel, Switzerland) using SYBR green I master mix (Invitrogen). Data were analyzed with the Light Cycler software version 3.5.3 using the fit point method by setting the noise band to the exponential phase of the reaction to exclude background fluorescence. The relative expression of the genes was calculated by normalizing to the house keeping gene (GAPDH) and comparing to the negative control group (without TGF β1) by the comparative $2^{-\Delta\Delta CT}$ method [203]. For all groups, the sample size was 3, representing three different pellets. If data passed the normality and variance tests, multiple student's t-tests were performed to compare the different groups. If not, the non parametric Mann-Whitney test was used. A p -value<0.05 was considered significant for all tests.

Results

1. Effect of TGF β1 supplementation rate on cartilage formation

Histological evaluation

The different delivery rates of TGF β1 to the culture medium resulted in different tissue organization of the pellets. Representative cross sections of the pellets cultured in various conditions and stained with Safranin O/fast green (stains negatively charged glycosaminoglycans (GAGs) red and nuclei green) are presented in Fig. 2.

Irrespective of the copolymer used as coating, the positive effect of TGF β1 on the differentiation of gMSC towards cartilage could clearly be observed. In the absence of TGF β1 (negative control) no GAG was found in the pellets, which were of smaller size than for the other conditions. The cells were small and a lot of debris was observed, suggesting a low cell survival during culture. In contrast, all the pellets cultured in the presence of TGF β1 (either supplemented or released from scaffolds) showed GAG formation at different intensities and localizations. The morphology of the cells present in the positively stained areas was similar regardless of the culturing conditions and resembled articular chondrocytes. The cells were rounded and located in lacunae surrounded by GAG positive extra cellular matrix. The chondrogenic differentiation of MSCs by TGF β1 is in line with previous studies conducted on goat [143], rabbit [115], or human [116, 204] cells.

The rate at which TGF β1 was applied to the pellets influenced chondrogenesis. For a 1000PEGS70PBS30 coating, a slow release of the protein (within 40 days) resulted in

the formation of GAG in discontinuous areas, mainly at the pellets rim and in the smaller structures present around it. The pellet core was of similar structure to the negative control, without apparent GAG formation, indicating a partial differentiation of the pellets. The bolus supplementation of the TGF β 1 at the beginning of the culture resulted in an intermediary GAG staining at the pellet rim and a small and less intensively stained core. The core was composed of a mix of distressed-looking and round cells surrounded by a faint positive staining. Surprisingly, the addition of TGF β 1 in the culture medium at regular time interval (10ng/ml every 3 days, positive control for long term release) resulted in a structure more comparable to the bolus than to the slow release.

2000PEOT80PBT20 coatings, either loaded or unloaded with TGF β 1, resulted in pellets of more homogeneous GAG distribution, with a lower amount of small and undifferentiated cells in the pellet core. In addition, the pellets were larger for similar culture conditions and some cells were stacked in chondron-like structures of two to five cells. The differences in GAG formation were less obvious between the delivery conditions (either released or supplemented) as compared to the 1000PEGS70PBS30 coating. The bolus supplementation resulted in a cartilage formation as effective as the fast release from the scaffolds or the repeated supplementation.

Quantitative characterization of the TGF β 1 supplementation rate effect

The differences in GAG formation due to the TGF β 1 supplementation rate was evaluated more accurately by a quantitative characterisation of the pellets GAG and DNA content. The pellet DNA content indicated that the number of cells was influenced by the culture conditions, as presented in Fig. 3 A. A slow delivery and a lack of TGF β 1 (negative control for both coating copolymers) resulted in a significantly lower DNA content ($p < 0.05$) than the other culture conditions. This indicates that the pellets cultured with slow releasing scaffolds or without TGF β 1 had a similarly low cell number. Apparently, the slow growth factor release resulted in a cell survival or proliferation rate similar to the one observed without TGF β 1. Nevertheless, the size of the pellets obtained for a slow TGF β 1 release (Fig. 1) confirmed the extra cellular matrix (ECM) production, as previously observed for human MSC [116, 202, 205]. All the other culture conditions resulted in higher and variable amount of DNA per pellet, without statistical difference.

The differentiation state of the cells was quantified by measuring the amount of GAG produced per DNA (Fig. 3B). As expected from the histological sections of the pellets, the lack of TGF β 1 (negative control) resulted in a minimal GAG formation ($p < 0.05$) for both coating copolymers. For the 1000PEGS70PBS30 coating, the bolus, repeated supplementation (positive control) and slow release of TGF β 1 showed intermediate GAG levels which seemed to increase from slow release to bolus, but not significantly ($p \approx 0.1$). The low amount of cartilage formation and low cell number observed for the slow release group is probably linked to the lower amount of TGF β 1 released over the 21 days of culture. As the release from the scaffold was completed in 40 days, only 75% of the protein was delivered to the culture medium at the end of the study. The localized and sporadic chondrogenic differentiation could therefore be linked to the TGF β 1 dose. This was confirmed in an independent experiment which demonstrated that lower doses of TGF β 1 (3ng/ml every 3 days) result in very few small conglomerates of cartilage like cells at the periphery of the pellet (data not shown).

The scaffolds coated with 2000PEOT80PBT20 copolymer induced as well an evolution of the GAG synthesis linked to the rate of TGF β 1 supplementation. The amount of GAG/DNA regularly and significantly increased from a slow supplementation of TGF β 1 in the medium over 21 days (positive control) to an instantaneous and unique

supplementation (bolus) ($p < 0.05$). In agreement with the histological observations, a 2000PEOT80PBT20 coating (unloaded or releasing TGF β 1) always showed a higher GAG formation in comparison to scaffolds coated with a 1000PEGS70PBS30 copolymer. As a result, the bolus group induced the highest GAG formation of all delivery conditions investigated. This suggests the a sustained delivery of the growth factor, either release from scaffolds or supplemented in the culture medium is not as effective as a bolus delivery.

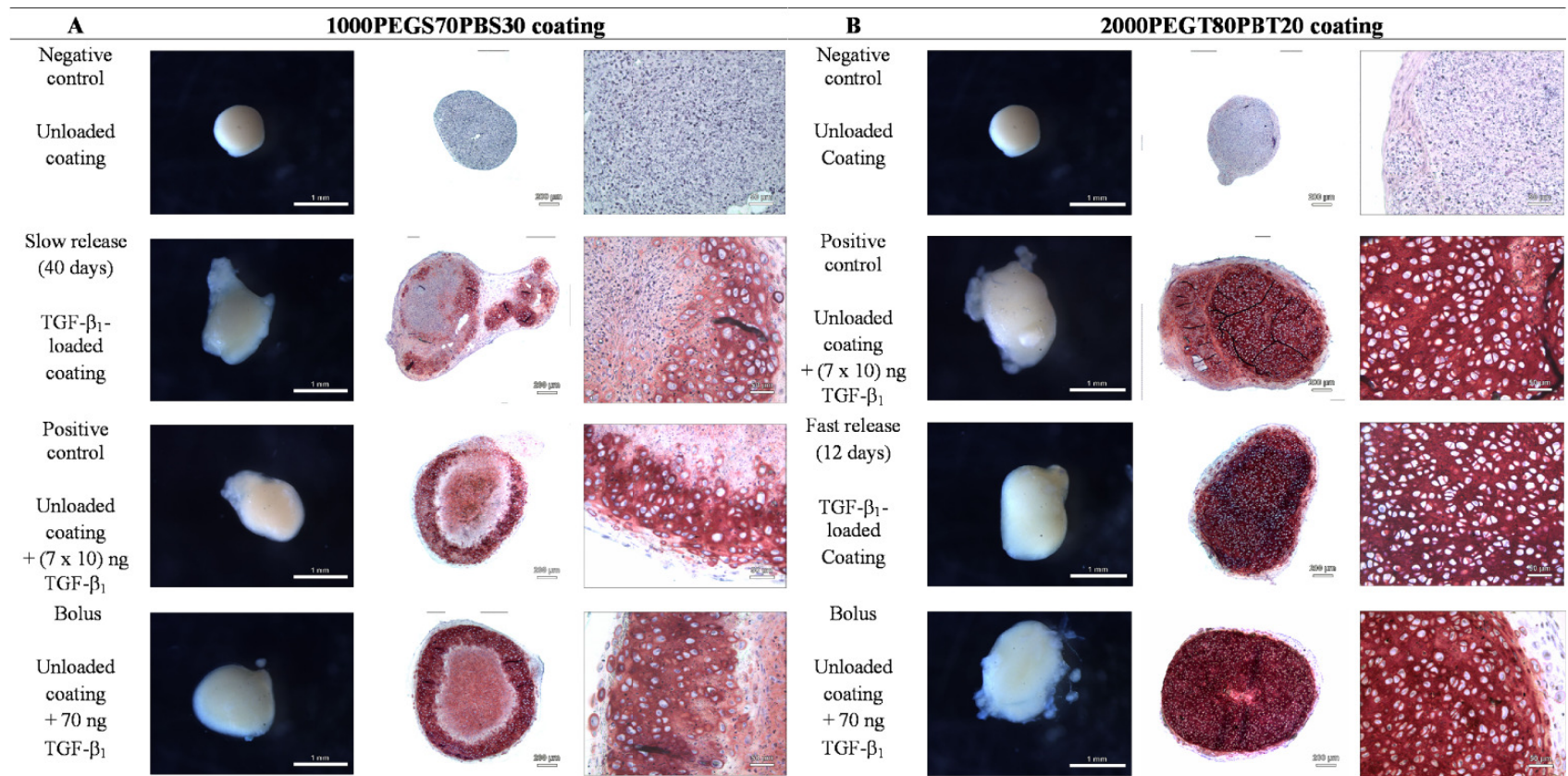


Figure 2: Gross evaluation and histological cross sections of MSC pellets cultured in the presence of porous scaffolds of different TGF β_1 release profiles and different coating copolymers: **A.** 1000PEGD70PBS30 coating **B.** 2000PEOT80PBT20coating. The cross sections were stained with Safranin O. The negative control pellets were not exposed to TGF β_1 . The positive control consists of unloaded scaffold where constant amounts of TGF β_1 were added to the culture medium regularly (10ng/3 days), while in the bolus groups 70ng of TGF β_1 were added at the start of culture (n=2).

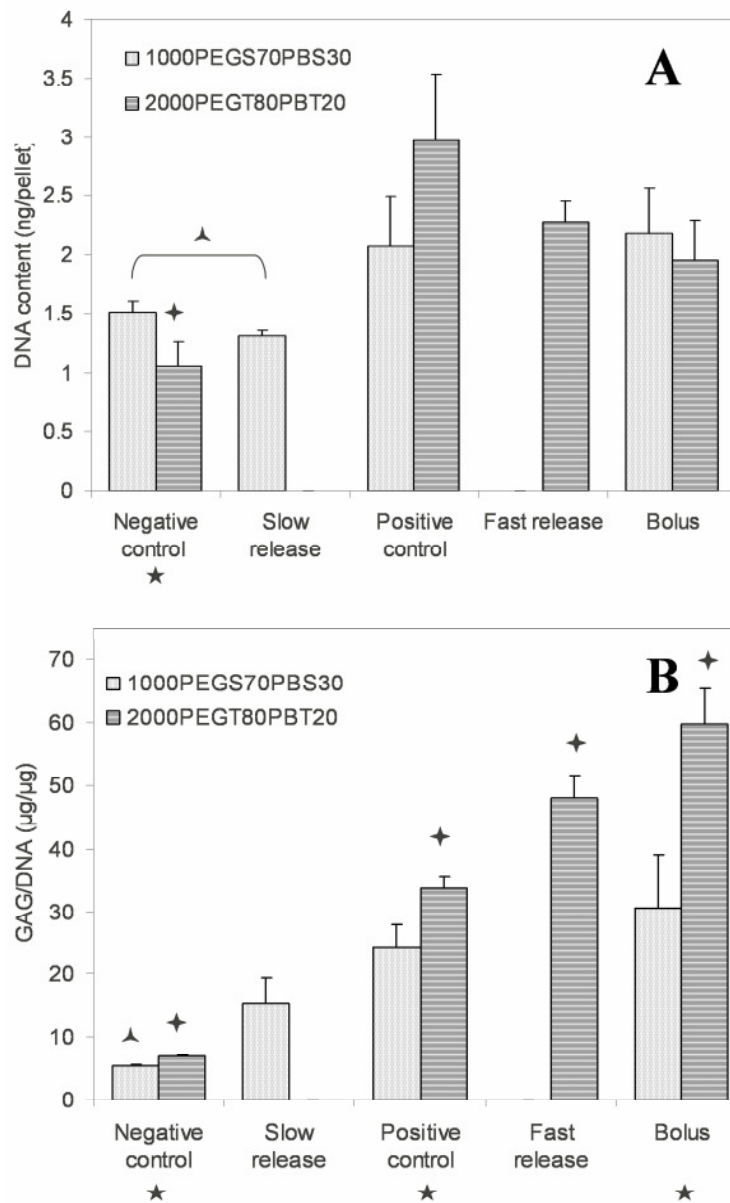


Figure 3: Effect of the TGF β 1 supplementation rate and coating copolymer composition on MSC pellets DNA (**A**) and GAG/DNA (**B**) content. TGF β 1 unloaded scaffolds were coated with 1000PEGS70PBS30 (dotted bars) or 2000PEOT80PBT20 (stripped bars) and were cultured without supplementation of TGF β 1 (negative control), with regular supplementation every 3 days (positive control), or with a bolus supplementation of TGF β 1 at the beginning of the culture. TGF β 1 loaded scaffolds released the growth factor over 12 days (fast release) or 40 days (slow release). \blacktriangle denotes a significant difference ($p < 0.05$) between culture conditions for a 1000PEGS70PBS30 coating copolymer, \blackstar denotes a significant difference ($p < 0.05$) between the different culture conditions for a 2000PEOT80PBT20 coating copolymer and \star denotes a significant difference ($p < 0.05$) between coated copolymer for a similar culture condition ($n = 3 \pm \text{s.d.}$).

Temporal pattern of chondrogenic gene expression

To better understand the relative effects of the different supplementation and release rates on the chondrogenic differentiation, the expressions of collagen type 1 (coll 1), collagen type 2 (coll 2) and aggrecan (AGC) genes were quantified as a function of time. Three different time points were evaluated (after 3, 12 and 21 days of culture). The pellets cultured with a 1000PEGS70PBS30 coating were used as the differences in GAG formation appeared more acute by histology when using this coating copolymer. As depicted in Fig. 4, the coll 1 expression remained unchanged after 12 days of culture while after 21 days all the culture conditions showed a higher gene expression. The increase of coll 1 expression varied between 1.7 and 6.6 folds as compared to the negative control (without TGF β 1). The coll 2 expression appeared highly upregulated after 12 days of culture. The bolus supplementation resulted in an upregulation close to 200 times, followed by the slow release scaffolds and the repeated supplementation (positive control, 50 times). The expression of coll 2 appeared to decrease for some culture conditions after 21 days (slow release and its control), although no statistically significant differences could be found in comparison with 12 days. The opposite trend was seen for the bolus condition, without significant difference. The expression of the AGC gene was highly upregulated by a bolus delivery after 12 days of culture (by 70 fold). Similarly to coll 2, a slow TGF β 1 release or the positive control resulted in the smallest upregulation of the gene (between 25 and 35 fold). Although the AGC expression was increasing slightly for all groups after 21 days, no statistically significant difference could be found between the gene expression at day 12 and day 21.

In all culture conditions containing TGF β 1, a high and variable ratio of coll 2 gene expression versus coll 1 was seen after 12 and 21 days, corroborating the chondrogenic differentiation of the gMSCs noticed by histology. Several publications outlined that a high ratio was representative of hyaline articular chondrocytes of different mammal species including goat [206-211].

The coll 2 and AGC gene expression of the pellets clearly confirms the beneficial effect of the bolus supplementation on cartilage formation, in comparison to slower deliveries (positive control and slow release from scaffolds). Interestingly, the different supplementation rates upregulated the coll 2 and AGC expression mainly over the first 12 days of culture. At later culture time, the gene expression was not significantly varied. This indicates that the upregulation of these cartilage related genes is mainly triggered over the first 12 days of culture. Moreover, it can even be assumed that the first 3 days are the most important as TGF β 1 is only available to the pellets over the first 3 days for the bolus group, which resulted in the highest upregulation.

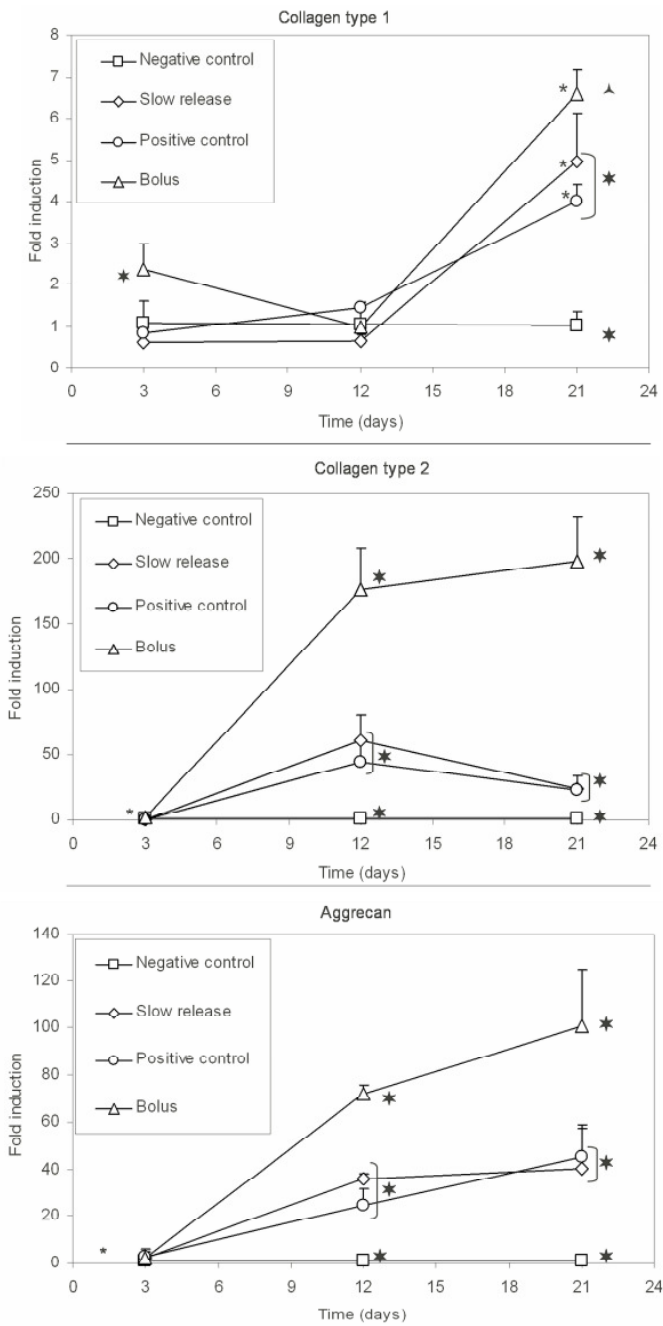


Figure 4: Gene expression for collagen type 1, 2, and aggrecan of pellets cultured in different conditions. Expression was analyzed by quantitative real time PCR and expressed as fold induction compared to negative controls normalized to GAPDH expression. ★ denotes a significant difference ($p < 0.05$) between culture times for a certain group, ★ indicates a significant difference ($p < 0.05$) between groups for a fixed culture time, ^ indicates a significant difference ($p < 0.05$) between all other groups for a fixed culture time, except the slow releasing one. ($n = 3 \pm$ s.d.)

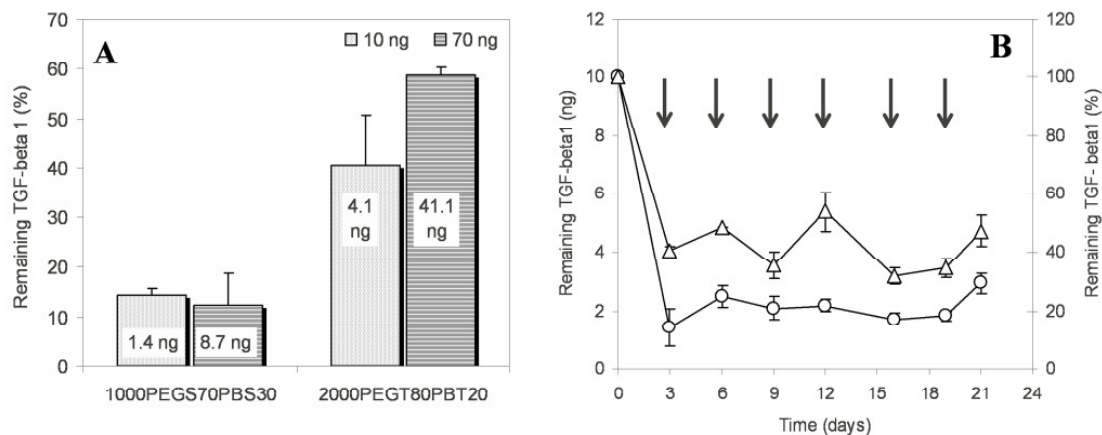


Figure 5: TGF β 1 decrease in the culture medium over three days (A) or after repeated refreshments over a culture period of 21 days (B). The growth factor depletion was monitored in the presence of unloaded scaffolds coated with 2000PEOT80PBT20 (Δ) or 1000PEGS70PBS30 (O) copolymers, after unique supplementation of 70 and 10ng of TGF β 1 (A), or after repeated supplementation of 10ng of TGF β 1 (B). In the latter, arrows indicate a complete refreshment of the medium, with a fresh solution containing 10ng/ml of TGF β 1 (1 ml). The difference between coating copolymers, was significant for similar TGF β 1 dose ($p < 0.05$). For repeated supplementations (B), no statistically significant difference was found between the time points, for a similar coating copolymer. ($n=3 \pm$ s.d.)

2. Effect of coating copolymer

Although the rate of TGF β 1 supplementation from slow (positive control) to instantaneous (bolus) resulted in an increasing beneficial effect on cartilage formation (evident from histological evaluation, GAG quantification and cartilage genes expression), the coating copolymer composition showed a large effect as well. The cause of the beneficial effect of the 2000PEOT80PBT20 copolymer observed by histology (Fig. 2) and GAG quantification (Fig. 3) is unclear. A direct induction of the cells to the cartilage lineage by the copolymer can be excluded as the culture of pellets without TGF β 1 did not show any cartilage formation.

Alternatively, the presence of smaller cells and cellular debris in the pellets core when cultured with a 1000PEGS70PBS30 coating suggests a cytotoxic effect on the cells. Nevertheless, this copolymer did not induce statistically significant differences in the pellets cells number when compared to the 2000PEOT80PBT20 copolymer, and succinated copolymers were not found cytotoxic in previous evaluations [74]. In addition, change in the culture medium pH due to polymer degradation occurred in the same fashion for both copolymers used (from 8.3 ± 0.1 to 7.8 ± 0.2 after three days).

A third possibility may reside in the effect of the copolymers on the amount of TGF β 1 available in the culture medium. TGF β 1 is known to be unstable and rapidly degraded [190]. *In vivo*, the half life time of TGF β 1 is less than to 30 minutes [171, 182] when in its active form. In addition, due to its high hydrophobicity, TGF β 1 tends to rapidly adsorb to plastic surfaces, reducing so the biologically active concentration of the protein in solution. Due to the difference in hydrophilicity of the two coating copolymers used, a different TGF β 1 adsorption behavior can be expected. To assess the effect of the copolymers on TGF β 1 availability in the culture medium, the protein concentration was measured at different time points and under different conditions schematically summarized in Fig. 1. Indeed the amount of TGF β 1 was decreased over the first three days of culture, in a different fashion for each coating copolymer (Fig. 5A). While only 12

to 14% of the TGF β 1 was still present when using an unloaded 1000PEGS70PBS30 coating, between 40 and 59% remained when using a 2000PEOT80PBT20 copolymer. Over longer culture times, the trend in the growth factor disappearance was similar, with always a more acute clearance when using a 1000PEGS70PBS30 copolymer (Fig. 5B). The complete refreshment of the TGF β 1 containing medium at regular time intervals (3-4 days) showed that two different concentration equilibria were reached for each coating copolymer. Around 20% of the protein was found after each refreshment of the 1000PEGS70PBS30 coating while 40 to 60% remained in the 2000PEOT80PBT20-containing medium. The presence of different equilibria supports the hypothesis of different adsorption affinities of the protein for the two copolymers. However, the differential concentration decrease could be due to other events. For instance the copolymer degradation products could interact or bind with the protein in a different fashion.

Discussion

In the perspective of repairing deficient cartilage, an increasing interest is given to the controlled release of TGF β 1 from porous supportive structure to enhance the differentiation of cells [197, 212, 213]. In general, it is assumed that a sustained release of TGF β 1 results in optimal cartilage formation. On the contrary, the present study indicates that the sustained exposition of TGF β 1 is not the most effective approach for a given amount of growth factor.

Irrespective of the copolymer used as coating, a bolus exposure to TGF β 1 resulted in the most successful cartilage differentiation of gMSC pellets. In general, the cartilage formation was increasing with an increasing delivery rate of growth factor to the cells, either released from a porous scaffold or supplemented in the culture medium. Even the repeated supplementation of TGF β 1 over 21 days (10ng/ml every 3 days), which is the way commonly used to induce cartilage differentiation of dedifferentiated chondrocytes or MSCs [116, 143, 202, 214-216], resulted in a lower chondrogenic differentiation as compared to a fast release (within 12 days) or a bolus supplementation.

These differences can be related to the TGF β 1 concentration readily available in the medium at a given point. This was suggested by the low cartilage formation observed from slow releasing scaffolds, which released less TGF β 1 than the other conditions. Besides, 2000PEOT80PBT20 coatings always resulted in a higher TGF β 1 concentration available for the cells and consequently showed a better and more homogeneous cartilage differentiation for all delivery conditions (release or supplementation). The effect of TGF β 1 concentration was as well indicated in previous studies on rabbit MSCs which reported the apparition of an undifferentiated core in pellets cultured with concentrations of TGF β 1 lower than 10ng/ml in the culture medium [115]. Therefore, the superiority of the bolus supplementation could simply be due to the higher amount of growth factor in the medium during the first three days of culture, before the first refreshment. Subsequently, although the amount of protein is important, the time frame where TGF β 1 is presented to the cells appears important as well.

This can be better understood in the light of the physiological mechanism of action of the growth factor. Studies investigating the signaling pathway of TGF β 1 mediated chondrogenesis of human MSC pellets reported that its triggering action on the cells was occurring rapidly [215, 217]. The TGF β 1 receptors are saturated within 25 minutes and the expression of N-cadherin (cell adhesion molecule functioning during precartilage mesenchymal condensation leading to chondrogenic differentiation) is upregulated

within one day and downregulated after 5, while changes in cell morphology and increase of ECM production are concomitant. The same rapid chondrogenic induction of the cells was suggested by the temporal pattern of gene expressions. For all culture conditions the upregulation of the collagen type 2 and aggrecan genes was seen during the first 12 days of culture. Over the next 9 days (till 21 days of culture), the gene expression decreased or increased not significantly. Similar results were observed when human MSCs were seeded on PLA scaffolds and exposed to 50ng/ml of TGF β 1 during the first three days of culture [147]. This indicates that the cells are most active in reaching the cartilage phenotype during the early time of culture, after being exposed to TGF β 1. At later time points, the cartilage phenotype is perhaps partially achieved and the cells are reaching a basal level of gene expression or initiating a de-differentiation towards hypertrophic or fibrous cartilage or a fibrotic tissue as was suggested by the increase of collagen type 1 expression. Cross sections of pellets from the positive control group after 12 days confirmed that the cartilage phenotype was mostly achieved within this time as they presented staining intensities close to the ones observed after 21 days (data not shown). Additionally, it seems that TGF β 1 is naturally not presented in a continuous fashion to cells in the body. Its high hydrophobicity induces a high binding affinity for extracellular matrix component, which is irreversible unless proteolytic cleavage occurs [171]. Rapidly upon secretion from the cell, the major fraction is covalently associated with the extracellular matrix and not available for the cells. A bolus supplementation is therefore closer to the physiological mechanism of action than a sustained delivery.

It is likely that once the cells are induced to the chondrogenic lineage at early culture time, they do not need further differentiation signals. Higher amount of growth factor would trigger more of the undifferentiated cells present towards the cartilage lineage. The triggered cells would then differentiate and proliferate as chondrocytes within the pellet, while those not triggered by TGF β 1 would remain undifferentiated and eventually die (in the pellet core). This hypothesis was further strengthened in a separate experiment evaluating the cartilage formation of gMSC aggregates subjected to different bolus of TGF β 1. A gradual increase in differentiation was seen from single cells up to complete aggregate when exposed from 10ng/ml to 100ng/ml for 24hrs (data not shown). Similarly, it was previously reported that the exposure of rabbit periosteal explants (containing undifferentiated mesenchymal stem cells) to TGF β 1 for 30 minutes was sufficient to induce cartilage formation after six weeks in a concentration dependent way [181].

To conclude, the experiments conducted clearly indicate that a long term delivery of TGF β 1 or its supplementation at regular time interval is not the most optimal way to induce the chondrogenic differentiation of MSCs. TGF β 1 is involved in the cell fate decision, which occurs immediately after exposure, but not in later phases of differentiation. Hence, a single bolus delivery is more effective, granted that all cells are available at that time, which might not be the case when scaffolds are implanted in chondral or osteochondral defects. In addition, this study reveals that the copolymers used as scaffolds have an indirect effect on chondrogenic differentiation of MSCs via TGF β 1 availability. This is important to consider as the nature of the scaffold can diminish the effect of the growth factor.

The quality of the cell differentiation appears mainly linked to the concentration of the growth factor present at the beginning of the culture. This has important implication for the use of TGF β 1 release systems for cartilage regeneration, as it might not be of interest to develop complex release systems providing a long term delivery. Additionally, it could be helpful to develop tissue engineered systems based on MSCs without

controlled release. One could think for instance to trigger the cells by a bolus administration and implant them without waiting for their differentiation *in vitro*. Alternatively, if the totality or part of the cells is to be recruited from the site of implantation *in vivo*, a bolus or burst delivery might not be the best option as the growth factor will probably be degraded faster than in the confined tube environment and as the number of cells present immediately after implantation might not be sufficient to induce a positive response. It has been reported that osteochondral defects in rabbits could be filled with mesenchymal stem cells about one week after surgery [23]. There, the delayed burst delivery of the growth factor after one week or its sustained release over more than one week days could be of advantage to respectively trigger a sufficient number of cells after one week or to continuously trigger newly recruited cells towards the chondrogenic lineage efficiently.

Chapter 4

A novel approach to improve seeding efficiency and chondrogenic differentiation of mesenchymal stem cells for tissue engineering application

Abstract

For the chondral part of osteochondral constructs the application of mesenchymal stem cells (MSCs) still faces particular difficulties like poor cell seeding efficiency and insufficient cartilage generation. For chondrogenic differentiation cell aggregation is required and previous studies have shown that it can be applied to increase seeding efficiency.

We aimed to investigate the optimal aggregation time and its dependency on growth factor concentration. The aggregate size is confined by the pore size of three-dimensional scaffolds used in cartilage TE. To allow sufficient cell seeding, aggregate size should not exceed the pore size of the applied scaffold. Furthermore, we studied the effect of shortterm incubation with different concentrations of transforming growth factor β 1 (TGF β 1) on chondrogenic differentiation of MSCs.

MSCs were aggregated in chondrogenic medium, supplemented with 0, 10, 70 or 100ng/ml TGF β 1 for 4, 6 and 24h. Subsequently, aggregates were incorporated in a gel and cultured in chondrogenic medium without TGF β 1 for 21 days. Quantification of loaded cells and qualitative analysis of chondrogenic components such as glycosaminoglycans were performed.

An appropriate aggregate size could be achieved by incubating MSCs for 4h. No differences in aggregate sizes could be observed in aggregates exposed to different TGF β 1 concentrations. Furthermore, cells did not undergo chondrogenesis when cultured for 4h, independent on TGF β 1 concentrations. However, when exposed to TGF β 1 for additional 20hrs, aggregated cells differentiated into the chondrogenic lineage. This approach provides a promising tool for the application of MSCs for osteochondral tissue engineering by increasing seeding efficiency and improving generation of cartilage like tissue *in vitro* and *in vivo*.

Introduction

In reconstructive surgery and in orthopedics, demand of cartilage is very high. Since cartilage lacks a system of self repair, several methods have been established to substitute damaged or lost cartilage tissue. However, conventional treatments such as the application of allografts or autografts are not without disadvantages. Allografts carry the risk of transmitting diseases, cell death or graft defragmentation [218-220], and within the last years the immune response as an underestimated drawback after allograft implantation has been received increased attention [221-223]. Autografts are limited available and the harvest procedure can be accompany by donor site degradation and morbidity [29, 85].

Tissue engineering (TE) of cartilage has been introduced into research and clinic with some promise. A wide range of synthetic polymers and natural carriers have been tested as scaffolds for cartilage TE [42, 70, 224-228]. These scaffolds aim to be biocompatible, biodegradable, intend to provide mechanical stability, as well as support tissue regeneration. There is clear evidence that the production of extracellular matrix by chondrocytes depends on the scaffold type. Comparing several biocompatible materials such as collagen type I and polyglycolic acid (PGA), chondrocytes increase their collagen production when cultured on collagen type I sponges, whereas they produce significantly higher amounts of proteoglycans on PGA scaffolds [128]. Freed *et al.* discovered in increased rate of chondrocyte proliferation and deposition of cartilage specific glycosaminoglycans by chondrocytes when seeded on PGA-based scaffolds [47].

Our research group concentrates on architecture and composition of polyethylene oxide terephthalate / polybutylene terephthalate (PEOT/PBT) copolymers. A tremendous pool of scaffold compositions distinguished by properties like swelling, degradability and mechanical stability can be tailor-made by varying the ratio of hydrophobic PEOT and hydrophilic PBT blocks [63, 130, 195]. Moroni *et al.* produced three-dimensional PEOT/PBT scaffolds matching the mechanical properties of native hyaline cartilage [68]. It has been suggested that the implantation of scaffolds with mechanical properties matching the recipient site can prevent degradation of the surrounding tissue [229]. Therefore, these PEOT/PBT scaffolds may find application in cartilage TE.

However, cartilage TE depends not only on the scaffold materials, but also on the *in vitro* culture conditions. To find appropriate cell sources to create tissues and organs is still the major challenge. For cartilage TE, mostly autologous chondrocytes are expanded in culture, incorporated in a carrier matrix and implanted into the defect side. But the use of autologous chondrocytes raises disadvantages like the low cell number obtained during harvest, the loss of the cartilage-specific phenotype during culture expansion as well as donor side morbidity [22, 230-232].

A promising alternative is the use of mesenchymal stem cells (MSCs) isolated from adipose tissue [108] or bone marrow [100]. These cells are easy to isolate, have a high proliferation capacity as well as a high regeneration potential. They can be differentiated into various types of tissue such as tendon, bone or cartilage. However, whereas the osteogenic generation can be induced by seeding MSCs on osteoinductive materials directly *in vivo* [233], chondrogenic differentiation is only achieved when cells are pelleted prior to the differentiation, followed by incubation in chondrogenic differentiation medium containing transforming growth factor β 1 (TGF β 1) for 21 days *in vitro* [204, 216, 234].

Regarding future clinical application, this standard protocol is time and cost intensive. A shorter incubation time directly after isolation of the cells would be more applicable. We previously studied the influence of the TGF β 1 release profiles from PEO/PBT scaffolds

on chondrogenic differentiation of goat MSCs [201]. However, TE drawbacks still remained, because 2mm large pellets were used in this study, which exceeded the pore size of appropriate three-dimensional scaffolds. Attempts to digest pellets and harvest differentiated cells were rejected since a huge discrepancy occurred between initial cell number and cell number harvested after digestion (unpublished data). Therefore, this study was conducted to achieve increased seeding efficiency by using aggregates of MSCs in scaffolds that match the mechanical properties of native hyaline cartilage, and to establish an optimal incubation time and growth factor concentration in terms of aggregate size and cell differentiation.

Materials

Culture media and supplements were from Sigma (Zwijndrecht, The Netherlands) and Gibco (Breda, The Netherlands) unless otherwise noted.

Methods

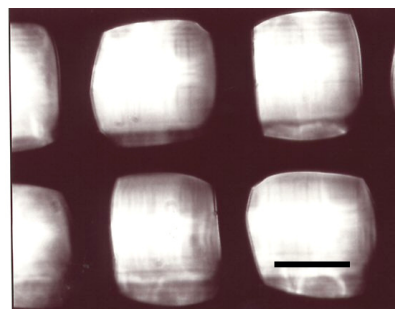
Bone marrow isolation and expansion

Caprine mesenchymal stem cells (MSCs) were harvested, isolated and cryopreserved as described previously [146]. For these experiments, MSCs were thawed at 37°C and replated at a density of 1000 cells/cm² in expansion medium containing α -modified Eagle's Medium, supplemented with 15% FBS, 1% Pen/Strep, 0.1mM ascorbate-2-phosphate acid and 2mM L-Glutamine. When 80% confluent, cells were trypsinized using 0.25% trypsin-EDTA and replated at a density of 1000 cells/cm². When reaching 80% confluence again, cells were trypsinized, washed twice in PBS and counted using a Burker Turk Counting chamber.

Aggregation and differentiation

An aggregate size that does not exceed the pore size of 3D fiber-deposited PEOT/PBT scaffolds with mechanical properties matching native cartilage (as described in chapter 1 of this thesis) was considered appropriate (Fig.1). Chondrogenic differentiation medium was composed of Dulbecco's modified eagle medium, supplemented with 1% penicillin/streptomycin, 1% ITS⁺, 100nM dexamethasone, 50 μ g/ml ascorbic 2-phosphate, 100 μ g/ml sodium pyruvate, 40 μ g/ml proline and TGF β 1 (R&D Systems, Abington, UK). MSCs were aggregated by inoculating a single cell suspension on an Ultra-Low Attachment Surface (Corning Life Sciences, later referred to as ultra-low attachment plate). 1x10⁶ cells/ml per well of a 24-well ultra-low attachment plate were incubated in differentiation medium with a concentration of 0, 10, 70 or 100ng/ml TGF β 1, respectively (Tab. 1) at 37°C in a humidified atmosphere of 5% carbon dioxide. Light microscopy pictures were taken after 4, 6 and 24hrs.

Figure 1: 3D fiber deposited PEOT/PBT scaffolds with critical pore size of 150 μ m matching native cartilage like mechanical properties. Aggregate size that does not exceed this pore size was considered appropriate. Light microscopy. Scale bar 250 μ m.



To investigate the influence of TGF β 1 on chondrogenic differentiation stage, we conducted three experiments.

In the first experiment, cells were inoculated in a 24-well ultra-low attachment plate with a density of 0.3×10^6 cells/well and incubated in differentiation medium, supplemented with 0, 10, 70 and 100ng/ml TGF β 1, respectively. After 24hrs, cells were collected per well in a separate polystyrene tube to avoid further aggregation, supernatant was removed and aggregates were mixed with 50 μ l matrigel® (1well/50 μ l matrigel®) (BD Bioscience, later referred to as matrigel). Mixtures were allowed to gel for 30 minutes at 37°C and subsequently cultured in differentiation medium without TGF β 1 for 20 days (Tab. 2).

In the second experiment, cells were inoculated in a 24-well ultra-low attachment plate with a density of 0.3×10^6 cells/well and incubated in differentiation medium, supplemented with 0, 10 and 70ng/ml TGF β 1, respectively for 4hrs. Following incorporation in 50 μ l matrigel/well as described above, aggregates were cultured in differentiation medium without TGF β 1 for 21 days (Tab. 3).

Table 1: Study design to assess aggregation of mesenchymal stem cells (MSCs) in different growth factor concentration for variable incubation periods.

		ng/ml TGF β 1			
		0	10	70	100
hrs	4	X	X	X	X
	6	X	X	X	X
	24	X	X	X	X

In the third experiment, cells were aggregated for 4hrs in differentiation medium, supplemented with 0, 10 and 70ng/ml TGF β 1 as described above. Subsequently, aggregates from each growth factor concentration were incorporated in matrigel and cultured in 0, 10 and 70ng/ml TGF β 1 for additionally 20hrs (Tab. 4).

All cultures were incubated at 37°C in a humidified atmosphere of 5% carbon dioxide.

Table 2: Study design to investigate the influence of different growth factor concentrations on chondrogenic differentiation of MSCs after 24hrs.

		ng/ml TGF β 1			
		0	10	70	100
hrs	24	X	X	X	X

Table 3: Study design to investigate the influence of different growth factor concentrations on chondrogenic differentiation of MSCs after 4hrs.

		ng/ml TGF β 1		
		0	10	70
hrs	4	X	X	X

Table 4: Study design to investigate chondrogenic differentiation of 4hrs aggregates incubated in different growth factor concentrations for additional 20hrs.

		ng/ml TGF β 1								
hrs	4	0			10			70		
	20	0	10	70	0	10	70	0	10	70

Analysis

SEM

Samples were fixed in 1,5% glutaraldehyde in 0,14 M sodium cacodylate buffer at 4°C for 48 h. After dehydration by graded ethanol series, samples were critical point dried using CO₂ in a Balzers model CPD 030 Critical Point Dryer. Next, samples were gold-sputtered (Cressington 108 Auto Cool Sputter Coater) and examined using a Philips XL30 FEG environmental SEM at a voltage of 10kV.

Histology

Samples were fixed in 1,5% glutaraldehyde in 0,14M sodium cacodylate buffer at 4°C for 48h. After dehydration by graded ethanol series, specimens were embedded in glycol methylacrylate (GMA). Histological sections of 5 μ m were made (Microtom HM 355S) and stained with Safranin O/ fast green. Nuclei were costained with hematoxyline.

Biochemical assays

At 14 and 21 days, samples were harvested, washed in PBS and frozen at -80°C followed by digesting in 1mg/ml proteinase K, 10 μ g/ml pepstatin A and 180 μ g/ml iodoacetamide overnight at 56 °C.

Total DNA was quantified by using the CyQuant dye kit (Invitrogen) and measuring with a spectrofluorometer at 520 nm., while glycosaminoglycans (GAGs) were determined by staining GAGs with dimethylene blue and measuring the color intensity at 540nm using a spectrofluorometer. Chondroitin-sulfate served here as a standard.

Statistical evaluation

All quantitative data are presented as means \pm standard deviations (n = 3). The data obtained were analyzed using SPSS software (version 12.0). Analysis of variance (ANOVA) was used and significant differences were determined by Bonferroni post-hoc test (p<0.05 was considered significant).

Results

The first part of this study addresses the feasibility to aggregate MSCs and to estimate the appropriate duration and growth factor concentration. We incubated single cells in wells for 4, 6 or 24hrs in differentiation medium containing TGF β 1 concentrations ranging from 0 to 100ng/ml.

Macroscopic analysis using light microscopy revealed that after 4h most aggregates were not attached to the bottom of the culture dish, but floated freely. Small aggregates of approximately 50 to 200 μ m in diameter were formed (Fig. 2A). These small aggregates maintained their integrity during pipetting, indicating their stability. Cells within the aggregates showed a rounded morphology. The aggregate size did not exceed the diameter of the pores of the scaffold. Results were independent on TGF β 1 concentration; no difference could be found when aggregates were cultured in 0, 10, 70 100ng/ml, respectively (data not shown).

After 6hrs, aggregates had increased in size indicating that aggregation had continued (Fig. 2B). Aggregates did not disintegrate and cells showed a round morphology. After 24hrs, aggregate morphology changed drastically (Fig. 2C). Large, round pellets of approximately 250 to 500 μ m in diameter were found.

The effects of culture condition on cell aggregation and aggregate size were independent on growth factor concentration. Results for 4, 6 and 24hrs incubation period were comparable for 0, 10, 70 and 100ng/ml, respectively; no differences in cell morphology or aggregate size could be revealed (data not shown).

In conclusion, within a short incubation period of 4 and up to 24hrs aggregation of MSCs is possible. The size of the aggregates is time depending; large aggregates after 24hrs, small aggregates after 4hrs. A short incubation period is more efficient regarding labor and costs when compared to the standard period of 21 days for chondrogenic differentiation of MSCs.

Therefore, in a second experiment we tested the hypothesis that 24hrs incubation in differentiation medium is sufficient to trigger chondrogenic differentiation of MSCs. 24hrs aggregates were produced as described in the first experiment. Subsequently, aggregates cultured in 0, 10, 70 or 100ng/ml TGF β 1 containing differentiation medium were incorporated in matrigel to avoid further aggregation, cultured without growth factors and analyzed after 21 days.

Prior to the gel incorporation, aggregate morphology and size were similar for 0, 10, 70 or 100ng/ml, no differences in cell morphology or aggregate size could be found

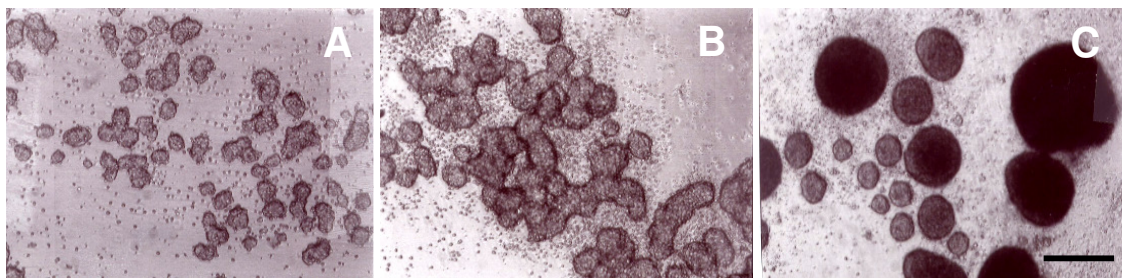


Figure 2: Aggregate size after 4, 6 and 24hrs. **(A)** 4hrs aggregates are appropriate in size, with approximately 50 - 100 μ m in diameter. **(B)** After 6hrs, aggregates increase in size (approximately 200 - 300 μ m). **(C)** After 24hrs, single pellets can be distinguished. Most pellets exceed the appropriate size (approximately 250 - 500 μ m in diameter). Light microscopy. Scale bar 250 μ m.

(Fig. 3 A-D). After 21 days, however, Safranin O staining revealed evident differences (Fig. 3 E-K). At 0ng/ml, samples were small and did not stain positive for Safranin O (Fig. 3 E). The biochemical assay did not detect chondrogenic markers such as glycosaminoglycans (GAGs). At 10ng/ml aggregates showed weak positive Safranin O staining (Fig. 3 F). GAGs could be detected clearly when biochemically analyzed. The cell number as distinguished by DNA analysis was significantly higher compared to 0ng/ml. At 70ng/ml, the ECM of the cells stained very strongly for Safranin O (Fig. 3 G). The cells exhibited a round, chondrocyte-like morphology (Fig. 3 J). Also biochemical analysis of GAGs showed significantly higher amounts than 10ng/ml, while DNA quantification showed no significant differences. At 100ng/ml, no further beneficial effects could be revealed when compared to 70ng/ml. Cells showed comparable extensive positive staining of the ECM and the cell morphology was similar (Fig. 3H, K). Also DNA and GAG quantification were not different. These results show that 24hrs incubation in TGF β 1 were sufficient to induce chondrogenic differentiation of MSCs *in vitro*. However, the size of 24hrs aggregates exceeded the pore size of the preferred scaffold.

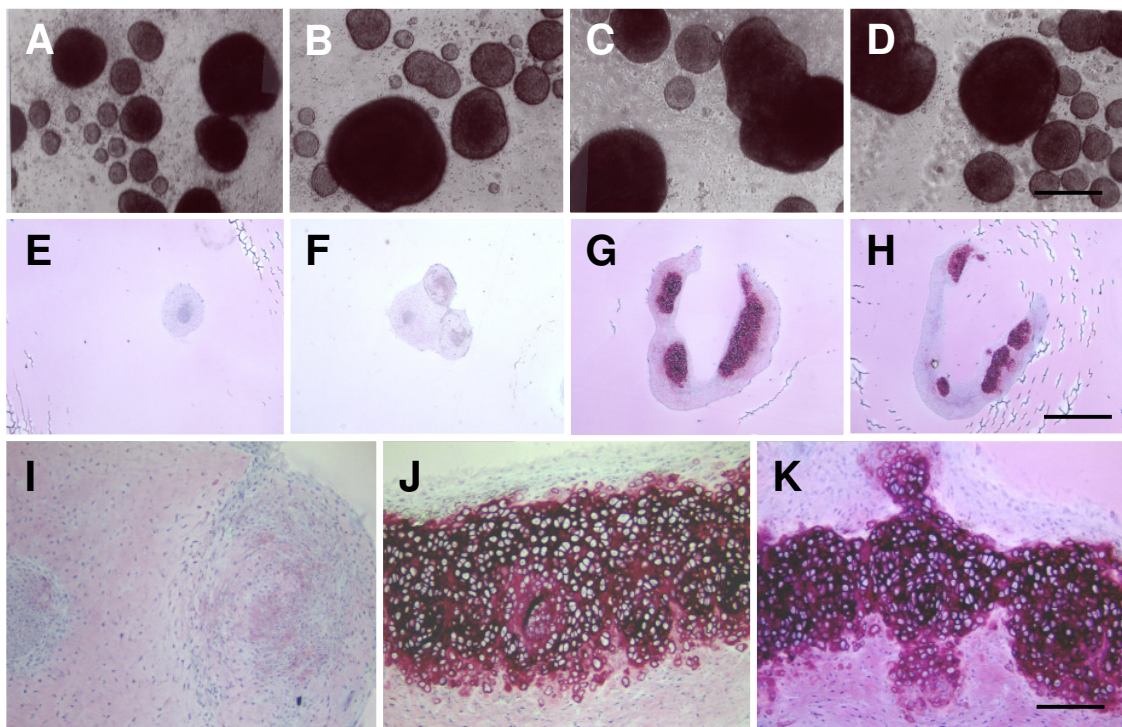


Figure 3: Aggregate size (A - D) and chondrogenic differentiation (E - K) depending on TGF β 1 concentration after 24hrs.

Aggregate size is independent on TGF β 1 concentration. Diameter is approximately 250 – 500 μ m at (A) 0ng/ml, (B) 10ng/ml, (C) 70ng/ml and (D) 100ng/ml TGF β 1, respectively. However, chondrogenic differentiation depends on growth factor concentration. (E) At 0ng/ml TGF β 1 no positive staining can be detected. (F, I) At 10ng/ml weak positive areas can be identified. (G, J) At 70ng/ml and (H, K) at 100ng/ml strong positive extracellular matrix surrounding chondrocyte like cells can be distinguished. Note the clear formation of lacunae.

(A – D) Light microscopy. Scale bar 250µm. (E – K) Safranin O staining. Scale bar 1mm (E - H), 200µm (I - K).

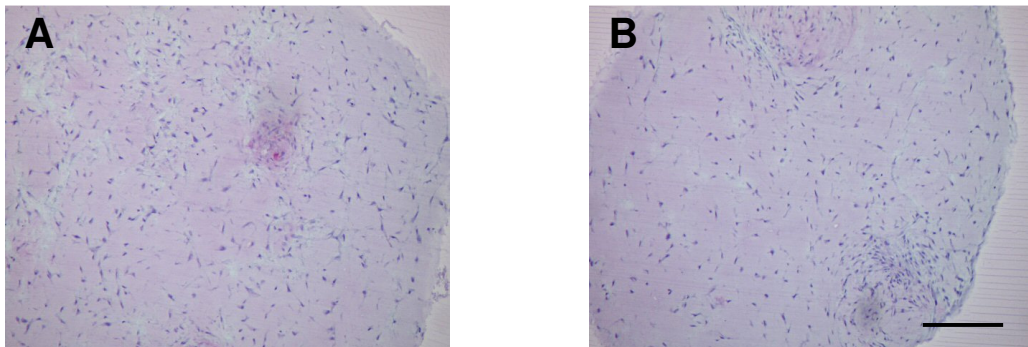


Figure 4: Histological analysis of aggregates in chondrogenic differentiation medium with different TGF β 1 concentrations after 4hrs. Samples cultures in (A) 10ng/ml and (B) 70ng/ml TGF β 1 are not stained positive. Due to instability during histological processing, histology of cultures of 0ng/ml TGF β 1 is not available. Safranin O staining. Scale bar 200µm.

Therefore, in a third experiment we investigated the influence of TGF β 1 on chondrogenic differentiation stage after 4hrs since 4hrs incubation was sufficient to form small aggregates. Results showed that samples did not sustain histological processing when cultured without TGF β 1 suggesting that no extracellular matrix was generated. Samples cultured with TGF β 1 were stable (Fig. 4). However, they did not stain positive for Safranin O when cultured with 10 (Fig. 4A) or 70ng/ml TGF β 1 (Fig. 4B), respectively. Biochemical analysis verified these findings; no GAGs could be detected for samples cultured in 0ng/ml and no substantial amounts using 10 or 70ng/ml TGF β 1 (Fig. 5).

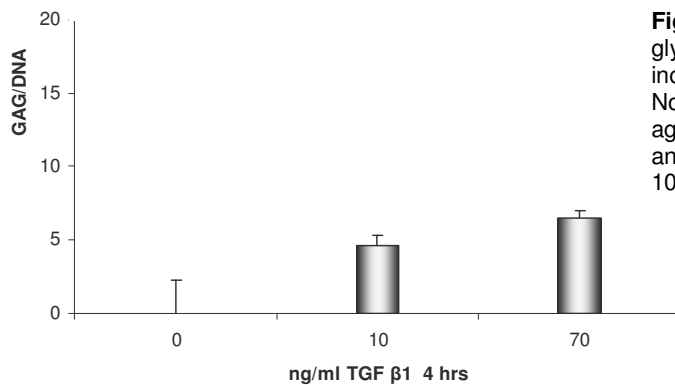


Figure 5: Quantification of glycosaminoglycans (GAGs) after 4hrs incubation in 0, 10 and 70ng/ml TGF β 1. No GAGs can be detected when aggregates are cultured in 0ng/ml TGF β 1 and no significant amounts for cultures in 10 or 70ng/ml.

These results suggest that 4hrs in differentiation medium is not sufficient to induce chondrogenic differentiation, independent on the growth factor concentration used. Finally, we conducted an experiment combining the conclusions from the three previous experiments. MSCs were aggregated for 4hrs in 0, 10 and 70ng/ml TGF β 1, respectively, incorporated in a gel to hinder further aggregation, but subsequently cultured with different concentrations TGF β 1 (0, 10 and 70ng/ml, respectively) for additional 20h. Surprisingly, the differentiation stage and the amount of GAGs were independent on the TGF β 1 concentration applied for the first 4h. Also, when cells were aggregated without

TGF β 1 in the first 4hrs additional incubation for 20hrs with TGF β 1 was sufficient to induce chondrogenic differentiation (Fig. 6 A, D). Cells exhibited a Safranin O positive

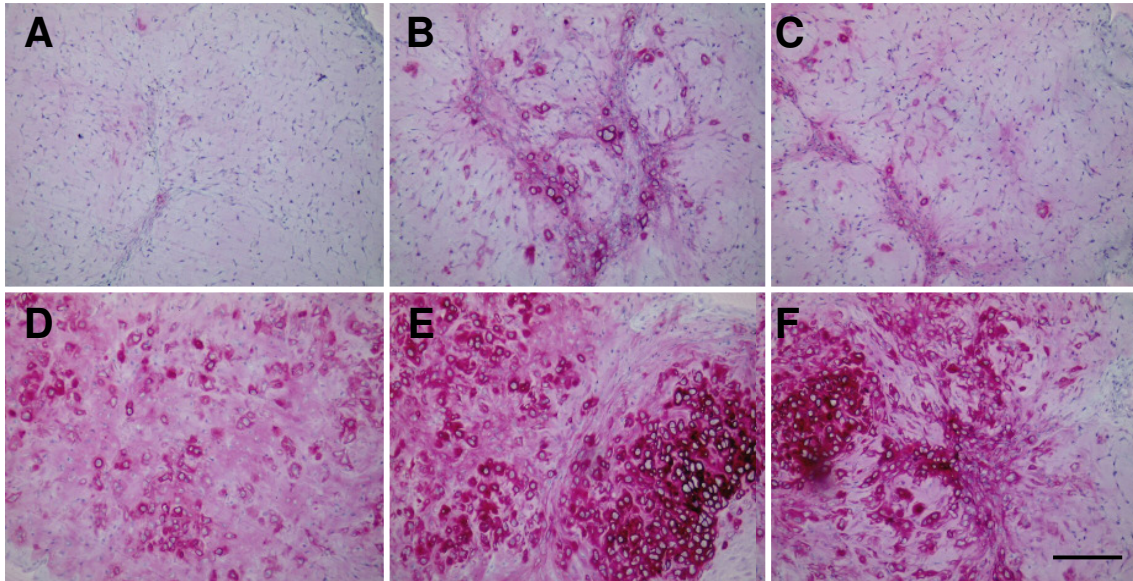


Figure 6: Histological analysis of 4hrs aggregates incubated in chondrogenic differentiation medium with different TGF β 1 concentrations for additional 20hrs. ECM stains positive when aggregates were cultured in 10ng/ml TGF β 1 for additional 20hrs, regardless if (A) 0, (B) 10 and (C) 70ng/ml, respectively, were applied in the first 4hrs. Cells exhibit a round morphology and are situated in lacunae. When cultured in 70ng/ml for additional 20hrs, ECM stains more intense. Also these results are independent on TGF β 1 concentration used for the first 4hrs ((D) 0, (E) 10 and (F) 70ng/ml, respectively). Safranin O staining. Scale bar 200 μ m.

matrix. They revealed a chondrocyte-like morphology and were located in lacunae. When compared to cultures in 10ng/ml (Fig. 6A-C), the amount of positive areas and the intensity of the staining were higher for aggregates additionally cultured in 70ng/ml TGF β 1 (Fig. 6 D-F) The biochemical analysis of the samples showed high amounts of GAGs; at 70ng/ml TGF β 1 significantly higher than at 10ng/ml TGF β 1 ($p > 0.05$; Fig. 7).

Discussion

The most widely described technique for differentiating MSCs into cartilage is the use of a micromass system and subsequent incubation in serum-free medium, supplemented with TGF β 1 for 21 days in vitro [116, 205]. However, when applied to three-dimensional biomaterials controvert mechanisms challenging research. On one hand, cell seeding efficiency is very poor due to the absence of adhesion proteins in serum-free differentiation medium. On the other hand, cell attachment enhanced by changing the surface tension or sealing cells with a gel onto the material does not enhance chondrogenesis of MSCs (this thesis). Another aspect is the cell density. The micromass model is applied because chondrogenic differentiation depends on cell density [235-238]. The importance of high-density cultures and appropriate cell-cell contact is further elucidated by studies conducted by Zhang *et al.* Inhibition of gap junction-mediated intercellular communication blocked growth factor dependent chondrogenesis in the limb bud model [239]. Therefore, a initially high cell number or the aggregation of cells prior to incorporation into the scaffold increases seeding efficiency and supports chondrogenesis.

In this study, we focused on the aggregation of MSCs to improve cell incorporation into synthetic, biodegradable scaffolds optimized for cartilage tissue engineering [68].

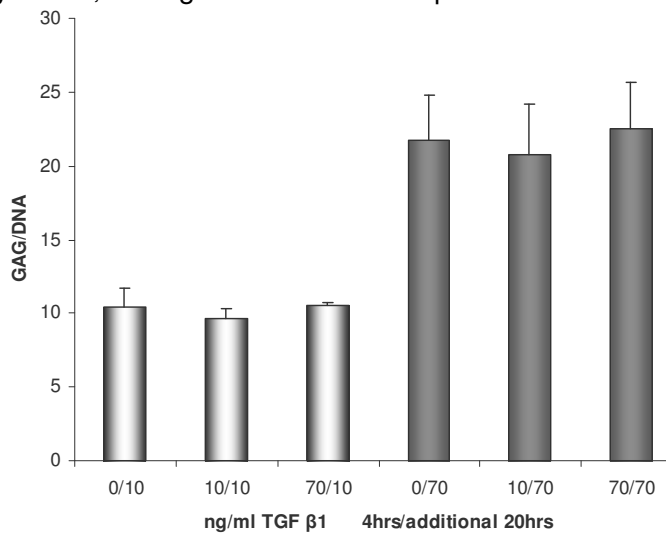


Figure 7: Quantification of GAGs of 4hrs aggregates after additional 20hrs incubation in 10 (light grey) and 70ng/ml (dark grey) TGF β 1, respectively. Significantly higher amounts are detected when aggregates were additionally incubated in 70ng/ml ($p>0.05$), independent on TGF β 1 concentration applied in the first 4hrs.

However, when centrifugal forces are applied to aggregate cells, the resulting pellets are oversized relatively to the pores of the scaffold. Undifferentiated MSCs express a variety of adhesion molecules [100] and exhibit a spindle-shaped morphology. On standard tissue culture, plastic protein adsorption occurs due to its hydrophobic surface. Extracellular matrix proteins from the culture medium or present at the cellular surface allow cell attachment and spreading. Usually, biomaterials are placed onto bacteriological plastic to increase seeding efficiency of MSCs. The plastic presents a negatively charged, hydrophilic surface where protein adsorption is blocked and cells remain in single cell suspension unless they attach onto the biomaterial. Aggregate formation of MSCs in bacteriological dishes has never been observed and the reason for that is unclear (internal communication). However, as described in this chapter, when cultured on a neutral charged, hydrophilic surface MSCs aggregated successfully. These surfaces have been applied effectively to maintain a spheroid phenotype of anchorage dependent cell types such as melanoma cells, fibroblasts and chondrocytes [240-243]. In addition, they are also used to study invasion of spheroid cell models in cancer research [244, 245]. In our study, we presented the same surface to MSCs. Cultured in chondrogenic medium, these cells maintained a spheroid phenotype. Furthermore, by varying the incubation time, we were able to aggregate the cells and to control the aggregate size. Incubation for 24 hrs resulted in large aggregates, which exceeded the pore size of the intended scaffold, whereas incubation for 4 hrs led to aggregates which were small, and which fitted into the pores of appropriate scaffolds.

However, regarding chondrogenic differentiation, our results show that only 24 hrs of incubation is sufficient to induce MSCs into the chondrogenic lineage in the presence of TGF β 1. These results are consistent with results from studies investigating the signaling pathway of TGF β 1-mediated chondrogenesis of human MSC pellets. Its triggering action on the cells occurred rapidly [215, 217]. Within 25 minutes the TGF β 1 receptors are saturated. Within one day the expression of cell adhesion molecules functioning during precartilaginous condensation and leading to chondrogenic differentiation were upregulated. After 5 days, they were already downregulated whereas changes in cell morphology and an increase of ECM production were observed. The same rapid chondrogenic induction of cells was suggested by temporal pattern of gene expression.

For all culture conditions, the upregulation of the collagen type II and aggrecan gene was seen during the first 12 days of culture [201]. Over the remaining culture period, the gene expression did not change significantly. And also Caterson *et al.* found that during the first three days of culture human MSCs underwent chondrogenesis when seeded on PLA scaffolds and exposed to 50ng/ml of TGF β 1 after a short incubation time [147]. The results of these studies suggest that TGF β 1 plays a crucial role during the initial phase of chondrogenesis and is not necessary during later phases. The majority of MSCs have made the cell fate decision to undergo chondrogenesis within the first 20hrs, after which TGF β 1 is not required anymore. Furthermore, at 4h, aggregate size was appropriate, but chondrogenic differentiation was not induced, while at 24 hrs aggregates were oversized but chondrogenic differentiation was induced. Therefore, to evaluate which growth factor concentration is required to obtain chondrogenic differentiation with the proper aggregate size, we applied a new method taking these two parameters into consideration. Our results demonstrate that the method, by which aggregation is inhibited after 4 hrs but chondrogenesis is induced for additional 20 hrs, is sufficient to achieve suitable aggregate size while chondrogenesis occurred. Since this aggregation proceeded independent on the presence or absence of TGF β 1, its influence on aggregate formation can be neglected. Moreover, applying different concentrations of TGF β 1 for 4 hrs had no effect on chondrogenic differentiation. However, analyses of chondrogenesis after incubation for additional 20 hrs suggest a concentration dependency; at 10ng/ml TGF β 1, GAG staining was weaker and quantitative data significantly lower compared to 70ng/ml. These data are consistent with previous publications showing the dose dependency of members of the TGF β family on chondrogenesis [179, 246-249]. However, when applied to MSCs as suggested by this study, it brings MSC-base cartilage TE one step closer to medical application.

Conclusion

MSCs form stable aggregates when cultured in chondrogenic differentiation medium using low attachment wells. Appropriate aggregate size can be achieved within 4 hrs. Aggregation is independent on TGF β 1 concentration, without growth factor cells also form aggregates. However, when growth factors are applied, it is not sufficient to induce chondrogenic differentiation within 4 hrs; cultivation for additional 20 hrs in TGF β 1 is required. In addition, our results suggest that an optimal growth factor concentration is between 10 and 70ng/ml TGF β 1. Further intensive studies are necessary to investigate the applicability in three-dimensional scaffolds. First attempts have been undertaken and preliminary results are promising. Advantages of this technique include easy handling, fast and efficient cell incorporation and cost and time efficient cell differentiation.

Chapter 5

3D fiber deposited electrospun integrated scaffolds enhance cartilage tissue formation

Abstract

Despite the periodical and completely interconnected pore network that characterize rapid prototyped scaffolds, cell seeding efficiency remains still a critical factor for optimal tissue regeneration due to the current resolution limits in pore size. We present here a novel three-dimensional (3D) scaffold fabricated by combining 3D fiber deposition (3DF) and electrospinning (ESP). Scaffolds consisted of integrated 3DF macrofiber periodical and ESP microfiber random networks (3DFESP), where the 3DF construction provides structural integrity and mechanical properties and the ESP network works as a “sieving” and cell entrapment system, at the same time offering cues at the extracellular matrix (ECM) scale. Primary bovine articular chondrocytes were isolated, seeded, and cultured for 4 weeks on 3DF and 3DFESP scaffolds to evaluate the influence of the integrated ESP network on cell entrapment and on cartilage tissue formation. 3DFESP scaffolds showed a better cell entrapment as compared to 3DF scaffolds. This was accompanied by a higher amount of ECM (expressed in terms of sulphated glycosaminoglycans or GAG) and a significantly higher GAG/DNA ratio after 28 days. SEM analysis of the constructs revealed a rounded cell morphology on 3DFESP scaffolds, whereas a spread morphology was observed on 3DF scaffolds, suggesting a direct influence of fiber dimensions on cell differentiation. Furthermore, also ESP surface topology influenced cell morphology. Thus, the integration of 3DF and ESP techniques provide a new set of “smart” scaffolds for tissue engineering applications.

Introduction

Rapid prototyped (RP) scaffolds are quite promising in tissue engineering, as they can be custom-shaped with a completely interconnected pore network [250-252]. Several studies focused on the development of different rapid prototyping techniques [132, 144, 253-257] and on scaffolds optimization [258-261]. In all of these techniques, pore volume and architecture can be designed in a CAD/CAM controlled manner, resulting in a modulation of scaffold's mechanical properties [145] and in a proficient nutrient perfusion determinant for cell survival [67]. They can be comprised of different materials [61, 254, 262, 263], they can combine gradients of porosities [152], and they can be designed to match specific tissue requirements, resulting in multifunctional constructs [32, 264, 265].

However, the scaffold's pore resolution poses still a limit in cell seeding efficiency and tissue formation. The pore size of RP scaffolds are relatively large as compared to cells dimensions and a high number of cells are needed to obtain a sufficient number of attached cells that produce enough extracellular matrix to functionalize the tissue engineered construct. This eventually results in expensive and extensive cell isolation, culture, and expansion processes, which may hamper the clinical relevance of RP scaffolds. A possible way to improve cell seeding efficiency is to aggregate cells [266-268] prior to seeding them onto the scaffolds, so that cell clumps will be better entrapped in the pores. Furthermore, cell aggregation is known to enhance cell-cell signaling [269], resulting in a better tissue formation [270]. Another possibility can be offered by introducing in RP scaffolds a micron scale fibril networks that have the double advantage to function as a "sieve" for cell entrapment and to provide extracellular matrix-like cues to cells. This can be achieved by integrating rapid prototyping with another technique like electrospinning (ESP). ESP fibers have typically dimensions varying from the nano- to the micro-scale, which results from the application of a high voltage electric field to a polymeric solution pumped into the field [271-273]. Depending on the pumping flow rate, the electric field intensity, and the polymer solution concentration, fibers of different diameter and surface topology can be obtained [273-276]. Furthermore, ESP scaffolds have been shown to influence cell proliferation rate and morphology depending on their size and surface texture [277-279].

Therefore, the aim of this study was to combine a rapid prototyping fabrication technique like 3D fiber deposition (3DF) with electrospinning (ESP) to fabricate integrated macro- and μ -fiber polymeric scaffolds (3DFESP) and to assess the influence of the microfibrillar network on cell entrapment and differentiation into cartilage tissue. Three scaffolds construct were considered: 3DF scaffolds as such, and 3DFESP integrated scaffolds with two different ESP network densities determined by varying the electrospinning time,

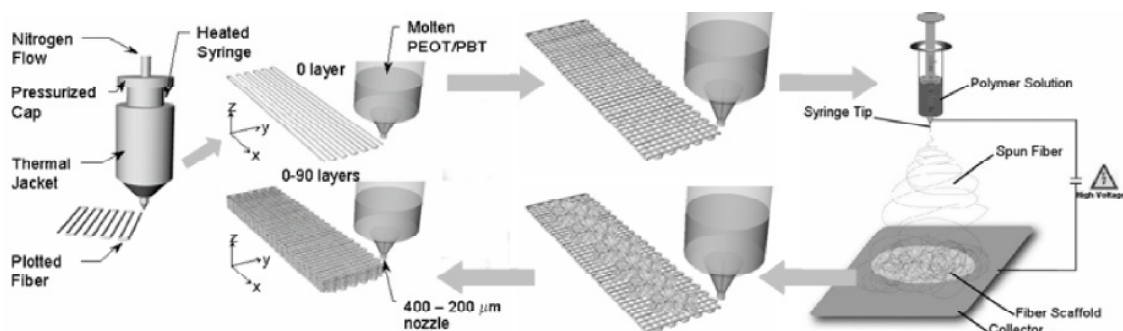


Figure 1: Schematic draw of the integration of 3DF and ESP fabrication techniques.

as depicted in Fig. 1. Primary bovine articular chondrocytes were seeded on the scaffolds and cultured for 4 weeks. The distribution and the amount of cells and extracellular matrix present on the scaffolds were considered as determinants for a better scaffold performance. 3DF and 3DFESP scaffolds were fabricated with block-copolymers of polyethyleneoxide-terephthalate(PEOT) and polybutylene-terephthalate (PBT). These poly(ether ester) multiblock copolymers are thermoplastic elastomers which display good physical properties like elasticity, toughness and strength in combination with easy processability. These properties result mainly from a phase separated morphology in which soft, hydrophilic PEO segments at environmental temperatures are physically cross-linked by the presence of hard, semi crystalline PBT segments. In contrast to chemically cross-linked materials, these cross-links are reversible and will be disrupted at temperatures above their glass transition- or melting point, which gives the material its good processability. This class of polymers have been extensively studied for in vitro and in vivo biocompatibility [280-283] and found commercial clinical applications (PolyActive™, IsoTis Orthopaedics S.A.) as cement stoppers and bone fillers in orthopedic [284, 285]. Being polyether-esters degradation occurs in aqueous media by hydrolysis and oxidation, the rate of which varying from very low for high PBT contents to medium and high for larger contents of PEOT and longer PEO segments [63, 195]. Similarly, by varying the PEOT/PBT ratio and the length of the PEO segments, a series of copolymers can be attained covering a wide range of mechanical properties with different abilities to swell in aqueous media.

We report here a novel strategy in scaffold design for tissue engineering applications, where the combination and integration of different scaffold fabrication technologies generates a family of multifunctional 3D scaffolds that significantly enhance tissue regeneration. Specifically, we show that the simultaneous presence of mechanical and physical cues at the macro, micro, and nano scale is responsible for this improvement and must be taken into account in the design of scaffolds for tissue engineering applications.

Materials

Polyethylene oxide terephthalate/polybutylene terephthalate (PEOT/PBT) copolymers were obtained from IsoTis S.A. (Bilthoven, The Netherlands). The copolymer composition used in this study was 300PEOT55PBT45 where, following an aPEOTbPBTc nomenclature, a is the molecular weight in g/mol of the starting PEG blocks used in the copolymerization, while b and c are the weight ratios of the PEOT and PBT blocks, respectively.

Methods

Scaffolds Fabrication

3D fiber deposited-electrospun integrated (3DFESP) scaffolds were manufactured by combining a Bioplotter device (Envisiontec GmbH, Germany) and a home-assembled electrospinning (ESP) apparatus. The Bioplotter is essentially an XYZ plotter device as previously described [258, 286]. Briefly, the polymers were put in a stainless steel syringe and heated at $T = 190\text{ }^{\circ}\text{C}$ through a thermo-stated cartridge unit, fixed on the "X"-mobile arm of the apparatus. When the molten phase was achieved, a nitrogen pressure of 5 Bars was applied to the syringe through a pressurized cap. Rectangular block models were loaded on the Bioplotter CAM (PrimCAM, Switzerland) software and deposited layer by layer, through the extrusion of the polymer on a stage as a fiber. The

deposition speed was set to 300 mm/min. Scaffolds were then characterized by the fiber diameter (through the nozzle diameter), the spacing between fibers in the same layer, the layer thickness and the configuration of the deposited fibers within the whole architecture. In this study, the nozzle internal diameter was 400 μ m, the fiber spacing was set to 800 μ m, the layer thickness was set to 225 μ m, and the scaffold architecture was determined by a 0-90 layer configuration where fibers were deposited with 90 $^{\circ}$ orientation steps between successive layers.

Electrospun fibrous networks were fabricated from a 20% w/v polymer solution in a 90%/10% v/v chloroform/hexafluoroisopropanol mixture. The ESP device consists of a high voltage (0-30 kV) generator (NCE 30000, Heinzinger Electronic GmbH, Germany) connected to a syringe, where the polymer solution is contained, and to a collector plate. When a high voltage is applied, an electric field is formed between the syringe needle (positive pole) and the collector (negative pole). The polymer solution is then pushed out of the syringe by a pump at variable flow rates depending on the electrostatic field strength. When the intensity of the electrostatic field is high enough to surpass the surface tension of the liquid drop at the tip of the needle, the drop is pulled out into a jetting filament and deposited as a dry fiber on the collector. The fibrous network is characterized by the voltage applied, the air gap (distance between the syringe needle and the collector plate), the pump flow rate, the syringe needle. In our experimental set up the voltage kept constant at 15 kV, the air gap was fixed at 15 cm, the flow rate at 0.39 ml/min, and the needle used had an internal diameter of 0.9 mm.

3DFESP scaffolds were fabricated by electrospinning a fibrous network layer every two layers of 3D fiber-deposited mesh until a scaffold height of 4 mm was reached (Fig. 1). Two different network densities were used to evaluate its influence on cell entrapment and tissue formation. The ESP fiber density was determined as the time frame used during electrospinning. Specifically, 3DFESP scaffolds with a fibrous network spun for 2 minutes (3DFESP-2) and for 30 seconds (3DFESP-30) were considered.

Scaffold Characterization

Cylindrical plugs of 4 mm in diameter by 4 mm in height were considered for characterization. The constructs were analyzed with a Philips XL 30 ESEM-FEG scanning electron microscopy (SEM). Samples were gold sputter (Carrington) before SEM analysis. The porosity of 3DF scaffolds was calculated following the theoretical approach by Landers *et al.*[286]:

$$P = 1 - \frac{V_{\text{scaffold}}}{V_{\text{cube}}} = 1 - \frac{\pi}{4} \cdot \frac{1}{\frac{d_2}{d_1}} \cdot \frac{1}{\frac{d_3}{d_1}}$$

(1)

where P is the scaffold porosity, d1 the fiber diameter, d2 the fiber spacing and d3 the layer thickness.

The porosity of ESP networks and 3DFESP scaffolds was experimentally measured by analyzing the mass and the volume of each structure, as:

$$P = 1 - \frac{M}{V} \cdot \frac{1}{\rho}$$

(2)

where, M and V are the measured mass and volume of the polymeric scaffolds, while ρ is the specific density of 300PEOT55PBT45 (1.2 g/cm 3).

3D scaffolds for culture experiments were sterilized in isopropanol (IPASEPT 70, VWR International) for 15 minutes, thoroughly washed with a phosphate buffered saline (PBS)

solution (Gibco-BRL) three times, and incubated over night in culture medium prior cell seeding.

Cell Seeding

Chondrocytes were isolated via collagenase digestion from articular cartilage harvested from an 18-month old bovine knee joint. Primary cells were aggregated with 300µg/ml of fibronectin (Invitrogen), statically seeded at a density of 3 millions in 50 µl of medium and cultured in scaffolds for 1, 7, and 28 days (n=6). 3DF, 3DFESP-2, and 3DFESP-30 scaffolds of 4mm in diameter and 4mm in height fabricated with 0-90 architecture were considered. The culture medium contained HEPES (Invitrogen)-buffered DMEM (Invitrogen), supplemented with 10% fetal bovine serum (FBS, Sigma-Aldrich), 0.2mM ascorbic acid 2-phosphate (Invitrogen), 0.1mM non-essential amino acids (Sigma-Aldrich), 0.4mM proline (Sigma-Aldrich), 100units/ml penicillin (Invitrogen), and 100µg/ml streptomycin (Invitrogen). Constructs were cultured at 37°C in a humid atmosphere with 5% CO₂. Medium was refreshed twice a week and subsets of chondrocytes were used for further subculturing or cryopreservation upon reaching near confluence. Scaffolds were compared to evaluate the influence of the ESP network on chondrocytes entrapment in the pores, differentiation and morphology.

Biochemical Analysis

DNA and glycosaminoglycans (GAG) assay were performed after 1, 7, and 28 days of culture. Constructs were also digested overnight at 56 °C in a Tris-EDTA buffered solution containing 1 mg/ml proteinase K, 18.5µg/ml pepstatin A, and 1µg/ml iodoacetamide (Sigma-Aldrich). Quantification of total DNA was done with Cyquant dye kit according to the manufacturers description (Molecular Probes) using a spectrofluorometer (LS 50B, Perkin Elmer). GAG amount was determined spectrophotometrically (EL 312e Bio-TEK Instruments) after reaction with dimethylmethylene blue dye (DMMB, Sigma-Aldrich) by measuring absorbance at 520 nm. The final amount was calculated using a standard of chondroitin sulphate B (Sigma-Aldrich).

Histology Analysis

Samples were fixed overnight in 0.14 M cacodylate buffer (pH = 7.2 – 7.4) containing 1.5% glutaraldehyde (Merck). Scaffolds were subsequently dehydrated in sequential ethanol series, plastic embedded in glycol-methacrylate (Merck) and cut using a microtome to yield 5 µm sections. Slices were stained with Safranin O (Sigma-Aldrich) to visualize extracellular matrix (glycosaminoglycans, GAGs), and counterstained with haematoxylin (Sigma-Aldrich) and fast green (Merck) to visualize cytoplasm and cells nuclei. Mounted slides were examined under a light microscope (Nikon Eclipse E400) and representative images captured using a digital camera (Sony Corporation, Japan) and Matrix Vision software (Matrix Vision GmbH, Germany). Tissue constructs on scaffolds were also analyzed by SEM. Specimens were fixed and dehydrated as described above and critical point dried from liquid carbon dioxide using a Balzers CPD 030 machine. Samples were then gold sputtered and studied under the SEM.

Statistical Analysis

Statistical analysis was performed using a Student's t-test, where the confidence level was set to 0.05 for statistical significance. Values in this study are reported as mean and standard deviation.

Results

1. Scaffold Characterization

The surface and cross section of 3DFESP scaffolds is illustrated in Fig. 2. SEM analysis revealed a fiber diameter of $268 \pm 32 \mu\text{m}$, a fiber spacing of $807 \pm 28 \mu\text{m}$, and a layer thickness of $227 \pm 20 \mu\text{m}$ for the 3DF scaffolds, and a fiber diameter of $10 \pm 2.8 \mu\text{m}$ for the ESP network. This corresponded to a porosity of $69 \pm 3\%$ for the 3DF scaffolds, and to a porosity of $94 \pm 1.6\%$ for the ESP network. The porosity of the integrated 3DFESP scaffolds was measured as $50 \pm 3\%$. The scaffolds produced were 100% interconnected porous structures and no layer delamination phenomenon occurred.

2. Cell entrapment and tissue formation

During the 4 weeks of culture on the 3DF and on the 3DFESP scaffolds, DNA amount and GAG formation were measured. Fig. 3 shows the DNA amount for the different scaffolds considered in the study. At day 1 DNA significantly increased from 3DF to 3DFESP-2, suggesting a better cell entrapment in the pores of the 3DFESP scaffolds. With increasing ESP network density, DNA did not significantly change. Specifically, DNA was measured as $5.21 \pm 0.94 \mu\text{g}$ for 3DF, $7.57 \pm 1.86 \mu\text{g}$ for 3DFESP-30, and $7.81 \pm 1.08 \mu\text{g}$ for 3DFESP-2 scaffolds. At day 7 a similar trend was found and the increase for 3DFESP-2 was significantly different as compared to 3DF scaffolds, indicating that cells were still more efficiently retained in the integrated scaffolds during the proliferation time. The cell amount, however, was found to be comparable between the scaffolds after 4 weeks of culture. This might imply a redistribution of the cells in the constructs due to extracellular matrix formation. More interestingly, the GAG amount increased in the whole culture period with the same trend as for DNA, suggesting a better tissue formation in the integrated scaffolds as depicted in Fig. 4. The increase was significantly for 3DFESP as compared to 3DF scaffolds all over the culture period. Specifically, GAG increased from $160.29 \pm 46.43 \mu\text{g}$ for 3DF, to $321.1 \pm 77.86 \mu\text{g}$ for 3DFESP-30, and to $316.84 \pm 75.93 \mu\text{g}$ for 3DFESP-2 scaffolds over a month. Even more interestingly, a higher degree of differentiation was found for chondrocytes cultured on 3DFESP scaffolds, as shown in Fig. 5 from the GAG/DNA ratio. GAG/DNA significantly increased in 3DFESP scaffolds as compared to 3DF scaffolds alone during the month of culture. In particular, the increase was measured at day 1 as 4.37 ± 2.13 for 3DF, 5.87 ± 1.11 for 3DFESP-30, 7.24 ± 1.59 for 3DFESP-2 scaffolds. At day 28 GAG/DNA ratios reached 22.23 ± 4.18 for 3DF, 54.26 ± 12.72 for 3DFESP-30, and 54.77 ± 8.11 for 3DFESP-2. Chondrocyte differentiation in 3DFESP scaffolds can be also qualitatively detected by SEM analysis. After 28 days of culture, chondrocytes appeared completely spread and attached to the 3DF scaffolds' macro-fibers (Fig. 6A, D), whereas they remained

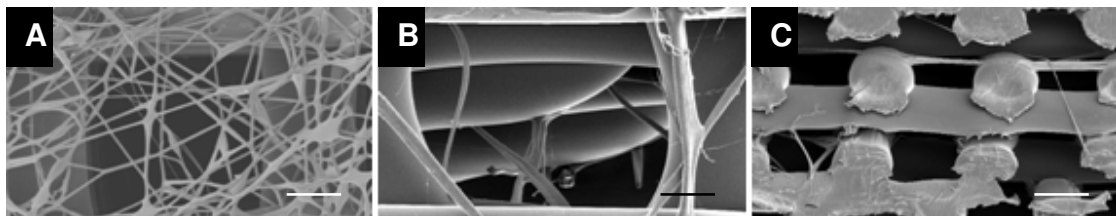


Figure 2: SEM micrographs of the surface (A, B) and of the cross section (C) of 3DFESP scaffolds. (A) ESP network spun for 2 minutes every two 3DF deposited layers (3DFESP-2); (B) ESP network spun for 30 seconds every two 3DF deposited layers (3DFESP-30); (C) cross section of a 3DFESP-30 scaffold. (A, B) Scale bar 200 μm ; (C) Scale bar 500 μm .

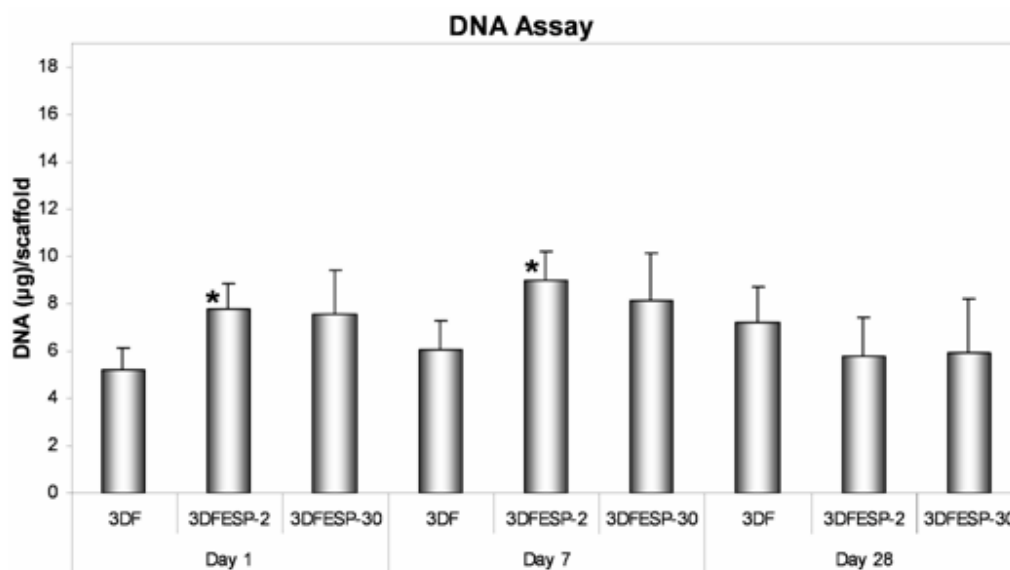


Figure 3: DNA assay on 3DF, 3DFESP-2, and 3DFESP-30 scaffolds after 1, 7, and 28 days of culture. (*) shows significant differences with respect to 3DF scaffolds ($p < 0.05$).

aggregated and maintained a rounded shape morphology in 3DFESP scaffolds (Fig. 6B, C). This is already evident after 1 day of culture, when chondrocytes in contact with big 3DF fibers attach and spread on their surface, while chondrocytes entrapped in the small ESP fiber network keep their rounded morphology (Fig. 6D, E), suggesting an influence on cell morphology. ECM formation can be also detected, as shown in Fig. 6F, and was confirmed by histology where the formed tissue responded to Safranin O staining (Fig. 7).

Discussion

3DFESP integrated scaffolds were successfully produced by combining two novel scaffold fabrication technologies: 3D fiber deposition and electrospinning. The scaffolds were characterized by a periodically interspersed network of rapid prototyped macrofibers and electrospun microfibers. Scaffolds with macrofibers of approximately 300 µm and microfibers of approximately 10 µm were used in this specific study. No delamination between layers of 3DF fibers or layers of 3DF and ESP fibers occurred resulting in a stable scaffold construct. Moreover, being the integration principles adopted in this study relatively simple, such a system can be extended to different kind of polymers and other rapid prototyping devices. Further investigations could also focus on the combination of different fiber diameter and surface texture. The two techniques offer, in fact, a wide versatility and range of solutions. The resolution limit of 3DF is currently 100µm and can be further downscaled by for example improving the extrusion mechanism [287, 288], while ESP fibers can be downscaled to few tens of nanometers [289, 290]. Furthermore, electrospun fibers can be fabricated with different surface morphology [275, 278, 291] and were shown to influence cell proliferation and morphology [278]. For instance, we also integrated in 3DF scaffolds an ESP network of nanoporous fibers with a fiber diameter of 10 µm and rounded shaped nanopores of 220nm. Seeded mesenchymal stem cells were found to attach, spread, and proliferate

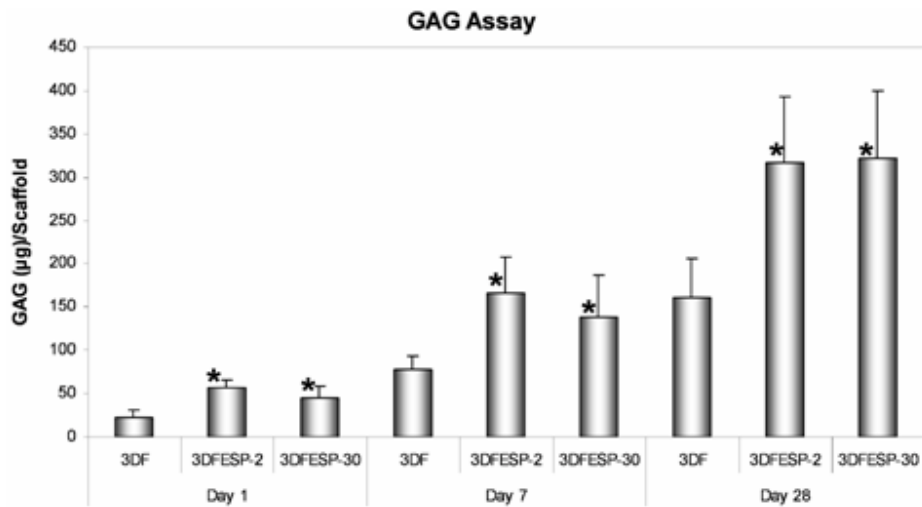


Figure 4: GAG assay on 3DF, 3DFESP-2, and 3DFESP-30 scaffolds after 1, 7, and 28 days of culture. (*) indicates significant differences with respect to 3DF scaffolds ($p < 0.05$).

most preferably on the electrospun fibers, while almost no cell adhered to the 3DF macrofibers (Fig. 8). Another interesting possibility is the direct integration of the two techniques in a single apparatus, since electrospinning of molten polymers has been successfully demonstrated [272] and characterized [292] by Larrondo *et al.* We have started to look into this direction and we could extend molten polymer electrospinning to PEOT/PBT copolymers, as shown in Fig. 9. However, more efforts need to be put in the insulation of the rapid prototyping robot from the electrospinning high voltage collector. Yet, the combination of these varieties might give origin to multifunctional structures useful in application where a hierarchical structure and a time response of such a construct are desired. As an example to show their improved functionality, these cellular structures were used as scaffolds for cartilage tissue engineering.

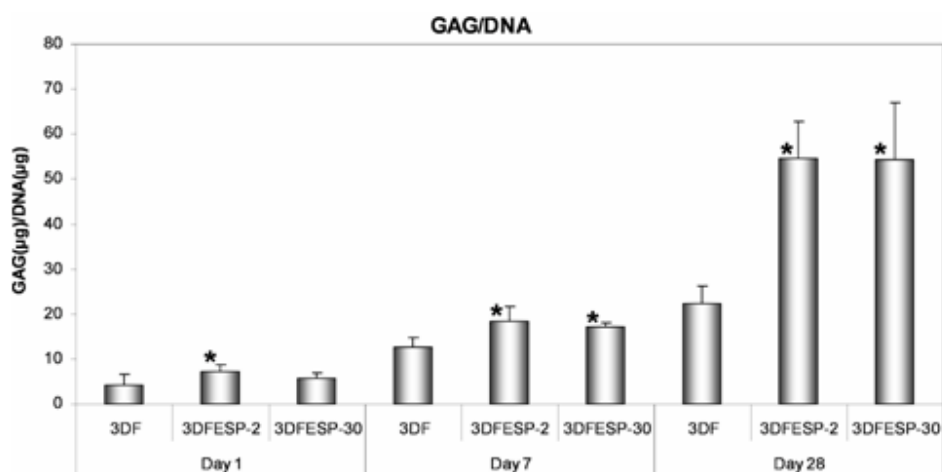


Figure 5: GAG/DNA ratio on 3DF, 3DFESP-2, and 3DFESP-30 scaffolds after 1, 7, and 28 days of culture. (*) depicts significant differences with respect to 3DF scaffolds ($p < 0.05$).

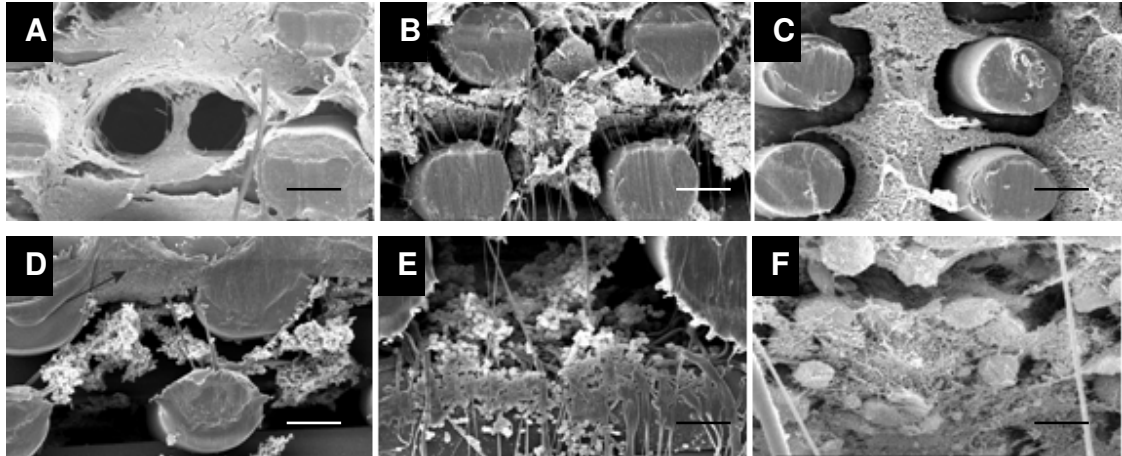


Figure 6: SEM micrographs illustrate chondrocytes distribution and morphology on 3DF (A), 3DFESP-30 (B,D), and 3DFESP-2 (C, E, F) scaffolds. After 28 days scaffolds pores were bridged by cells (A-C) and ECM (F). Chondrocytes were spread on 3DF scaffolds (A) and maintained their rounded morphology on 3DFESP scaffolds (B, C). Cell morphology was influenced by the fiber diameter (D, E) already at day 1. (A-D) Scale bar 200 μ m; (E) Scale bar 100 μ m; (F) Scale bar 20 μ m.

Bovine primary chondrocytes were cultured for one month on 3DF and 3DFESP scaffolds with different ESP network density. Cells were better retained in 3DFESP. This can be deputed to the “sieving” effect of the ESP integrated network, which entraps cells within the scaffolds. The entrapment efficiency of 3DFESP constructs was enhanced after cell seeding and during cell proliferation (day 7), since the increase in DNA amount was significant as compared to 3DF scaffolds alone. Furthermore, a homogeneous distribution of cells could be detected throughout the entire scaffold. Therefore, it can be inferred that the pores of the electrospun network are accessible and do not obstruct cell migration in the scaffold. However, after 4 weeks DNA decreased in the 3DFESP scaffolds. This might be due to a redistribution of cells in favor of a higher extracellular matrix production, as also supported by a higher GAG formation in the combined constructs. The production of more GAG can also be to a better cell differentiation in the 3DFESP scaffolds, as analyzed by SEM and quantitatively confirmed by the GAG/DNA ratio. In fact, chondrocytes appeared to maintain a rounded morphology when in contact with smooth microfibers and started to spread already after 1 day only when in contact with smooth macrofibers (Fig. 6D, E). It is known that when chondrocytes maintain their natural spherical shape they produce more GAG and a higher collagen type 2 versus collagen type I ratio [152, 161, 293-295]. This is partly corroborated by the GAG/DNA ratio, which determines how much GAG is produced per cell. A higher value of this ratio implies a higher degree of differentiation of the cells. Therefore, a better articular cartilage tissue formation can be expected from the 3DFESP constructs. No significant difference was found by varying the ESP network density. A comparable amount of DNA was found during the cell attachment (day 1) and proliferation (day 7) stages when a higher density network (3DFESP-2) was integrated as compared to a lower density network (3DFESP-30). This was also reflected in a similar GAG formation and a comparable GAG/DNA ratio. Therefore, no implications between the density of the network chosen in this study and the efficiency of the cell “sieving” and entrapment effect can be drawn. These results make of 3DFESP a very promising new type of scaffolds for

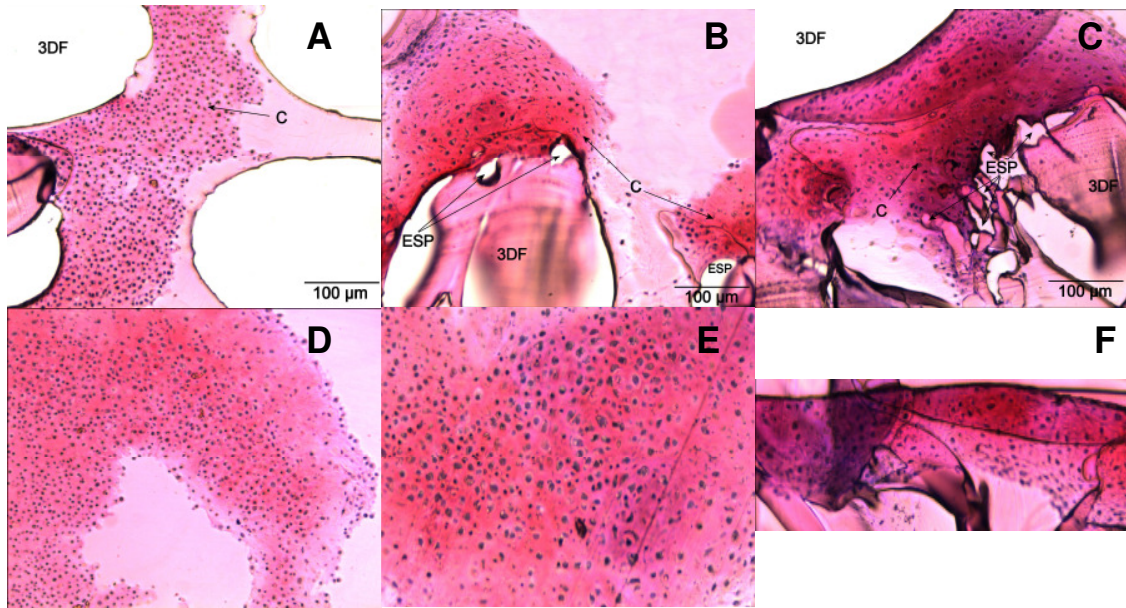


Figure 7: Histological cross sections show sulphated GAG formation in 3DF (A), 3DFESP-30 (B), and 3DFESP-2 (C) scaffolds by Safranin O staining. Inserts show staining in the middle of the scaffolds (D, E) and close to the ESP micron-size fibers. Differences in 3DF and ESP fiber coloration are due to partial or total dissolution of PEOT/PBT in the embedding material (GMA). C indicates cartilage formation (GAG), 3DF refers to the macro fibers, while ESP to the micro fibers. Scale bar: 100 μm .

cartilage tissue formation. Since they combine a macrostructure that provides the required mechanical properties and a microstructure that supplies topological cues at the extracellular matrix level, 3DFESP scaffolds can also find applications for other engineered tissue. Furthermore, the possibility to incorporate biological factors in the ESP network [296, 297] gives the possibility to control layer by layer the differentiation of cell and the formation of hierarchically structured tissues.

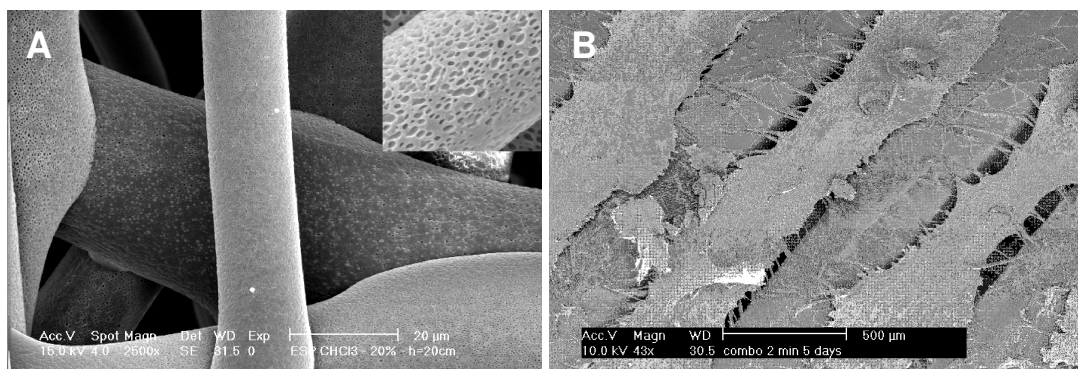


Figure 8: SEM micrographs showing (A) the nanopore surface topology of the ESP fibers and (B) stem cells selective attachment and spreading on the 10 μm nanoporous electrospun network, which suggests an influence of fiber nanoporosity on cell morphology and a cell-fiber size preferential interaction. Scale bar 500 μm .

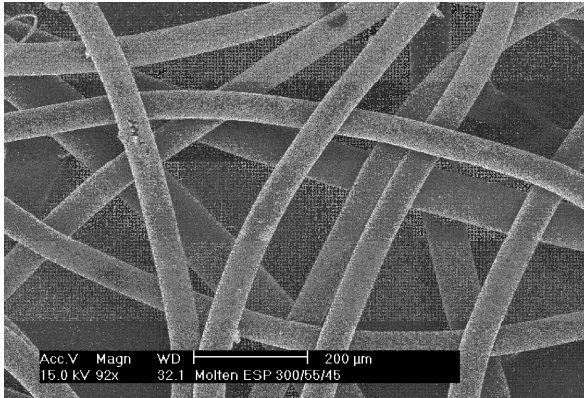


Figure 9: SEM micrographs of molten-electrospun 300PEOT55PBT45. Scale bar 200μm.

Conclusion

A novel type of scaffold (3DFESP) that combines a periodical rapid prototyped macrostructure with a random electrospun microstructure integrated in the same construct has been fabricated, characterized and evaluated for cartilage tissue engineering. 3DFESP showed a higher amount of entrapped cells during attachment and proliferation and a higher amount of extracellular matrix produced after 4 weeks of culture as compared to 3DF scaffolds alone. Furthermore, a better cell differentiation was supported by these constructs, as shown by the GAG/DNA ratio and by SEM analysis. Chondrocytes maintained their rounded morphology in 3DFESP scaffolds while they spread in 3DF scaffolds. Being the two fabrication technologies versatile to process different kind of materials with a number of topological superficial cues, these new kinds of scaffolds can be used to create different multifunctional 3D matrices that will improve the current status of tissue engineering applications.

Chapter 6

Osteochondral tissue engineering: mechanical characterization and biological performance of triphasic 3D fiber deposited scaffolds utilizing mesenchymal stem cells

Abstract

Scaffolds used for osteochondral Tissue Engineering (TE) should mimic both mechanical properties of cartilage and bone, respectively, and structural niches supporting either chondral or osteogenic cell differentiation. In this study, we explore the feasibility of scaffolds providing specific cell niches. Furthermore, the use of bone marrow as a single cell source for mesenchymal stem cells (MSCs) to create osseous and chondrogenic tissue respectively has been evaluated.

Three-dimensional fiber deposition technique was used to produce porous 3D PEOT/PBT scaffolds. The scaffolds were composed of a chondral compartment and an integrated osseous compartment with inserted biphasic calcium phosphate blocks (BCP) which were produced by an indirect photolithographic technique. Goat MSCs were aggregated and differentiated in chondrogenic differentiation medium and subsequently incorporated into the chondral part. Undifferentiated MSCs were seeded as single cell suspension into the osseous compartment. Constructs were subcutaneously implanted in nude mice.

25 days after implantation, the scaffolds retained their size and shape, and maintained their structural integrity throughout histological processing. In the bone part, the implants exhibited *de novo* bone formation. In the chondral compartment, cartilage-like structures could be observed.

The osteochondral scaffolds proposed here are of interest, as they are produced with combined cartilage and bone compartments. Both match the mechanical properties of natural tissue and promote cartilage and bone tissue formation.

Introduction

Articular cartilage is the layer of connective tissue covering each bone end within the joint. Damage to the articular cartilage leads to joint pain and progressive erosion of the cartilage due to its limited self repair capability. Repair results in fibrocartilage of inadequate quality. Injuries are maintained for years and lead to further degeneration like the loss of cartilage and underlying bone or osteoarthritis.

Conventional options for operative treatments are limited, involving the restoration of the joint surface, transplantation of cartilage or an artificial replacement. However, restorations like abrasion, subchondral drilling or production of microfractures do not induce appropriate tissue repair and replacement by allografts carries the risk of infections.

Therefore, autograft approaches like mosaicplasty have been introduced into the clinic successfully [30]. Grafting of osteochondral plugs has been shown to be advantageous due to the good fixation and integration into surrounding tissue. Unfortunately, this approach requires skilled and costly extensive surgical experience to obtain donor tissue [85]. In addition, only limited amounts of tissue can be transplanted, making it difficult to apply for large defects. Furthermore, at the donor site morbidity and degradation can occur [29].

To minimize these limitations, biological substitutes for osteochondral plugs can be developed using tissue engineering (TE). It involves the use of both an appropriate cell source and an appropriate biocompatible material as a cell substrate or cell-encapsulation material [298]. Further advantages of this technology are the scale production of implants with defined size, shape and mechanical properties.

First TE approaches have focused on the use of chondrocytes for the chondral part in combination with a cell free [42, 46, 299] or cell containing bone substitute [53]. However, the use of cartilage as cell source requires cost intensive isolation, expansion and redifferentiation, because chondrocytes tend to lose their phenotype during culture. Further limitations of the different approaches are the lack of integration of the bone and cartilage part [46], cell death [135], the poor integration into the surrounding bone [42] and the need of time consuming preculture systems [53]. Therefore, mesenchymal stem cells (MSCs) might be very promising. MSCs can be easily isolated from bone marrow by taking a punch biopsy. They have a high *in vitro* expansion potential and can be differentiated into several cell types such as osteocytes and chondrocytes.

Several studies have addressed the application of biodegradable materials to engineer functional cartilage [128, 300, 301] or bone like tissues [302]. However, scaffolds used for osteochondral TE based on MSCs should provide mechanical properties of both cartilage and bone respectively, but also structural niches supporting either chondrogenic or osteogenic cell differentiation. Different *in vitro* and *in vivo* studies have demonstrated both the biocompatibility and biodegradability of polyethylene oxide terephthalate/ polybutylene terephthalate (PEOT/PBT) segmented copolymers [63, 130, 195] as well as their applicability in cartilage tissue engineering [131, 132]. Additionally, it has been used as bone bonding material [200, 274, 303]. Biphasic calcium phosphates (BCP) have been shown to induce bone ectopically [304, 305]. With these characteristics respective environments as in cartilage and bone can be mimicked by combining different polymer compositions and osteoinductive ceramics.

The objectives of the current study were (1) to explore the feasibility of fabricating osteochondral composite scaffolds which provide specific cell niches by using PEOT/PBT and BCP and (2) to evaluate the use of bone marrow as single cell source of mesenchymal stem cells to create bone and cartilage respectively. We applied state of the art technology to produce threedimensional, porous implants. 3D fiber-deposited

PEOT/PBT scaffolds with cartilage like mechanical properties have been combined by a tide mark like structure with 3D fiber deposition PEOT/PBT scaffolds with bone bonding characteristics, in which photolithographically produced BCP particles were inserted. For the chondral part, MSCs were induced into chondrogenic lineage 3 days prior to the seeding, while MSCs for the bone part were seeded undifferentiated onto the BCP particles.

Materials

Culture media and supplements were from Sigma (Zwijndrecht, The Netherlands) and Gibco (Breda, The Netherlands) unless otherwise noted. Biodegradable poly(ethylene oxide)-terephthalate/polybutylene terephthalate (PEOT/PBT) block copolymers were obtained from IsoTis Inc. (Irvine, USA).

Methods

Scaffold fabrication

Polymer

The biodegradable PEOT/PBT copolymers have been characterized previously [132, 145] with the composition denoted as a/b/c, where a represents the PEG MW (g/mol), and b and c represent the wt% of the PEOT and PBT blocks, respectively. Triphasic scaffolds have been fabricated using the 300/55/45 for the chondral part and the 1000/70/30 as a carrier for biphasic calcium phosphate (BCP) particles for the bone part of the defect. Three-dimensional (3D) sheets of copolymer were produced using a Bioplotter device (Envisiontec GmbH, Germany) [144]. To extrude highly viscoelastic fibers, the bioplotter underwent few modifications reported by Moroni et al.[145].

The polymer was put in a stainless steel syringe and heated at $T = 190\text{ }^{\circ}\text{C}$ through a thermoset cartridge unit, fixed on the "X"-mobile arm of the apparatus. When the molten phase was achieved, a nitrogen pressure of 5 bars was applied to the syringe through a pressurized cap. The scaffold models were loaded on the Bioplotter CAM (PrimCAM, Switzerland) software and deposited layer by layer, through the extrusion of the polymer on a stage as a fiber. The deposition speed was set to 300 mm/min. Scaffolds were then characterized by the fiber diameter (through the nozzle diameter), the spacing between fibers in the same layer, the layer thickness and the configuration of the deposited fibers within the whole architecture. The nozzle used was a stainless steel Luer Lock needle with internal diameter (ID) of 400 μm , shortened to a length of 16.2mm. The fiber spacing was set to 1650 μm , while the layer thickness to 225 μm . A 0-90 scaffold architecture was chosen, where fibers were deposited with 90 $^{\circ}$ orientation steps between successive layers.

Ceramic

Porous BCP designed particles were fabricated by an indirect rapid-prototyping technique (Fig. 1). First, negative masks were designed with a CAD/CAM software (Rhinoceros[®]) and fabricated with an acrylic photopolymerizable resin by photolithography (PreFAB, Envisiontec, Germany). Biphasic calcium phosphate (BCP) slurry was made by adding 32.8 grams of calcinated BCP powder (20hrs in an oven at 1000 $^{\circ}\text{C}$), 14.2 grams of non calcinated BCP powder, 20 grams of demineralized water, 1.2 grams of methylcellulose solution (2% w/v methylcellulose in demineralized water),

2.2 grams of ammonia, and 14.1 grams of 300 – 500 µm sieved naphthalene particles, resulting in a 30% macro porosity of the final BCP particles. All components were blended and vigorously stirred with a mixer for approximately 30 minutes, until a homogen slurry was obtained. The slurry was filled into the resin masks, and BCP particles were then obtained by debonding and sintering in a furnace (Nabertherm, Germany) at T = 1150 °C. Irregular BCP particles with an average size between 1.4 mm and 2 mm were also used. These latter particles were fabricated by hydrogen peroxide foaming, as described elsewhere [38]. BCP particles were pressed into the pores of the 3DF matrix by exploiting the swelling behavior of 1000PEOT70PBT30. The polymeric matrix was left in demineralized water for 24hrs to allow swelling prior to insertion of the BCP particles. BCP particles were of pillar (side: 1.6 mm; height: 4.3 mm), truncated cone (large base diameter: 2 mm; small base diameter: 1.6 mm; height: 4 mm), spherical (diameter: 1.8 mm) and irregular (between 1.4 mm and 2 mm in their maximum dimension) shapes (Fig. 1). Additional spherical and irregular particles were pressed into the pores of the 3DFM scaffolds until covering the total thickness of the polymeric matrix. Different ceramic particle shapes were considered to address the optimal amount of included BCP and the influence of the particle geometry on mechanical properties, while maintaining the flexibility of the construct. The 3DFM scaffold had a block shape, with a square base of 10 mm, and a height of 3.15 mm. Since 1000PEOT70PBT30 is known to swell in an aqueous environment [63, 145, 195], the scaffolds were under-dimensioned to match exactly the BCP designed particles in a wet milieu.

Assembly of osteochondral scaffolds

A first scaffold of PEOT/PBT 300/55/45 was 3D fiber-deposited with dimensions 11mm x 11mm x 1.95mm ($d_1=175\mu\text{m}$, $d_2=600\mu\text{m}$ and $d_3=150\mu\text{m}$) followed by two layers of circular and concentric fibers of 300/55/45 and 1000/70/30 respectively to prevent delamination at the interface. The fiber thickness was 135µm. On the top of these two layers a 11mm x 11mm x 3.45mm block of 1000/70/30 was deposited using the parameters $d_1=175\mu\text{m}$, $d_2=1650\mu\text{m}$ and $d_3=150\mu\text{m}$. The construct was left swelling until equilibrium was reached, and BCP blocks (1.64mm x 1.64mm x 3.8mm) were inserted in the 1000/70/30 scaffold pores.

Scaffolds Characterization

Cylindrical plugs of 6 mm in diameter by 8 mm in height were taken as samples for characterization. The constructs were analyzed with an optical microscope (OM) to assess their integrity over time and by scanning electron microscopy (SEM) analysis with a Philips XL 30 ESEM-FEG. Samples were gold sputter coated (Carrington) before SEM analysis.

The porosity of the 3DF cartilage scaffold and of the bone scaffold in its separated components and as a final whole construct was experimentally measured by analyzing the mass and the volume of each structure, as:

$$P = 1 - \frac{M}{V} \cdot \frac{1}{\rho} \quad (1)$$

where M and V are the measured mass and volume of the scaffolds components, while ρ is the specific density of the materials (1.25 g/cm³ for 1000PEOT70PBT30, 3.15 g/cm³ for BCP). The composition of BCP particles was analyzed by x-ray diffraction (XRD) (Rigaku Miniflex, China) and Fourier Transform Infrared analysis (FTIR) (Spectrum 1000,

Perkin Elmer, USA). For the bone hybrid construct, the weight and volume percentage of BCP included in each scaffold was also measured as the ratio between the BCP particles weight and volume and the weight and volume of the final construct, respectively.

Mechanical Characterization of the Bone Hybrid Scaffolds

A DMA instrument (Perkin Elmer 7e) was used to evaluate the bending and compressive dynamic stiffness of the 3D assembled scaffolds of the bone compartment and of the single biomaterials used. In the dynamic bending test, three slabs of 15 mm in length by 5 mm in width by 6 mm in height were used as samples. A 3-point bending test was chosen for the characterization. Scaffolds were loaded with a dynamic force varying from 350 mN to 450 mN. A ramp of 5 mN/min at a constant frequency of 1Hz was applied. A lower range of forces was applied with respect to the compressive dynamic test to prevent sample deformation that impinged with the test setting.

In the compressive dynamic test, for each hybrid design and for each single biomaterial used three cylindrical samples of 6 mm in diameter by approximately 6 mm in height were tested. Cylindrical fixtures were chosen to test the specimens and evaluate their behavior as a whole structure along their compression axis, in the “z-direction”. Scaffolds were loaded with a dynamic force varying from 3.5N to 4.5N. A ramp of 50mN/min at a constant frequency of 1Hz was used. In the two test configurations, the dynamic stiffness, or storage modulus E' , was calculated in the elastic region of the composites. The theoretical modulus as proposed by the Reuss-Voigt model for a composite was also calculated [306, 307]. In this case we assumed the ceramic particles as mainly oriented along the longitudinal direction where compression occurs. The modulus can then be calculated as:

$$E = E_i V_i + E_m V_m$$

(2)

Where E is the modulus of the final construct, E_i and V_i are the modulus and the volume fraction of the inclusions (here considered as the BCP particles), while E_m and V_m are the modulus and the volume fraction of the polymeric matrix.

The stress and deformation at break were measured with a Zwick Z050 mechanical testing apparatus (Zwick, Germany), in a failure test under compression with a crosshead speed of 1mm/min.

2.6. Statistical Analysis

Statistical Analysis was performed using a Student's t-test, where the confidence level was set to 0.05 for statistical significance. Values in this study are reported as mean and standard deviation.

Bone marrow isolation and cell expansion

Goat bone marrow cells (gBMCs) were isolated and culture expanded as described previously [146]. Briefly, bone marrow aspirates from the iliac wing of Dutch milk goats were plated in tissue culture flasks (0.5×10^6 nucleated cells/cm²) and cultured in expansion medium containing α -Modified eagle medium, supplemented with 15% FBS, 1% Pen/Strep, 0.1mM ascorbate-2-phosphate acid and 2mM L-Glutamine until reaching 80% confluence. gBMCs were harvested using 0.25% trypsin-EDTA, counted and replated at 1000 cells/cm². Cells were cultured in monolayer in a humidified atmosphere with 5%CO₂ at 37°C. Medium was changed every 2-3 days. When reaching 80% confluency again, cells were trypsinated, washed twice in PBS and counted using a Burker Turk Counting chamber.

Cell seeding

Osteochondral grafts were incubated in expansion medium 48 h prior to the implantation. Four samples without cells served as controls. For the cell-based constructs, two different methods were used to seed the two different parts of the osteochondral graft.

For the osseous part, 4h prior to the implantation, gBMCs were seeded at a density of 2.5×10^6 cells/graft onto the BCP particles (4 particles per graft).

For the chondral component, 48 h prior to the implantation, cells were incubated in a 24-well plate (Ultra Low Attachment Surface, Corning) at a cell density of 1×10^6 cells/well in Dulbecco's modified eagle medium, supplemented with 1% penicillin/streptomycin, 1% ITS⁺, 100nM dexamethasone, 50µg/ml ascorbic 2-phosphate, 100µg/ml sodium pyruvate, 40µg/ml proline and 10ng/ml TGF β1 (R&D Systems, Abington, UK). Prior to the implantation, cells of five wells were collected ($\approx 5 \times 10^6$), spun down at 300g for 30 seconds and supernatant was removed. Cells were resuspended in 50µl Matrigel® (BD Bioscience, Alphen aan den Rijn, The Netherlands) and placed into the pores of the chondral part of the graft (total of 5×10^6 cells/graft). Samples were incubated for 20 minutes at 37°C in order to let a gel be formed.

Implantation

The animal experiments were approved by a local Ethics Committee. Tissue engineered osteochondral grafts and controls were implanted into immunosufficient, six weeks old, male mice (HdCpb:NMRI-nu, Harlan B.V., Horst, The Netherlands). All animals were operated under aseptic conditions. After subcutaneous injection of 0,05mg/kg Temgesic for analgesia the mice were put under general inhalation anesthesia using Isofluran. Two subcutaneous pockets were created on the dorsum of each mouse by blunt dissection. One osteochondral graft was inserted per pocket. In total five mice were used for the implantation.

Histological analysis

25 days after implantation, mice were euthanized by CO₂ asphyxiation. The implants were carefully removed and fixed in 1,5% glutaraldehyde in 0,14 M sodium cacodylate buffer for 24 h at 4°C. Following dehydration by graded ethanol series, specimens were embedded in polymethylmethacrylate. Histological sections of 10µm were made using a sawing microtome (Leica, Nussloch, Germany) and stained with 1% methylene blue and 0,3% basic fuchsin to visualize bone formation or 0,04% thionine to distinguish cartilage like tissue formation.

Results

1. Characterization of osteochondral grafts

The principles of scaffold assembly for the bone compartment of the osteochondral scaffold are illustrated in Fig. 1. The constructs were macroscopically examined. They kept their integrity both in a dry and in a wet (immersed in PBS) environment. The characteristic dimensions of the scaffolds such as fiber diameter, fiber spacing and layer thickness, were in good correlation with the parameters set on the device software. Shrinkage following sintering of BCP particles was shown to vary from $7 \pm 0.7\%$ to $18 \pm 1.9\%$. The composition of the BCP particles was analyzed by XRD and was comprised of 24.6% of tricalcium phosphate (TCP) and 75.4% of hydroxyapatite (HA). FTIR spectra showed the typical pattern of BCP (not shown), as also described [308].

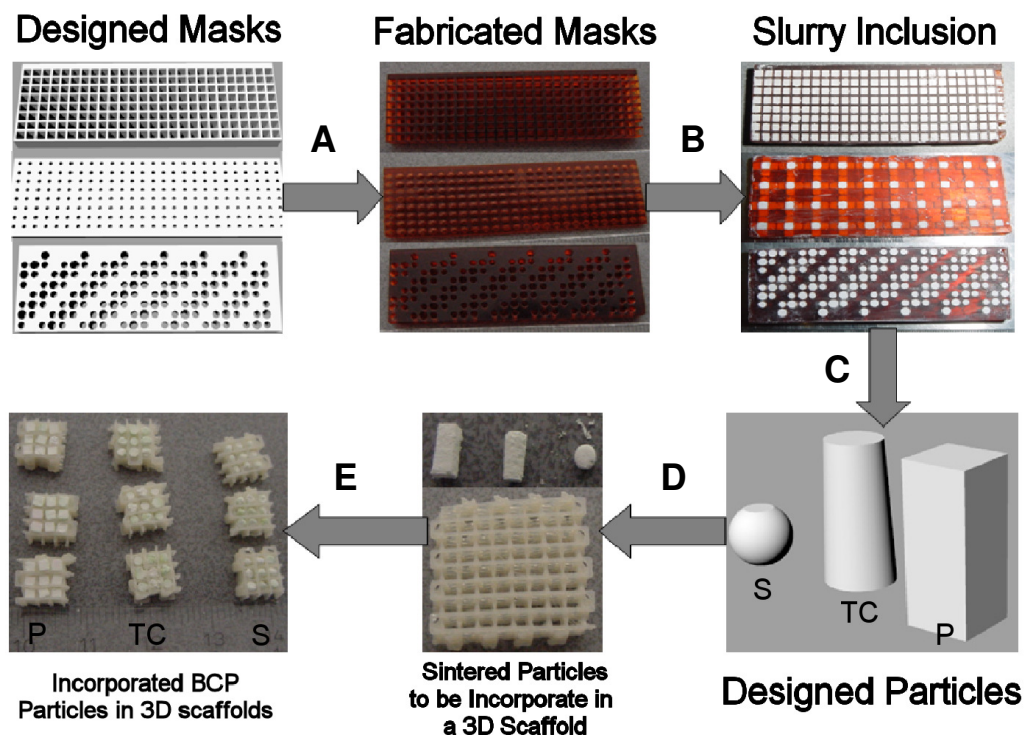


Figure 1: The schema illustrates the principles of scaffold assembly for the bone compartment of the osteochondral scaffold. A computer designed mask is fabricated in a resin by photolithography (A). The negative mask is filled with BCP slurry (B) and particles are obtained subsequently by debonding and sintering at 1150°C (C). Particles are incorporated into 3D scaffolds (D) to be used as bone compartment of the osteochondral construct (E). S = sphere; TC = truncated cone; P = pillar.

No fiber delamination occurred after BCP assembly as SEM analysis revealed (Fig. 2). The pillar particles were found to fit better in the pores of the 3D scaffolds when compared to the spherical and truncated architecture. As a result, the maximum BCP weight percentage was $61 \pm 3.15\%$, which corresponded to a volume fraction of $27.98 \pm 0.81\%$ (Tab. 1).

Osteochondral constructs with and without the interlocking system were fabricated. Due to the different swelling properties of the two PEOT/PBT compositions (bone =

Table 1: BCP weight percentages included in assembled scaffolds depending on particle design.

Designed Particle	BCP (weight%)	BCP (volume%)
Irregular	38.32±9.9	11.83±2.5
Sphere	38.24±1.45	14.12±0.37
Truncated cone	46.96±3.99	21.23±0.95
Pillar	61.06±3.15	27.98±0.81

1000PEOT70PBT30 – cartilage = 300PEOT55PBT45), instability at the interface of the two compartments occurred when no interlocking system was applied (Fig. 3 A).

However, when an interlocking fibrous system made of intertwined concentric 1000PEOT70PBT30 and 300PEOT55PBT45 fibers was deposited at the interface between the bone and the chondral part of the construct, constructs kept their architecture under forceps traction (Fig. 3 B, C). SEM analysis revealed a fiber diameter d_1 of $170 \pm 15 \mu\text{m}$, a fiber spacing d_2 of $605 \pm 12 \mu\text{m}$, and a layer thickness d_3 of $148 \pm 10 \mu\text{m}$ for the cartilage compartment. This corresponded to a porosity of $74 \pm 2\%$ and, consequently, to a dynamic stiffness of approximately 13 MPa, as calculated from previous studies [258].

The 3D hybrid bone compartment of the osteochondral construct were mechanically characterized by measuring the bending and compressive storage modulus (or dynamic stiffness, E') and the breaking stress and strain. The bending and compressive dynamic stiffness of the constructs with and without the inclusion of BCP particles are shown in Fig. 4. In the bending test, the bending dynamic stiffness was $0.134 \pm 0.035 \text{ MPa}$ for the bare 3DFM scaffold. When the designed BCP particles were pressed into the pores of the 3DFM scaffolds, the bending test significantly increased to $0.94 \pm 0.15 \text{ MPa}$ for irregular particles, to $3.72 \pm 0.03 \text{ MPa}$ for spherical particles, to $8.86 \pm 0.65 \text{ MPa}$ for truncated cones, and to $18.99 \pm 0.14 \text{ MPa}$ for pillar particles ($p < 0.05$). In the compression test, the compressive storage modulus E' significantly increased from $0.692 \pm 0.16 \text{ MPa}$ for 3DFM bare matrices to $0.935 \pm 0.165 \text{ MPa}$ for irregular particles, to $17.38 \pm 5.38 \text{ MPa}$ for spherical particles, to $26.2 \pm 4.76 \text{ MPa}$ for pillar particles, to $37.97 \pm 6.14 \text{ MPa}$ for truncated conical particles. The elastic moduli of the different construct configurations were also calculated with the theoretical model proposed by Voigt for composites and were found to be in the same range as the bending measured values, but not comparable to the compression ones (Table 2). The bending ($r^2 = 0.96$) and the Reuss-Voigt ($r^2 = 0.99$) modulus seemed to increase with a power law, with increasing the BCP volume fraction. However, this was not the case for the compression modulus ($r^2 = 0.87$). The stress at break was also dependent on the design of the hybrid scaffolds. Stress changed from $0.52 \pm 0.14 \text{ MPa}$ for irregular particles to $14.01 \pm 1.19 \text{ MPa}$ for pillar particles. The strain varied from $9.92 \pm 1.78\%$ to $33.74 \pm 0.49\%$, but did not appear to depend on the scaffold design, as presented in Table 4. 3DFM alone did not break under compression.

2. *In vivo*

After 48 h incubation in chondrogenic medium, MSCs formed small cell aggregates between $140\mu\text{m}$ and $1400\mu\text{m}$ (Fig. 5A). Unfortunately, during cell seeding into the porous chondral part, the size of the aggregates turned out to be not advantageous. After fixation with a gel, the majority of cell aggregates was located at the seeding site of the chondral component and only low amount was integrated within the fibers of the

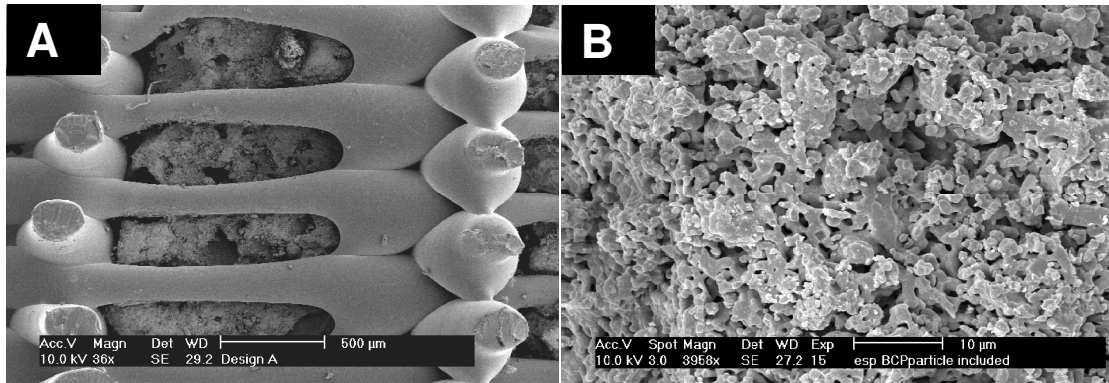


Figure 2: SEM micrograph of hybrid osteochondral scaffolds. **(A)** Bone part after insertion of BCP particles into three-dimensional 1000/70/30 matrix. **(B)** Microstructure of BCP particles sintered at 1150°C.

polymer (Fig. 5 B). In contrast, MSCs seeded in the osseous part were homogeneously distributed and attached evenly throughout the scaffolds. While in the chondral part cells kept a round morphology, MSCs in the bone part exhibited a flat, spread morphology (Fig. 5 C, D). After 25 days of subcutaneous implantation in the dorsum of nude mice all implants were surrounded by a fibrous capsule. Macroscopically, the two components revealed their original size and shape and maintained their structural integrity during the period of implantation. Furthermore, after histological processing, a separation of the polymer part and the BCP component did not occur in any of the samples. Histological analysis revealed that *in vivo* tissue engineered grafts exhibited at the bone part *de novo* bone formation (Fig. 6 A). Tissue generation took place in direct apposition to the ceramic surface. Osseous tissue was composed of a mineralized matrix strongly positive for Fuchsin red. Osteocytes could be detected, which were embedded in the matrix, and layers of osteoblasts lining the outer edges of the newly formed bone. Bone marrow-like tissue characterized by hematopoietic cells, blood vessels and fat could also be observed in most of the implants. In few cases, hyaline cartilage-like islands appeared within the pores of the BCP (Fig. 6 B).

In the chondral part, histological staining revealed the presence of cartilage-like tissue. Cells exhibited a round morphology. They were located in lacunae and their pericellular matrix was strongly positive for Thionine (Fig. 7 A). However, we also found mineralized matrix within the chondral part. Clearly, hypertrophic cells were still distinguishable in the center of the mineralized nodules suggesting endochondral ossification (Fig. 7 B). Control grafts implanted without cells did not show any evidence of osseous or chondral structures (not shown).

Table 2: Comparison between the experimental and the theoretical values of the storage moduli of three-dimensional scaffolds with custom designed assemblies BCP particles.

	$E'_{\text{bend exp}}$ (MPa)	$E'_{\text{comp exp}}$ (MPa)	E'_{theor} (MPa)
Sphere	3.72 ± 0.03	17.38 ± 5.38	6.99
Truncated cone	8.86 ± 0.65	37.97 ± 6.14	10.17
Pillar	18.99 ± 0.14	26.2 ± 4.76	13.19

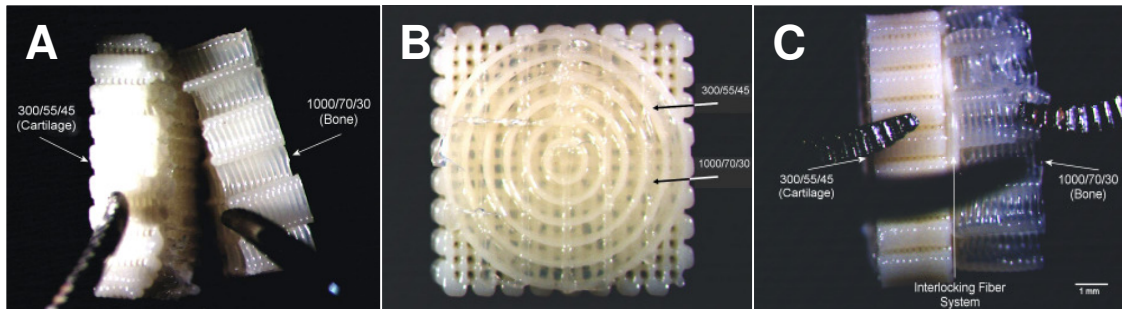


Figure 3: Osteochondral scaffolds with and without interlocking system were fabricated. **(A)** Without the interlocking system scaffolds delaminate after swelling in PBS due to different swelling properties of the two polymer compositions 300/55/45 and 1000/70/30 **(B)** The interlocking system is made of intertwining fibers of both polymer compositions. **(C)** With the interlocking system scaffolds remain integrated after swelling in PBS. Scale bar 1mm.

Discussion

Osteochondral scaffolds comprised of a three-dimensional cartilage and bone compartment were successfully fabricated and showed to possess the mechanical flexibility of polymers and the strength of ceramics. Furthermore, the rapid prototyping approach used in the design allowed the creation of scaffolds with a completely interconnected and accessible pore network. Different triphasic 3D scaffolds were considered and characterized in terms of their structural and mechanical properties for the bone compartment. In addition, seeding of mesenchymal stem cells was successfully on both the cartilage and the bone part. Cells differentiated into chondrogenic and osteogenic lineage and produced cartilage-like and bone-like extracellular matrix, respectively. This is the first report of osteochondral tissue engineering using mesenchymal stem cells for both the chondral and the bone part, and subsequent generation of appropriate tissue after implantation.

Bending Storage Modulus of Assembled Scaffolds

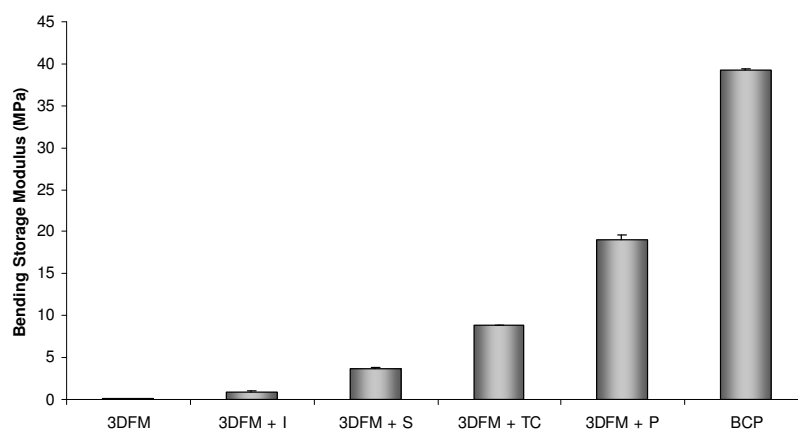


Figure 4: Influence of scaffold design on bending storage modulus. The dynamic stiffness of the single components comprising the hybrid scaffold was also measured for comparison. All groups are significantly different from each other ($p < 0.05$). Particle shape legend: I = irregular; S = spherical; P = pillar; TC = truncated cone.

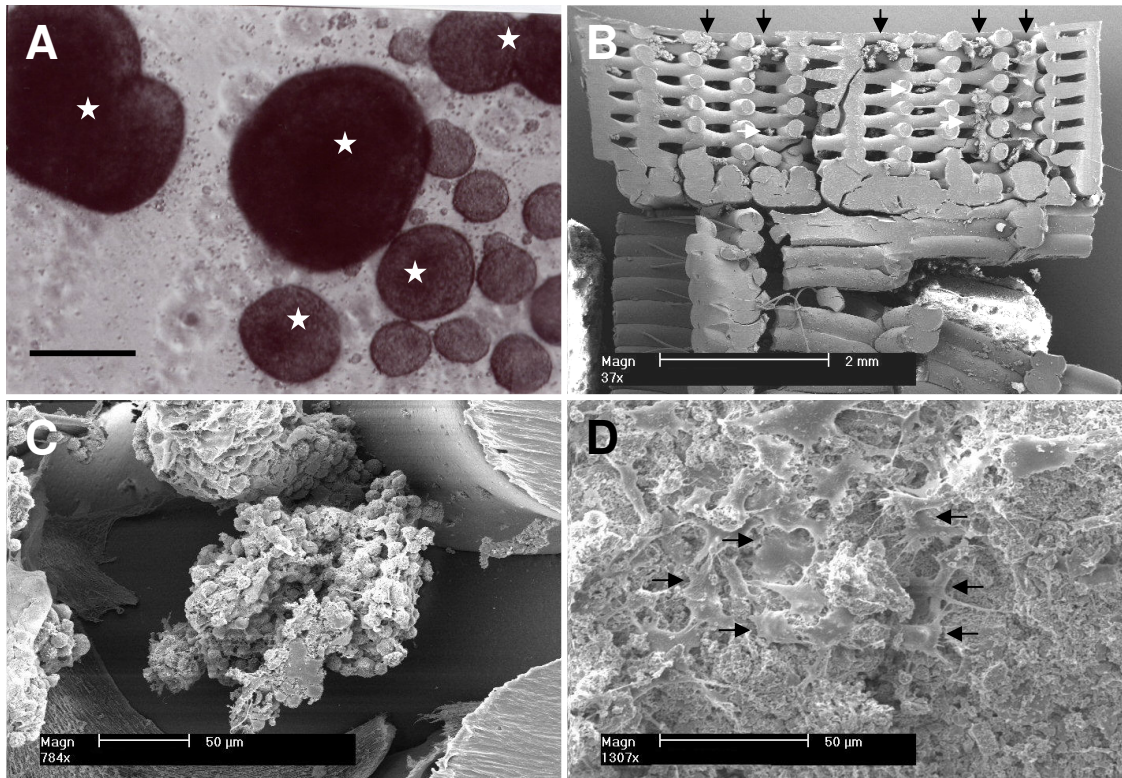


Figure 5: Cell aggregation and loading into three-dimensional scaffolds. **(A)** Cells form stable aggregates after 48hrs in chondrogenic differentiation medium. The majority of aggregates exceed the pore size (stars). **(B)** SEM micrograph shows a cross section of osteochondral constructs. Only at the surface of the construct cells can be found (black arrowhead) and occasionally in the inner part (white arrowhead). **(C)** Cells exhibit a round morphology in the chondral part, whereas in the bone part they appear flat and spread (arrows). Scale bar in (A) 250 μ m.

Two parameters are important in this study: Firstly, the mechanical properties of the biomaterials with respect to cartilage and bone. Secondly, the bone marrow as cell source for cartilage and bone.

Since ceramics are typically characterized by their behavior at break, the breaking stress and strain of the composite scaffolds were measured. Strain did not seem to depend on scaffold design. The variable increase of the stiffness and of the breaking stress might be linked to the different packing degree of the ceramic in the polymeric matrix, resulting in a progressively higher coupling of the two materials. The increasing fit with the polymer, thus, resulted in a more efficient strengthening of the construct, increasing the overall stiffness and the stress at break.

With increasing BCP weight and/or volume percentage in the hybrid 3D scaffolds, the bending modulus increased accordingly. This can be expected as, with higher BCP content, the scaffolds are more densely packed, resulting in an increase of the stiffness given that BCP is the stiffest component in the assembled construct. A similar trend was seen for the compressive stiffness, although the highest value was measured when truncated conical ceramic particles were press-fitted in the polymeric matrix. The higher performance of these particles within the matrix, despite a non-correspondent higher weight percentage, might be due to a higher localization of the surface stresses in a cylindrical section as compared to the rectangular one characteristic of the pillar particles. The higher localization is originated by a “confinement” or “focusing” effect of the

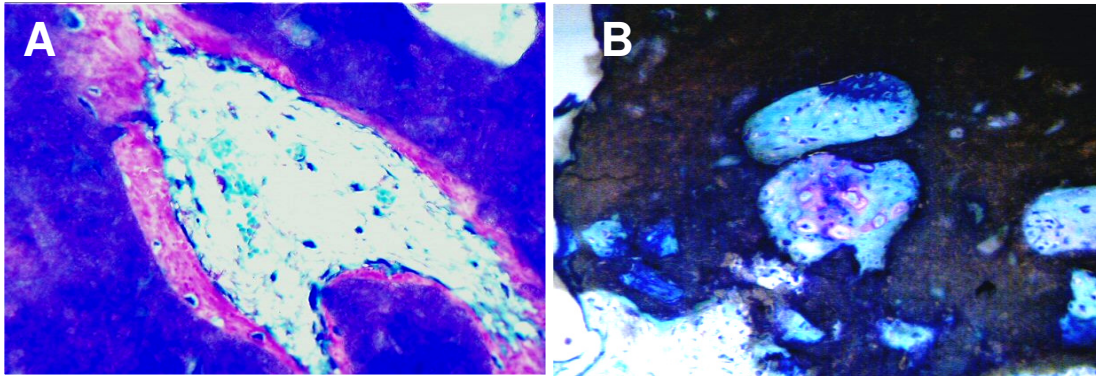


Figure 6. Bone part of the osteochondral construct. **(A)** Pores are filled with de novo bone. Note the embedded osteocytes and the osteoblasts laying at the outer edge of the mineralized matrix. **(B)** Occasionally, hypertrophic cells with positive stained matrix can be seen in the pores. **(A)** Fuchsin red staining. **(B)** Thionine staining. Scale bar 200 μ m.

ceramic particle in the polymeric matrix, which is dependent on the particle section and results in a stiffer response. This is theoretically quantified as a 10-20% increase for a cylindrical section as compared to a cubical one [309, 310] and falls within the variation experimentally measured for truncated conical and pillar particles. Since the experimental values of the bending stiffness were in the same range of the calculated stiffness values from the Reuss-Voigt model, this might suggest that the assembly of the different biomaterials can be considered close to a composite when subjected to a flexion load [306, 307]. Although it cannot be strictly defined as such, since this is typically formed by chemically bonded materials. It is clear that the hybrid scaffolds do not mechanically respond as real composites when their mechanical behavior in compression is considered. In this case the theoretical and the experimental values do not follow the same power law. As previously explained, it might be that the different stress localization on ceramic particles with different shapes is predominant in compression as compared to a volumetric increase of BCP in the assembly.

As reviewed by Athanasiou *et al.*, cancellous bone has a bending modulus varying between 49 MPa and 336 MPa, and a compressive modulus varying between 12 MPa and 900 MPa [311]. Cortical bone has a bending modulus ranging from 5.44 GPa to 15.8 GPa, and a compressive modulus ranging from 4.9 GPa to 27.6 GPa. The variations are related to different bone sources, different locations within the sources, and to different mechanical testing conditions. Cancellous bone has a strength varying between 0.15 MPa and 10.2 MPa, while cortical bone has a strength ranging from 90 MPa to 193 MPa. If the stiffness and stress/deformation at break of the different hybrid 3D assembled scaffolds are compared to the stiffness of cortical and cancellous bone, constructs with pillar or conical-cylindrical ceramic particles seems to better approach the mechanical behavior of cancellous bone. Cortical bone still has a much greater stiffness and strength as compared to the scaffolds here presented. Therefore, if mimicking the mechanical properties of the tissue to regenerate (in this specific case cortical bone) further investigation for appropriate materials seems to be required.

The advantage of using a 3D polymeric matrix in the bone part to enclose osteoinductive components is that it is possible to directly fabricate all polymer structure of the osteochondral scaffold by 3DF. Specifically, the chondral part of the scaffold can be

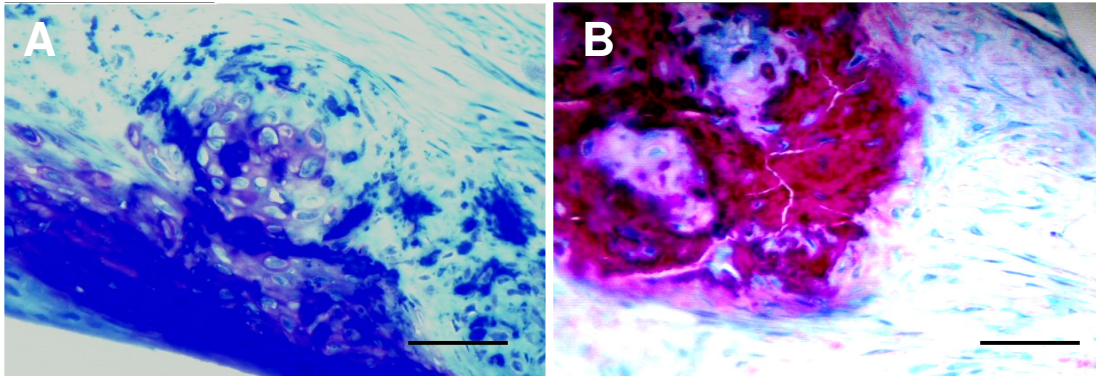


Figure 7. Cartilage part of the osteochondral construct. **(A)** Cartilage like tissue can be observed in the chondral part. Cells exhibit a round, chondrocyte like morphology, are located in lacunae and surrounded by positive extracellular matrix. **(B)** Hypertrophic cells in the center of mineralized matrix and embedded osteocytes can be found. **(A)** Thionine staining. **(B)** Fuchsin red staining. Scale bar 200 μ m.

fabricated on top of the bone part with 300PEOT55PBT45, a PEOT/PBT composition that has been considered for cartilage tissue engineering [132, 148, 152]. Since the two PEOT/PBT compositions (bone = 1000PEOT70PBT30 – cartilage = 300PEOT55PBT45) have different swelling properties, an interlocking fibrous system made of intertwined concentric 1000PEOT70PBT30 and 300PEOT55PBT45 fibers was deposited at the interface between the bone and the chondral parts of the construct. This system also mimics the tidemark in natural osteochondral tissue, as 1000PEOT70PBT30 is known to calcify and interconnects with the bone part. As shown qualitatively in Fig. 4, when the osteochondral scaffold was simply pulled apart with forceps, the presence of the interlocking system prevented the delamination of the two parts of the scaffold. The system retained this stability even after one month in culture medium at physiological conditions. However, after subcutaneous implantation, no cell ingrowth could be observed. This might be that the hydrophilic fibers of PEOT/PBT 1000/70/30 swelled in such an extent, that due to the limited available space no cells were able to invade the tidemark-like structure. The absence of host tissue supports this hypothesis, that the fibers of the two PEOT/PBT compositions built a dense layer between the chondral and the bone part.

MSCs are known to be multipotent; they are able to differentiate into chondrocytes or osteocytes under the appropriate culture conditions. The use of MSCs is also advantageous regarding clinical application, since they can be easily and minimally invasively isolated by bone marrow aspiration from the iliac crest under partial anesthesia. However, they do not differentiate spontaneously. In this study design, osteogenic differentiation was successfully induced. Important to note is: cells were not differentiated prior to the seeding, but nevertheless bone was formed *in vivo*. Osteoinductive properties of calcium phosphates have been demonstrated previously. Since they exhibit specific chemical and structural characteristics (biphasic, three-dimensional, microporous) [304, 308, 312] we assume that osteoinduction by the porous ceramic took place. However, we also observed cartilage-like tissue within the pores of BCP. We hypothesize that the enclosure of MSCs supported the regeneration of cartilage-like tissue. Parameters such as high cell density, condensation, and the low oxygen concentration might have occurred, which favor the chondrogenic differentiation of mesenchymal stem cells [124, 153, 313-315].

It has been shown that 300/55/45 PEOT/PBT with matching mechanical properties of cartilage favors chondrocyte redifferentiation *in vitro* [316]. However, no

chondroinductive property could be detected *in vivo* so far. Therefore, unlike for the bone part, MSCs intended for the chondral part were precultured in TGF β 1-containing differentiation medium. In general, a culture period of 21 days is applied. However, after 72 h of incubation, cells formed large aggregates; most of them were oversized for the pores of 3D fiber-deposited PEOT/PBT scaffold of the chondral part. Only a minority of the initial cell number could be loaded. Beside cartilage-like tissue, mineralized matrix with embedded osteocytes was found in the chondral part. The process behind this remains unknown, however, we hypothesize processes as they take place during endochondral bone formation may have occurred. Hypotrophy is often seen during chondrogenic differentiation of MSCs *in vitro* [204]. In addition, the presence of blood vessel ingrowth creates a microenvironment favoring osteogenesis. Consequently, optimizations regarding aggregate size and control of differentiation stage need to be conducted to fully load the construct with cartilaginous tissue

Conclusions

A novel approach to build scaffolds for osteochondral tissue engineering was introduced based on biomaterial assembly. Three-dimensional scaffolds made of polymers and ceramics were fabricated by integrating different scaffold fabrication technologies, and found to couple the flexibility of polymers with the mechanical strength of ceramics, at the same time maintaining a completely interconnected pore network. The mechanical properties of these constructs were modulated depending on the assembly design, and matched both cartilage and cancellous bone stiffness and strength. Their design and their biological performance *in vivo* make these scaffolds promising candidates for osteochondral regeneration.

Chapter 7

A clinical feasibility study to evaluate the safety and efficacy of PEOT/PBT implants for human donor site filling during mosaicplasty

Abstract

Transplantation of autologous osteochondral plugs (mosaicplasty) has become a valid and well-accepted treatment modality for articular cartilage lesions in the knee. Postoperative bleeding, progressing into haemarthrosis, however, remains a potential concern. The aim of this clinical feasibility study was to evaluate the safety and efficacy of porous polyethylene oxide terephthalate / polybutylene terephthalate (PEOT/ PBT) PEOT/PBT implants to fill donor sites during mosaicplasty. Empty donor sites were included as a control. Groups were assessed after 9 months using MRI, macroscopical and histological analysis.

Postoperative intra-articular bleeding was absent in all treated defects evaluated. Empty controls occasionally revealed effusions. No adverse events, synovitis or inflammatory responses were observed. PEOT/PBT implants were well integrated with the surrounding host tissue. MRI indicated surface congruence of all filled donor sites and an osseous integration throughout the implant. By contrast, empty controls occasionally showed protrusion of repair tissue at the defect margins. The stiffness of the surface repair tissue of filled donor sites was equal or slightly improved when compared to empty controls. Biocompatibility of PEOT/PBT implants was demonstrated by the absence of a chronic inflammation and the presence of a mild foreign body response. The presence and amount of polymer fragments indicated considerable biodegradation. Histological evaluation of the filled donor sites revealed congruent fibrocartilaginous surface repair with proteoglycan rich domains after 9 months follow up. Dense fibrous connective tissue was occasionally observed. Subchondral cancellous bone formation with interspersed fibrous tissue was observed in all implant filled sites.

It is concluded that by preventing postoperative bleeding, supporting bone bonding and bone formation as well as regenerating fibrocartilagenous repair tissue, the filling of donor sites using PEOT/PBT implants offers a therapeutic opportunity to reduce donor site morbidity after mosaicplasty.

Introduction

Mosaicplasty (MP) involves the collection of small-sized cylindrical osteochondral grafts ranging from 2.7 to 9mm from the minimal weight bearing periphery of the femoral condyles, followed by their transplantation to a pre-prepared recipient site. Surface congruence comprised of hyaline cartilage, and progressive fibrocartilagenous sprouting between the grafts resulting in appropriate integration have been demonstrated up to 5 years follow up. Multicenter clinical studies revealed superior outcomes of MP in comparison to subchondral abrasion, microfracture or Pridie perforations as based on arthoscopic follow up, MRI and modified HSS and Cincinnati scores. As a result, MP has become a valid technique for the treatment of articular cartilage lesions in the knee joint and is one of the major internationally accepted articular cartilage reconstructions in humans [29, 30].

Despite the good-to-excellent results, donor site morbidity remains a concern [30]. Donor site bleeding in particular has to be taken into consideration as it can potentially progress into haemarthrosis. Sokoloff *et al.* showed that trivalent cations such as Fe^{3+} can cause irreversible collapse of hydrated glycosaminoglycan side chains of proteoglycan molecules which are predominantly responsible for the load bearing capacity of the hyaline cartilage [317]. Extensive *in vitro* studies suggest that interleukins such as IL-1, produced by activated monocytes, stimulate chondrocytes to increase the production of hydrogen peroxide. In reaction with haemoglobin-derived iron, hydroxyl radicals are formed within the joint environment. These radicals irreversibly inhibit cartilage matrix synthesis by induction of chondrocyte apoptosis [318-323]. While Jansen *et al.* claim a complete reversible inhibition by blood on matrix synthesis after 24hrs, they also found a prolonged damage of joint cartilage already after 48 h blood exposure to cartilage [324]. Clearly, the potential risk of postoperative bleeding progressing into haemarthrosis needs to be addressed.

Numerous implants, both of natural and synthetic origin, have been applied in cartilage repair. Only few studies, however, have addressed osteochondral donor site filling. Using the German shepherd dog model, Feczko and Hangody *et al.* evaluated hydroxylapatite, polycaprolactone, carbon and collagen implants [29]. With the exception of compressed collagen, acceptable fibrocartilagenous resurfacing was not observed. Initial mechanical properties of collagen implants, however, are substantially inferior to their synthetic counterparts.

Based on its biocompatibility, biodegradability and mechanical properties it is suggested that porous PEOT/PBT implants are suitable candidates for donor site filling. *In vitro* cartilage engineering is facilitated by PEOT/PBT implants [69, 132, 199]. Pre-clinical studies using the rabbit femoral osteochondral defect model demonstrated surface congruent fibrocartilagenous resurfacing with robust subchondral bone formation at 12 and 52 weeks follow up [325].

To our knowledge, this is the first publication on treatment of donor sites after mosaicplasty in humans. In this clinical feasibility study, porous PEOT/PBT implants were used to fill donor sites during mosaicplasty. Its safety and efficacy was assessed arthroscopically, histologically and using MRI scans after 9 months follow up.

Materials and Methods

PEOT/PBT Implants

The elastomeric copolymer polyethylene oxide terephthalate/polybutylene terephthalate (PEOT/PBT) was used to prepare porous implants by compression molding/porogen leaching as described previously [132, 148]. This resulted in implants with a porosity of 75%, average pore size of 182 μ m, and dynamic stiffness at 0.1 Hz is 1.7 MPa. The specific composition of the PEOT/PBT implant is 55% by weight of PEOT and 45% by weight of PBT. The molecular weight of the polyethylene oxide is 300 Da. The compositional code of this PEOT/PBT copolymer is thus 300PEOT55PBT45. Implant dimensions were 7.5 mm in diameter and 10 mm in length (Fig. 1A). Implants were sterilized using gamma-irradiation at 25 kGy.

Study design

The described study followed an open, non-randomized, concurrent controlled, single centre, clinical feasibility design to evaluate the safety and effectivity of PEOT/PBT in reconstruction of the donor sites during autologous osteochondral grafting. The study was approved by an independent medical Ethics Committee, and performed in accordance with the Declaration of Helsinki (2000), ICH GCP, and EN540 guidelines. Informed consent was provided to all patients. Patients included in the PEOT/PBT group underwent a MRI within 7 days and 9 months post surgery. In addition, a rearthroscopy was performed at 9 months post surgery for macroscopic evaluation and biopsy collection.

Patients who met the inclusion criteria and who underwent the same procedure within the timeframe of the study, but who did not wish to be treated in the treatment group, were included in a concurrent control group. These patients were evaluated at 9 months follow up for clinical outcome. No additional analysis was performed in this group.

Patient inclusion criteria

All patients participating in this study met the following inclusion and exclusion criteria: The patients were male or female aged between 18 and 55 years. They were qualifying for an autologous osteochondral grafting procedure for femoral condyle cartilage lesions with a maximum defect size of 4cm² with a stable knee with no malalignment. Concomitant procedures (six ACL reconstructions, one HTO, one meniscus resection, one lateral release) were no exclusion criteria. The total number of patients included in the PEOT/PBT implant treatment and control were ten and four, respectively.

Surgical procedure

The study was approved by an independent medical Ethics Committee and performed in accordance with the Declaration of Helsinki (2000), ICH-GCP and EN540 guidelines. Mosaicplasty was performed as described previously [29, 85]. The procedure was either performed arthroscopically (8 patients, Fig.1D) or via an open procedure (2 patients, Fig.1C). The latter was chosen when an arthroscopic approach was not practical due to the size or location of the lesion or due to the inability to appropriately flex the knee.

During the open procedure, the peripheries of both femoral condyles at the level of the patellofemoral joint served as donor sites. During the arthroscopic technique, the medial border of the femoral condyle was used as the primary donor site. Donor grafts with a diameter of 6.5 mm and a length of approximately 15 mm were harvested perpendicularly to the donor sites using a tubular chisel and harvesting tamp. PEOT/PBT implants were allowed to hydrate for at least 15 minutes in sterile saline at room temperature.

Implants were applied to the donor sites slightly indented via press fit insertion using the digital application (open procedure) or via an adjustable plunger (arthroscopy) (Fig. 1D). In the PEOT/PBT group two to six scaffolds were used per patient with an average of 3.5. In the control group the donor sites were left empty (two open procedures and two arthroscopically). In the 10 PolyActive B group the concomitant interventions: 6 ACL reconstruction, 1 HTO, 1 meniscus resection, 1 lateral retinaculum incision. In the control group there was no concomitant intervention.

For postoperative pain control intravenous (on the day of surgery) or oral pain medication was prescribed. Post-operatively, the patients were kept non-weight bearing and partial weight-bearing for 4 to 8 weeks. Return to full activities was accomplished within 3 to 6 months.

Evaluation and analysis

Adverse events, general clinical outcome (HSS, Cincinnati, Lysholm, and ICRS scores), postoperative bleeding, arthroscopy and MRI for surface congruence as well as cartilage stiffness measurements were used to evaluate clinical outcomes and quality of the repair tissue at the donor sites. In addition, a histological analysis was performed on biopsies (2.7mm in diameter, 10mm length) taken from the defect margins during arthroscopy after 9 months follow up. At the upper surface of 5 cylindrical samples, white, "cartilaginous cap" was observed (Fig.1B). Postoperative bleeding, clinical symptoms were assessed in both groups, and in the PolyActive group MRI and second look arthroscopy were also used to check the surface congruence. MRI was repeatedly done before the operation, on the 7th postoperative day, in the 3rd postoperative month and at one year postoperatively Clinical scoring systems (modified HSS, Lysholm, Cincinnati) were employed before the operation and 3, 9 and 12 months postoperatively to check the clinical outcome. A second look was performed 9 months postoperatively (Tab. 1). During the control arthroscopies biopsies were harvested for histological analysis. Only 7 patients agreed to undergo biopsy harvest. As biopsy materials osteochondral cylinders with a diameter of 2.7mm were taken at the defect margin to evaluate quality of tissue repair in donor sites. All patients had clinical and MRI examinations. All patients (10 PolyActive - filled and 4 control patients) had the preoperative 3rd , 9th , 12th months scoring and preoperative, 7th day, 3rd month and 12th months postoperative MRI assessments.

Table 1. Overview of the study follow up

	Preop.	1-7 day	7d FU	3m FU	9m FU	12m FU
Postoperative bleeding		x				
Clinical score	x			x	x	x
MRI	x		x	x		x
Controlarthroscopy					x	

For histological analyses, biopsies were fixed in Sainte-Marie's fixative, decalcified in 10% EDTA and embedded in paraffin. Longitudinal serial sections of 5-8 μ m thickness were stained with hematoxylin-eosin for general histology, dimethylmethylene blue DMMB and Safranin O for proteoglycans, and picosirius red for collagen and evaluated using normal and polarized light microscopy. In addition, sections were also immunostained for type I collagen and osteonectin to assess fibrous tissue and bone formation, respectively. Hyaluronic acid (HA) was detected by using a highly specific biotinylated hyaluronon-binding probe bHABS kindly provided by R. and M. Tammi, University of Kuopio, Finland) [326].

Results

This clinical study evaluated the safety and efficacy of biodegradable PEOT/PBT implants to fill donor sites during mosaicplasty in a 1 year follow up period.

Postoperative intra-articular bleeding was absent in all treated defects. No adverse events, synovitis, heamarthrosis, arthrofibrosis or inflammatory responses were observed. No significant differences were observed in clinical outcome between filled groups and empty controls. Arthroscopical assessment demonstrated surface congruence and integration of implants with the host tissue after 9 months (Fig. 2A).

The reparative tissue here was yellow - whitish. The Polyactive B plugs were macroscopically well integrated to the surroundings. The surface of the filled up areas was flush with the neighboring surface, and checking with the probe it was similar, or even more firm, than the reparative tissue at the donor sites left empty. No signs of haemosiderosis or any bleeding was found.

In addition, MRI revealed surface congruence of all filled donor sites and indicated appropriate osteointegration of the implants (Fig. 2B, C, D). In contrast, empty controls

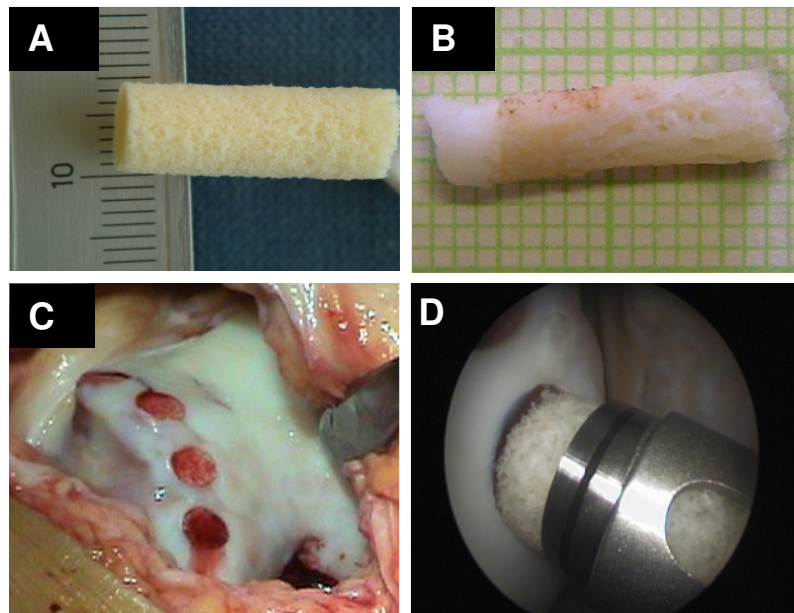


Figure 1. Application of PEOT/PBT implants to fill donor during during mosaicplasty. (A) PEOT/PBT plug prior to the insertion and (B) biopsy after 9 months. Insertion of PEOT/PBT during (C) an open procedure and (D) an arthroscopic procedure.

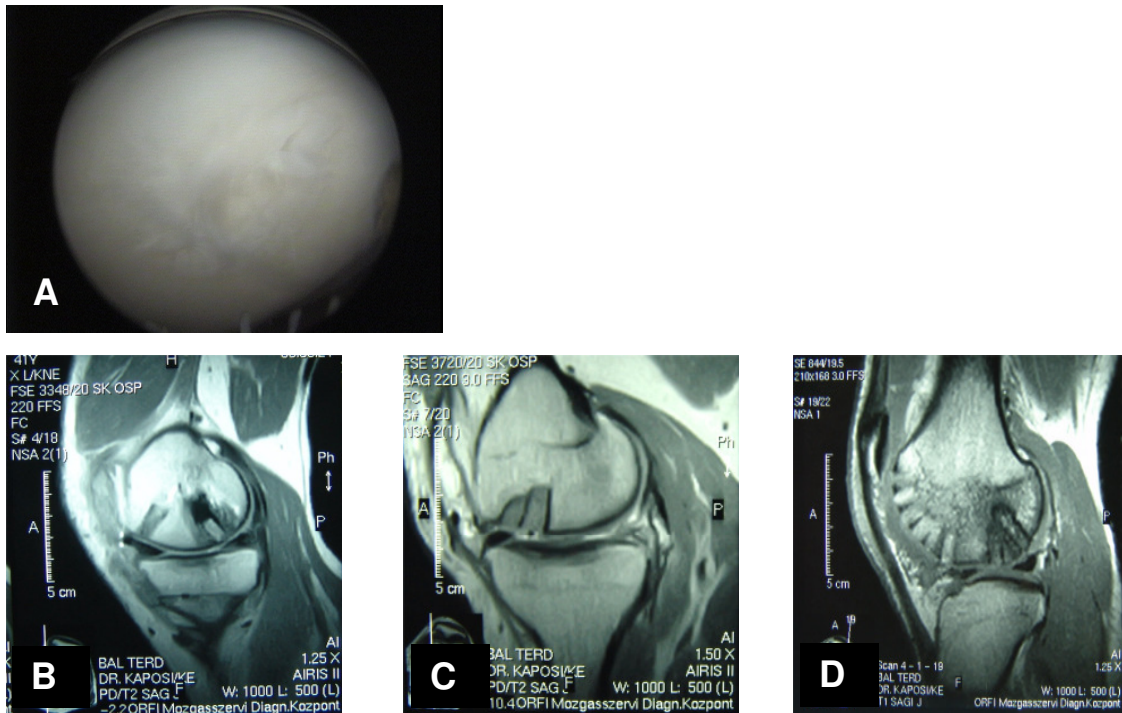


Figure 2. Arthroscopy and MRI evaluation of the filled donor sites after 9 months.

(A) Arthroscopy of the donor site. Note the surface congruence and integration with surrounding host tissue. (B) MRI showing the filled donor site (left) and recipient site (right). Donor site indicates homogenous scaffold filling and osseous integration. (C) MRI showing two filled donor sites. Note the homogenous filling. (D) MRI showing six filled donor sites and the recipient site indicating surface congruence of the filled sites and the osseous integration of the scaffolds.

occasionally showed protrusion of repair tissue at the defect margins. Subchondral cortical bone formation was not observed at this stage. The stiffness of the repair tissue at the surface of filled donor sites was equal or slightly improved when compared to empty controls.

By histological evaluation of the filled donor sites formation of fibrocartilaginous surface repair was observed in 5 out of 7 biopsies (Fig. 3). The tissue was characterized by the presence of large proteoglycan rich areas indicated by intense metachromatic staining: purple after DMMB reaction (Fig. 3A, C), and red after Safranin O staining (Fig. 3B). Furthermore, induced optical anisotropy was observed after DMMB staining reaction in polarized light microscope suggesting the spatial orientation proteoglycan molecules stained (Fig. 3D). This feature is generally typical for the extracellular matrix of hyaline cartilage. In 2 other cases the articular surface was covered by a dense connective tissue.

Interestingly, despite the relative hydrophobic composition of the PEOT/PBT implant (300PEOT55PBT45), histological evaluation showed substantial fragmentation in all filled donor sites (Fig. 3A-D). This demonstrates the biodegradability of the implant. In addition, the presence of these fragments did not induce an increased inflammatory response. The integration of the PEOT/PBT implant and the absence of a chronic inflammatory response demonstrate the long-term biocompatibility of this polymer. The polymer fragments are frequently surrounded by a few multinucleated giant cells indicating active ongoing phagocytotic degradation. Furthermore, histological analysis detected connective tissue rich in collagen fibers and HA as well as trabecular bone.

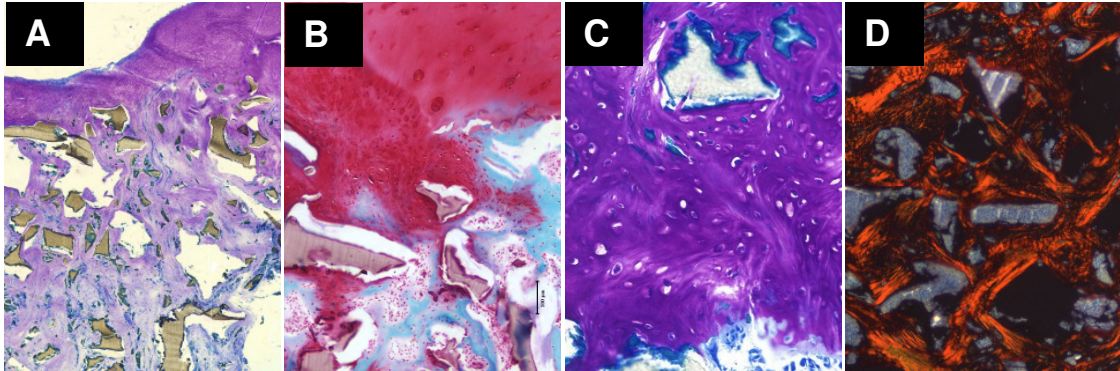


Figure 3. Histological evaluation of biopsies after 9 month. **(A)** Fibrocartilage formation at the surface of PEOT/PBT. Dimethylmethylene blue staining (DMMB); magnification 4x. **(B)** Intense metachromatic staining indicating proteoglycan rich domains. Safranin O staining; magnification 10x. **(C)** Calcification throughout the biopsy. DMMB staining; magnification 20x. **(D)** Strong optical anisotropy of collagen fibers. Picosirius Red staining and polarized light microscopy. Magnification 10x.

Polarized microscopy revealed that the collagen fibers of the connective tissue and trabecular bone exhibited a strong induced optical anisotropy suggesting a high degree of spatial orientation of the collagen (Fig. 3D). In the fibrous surface and underlying connective tissue collagen type I and HA could be detected (Fig. 4A). Some traces of collagen type 2 could be detected by immunohistochemistry at the periphery of the implants (data not shown).

In addition, newly formed bone has been found in all biopsies. Biopsies stained positively for osteonectin (Fig. 4B). Moreover, the osteoconductive property of the PEOT/PBT implants could be verified by the detection of osteoblasts and osteocytes.

Discussion

This clinical feasibility study evaluated the safety and efficacy of biodegradable PEOT/PBT implants to fill donor sites during mosaicplasty after 9 months of surgery. We were able to demonstrate, that PEOT/PBT is a safe and biocompatible filler and of added value to prevent postoperative bleeding, support subchondral integration and facilitate congruent resurfacing with mainly fibrocartilagenous tissue.

Safety was demonstrated by the absence of adverse intra-articular events or implant related complications. Long term biocompatibility was proven by the absence of a chronic inflammatory response or adverse cellular events and the presence of a mild foreign body response. The latter is inherent to biodegradable synthetic biomaterials. Few giant cells were occasionally observed adjacent to PEOT/PBT fragments. This is indicative for ongoing phagocytosis. The ability of phagocytosing cells with normal cell morphology to further erode and degrade PEOT/PBT polymer fragments has previously been established using transmission electron microscopic analysis [327]. The presence and amount of PEOT/PBT fragments after 9 months follow up indicated considerable implant biodegradation. Fragments were mainly observed in the subchondral area. Extrusion was not observed. Fragments occasionally revealed a clear demarcation following DMMB staining reaction, indicative for polymer calcification. Calcification of PEOT/PBT has been demonstrated to be key attribute for its bone bonding and osteoconductive character [64, 65, 200, 303].

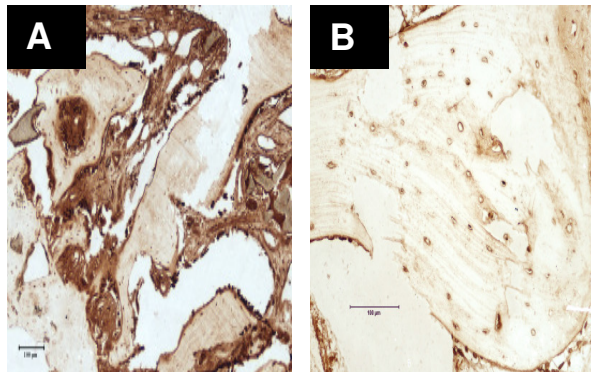


Figure 4. Histological evaluation of biopsies after 9 month. **(A)** Densely packed collagen type 1 at the surface of the PEOT/PBT. Immunohistochemistry, magnification 10x. **(B)** Detection of osteonectin in biopsies after 9 months indicating newly formed bone. Immunohistochemistry. Magnification 20x.

Lamme et al. previously implanted porous PEOT/PBT subcutaneously in mini pigs [328]. Using the identical implant structure and copolymer composition 300PEOT55PBT45, a decrease in the Mw of 34% was observed after 52 weeks. Based on the 90% decrease in MW for hydrophilic compositions, while preserving high amounts of PEOT in the copolymer, it was indicated as unlikely that crystalline PBT domains would remain. The rate and extent of polymer fragmentation was identified as the determining factor for successful soft tissue augmentation. Hydrophobic compositions performed better in comparison to hydrophilic compositions with respect to soft tissue biocompatibility and the amount and quality of deposited soft tissue. Analogously, the hydrophobic composition in this clinical trial seems to have supported appropriate biocompatibility, tissue integration and osteochondral healing. An interesting observation was also the absence of soft tissue encapsulation following subcutaneous implantation. The prevention of postoperative bleeding following press-fit insertion of PEOT/PBT implants can be explained by its hydrogel behavior which induces implant swelling thereby sealing off the defect [63].

Good integration of implants with the surrounding bone was established at the MRI and histological level. Osteolytic responses were absent. In the subchondral area, ample newly formed cancellous bone interspersed with fibrous tissue was observed. The properties of bone bridging and bone bonding by PEOT/PBT has been described in animal experiments using goats [200], beagle dogs [329] and rabbits [330]. Next to calcification, it is known that factors such as close contact between surrounding bone and implant material, appropriate porous and interconnected structures and the absence of micro-movement support bone ingrowth into the implant and allows good integration [331]. These critical parameters appear to be provided by the press-fit insertion and physico-chemical and structural properties of the PEOT/PBT implants and facilitate osteoconduction.

The postoperative behavior of empty donor sites after mosaicplasty has already been evaluated in previous experimental studies [29, 30]. These evaluations showed that fibrous or cancellous bone filling occurs, and natural healing processes result in mainly fibrous or fibrocartilagenous tissue resurfacing of the defects providing an acceptable gliding surface in these limited weight-bearing areas. This healing process, however, takes approximately 8 to 10 weeks and complications such as postoperative bleeding and donor side morbidity during this period have been reported [85].

The PEOT/PBT implants supported and favored fibrocartilage rather than fibrous tissue formation at the surface. The absence of fissures indicated an appropriate integration of the newly formed tissue with cartilage host tissue. Arthroscopically, the quality and stiffness of surface repair appeared comparable or slightly improved when compared to the repair tissue of empty donor sites. Surface fibrillation, for example, was occasionally observed in control defects. Although the increased cellular density indicates its reparative nature, the presence of several intense metachromatically stained hyaline-like areas in the implant filled defects is worth while mentioning.

Bone marrow derived progenitor cells play a key role in the osteochondral repair process. The PEOT/PBT implants likely provided the appropriate microenvironment for the attachment proliferation and differentiation of these cells thereby enabling fibrocartilagenous tissue formation and subchondral bone remodeling [23, 122]. It has been shown, for example, that PEOT/PBT copolymers can support the culture of fibroblasts [62], chondrocytes [332], bone and mesenchymal stem cells [63-65, 200, 303, 333, 334]. In addition, conditions such as high cell density, condensation and the low oxygen concentration might have occur, which all favor the chondrogenic differentiation of mesenchymal stem cells [124, 135, 153, 314, 315].

Another essential factor which allows cartilage formation in the defect site is the mechanical property of the filling material. Although the donor sites are located at limited weight-bearing areas, studies have indicated that there is a relationship between a defect and mechanically induced degeneration [335-338]. In addition, a reduction in local stress concentrations around defects favors cartilage repair [229]. Their results suggest to fill the donor site and by this reducing the local stress. Furthermore, it is crucial that the filling material can withstand the forces and even simulate cartilage like qualities [42, 46]. The PEOT/PBT composition and porous matrix morphology used for osteochondral defect filling have been tailored to establish mechanical properties compliant with native cartilage [42, 46, 293].

Conclusion

This study demonstrates the safety, long-term biocompatibility and osteoconductivity of porous PEOT/PBT implants. In addition, the ease of arthroscopic scaffold insertion, the congruent surface tissue repair of predominantly fibrocartilagenous nature, and the absence of intraarticular adverse events indicates its suitability for the filling of donor sites during mosaicplasty to prevent postoperative bleeding and donor site morbidity.

Conclusions and future perspectives

The objectives of this thesis were to investigate critical steps of tissue engineering to develop an osteochondral construct for the repair of degenerated joints.

The most advanced method would be to recognize early degradation of the articular cartilage surface and to replace only that specific region by cell-based implants. In that way high impact joint replacements could be evaded. The variety of proposed strategies in literature indicates the high expectations of such implants. Currently, it has been proven to be feasible to produce both materials similar in composition to bone and mechanical properties as in native articular cartilage. Combining both productions, researchers are able to build constructs with integrated osseous and chondral compartments. This offers a promising approach regarding future clinical application of osteochondral tissue engineering.

A variety of different studies have been conducted: osteochondral tissue engineering as cell-free approach, and cell-based by loading with (i) a single cell source with chondrogenic differentiation capacity such as chondrocytes, (ii) two different cell sources with either chondrogenic or osteogenic capacities, and (iii) a single cell source with both chondrogenic and osteogenic capacity. Various investigations on cell-based strategies show the advantage over cell free approaches. While most studies utilize chondrocytes or two different cell sources, the application of a single cell source with both chondrogenic and osteogenic differentiation capacities has not been investigated in such a plurality. So the question remains, which source of cells might be most applicable?

In this thesis a cell-based approach using a single cell source with both chondrogenic and osteogenic capacity has been applied for osteochondral tissue engineering. In the introduction, critical steps accompanying the use of bone marrow as single cell source for mesenchymal stem cells (MSCs) have been identified. Since numerous research groups have applied MSCs for bone tissue engineering, these critical steps are accompanied with the use of MSCs for cartilage tissue engineering. The findings regarding these issues will be discussed in the sections below.

1. What is the most suitable polyethylene oxide terephthalate / polybutylene terephthalate (PEOT/PBT) polymer composition and what seeding method needs to be applied to facilitate cell loading on scaffolds and concomitant chondrogenic differentiation?

While for the osseous compartment osteoinductive biomaterials can initiate cellular differentiation into the osteogenic lineage, for the cartilage part no chondroinductive material is known. Therefore, application of porous materials matching cartilage like mechanical properties was proposed. PEOT/PBT copolymers are implemented as model for the chondral compartment since numerous publications from our research group are available concerning successful cartilage tissue engineering using chondrocytes on these materials. Nevertheless, the question remained, which parameters influence successful cell loading and chondrogenic differentiation of MSCs to be applied on these copolymers. In chapter 1 we investigated parameters such as scaffold composition and cell seeding methods. No difference regarding cell seeding efficiency and chondrogenic differentiation of MSCs could be seen using hydrophilic and hydrophobic scaffold compositions, respectively.

In chapter 2 was demonstrated that the generation of cartilage is not depending on an initial high cell density or the chemical composition of the investigated scaffold material, but on the seeding method. Methods that attach the cells onto fibers of the scaffold allow

a homogeneously cell distribution. However, they are not applicable to generate cartilage on three-dimensional polymeric scaffolds, since the spread, spindle shaped morphology accompanying attached cells does not favor chondrogenesis. In contrast, methods that incorporate single or aggregated cells into the three-dimensional structure of the scaffolds support the differentiation. MSCs differentiated into the chondrogenic lineage, revealed a round, chondrocyte like morphology and were surrounded by an ECM rich in glycosaminoglycans (GAGs). These findings were obtained by *in vitro* studies, but chapter 1 also describes the stability of the *in vitro* generated cartilage *in vivo*.

The study results show that methods by which cartilage generation was not accomplished *in vitro* were not successful either when loaded constructs were implanted. Cartilage could be detected in constructs, that were loaded with cells by incorporation or aggregation; methods which were successful *in vitro* as well. However, for these constructs the amount was very little compared to the related *in vitro* constructs. The soft tissue, the presence of blood vessels as well as the absence of load questions does not offer an appropriate environment. Therefore, we question the subcutaneous implantation as an appropriate model to study the generation and stability of generated cartilage.

Consequently, the question still remains if different seeding methods can enhance the formation of cartilage that is stable and furthermore functional in a clinical relevant environment and further research needs to be conducted to answer it.

2. Are synthetic PEOT/PBT scaffolds used in cartilage TE suitable for incorporation and controlled release of chondrogenic growth factors and do incorporated growth factors maintain their stability and their biological activity after controlled release?

A different proposal to realize osteochondral TE is to release chondrogenic growth factors into the osteochondral defect to initiate chondrogenic differentiation of MSCs recruited by infiltration from the subchondral bone during surgery. In chapter 3 we describe a new method to prepare porous polymeric scaffolds containing and releasing TGF β 1, a potent chondrogenesis inducing growth factor. The application of PEOT/PBT and PEOT(T/S) /PB(T/S) copolymers allow the preparation of TGF β 1 releasing porous scaffolds by emulsion coating. By modifying factors such as vacuum and w/o emulsion volume, the loss of emulsion could be reduced to 50% and tailored release rate of TGF β 1 from 10 to 40 days *in vitro* was accomplished. The potential use of this release system in cartilage tissue engineering using MSCs was further described in chapter 4. The bioactivity of the released growth factor was examined in a pellet model since TGF β 1 is highly unstable. When MSCs were incubated with TGF β 1 releasing scaffolds for 15 days, histological analysis revealed chondrogenic differentiation by chondrocyte like cell morphology and intense staining of cartilage specific extracellular GAGs, which was further increased after 21 days. In addition, the implantation of similar scaffolds in osteochondral defects of rabbits emphasizes the applicability of such scaffolds to allow tissue ingrowth and integration [192]. Therefore, the release of chondrogenic TGF β 1 is a feasible approach to initiate chondrogenic differentiation of MSCs.

3. How feasible is respective cell loading and cell differentiation of MSCs in osteochondral scaffolds?

In chapter 5 we investigated the possibility to preaggregate MSCs to a size of approximately 150 μ m to increase cell seeding efficiency on porous three-dimensional scaffolds. This size equals the pore size of three-dimensional polymeric scaffolds which have to be proven to favor cartilage tissue engineering [68]. After incubation of only 4h MSC aggregates reached the desired size. Further aggregation was stopped by

incorporating aggregates in a thermosensitive gel. Additional incubation for 20h with TGF β 1-supplemented chondrogenic medium induces chondrogenesis. After 21 days in medium without TGF β 1 cells were differentiated into the chondrogenic lineage. Conclusively, in contrast to standard differentiation protocols applying TGF β 1 for 21 days, this study shows that no further incubation with expensive growth factors is required. The information from chapter 2, 4 and 5 combined allows the hypothetical set up of an ideal situation applying MSCs on a biphasic osteochondral construct in clinical practice. Bone marrow is harvested and MSCs are isolated and culture expanded using autologous serum. One day prior to the surgery, one half of the culture expanded MSCs is aggregated for 4h, incorporated into the chondral part of an osteochondral construct and incubated in chondrogenic, serum-free medium for additional 20h. 4h prior to the surgery, the other half of culture expanded MSCs is seeded onto the osseous part and allowed to attach. By this, the osteochondral construct is cell-based with chondrogenic and osteogenic cells, respectively, and ready to replace worn out osteochondral tissue in the defect. In conclusion, short incubation of MSCs in chondrogenic medium using low attachment wells is required to offer a clinical and commercial interesting cell-based osteochondral strategy.

4. How can novel scaffold fabrication techniques be applied to support cartilage generation and create integrated three-dimensional osteochondral scaffolds?

In the load bearing environment of joints, the primary mechanical properties of a osteochondral scaffold should match the mechanical properties of the surrounding tissue and are therefore crucial for the survival of implanted cells and their generation of a osseous and cartilaginous extracellular matrix, respectively.

Moroni *et al.* applied three-dimensional fiber deposition technology to fabricate scaffolds matching mechanical properties of native cartilage. Cartilage generation was significant greater on hydrophilic PEOT/ PBT (1000/70/30) *in vitro*. But these polymers show a strong tendency to swell in a wet environment, resulting in poor mechanical stability and might fail when used *in vivo* in a load bearing environment. More hydrophobic and mechanical stiffer PEOT/PBT (300/55/45) are an alternative. When three-dimensional fiber deposition technique is used to produce scaffolds with properties matching cartilage, the resulting pore size and porosity are large in relation to the cell size. In such an open structure, the cell seeding efficiency is very low. In chapter 6 we investigated the possibility to increase entrapment and differentiation of cells by integrating microfibrillar structures within the macrofibers of porous three-dimensional 300/55/45 scaffolds using electrospinning. When seeded with bovine chondrocytes, results showed a significant higher cell number and increased proliferation and cartilaginous matrix production as compared to scaffolds without microfibers. When MSCs were seeded, selective attachment and spreading on the electrospun network was observed, whereas scaffolds without microfibers revealed empty. These results indicate how different scaffold fabrication techniques combined can be exploited to realize material properties in terms of matching mechanical properties of desired tissue, increasing cell seeding and supporting cell differentiation. Going one step further, it can be adopted to assemble osteochondral constructs composed of polymers and ceramics, which is described in chapter 7.

The photolithographic technology was applied to produce porous, three-dimensional biphasic calcium phosphate structures of tailor-made architecture. These particles were integrated into the pores of a three-dimensional fiber-deposited osteochondral matrix composed of PEOT/PBT 1000/70/30 for the osseous part and PEOT/PBT 300/55/45 for the chondral part. Delamination of both compartments was prevented by utilizing the

hydrophilic and hydrophobic characteristic of the two polymer compositions. They were looped while printing and by swelling in culture medium this formed an interlocking system.

Results from chapter 2 and 5 were adopted to implement respective seeding of undifferentiated MSCs into the osseous part and chondrogenic MSCs into the chondral part. Cell-based osteochondral constructs were implanted subcutaneous in the back of nude mice. Analysis after 4 weeks showed cartilage tissue generation in the chondral part and bone tissue in the osseous part. In conclusion, the applied technologies to fabricate three-dimensional scaffolds facilitate efficient cell entrapment, cartilage generation and production of integrated osteochondral constructs and offer great potential for clinical practice.

Outlook

At this stage of development, it is important to notice that the application of successful aggregation, loading and differentiation of caprine MSCs into osteochondral constructs need to be extrapolated to human MSCs.

Within the last years our research group investigated intensively osteogenic and chondrogenic differentiation of human MSCs. Applying MSCs onto ceramic particles, we were able to reproducibly form bone *in vitro* and *in vivo* in animal models. As a result, Meijer et al. conducted a clinical feasibility trial where 10 patients underwent reconstruction of intra oral defects with MSC seeded hydroxyapatite. The defect of one patient was filled with newly formed bone produced by the implanted cells [339]. However, the amount of bone tissue produced is insufficient and not fully bridged to the implant. These data are in contrast to results obtained with goat and rat MSCs, which completely fitted the implant by newly formed bone [340]. Discrepancies are also seen when chondrogenic differentiation of human MSCs is compared with caprine MSCs (Fig. 1). In addition, in bone tissue engineering, a large variability in bone forming capacity of MSCs among donors has been reported [341-344]. It is concluded that bone marrow biopsies contain a heterogenous cell pool, which might have also a critical impact on the chondrogenic differentiation capacity of MSCs.

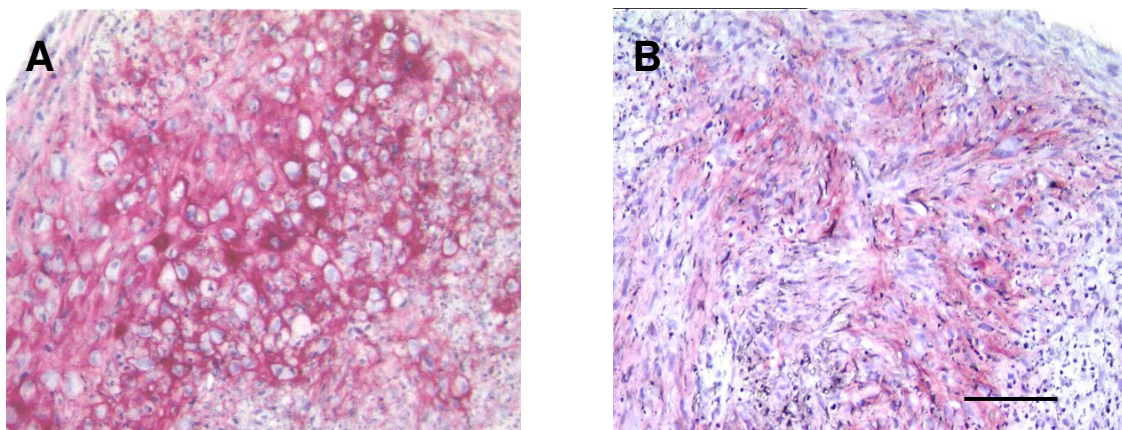


Figure 1: Safranin O staining of pellets containing MSCs differentiated into chondrogenic lineage. **(A)** Majority of caprine MSCs differentiate into chondrogenic lineage showing large lacunae and an intense Safranin O positive extracellular matrix. **(B)** In contrast, cultured under the same conditions, from human

MSCs only a minority show chondrocyte like morphology within the pellet, and their extracellular matrix does not stain in such intensity for Safranin O. Scale bar 200 μ m.

Therefore, current research is focused on the identification of new diagnostic markers to predict osteogenic and chondrogenic differentiation capacity. We approach this by isolating human MSCs from over 80 donors, analyzing their gene expression profiles and in parallel assessing their in vitro chondrogenic and osteogenic differentiation capacity and their in vivo bone and cartilage forming ability. First quantitative analysis of chondrogenic differentiation revealed significant differences between donors, but so far no conclusions can be drawn regarding influencing factors such as gender, source of bone marrow or age due the limited group size (Fig. 2).

Another essential issue that needs to be stressed out at this phase of osteochondral construct development is, that a subcutaneous implantation model as described in chapter 7 is not load bearing. Therefore, the stability and functionality of such tissue engineered osteochondral constructs remains to be investigated in a load bearing model and it might be also of great interest to implant such constructs in donor sites during mosaicplasty. In chapter 8 we describe the importance to fill donor sites after biopsy harvest for mosaicplasty. In this study we implanted cell free PEOT/PBT plugs into the steochondral defects created after biopsy harvest for mosaicplasty. MRI shows osseous integration throughout the implant. In addition, histological evaluation of the filled donor sites revealed subchondral cancellous bone formation with interspersed fibrous tissue and fibrocartilaginous repair at the surface.

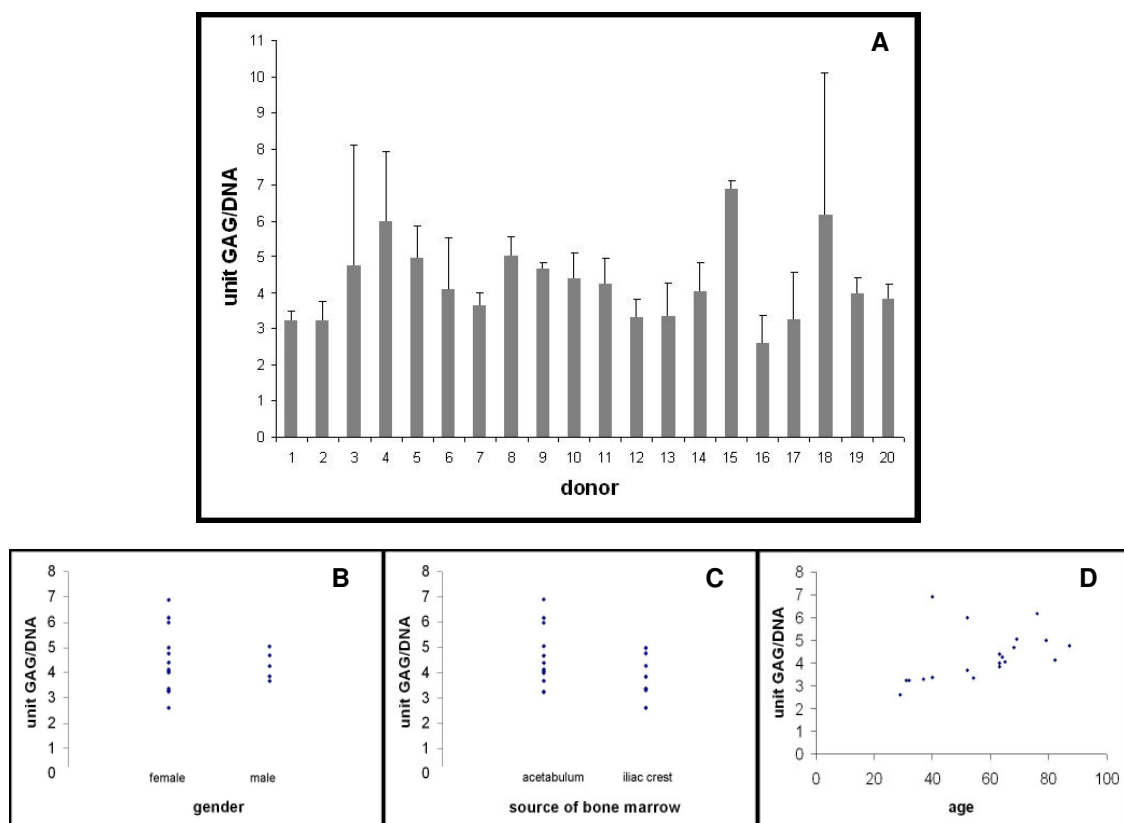


Figure 2: Preliminary results regarding the influence on donor variation on chondrogenic differentiation of mesenchymal stem cells. **(A)** Quantitative analysis of 20 donors shows significant variations between the donors. Parameters such as **(B)** gender, **(C)** source of bone marrow and **(D)** donor age are investigated, but do not reveal conclusive results due to the limited group size analyzed so far.

To improve the quality of the repair tissue, cell-based osteochondral tissue engineering as described in chapter 7 of this thesis might offer a promising approach and eventually replace conventional mosaicplasty. Subsequently, severe osteochondral defects in fully load bearing joints might be repaired in the future by this novel cell therapy.

Despite the last four years of research to develop the osteochondral construct, there are still numerous critical elements:

- Constructs completely filled with cartilage and bone, respectively, need to be developed. So far only limited and not clinical relevant amounts are feasible.
- The parameters that have impact on the development of hypertrophy in the cartilage part of subcutaneously implanted osteochondral constructs need to be determined. The knowledge might be applied to increase cartilage formation in the chondral part by inhibition of hypertrophic factors, but also to enhance bone formation in the osseous part by endochondral ossification.
- The feasibility to produce vascularized and thereby viable large osseous compartments and the influence of vascular invasion on cartilage formation in the chondral compartment need to be addressed.
- The stability and functionality of the cell-based osteochondral construct in a load bearing environment needs to be investigated.

The research on these significant aspects will bring osteochondral tissue engineering again a step closer to clinical application.

References

1. http://www.edcenter.med.cornell.edu/CUMC_PathNotes/Skeletal/3092.GIF.
2. Chambers TJ. The regulation of osteoclastic development and function. Ciba Foundation symposium 1988;136:92-107.
3. Heino TJ, Hentunen TA, Vaananen HK. Osteocytes inhibit osteoclastic bone resorption through transforming growth factor-beta: enhancement by estrogen. Journal of cellular biochemistry 2002;85(1):185-197.
4. Gay CV, Weber JA. Regulation of differentiated osteoclasts. Critical reviews in eukaryotic gene expression 2000;10(3-4):213-230.
5. Baron R, Neff L, Louvard D, Courtoy PJ. Cell-mediated extracellular acidification and bone resorption: evidence for a low pH in resorbing lacunae and localization of a 100-kD lysosomal membrane protein at the osteoclast ruffled border. The Journal of cell biology 1985 Dec;101(6):2210-2222.
6. Miller SC, de Saint-Georges L, Bowman BM, Jee WS. Bone lining cells: structure and function. Scanning microscopy 1989 Sep;3(3):953-960; discussion 960-951.
7. Bilezikian JP. Current and future nonhormonal approaches to the treatment of osteoporosis. International journal of fertility and menopausal studies 1996 Mar-Apr;41(2):148-155.
8. Wolff J. Das Gesetz der Transformation der Knochen. In: Hirschwald A, editor. Berlin, 1892.
9. Riesle J, Hollander AP, Langer R, Freed LE, Vunjak-Novakovic G. Collagen in tissue-engineered cartilage: types, structure, and crosslinks. Journal of cellular biochemistry 1998 Dec 1;71(3):313-327.
10. Garnero P, Rousseau JC, Delmas PD. Molecular basis and clinical use of biochemical markers of bone, cartilage, and synovium in joint diseases. Arthritis and rheumatism 2000 May;43(5):953-968.
11. Studer D, Chiquet M, Hunziker EB. Evidence for a distinct water-rich layer surrounding collagen fibrils in articular cartilage extracellular matrix. Journal of structural biology 1996 Sep-Oct;117(2):81-85.
12. DiMicco MA, Sah RL. Integrative cartilage repair: adhesive strength is correlated with collagen deposition. 2001. p. 1105-1112.
13. <http://anatomy.iupui.edu>. [cited; Available from:
14. Eckstein F, Winzheimer M, Hohe J, Englmeier KH, Reiser M. Interindividual variability and correlation among morphological parameters of knee joint cartilage plates: analysis with three-dimensional MR imaging. Osteoarthritis and Cartilage 2001;9(2):101-111.
15. Hunziker EB, Rosenberg LC. Repair of partial-thickness defects in articular cartilage: cell recruitment from the synovial membrane. The Journal of bone and joint surgery 1996 May;78(5):721-733.
16. Buckwalter JAM. Articular Cartilage Injuries
Source Clinical Orthopaedics & Related Research 2002
402(September):21-37.
17. Wezeman FH. Morphological foundations of precartilage development in mesenchyme. Microscopy research and technique 1998 Oct 15;43(2):91-101.
18. Williamson AK, Chen AC, Sah RL. Compressive properties and function-composition relationships of developing bovine articular cartilage. J Orthop Res 2001 Nov;19(6):1113-1121.
19. Metsaranta M, Kujala UM, Pelliniemi L, Osterman H, Aho H, Vuorio E. Evidence for insufficient chondrocytic differentiation during repair of full-thickness defects of articular cartilage. Matrix Biol 1996 Apr;15(1):39-47.
20. Giurea A, DiMicco MA, Akeson WH, Sah RL. Development-associated differences in integrative cartilage repair: roles of biosynthesis and matrix. J Orthop Res 2002 Nov;20(6):1274-1281.
21. Martin JA, Buckwalter JA. Aging, articular cartilage chondrocyte senescence and osteoarthritis. Biogerontology 2002;3(5):257-264.

22. Hunziker EB. Articular cartilage repair: basic science and clinical progress. A review of the current status and prospects. *Osteoarthritis and cartilage / OARS, Osteoarthritis Research Society* 2002 Jun;10(6):432-463.
23. Shapiro F, Koide S, Glimcher MJ. Cell origin and differentiation in the repair of full-thickness defects of articular cartilage. *The Journal of bone and joint surgery* 1993 Apr;75(4):532-553.
24. <http://www.hipresurfacingcenter.com/knee.htm>. [cited; Available from:
25. <http://www.kneesurgeryaustralia.com/kneereplacement/>. [cited; Available from:
26. Narmoneva DA, Cheung HS, Wang JY, Howell DS, Setton LA. Altered swelling behavior of femoral cartilage following joint immobilization in a canine model. *J Orthop Res* 2002 Jan;20(1):83-91.
27. O'Driscoll SW. The healing and regeneration of articular cartilage. *The Journal of bone and joint surgery* 1998 Dec;80(12):1795-1812.
28. Brittberg M, Tallheden T, Sjogren-Jansson B, Lindahl A, Peterson L. Autologous chondrocytes used for articular cartilage repair: an update. *Clin Orthop* 2001:S337-S348.
29. Hangody L, Fules P. Autologous osteochondral mosaicplasty for the treatment of full-thickness defects of weight-bearing joints: ten years of experimental and clinical experience. *The Journal of bone and joint surgery* 2003;85-A Suppl 2:25-32.
30. Hangody L, Kish G, Karpati Z, Szerb I, Udvarhelyi I. Arthroscopic autogenous osteochondral mosaicplasty for the treatment of femoral condylar articular defects. A preliminary report. *Knee Surg Sports Traumatol Arthrosc* 1997;5(4):262-267.
31. Langer R. Tissue engineering: a new field and its challenges. *Pharmaceutical research* 1997 Jul;14(7):840-841.
32. Ylanen HO, Helminen T, Helminen A, Rantakokko J, Karlsson KH, Aro HT. Porous bioactive glass matrix in reconstruction of articular osteochondral defects. *Annales chirurgiae et gynaecologiae* 1999;88(3):237-245.
33. Suominen E, Aho AJ, Vedel E, Kangasniemi I, Uusipaikka E, Yli-Urpo A. Subchondral bone and cartilage repair with bioactive glasses, hydroxyapatite, and hydroxyapatite-glass composite. *Journal of biomedical materials research* 1996 Dec;32(4):543-551.
34. Rey C. Calcium Phosphate biomaterials and bone mineral. Differences in Composition and structure and properties. *Biomaterials* 1990;Jul(11):13-15.
35. De Bruijn JD, Klein CP, De Groot K, van Blitterswijk CA. The Ultrastructure of the Bone-Hydroxyapatite interface in vitro. *Journal of biomedical materials research* 1992;26(10):1365-1382.
36. De Bruijn JD, Van Blitterswijk CA, Davies JE. Initial Bone Matrix Formation at the Hydroxyapatite Interface in vivo. *Journal of biomedical materials research* 1995;29(1):89-99.
37. Ripamonti U. Osteoinduction in porous hydroxyapatite implanted in heterotopic sites of different animal models. *Biomaterials* 1996 Jan;17(1):31-35.
38. Yuan H, Kurashina K, de Bruijn JD, Li Y, de Groot K, Zhang X. A preliminary study on osteoinduction of two kinds of calcium phosphate ceramics. *Biomaterials* 1999 Oct;20(19):1799-1806.
39. Yuan H, Li Y, de Bruijn JD, de Groot K, Zhang X. Tissue responses of calcium phosphate cement: a study in dogs. *Biomaterials* 2000 Jun;21(12):1283-1290.
40. Yuan H, Yang Z, De Bruijn JD, De Groot K, Zhang X. Material-dependent bone induction by calcium phosphate ceramics: a 2.5-year study in dog. *Biomaterials* 2001 Oct;22(19):2617-2623.
41. Ripamonti U, Tasker JR. Advances in biotechnology for tissue engineering of bone. *Current pharmaceutical biotechnology* 2000 Jul;1(1):47-55.
42. Niederauer GG, Slivka MA, Leatherbury NC, Korvick DL, Harroff HH, Ehler WC, et al. Evaluation of multiphase implants for repair of focal osteochondral defects in goats. *Biomaterials* 2000 Dec;21(24):2561-2574.
43. Guo X, Wang C, Duan C, Descamps M, Zhao Q, Dong L, et al. Repair of osteochondral defects with autologous chondrocytes seeded onto bioceramic scaffold in sheep. *Tissue Eng* 2004 Nov-Dec;10(11-12):1830-1840.

44. Guo X, Wang C, Zhang Y, Xia R, Hu M, Duan C, et al. Repair of large articular cartilage defects with implants of autologous mesenchymal stem cells seeded into beta-tricalcium phosphate in a sheep model. *Tissue Eng* 2004 Nov-Dec;10(11-12):1818-1829.
45. Tanaka T, Komaki H, Chazono M, Fujii K. Use of a biphasic graft constructed with chondrocytes overlying a beta-tricalcium phosphate block in the treatment of rabbit osteochondral defects. *Tissue Eng* 2005 Jan-Feb;11(1-2):331-339.
46. van Susante JL, Buma P, Homminga GN, van den Berg WB, Veth RP. Chondrocyte-seeded hydroxyapatite for repair of large articular cartilage defects. A pilot study in the goat. *Biomaterials* 1998 Dec;19(24):2367-2374.
47. Freed LE, Grande DA, Lingbin Z, Emmanuel J, Marquis JC, Langer R. Joint resurfacing using allograft chondrocytes and synthetic biodegradable polymer scaffolds. *Journal of biomedical materials research* 1994 Aug;28(8):891-899.
48. Hutmacher DW. Scaffolds in tissue engineering bone and cartilage. *Biomaterials* 2000 Dec;21(24):2529-2543.
49. Lu L, Zhu X, Valenzuela RG, Currier BL, Yaszemski MJ. Biodegradable polymer scaffolds for cartilage tissue engineering. *Clinical orthopaedics and related research* 2001 Oct(391 Suppl):S251-270.
50. Temenoff JS, Mikos AG. Review: tissue engineering for regeneration of articular cartilage. *Biomaterials* 2000 Mar;21(5):431-440.
51. Kreklau B, Sittinger M, Mensing MB, Voigt C, Berger G, Burmester GR, et al. Tissue engineering of biphasic joint cartilage transplants. *Biomaterials* 1999 Sep;20(18):1743-1749.
52. Gao J, Dennis JE, Solchaga LA, Awadallah AS, Goldberg VM, Caplan AI. Tissue-engineered fabrication of an osteochondral composite graft using rat bone marrow-derived mesenchymal stem cells. *Tissue Eng* 2001 Aug;7(4):363-371.
53. Schaefer D, Martin I, Shastri P, Padera RF, Langer R, Freed LE, et al. In vitro generation of osteochondral composites. *Biomaterials* 2000 Dec;21(24):2599-2606.
54. Schaefer D, Martin I, Jundt G, Seidel J, Heberer M, Grodzinsky A, et al. Tissue-engineered composites for the repair of large osteochondral defects. *Arthritis and rheumatism* 2002 Sep;46(9):2524-2534.
55. Isogai N, Landis W, Kim TH, Gerstenfeld LC, Upton J, Vacanti JP. Formation of phalanges and small joints by tissue-engineering. *The Journal of bone and joint surgery* 1999 Mar;81(3):306-316.
56. Alhadlaq A, Mao JJ. Tissue-engineered osteochondral constructs in the shape of an articular condyle. *The Journal of bone and joint surgery* 2005 May;87(5):936-944.
57. Taboas JM, Maddox RD, Krebsbach PH, Hollister SJ. Indirect solid free form fabrication of local and global porous, biomimetic and composite 3D polymer-ceramic scaffolds. *Biomaterials* 2003 Jan;24(1):181-194.
58. Holland TA, Bodde EW, Baggett LS, Tabata Y, Mikos AG, Jansen JA. Osteochondral repair in the rabbit model utilizing bilayered, degradable oligo(polyethylene oxide) fumarate hydrogel scaffolds. *Journal of biomedical materials research* 2005 Oct 1;75(1):156-167.
59. Gao J, Dennis JE, Solchaga LA, Goldberg VM, Caplan AI. Repair of osteochondral defect with tissue-engineered two-phase composite material of injectable calcium phosphate and hyaluronan sponge. *Tissue Eng* 2002 Oct;8(5):827-837.
60. Ito Y, Ochi M, Adachi N, Sugawara K, Yanada S, Ikada Y, et al. Repair of osteochondral defect with tissue-engineered chondral plug in a rabbit model. *Arthroscopy* 2005 Oct;21(10):1155-1163.
61. Sherwood JK, Riley SL, Palazzolo R, Brown SC, Monkhouse DC, Coates M, et al. A three-dimensional osteochondral composite scaffold for articular cartilage repair. *Biomaterials* 2002 Dec;23(24):4739-4751.
62. Beumer GJ, van Blitterswijk CA, Bakker D, Ponec M. Cell-seeding and in vitro biocompatibility evaluation of polymeric matrices of PEO/PBT copolymers and PLLA. *Biomaterials* 1993 Jul;14(8):598-604.
63. Deschamps AA, Claase MB, Sleijster WJ, de Bruijn JD, Grijpma DW, Feijen J. Design of segmented poly(ether ester) materials and structures for the tissue engineering of bone. *J Control Release* 2002 Jan 17;78(1-3):175-186.

64. Radder AM, Davies JE, Leenders H, van Blitterswijk CA. Interfacial behavior of PEO/PBT copolymers (Polyactive) in a calvarial system: an in vitro study. *Journal of biomedical materials research* 1994 Feb;28(2):269-277.
65. Radder AM, Leenders H, van Blitterswijk CA. Interface reactions to PEO/PBT copolymers (Polyactive) after implantation in cortical bone. *Journal of biomedical materials research* 1994 Feb;28(2):141-151.
66. Hendriks JA, Moroni L, Riesle J, van Blitterswijk CA. Fibronectin enhances cartilage tissue formation of articular chondrocytes on 3D-deposited scaffolds through aggregation mediated seeding. submitted.
67. Malda J, Woodfield TB, van der Vloodt F, Kooy FK, Martens DE, Tramper J, et al. The effect of PEOT/PBT scaffold architecture on oxygen gradients in tissue engineered cartilaginous constructs. *Biomaterials* 2004 Nov;25(26):5773-5780.
68. Moroni L, Hendriks JA, Schotel R, de Wijn JR, van Blitterswijk CA. Design of biphasic polymeric 3-dimensional fiber-deposited scaffolds for cartilage tissue engineering applications. *Tissue Eng* 2007 Feb;13(2):361-371.
69. Papadaki M, Mahmood T, Gupta P, Claase MB, Grijpma DW, Riesle J, et al. The different behaviors of skeletal muscle cells and chondrocytes on PEOT/PBT block copolymers are related to the surface properties of the substrate. *Journal of biomedical materials research* 2001 Jan;54(1):47-58.
70. Woodfield TB, Bezemer JM, Pieper JS, van Blitterswijk CA, Riesle J. Scaffolds for tissue engineering of cartilage. *Critical reviews in eukaryotic gene expression* 2002;12(3):209-236.
71. Bezemer JM, Radersma R, Grijpma DW, Dijkstra PJ, Feijen J, van Blitterswijk CA. Zero-order release of lysozyme from polyethylene oxide/polybutylene terephthalate matrices. *J Control Release* 2000 Feb 14;64(1-3):179-192.
72. Sohier J, Vlugt TJ, Cabrol N, Van Blitterswijk C, de Groot K, Bezemer JM. Dual release of proteins from porous polymeric scaffolds. *J Control Release* 2006 Mar 10;111(1-2):95-106.
73. van de Weert M, van Dijkhuizen-Radersma R, Bezemer JM, Hennink WE, Crommelin DJ. Reversible aggregation of lysozyme in a biodegradable amphiphilic multiblock copolymer. *Eur J Pharm Biopharm* 2002 Jul;54(1):89-93.
74. van Dijkhuizen-Radersma R, Roosma JR, Sohier J, Peters FL, van den Doel M, van Blitterswijk CA, et al. Biodegradable poly(ether-ester) multiblock copolymers for controlled release applications: An in vivo evaluation. *Journal of biomedical materials research* 2004 Oct 1;71(1):118-127.
75. LiVecchi AB, Tombes RM, LaBerge M. In vitro chondrocyte collagen deposition within porous HDPE: substrate microstructure and wettability effects. *Journal of biomedical materials research* 1994 Aug;28(8):839-850.
76. Woodfield TB, Miot S, Martin I, van Blitterswijk CA, Riesle J. The regulation of expanded human nasal chondrocyte re-differentiation capacity by substrate composition and gas plasma surface modification. *Biomaterials* 2006 Mar;27(7):1043-1053.
77. Quarto R, Campanile G, Cancedda R, Dozin B. Modulation of commitment, proliferation, and differentiation of chondrogenic cells in defined culture medium. *Endocrinology* 1997 Nov;138(11):4966-4976.
78. De Bari C, Dell'Accio F, Luyten FP. Human periosteum-derived cells maintain phenotypic stability and chondrogenic potential throughout expansion regardless of donor age. *Arthritis and rheumatism* 2001 Jan;44(1):85-95.
79. Mason JM, Breitbart AS, Barcia M, Porti D, Pergolizzi RG, Grande DA. Cartilage and bone regeneration using gene-enhanced tissue engineering. *Clinical orthopaedics and related research* 2000 Oct(379 Suppl):S171-178.
80. Haisch A, Schultz O, Perka C, Jahnke V, Burmester GR, Sittinger M. [Tissue engineering of human cartilage tissue for reconstructive surgery using biocompatible resorbable fibrin gel and polymer carriers]. *Hno* 1996 Nov;44(11):624-629.
81. Sittinger M, Perka C, Schultz O, Haupl T, Burmester GR. Joint cartilage regeneration by tissue engineering. *Zeitschrift fur Rheumatologie* 1999 Jun;58(3):130-135.
82. Gugala Z, Gogolewski S. In vitro growth and activity of primary chondrocytes on a resorbable polylactide three-dimensional scaffold. *Journal of biomedical materials research* 2000 Feb;49(2):183-191.

83. Lee CR, Grodzinsky AJ, Spector M. The effects of cross-linking of collagen-glycosaminoglycan scaffolds on compressive stiffness, chondrocyte-mediated contraction, proliferation and biosynthesis. *Biomaterials* 2001 Dec;22(23):3145-3154.
84. Sechriest VF, Miao YJ, Niyibizi C, Westerhausen-Larson A, Matthew HW, Evans CH, et al. GAG-augmented polysaccharide hydrogel: a novel biocompatible and biodegradable material to support chondrogenesis. *Journal of biomedical materials research* 2000 Mar 15;49(4):534-541.
85. Hangody L, Rathonyi GK, Duska Z, Vasarhelyi G, Fules P, Modis L. Autologous osteochondral mosaicplasty. Surgical technique. *The Journal of bone and joint surgery* 2004 Mar;86-A Suppl 1:65-72.
86. Kafienah W, Jakob M, Demarteau O, Frazer A, Barker MD, Martin I, et al. Three-dimensional tissue engineering of hyaline cartilage: comparison of adult nasal and articular chondrocytes. *Tissue Eng* 2002 Oct;8(5):817-826.
87. Thomson JA, Itskovitz-Eldor J, Shapiro SS, Waknitz MA, Swiergiel JJ, Marshall VS, et al. Embryonic stem cell lines derived from human blastocysts. *Science (New York, NY)* 1998 Nov 6;282(5391):1145-1147.
88. Shambloott MJ, Axelman J, Littlefield JW, Blumenthal PD, Huggins GR, Cui Y, et al. Human embryonic germ cell derivatives express a broad range of developmentally distinct markers and proliferate extensively in vitro. *Proceedings of the National Academy of Sciences of the United States of America* 2001 Jan 2;98(1):113-118.
89. Schuldiner M, Yanuka O, Itskovitz-Eldor J, Melton DA, Benvenisty N. Effects of eight growth factors on the differentiation of cells derived from human embryonic stem cells. *Proceedings of the National Academy of Sciences of the United States of America* 2000 Oct 10;97(21):11307-11312.
90. Kehat I, Kenyagin-Karsenti D, Snir M, Segev H, Amit M, Gepstein A, et al. Human embryonic stem cells can differentiate into myocytes with structural and functional properties of cardiomyocytes. *The Journal of clinical investigation* 2001 Aug;108(3):407-414.
91. Metzger JM, Lin WI, Samuelson LC. Vital staining of cardiac myocytes during embryonic stem cell cardiogenesis in vitro. *Circulation research* 1996 Apr;78(4):547-552.
92. Rohwedel J, Guan K, Zuschratter W, Jin S, Ahnert-Hilger G, Furst D, et al. Loss of beta1 integrin function results in a retardation of myogenic, but an acceleration of neuronal, differentiation of embryonic stem cells in vitro. *Developmental biology* 1998 Sep 15;201(2):167-184.
93. Tropepe V, Coles BL, Chiasson BJ, Horsford DJ, Elia AJ, McInnes RR, et al. Retinal stem cells in the adult mammalian eye. *Science (New York, NY)* 2000 Mar 17;287(5460):2032-2036.
94. McDonald JW, Liu XZ, Qu Y, Liu S, Mickey SK, Turetsky D, et al. Transplanted embryonic stem cells survive, differentiate and promote recovery in injured rat spinal cord. *Nature medicine* 1999 Dec;5(12):1410-1412.
95. Klug MG, Soonpaa MH, Koh GY, Field LJ. Genetically selected cardiomyocytes from differentiating embryonic stem cells form stable intracardiac grafts. *The Journal of clinical investigation* 1996 Jul 1;98(1):216-224.
96. Slack JM. Stem cells in epithelial tissues. *Science (New York, NY)* 2000 Feb 25;287(5457):1431-1433.
97. Smith C, Storms B. Hematopoietic stem cells. *Clinical orthopaedics and related research* 2000 Oct(379 Suppl):S91-97.
98. Gage FH. Mammalian neural stem cells. *Science (New York, NY)* 2000 Feb 25;287(5457):1433-1438.
99. McKay R. Stem cells in the central nervous system. *Science (New York, NY)* 1997 Apr 4;276(5309):66-71.
100. Pittenger MF, Mackay AM, Beck SC, Jaiswal RK, Douglas R, Mosca JD, et al. Multilineage potential of adult human mesenchymal stem cells. *Science (New York, NY)* 1999 Apr 2;284(5411):143-147.
101. Prockop DJ. Marrow stromal cells as stem cells for nonhematopoietic tissues. *Science (New York, NY)* 1997 Apr 4;276(5309):71-74.
102. Weissman IL. Translating stem and progenitor cell biology to the clinic: barriers and opportunities. *Science (New York, NY)* 2000 Feb 25;287(5457):1442-1446.

103. Bjornson CR, Rietze RL, Reynolds BA, Magli MC, Vescovi AL. Turning brain into blood: a hematopoietic fate adopted by adult neural stem cells in vivo. *Science (New York, NY)* 1999 Jan 22;283(5401):534-537.
104. Galli R, Borello U, Gritti A, Minasi MG, Bjornson C, Coletta M, et al. Skeletal myogenic potential of human and mouse neural stem cells. *Nature neuroscience* 2000 Oct;3(10):986-991.
105. Clarke DL, Johansson CB, Wilbertz J, Veress B, Nilsson E, Karlstrom H, et al. Generalized potential of adult neural stem cells. *Science (New York, NY)* 2000 Jun 2;288(5471):1660-1663.
106. Anderson DJ. Stem cells and pattern formation in the nervous system: the possible versus the actual. *Neuron* 2001 Apr;30(1):19-35.
107. Toma JG, Akhavan M, Fernandes KJ, Barnabe-Heider F, Sadikot A, Kaplan DR, et al. Isolation of multipotent adult stem cells from the dermis of mammalian skin. *Nature cell biology* 2001 Sep;3(9):778-784.
108. Zuk PA, Zhu M, Mizuno H, Huang J, Futrell JW, Katz AJ, et al. Multilineage cells from human adipose tissue: implications for cell-based therapies. *Tissue Eng* 2001 Apr;7(2):211-228.
109. Petersen BE, Bowen WC, Patrene KD, Mars WM, Sullivan AK, Murase N, et al. Bone marrow as a potential source of hepatic oval cells. *Science (New York, NY)* 1999 May 14;284(5417):1168-1170.
110. Fukuda K. Development of regenerative cardiomyocytes from mesenchymal stem cells for cardiovascular tissue engineering. *Artificial organs* 2001 Mar;25(3):187-193.
111. Makino S, Fukuda K, Miyoshi S, Konishi F, Kodama H, Pan J, et al. Cardiomyocytes can be generated from marrow stromal cells in vitro. *The Journal of clinical investigation* 1999 Mar;103(5):697-705.
112. Mezey E, Chandross KJ, Harta G, Maki RA, McKercher SR. Turning blood into brain: cells bearing neuronal antigens generated in vivo from bone marrow. *Science (New York, NY)* 2000 Dec 1;290(5497):1779-1782.
113. Kopen GC, Prockop DJ, Phinney DG. Marrow stromal cells migrate throughout forebrain and cerebellum, and they differentiate into astrocytes after injection into neonatal mouse brains. *Proceedings of the National Academy of Sciences of the United States of America* 1999 Sep 14;96(19):10711-10716.
114. Friedenstein AJ, Chailakhyan RK, Gerasimov UV. Bone marrow osteogenic stem cells: in vitro cultivation and transplantation in diffusion chambers. *Cell and tissue kinetics* 1987 May;20(3):263-272.
115. Johnstone B, Hering TM, Caplan AI, Goldberg VM, Yoo JU. In vitro chondrogenesis of bone marrow-derived mesenchymal progenitor cells. *Experimental cell research* 1998 Jan 10;238(1):265-272.
116. Yoo JU, Barthel TS, Nishimura K, Solchaga L, Caplan AI, Goldberg VM, et al. The chondrogenic potential of human bone-marrow-derived mesenchymal progenitor cells. *The Journal of bone and joint surgery* 1998 Dec;80(12):1745-1757.
117. Wakitani S, Saito T, Caplan AI. Myogenic cells derived from rat bone marrow mesenchymal stem cells exposed to 5-azacytidine. *Muscle & nerve* 1995 Dec;18(12):1417-1426.
118. Ferrari G, Cusella-De Angelis G, Coletta M, Paolucci E, Stornaiuolo A, Cossu G, et al. Muscle regeneration by bone marrow-derived myogenic progenitors. *Science (New York, NY)* 1998 Mar 6;279(5356):1528-1530.
119. Dormady SP, Bashayan O, Dougherty R, Zhang XM, Basch RS. Immortalized multipotential mesenchymal cells and the hematopoietic microenvironment. *Journal of hematotherapy & stem cell research* 2001 Feb;10(1):125-140.
120. Friedenstein AJ, Gorskaja JF, Kulagina NN. Fibroblast precursors in normal and irradiated mouse hematopoietic organs. *Experimental hematology* 1976 Sep;4(5):267-274.
121. Brazelton TR, Rossi FM, Keshet GI, Blau HM. From marrow to brain: expression of neuronal phenotypes in adult mice. *Science (New York, NY)* 2000 Dec 1;290(5497):1775-1779.
122. Wakitani S, Goto T, Pineda SJ, Young RG, Mansour JM, Caplan AI, et al. Mesenchymal cell-based repair of large, full-thickness defects of articular cartilage. *The Journal of bone and joint surgery* 1994 Apr;76(4):579-592.

123. Wakitani S, Mitsuoka T, Nakamura N, Toritsuka Y, Nakamura Y, Horibe S. Autologous bone marrow stromal cell transplantation for repair of full-thickness articular cartilage defects in human patellae: two case reports. *Cell transplantation* 2004;13(5):595-600.
124. Akiyama H, Chaboissier MC, Martin JF, Schedl A, de Crombrughe B. The transcription factor Sox9 has essential roles in successive steps of the chondrocyte differentiation pathway and is required for expression of Sox5 and Sox6. *Genes & development* 2002 Nov 1;16(21):2813-2828.
125. Wayne JS, McDowell CL, Shields KJ, Tuan RS. In vivo response of polylactic acid-alginate scaffolds and bone marrow-derived cells for cartilage tissue engineering. *Tissue Eng* 2005 May-Jun;11(5-6):953-963.
126. De Bari C, Dell'Accio F, Luyten FP. Failure of in vitro-differentiated mesenchymal stem cells from the synovial membrane to form ectopic stable cartilage in vivo. *Arthritis and rheumatism* 2004 Jan;50(1):142-150.
127. Pelttari K, Winter A, Steck E, Goetzke K, Hennig T, Ochs BG, et al. Premature induction of hypertrophy during in vitro chondrogenesis of human mesenchymal stem cells correlates with calcification and vascular invasion after ectopic transplantation in SCID mice. *Arthritis and rheumatism* 2006 Oct;54(10):3254-3266.
128. Grande DA, Halberstadt C, Naughton G, Schwartz R, Manji R. Evaluation of matrix scaffolds for tissue engineering of articular cartilage grafts. *Journal of biomedical materials research* 1997 Feb;34(2):211-220.
129. Freed LE, Marquis JC, Nohria A, Emmanuel J, Mikos AG, Langer R. Neocartilage formation in vitro and in vivo using cells cultured on synthetic biodegradable polymers. *Journal of biomedical materials research* 1993 Jan;27(1):11-23.
130. Sakkars RJ, de Wijn JR, Dalmeyer RA, van Blitterswijk CA, Brand R. Evaluation of copolymers of polyethylene oxide and polybutylene terephthalate (polyactive): mechanical behaviour. *Journal of materials science* 1998 Jul;9(7):375-379.
131. Mahmood TA, Miot S, Frank O, Martin I, Riesle J, Langer R, et al. Modulation of chondrocyte phenotype for tissue engineering by designing the biologic-polymer carrier interface. *Biomacromolecules* 2006 Nov;7(11):3012-3018.
132. Woodfield TB, Malda J, de Wijn J, Peters F, Riesle J, van Blitterswijk CA. Design of porous scaffolds for cartilage tissue engineering using a three-dimensional fiber-deposition technique. *Biomaterials* 2004 Aug;25(18):4149-4161.
133. Hendriks JAA. The influence of cellular Interactions in tissue engineering for cartilage repair [PhD thesis]. Enschede: University of Twente; 2006.
134. Worster AA, Brower-Toland BD, Fortier LA, Bent SJ, Williams J, Nixon AJ. Chondrocytic differentiation of mesenchymal stem cells sequentially exposed to transforming growth factor-beta1 in monolayer and insulin-like growth factor-I in a three-dimensional matrix. *J Orthop Res* 2001 Jul;19(4):738-749.
135. Wang Y, Kim UJ, Blasioli DJ, Kim HJ, Kaplan DL. In vitro cartilage tissue engineering with 3D porous aqueous-derived silk scaffolds and mesenchymal stem cells. *Biomaterials* 2005 Dec;26(34):7082-7094.
136. Claase MB, Grijpma DW, Mendes SC, De Bruijn JD, Feijen J. Porous PEOT/PBT scaffolds for bone tissue engineering: preparation, characterization, and in vitro bone marrow cell culturing. *Journal of biomedical materials research* 2003 Feb 1;64(2):291-300.
137. van den Dolder J, Spauwen PH, Jansen JA. Evaluation of various seeding techniques for culturing osteogenic cells on titanium fiber mesh. *Tissue Eng* 2003 Apr;9(2):315-325.
138. Vunjak-Novakovic G, Obradovic B, Martin I, Bursac PM, Langer R, Freed LE. Dynamic cell seeding of polymer scaffolds for cartilage tissue engineering. *Biotechnology progress* 1998 Mar-Apr;14(2):193-202.
139. Kim SS, Sundback CA, Kaihara S, Benvenuto MS, Kim BS, Mooney DJ, et al. Dynamic seeding and in vitro culture of hepatocytes in a flow perfusion system. *Tissue Eng* 2000 Feb;6(1):39-44.
140. Saini S, Wick TM. Concentric cylinder bioreactor for production of tissue engineered cartilage: effect of seeding density and hydrodynamic loading on construct development. *Biotechnology progress* 2003 Mar-Apr;19(2):510-521.

141. Hannouche D, Terai H, Fuchs JR, Terada S, Zand S, Nasser BA, et al. Engineering of Implantable Cartilaginous Structures from Bone Marrow-Derived Mesenchymal Stem Cells. *Tissue Eng* 2006 Dec 1.
142. Solchaga LA, Tognana E, Penick K, Baskaran H, Goldberg VM, Caplan AI, et al. A rapid seeding technique for the assembly of large cell/scaffold composite constructs. *Tissue Eng* 2006 Jul;12(7):1851-1863.
143. Williams CG, Kim TK, Taboas A, Malik A, Manson P, Elisseeff J. In vitro chondrogenesis of bone marrow-derived mesenchymal stem cells in a photopolymerizing hydrogel. *Tissue Eng* 2003 Aug;9(4):679-688.
144. Landers R, Pfister A, Hübner U, John H, Schmelzeisen R, Mülhaupt R. Fabrication of soft tissue engineering scaffolds by means of rapid prototyping techniques. *Journal of materials science* 2002;37(15):3107-3116.
145. Moroni L, de Wijn JR, van Blitterswijk CA. Three-dimensional fiber-deposited PEOT/PBT copolymer scaffolds for tissue engineering: influence of porosity, molecular network mesh size, and swelling in aqueous media on dynamic mechanical properties. *Journal of biomedical materials research* 2005 Dec 15;75(4):957-965.
146. Kruyt MC, de Bruijn JD, Wilson CE, Oner FC, van Blitterswijk CA, Verbout AJ, et al. Viable osteogenic cells are obligatory for tissue-engineered ectopic bone formation in goats. *Tissue Eng* 2003 Apr;9(2):327-336.
147. Catterson EJ, Nesti LJ, Li WJ, Danielson KG, Albert TJ, Vaccaro AR, et al. Three-dimensional cartilage formation by bone marrow-derived cells seeded in polylactide/alginate amalgam. *Journal of biomedical materials research* 2001 Dec 5;57(3):394-403.
148. Malda J, Woodfield TB, van der Vloodt F, Wilson C, Martens DE, Tramper J, et al. The effect of PEOT/PBT scaffold architecture on the composition of tissue engineered cartilage. *Biomaterials* 2005 Jan;26(1):63-72.
149. Lydon MJ, Minett TW, Tighe BJ. Cellular interactions with synthetic polymer surfaces in culture. *Biomaterials* 1985 Nov;6(6):396-402.
150. van Wachem PB, Beugeling T, Feijen J, Bantjes A, Detmers JP, van Aken WG. Interaction of cultured human endothelial cells with polymeric surfaces of different wettabilities. *Biomaterials* 1985 Nov;6(6):403-408.
151. De Bartolo L, Morelli S, Bader A, Drioli E. Evaluation of cell behaviour related to physico-chemical properties of polymeric membranes to be used in bioartificial organs. *Biomaterials* 2002 Jun;23(12):2485-2497.
152. Woodfield TB, Van Blitterswijk CA, De Wijn J, Sims TJ, Hollander AP, Riesle J. Polymer scaffolds fabricated with pore-size gradients as a model for studying the zonal organization within tissue-engineered cartilage constructs. *Tissue Eng* 2005 Sep-Oct;11(9-10):1297-1311.
153. Kramer J, Hegert C, Guan K, Wobus AM, Muller PK, Rohwedel J. Embryonic stem cell-derived chondrogenic differentiation in vitro: activation by BMP-2 and BMP-4. *Mechanisms of development* 2000 Apr;92(2):193-205.
154. Vacanti JP, Morse MA, Saltzman WM, Domb AJ, Perez-Atayde A, Langer R. Selective cell transplantation using bioabsorbable artificial polymers as matrices. *Journal of pediatric surgery* 1988 Jan;23(1 Pt 2):3-9.
155. Zeltinger J, Sherwood JK, Graham DA, Mueller R, Griffith LG. Effect of pore size and void fraction on cellular adhesion, proliferation, and matrix deposition. *Tissue Eng* 2001 Oct;7(5):557-572.
156. Hiraki Y, Inoue H, Shigeno C, Sanma Y, Bentz H, Rosen DM, et al. Bone morphogenetic proteins (BMP-2 and BMP-3) promote growth and expression of the differentiated phenotype of rabbit chondrocytes and osteoblastic MC3T3-E1 cells in vitro. *J Bone Miner Res* 1991 Dec;6(12):1373-1385.
157. Mankin HJ, Jennings LC, Treadwell BV, Trippel SB. Growth factors and articular cartilage. *J Rheumatol Suppl* 1991 Feb;27:66-67.
158. Isobe M, Yamazaki Y, Oida S, Ishihara K, Nakabayashi N, Amagasa T. Bone morphogenetic protein encapsulated with a biodegradable and biocompatible polymer. *Journal of biomedical materials research* 1996 Nov;32(3):433-438.

159. Kim SE, Park JH, Cho YW, Chung H, Jeong SY, Lee EB, et al. Porous chitosan scaffold containing microspheres loaded with transforming growth factor-beta1: implications for cartilage tissue engineering. *J Control Release* 2003 Sep 4;91(3):365-374.
160. Lee SJ. Cytokine delivery and tissue engineering. *Yonsei medical journal* 2000 Dec;41(6):704-719.
161. Murphy WL, Peters MC, Kohn DH, Mooney DJ. Sustained release of vascular endothelial growth factor from mineralized poly(lactide-co-glycolide) scaffolds for tissue engineering. *Biomaterials* 2000 Dec;21(24):2521-2527.
162. Aspenberg P, Jeppsson C, Wang JS, Bostrom M. Transforming growth factor beta and bone morphogenetic protein 2 for bone ingrowth: a comparison using bone chambers in rats. *Bone* 1996 Nov;19(5):499-503.
163. Ikada Y, Tabata Y. Protein release from gelatin matrices. *Adv Drug Deliv Rev* 1998 May 4;31(3):287-301.
164. Park YJ, Ku Y, Chung CP, Lee SJ. Controlled release of platelet-derived growth factor from porous poly(L-lactide) membranes for guided tissue regeneration. *J Control Release* 1998 Feb 12;51(2-3):201-211.
165. Sakano S, Hasegawa Y, Murata Y, Ito T, Genda E, Iwata H, et al. Inhibitory effect of bFGF on endochondral heterotopic ossification. *Biochemical and biophysical research communications* 2002 May 3;293(2):680-685.
166. Uludag H, D'Augusta D, Golden J, Li J, Timony G, Riedel R, et al. Implantation of recombinant human bone morphogenetic proteins with biomaterial carriers: A correlation between protein pharmacokinetics and osteoinduction in the rat ectopic model. *Journal of biomedical materials research* 2000 May;50(2):227-238.
167. Yamamoto M, Tabata Y, Hong L, Miyamoto S, Hashimoto N, Ikada Y. Bone regeneration by transforming growth factor beta1 released from a biodegradable hydrogel. *J Control Release* 2000 Feb 14;64(1-3):133-142.
168. Sherris DA, Murakami CS, Larrabee WF, Jr., Bruce AG. Mandibular reconstruction with transforming growth factor-beta1. *The Laryngoscope* 1998 Mar;108(3):368-372.
169. Steinbrech DS, Mehrara BJ, Rowe NM, Dudziak ME, Luchs JS, Saadeh PB, et al. Gene expression of TGF-beta, TGF-beta receptor, and extracellular matrix proteins during membranous bone healing in rats. *Plastic and reconstructive surgery* 2000 May;105(6):2028-2038.
170. Ueda H, Nakamura T, Yamamoto M, Nagata N, Fukuda S, Tabata Y, et al. Repairing of rabbit skull defect by dehydrothermally crosslinked collagen sponges incorporating transforming growth factor beta1. *J Control Release* 2003 Feb 14;88(1):55-64.
171. Dinbergs ID, Brown L, Edelman ER. Cellular response to transforming growth factor-beta1 and basic fibroblast growth factor depends on release kinetics and extracellular matrix interactions. *The Journal of biological chemistry* 1996 Nov 22;271(47):29822-29829.
172. Phillips GD, Whitehead RA, Stone AM, Ruebel MW, Goodkin ML, Knighton DR. Transforming growth factor beta (TGF-B) stimulation of angiogenesis: an electron microscopic study. *Journal of submicroscopic cytology and pathology* 1993 Apr;25(2):149-155.
173. Blottner D, Wolf N, Lachmund A, Flanders KC, Unsicker K. TGF-beta rescues target-deprived preganglionic sympathetic neurons in the spinal cord. *The European journal of neuroscience* 1996 Jan;8(1):202-210.
174. Beck LS, Chen TL, Mikalauski P, Ammann AJ. Recombinant human transforming growth factor-beta 1 (rhTGF-beta 1) enhances healing and strength of granulation skin wounds. *Growth factors (Chur, Switzerland)* 1990;3(4):267-275.
175. Chin D, Boyle GM, Parsons PG, Coman WB. What is transforming growth factor-beta (TGF-beta)? *British journal of plastic surgery* 2004 Apr;57(3):215-221.
176. O'Kane S, Ferguson MW. Transforming growth factor beta s and wound healing. *The international journal of biochemistry & cell biology* 1997 Jan;29(1):63-78.
177. Igotz RA, Endo T, Massague J. Regulation of fibronectin and type I collagen mRNA levels by transforming growth factor-beta. *The Journal of biological chemistry* 1987 May 15;262(14):6443-6446.
178. Streuli CH, Schmidhauser C, Kobrin M, Bissell MJ, Derynck R. Extracellular matrix regulates expression of the TGF-beta 1 gene. *The Journal of cell biology* 1993 Jan;120(1):253-260.

179. Hunziker EB, Driesang IM, Morris EA. Chondrogenesis in cartilage repair is induced by members of the transforming growth factor-beta superfamily. *Clinical orthopaedics and related research* 2001 Oct(391 Suppl):S171-181.
180. Mierisch CM, Cohen SB, Jordan LC, Robertson PG, Balian G, Diduch DR. Transforming growth factor-beta in calcium alginate beads for the treatment of articular cartilage defects in the rabbit. *Arthroscopy* 2002 Oct;18(8):892-900.
181. Miura Y, Parvizi J, Fitzsimmons JS, O'Driscoll SW. Brief exposure to high-dose transforming growth factor-beta1 enhances periosteal chondrogenesis in vitro: a preliminary report. *The Journal of bone and joint surgery* 2002 May;84-A(5):793-799.
182. Nimni ME. Polypeptide growth factors: targeted delivery systems. *Biomaterials* 1997 Sep;18(18):1201-1225.
183. Sohier J, van Dijkhuizen-Radersma R, de Groot K, Bezemer JM. Release of small water-soluble drugs from multiblock copolymer microspheres: a feasibility study. *Eur J Pharm Biopharm* 2003 Mar;55(2):221-228.
184. Bezemer JM, Radersma R, Grijpma DW, Dijkstra PJ, van Blitterswijk CA, Feijen J. Microspheres for protein delivery prepared from amphiphilic multiblock copolymers. 2. Modulation of release rate. *J Control Release* 2000 Jul 3;67(2-3):249-260.
185. van Dijkhuizen-Radersma R, Roosma JR, Kaim P, Metairie S, Peters FL, de Wijn J, et al. Biodegradable poly(ether-ester) multiblock copolymers for controlled release applications. *Journal of biomedical materials research* 2003 Dec 15;67(4):1294-1304.
186. van Dijkhuizen-Radersma R, Metairie S, Roosma JR, de Groot K, Bezemer JM. Controlled release of proteins from degradable poly(ether-ester) multiblock copolymers. *J Control Release* 2005 Jan 3;101(1-3):175-186.
187. Grimm MJ, Williams JL. Measurements of permeability in human calcaneal trabecular bone. *Journal of biomechanics* 1997 Jul;30(7):743-745.
188. Hui PW, Leung PC, Sher A. Fluid conductance of cancellous bone graft as a predictor for graft-host interface healing. *Journal of biomechanics* 1996 Jan;29(1):123-132.
189. Li S, De Wijn JR, Li J, Layrolle P, De Groot K. Macroporous biphasic calcium phosphate scaffold with high permeability/porosity ratio. *Tissue Eng* 2003 Jun;9(3):535-548.
190. McKay I, Leigh I, editors. *Growth factors - A practical approach*: IRL Press at Oxford University Press, 1993.
191. Sohier J, Haan RE, de Groot K, Bezemer JM. A novel method to obtain protein release from porous polymer scaffolds: emulsion coating. *J Control Release* 2003 Feb 21;87(1-3):57-68.
192. Cucchiari M, Sohier J, Mitoš K, Kaul G, Zurakowski D, Bezemer J, et al. Effect of transforming growth factor-beta 1 (TGF-β1) released from a scaffold on chondrogenesis in an osteochondral defect model in the rabbit. *Central European Journal of Biology* 2006;1(1):43-60.
193. Bezemer JM, Radersma R, Grijpma DW, Dijkstra PJ, van Blitterswijk CA, Feijen J. Microspheres for protein delivery prepared from amphiphilic multiblock copolymers. 1. Influence of preparation techniques on particle characteristics and protein delivery. *J Control Release* 2000 Jul 3;67(2-3):233-248.
194. van Dijkhuizen-Radersma R, Peters FL, Stienstra NA, Grijpma DW, Feijen J, de Groot K, et al. Control of vitamin B12 release from poly(ethylene oxide)/polybutylene terephthalate multiblock copolymers. *Biomaterials* 2002 Mar;23(6):1527-1536.
195. Bezemer JM, Grijpma DW, Dijkstra PJ, van Blitterswijk CA, Feijen J. A controlled release system for proteins based on poly(ether ester) block-copolymers: polymer network characterization. *J Control Release* 1999 Dec 6;62(3):393-405.
196. Babensee JE, McIntire LV, Mikos AG. Growth factor delivery for tissue engineering. *Pharmaceutical research* 2000 May;17(5):497-504.
197. Elisseeff J, McIntosh W, Fu K, Blunk BT, Langer R. Controlled-release of IGF-I and TGF-beta1 in a photopolymerizing hydrogel for cartilage tissue engineering. *J Orthop Res* 2001 Nov;19(6):1098-1104.
198. Lee JE, Kim KE, Kwon IC, Ahn HJ, Lee SH, Cho H, et al. Effects of the controlled-released TGF-beta 1 from chitosan microspheres on chondrocytes cultured in a collagen/chitosan/glycosaminoglycan scaffold. *Biomaterials* 2004 Aug;25(18):4163-4173.

199. Mahmood TA, Shastri VP, van Blitterswijk CA, Langer R, Riesle J. Tissue engineering of bovine articular cartilage within porous poly(ether ester) copolymer scaffolds with different structures. *Tissue Eng* 2005 Jul-Aug;11(7-8):1244-1253.
200. Radder AM, Leenders H, van Blitterswijk CA. Application of porous PEO/PBT copolymers for bone replacement. *Journal of biomedical materials research* 1996 Mar;30(3):341-351.
201. Sohler J, Hamann D, Koenders M, Cucchiari M, Madry H, van Blitterswijk C, et al. Tailored release of TGF-beta1 from porous scaffolds for cartilage tissue engineering. *International journal of pharmaceutics* 2007 Mar 6;332(1-2):80-89.
202. Noth U, Osyczka AM, Tuli R, Hickok NJ, Danielson KG, Tuan RS. Multilineage mesenchymal differentiation potential of human trabecular bone-derived cells. *J Orthop Res* 2002 Sep;20(5):1060-1069.
203. Livak KJ, Schmittgen TD. Analysis of relative gene expression data using real-time quantitative PCR and the 2(-Delta Delta C(T)) Method. *Methods (San Diego, Calif)* 2001 Dec;25(4):402-408.
204. Barry F, Boynton RE, Liu B, Murphy JM. Chondrogenic differentiation of mesenchymal stem cells from bone marrow: differentiation-dependent gene expression of matrix components. *Experimental cell research* 2001 Aug 15;268(2):189-200.
205. Mackay AM, Beck SC, Murphy JM, Barry FP, Chichester CO, Pittenger MF. Chondrogenic differentiation of cultured human mesenchymal stem cells from marrow. *Tissue Eng* 1998 Winter;4(4):415-428.
206. Naumann A, Dennis JE, Awadallah A, Carrino DA, Mansour JM, Kastenbauer E, et al. Immunohistochemical and mechanical characterization of cartilage subtypes in rabbit. *J Histochem Cytochem* 2002 Aug;50(8):1049-1058.
207. Martin I, Jakob M, Schafer D, Dick W, Spagnoli G, Heberer M. Quantitative analysis of gene expression in human articular cartilage from normal and osteoarthritic joints. *Osteoarthritis and cartilage / OARS, Osteoarthritis Research Society* 2001 Feb;9(2):112-118.
208. Marlovits S, Hombauer M, Truppe M, Vecsei V, Schlegel W. Changes in the ratio of type-I and type-II collagen expression during monolayer culture of human chondrocytes. *J Bone Joint Surg Br* 2004 Mar;86(2):286-295.
209. Marlovits S, Hombauer M, Tamandl D, Vecsei V, Schlegel W. Quantitative analysis of gene expression in human articular chondrocytes in monolayer culture. *International journal of molecular medicine* 2004 Feb;13(2):281-287.
210. Darling EM, Athanasiou KA. Rapid phenotypic changes in passaged articular chondrocyte subpopulations. *J Orthop Res* 2005 Mar;23(2):425-432.
211. Buckwalter JA, Mankin HJ. Instructional Course Lecture, The American Academy of Orthopaedic Surgeons - Articular Cartilage. Part I: Tissue Design and Chondrocyte-Matrix Interactions. *J Bone Joint Surg* 1997;79(4):600-611.
212. Lee JE, Kim SE, Kwon IC, Ahn HJ, Cho H, Lee SH, et al. Effects of a chitosan scaffold containing TGF-beta1 encapsulated chitosan microspheres on in vitro chondrocyte culture. *Artificial organs* 2004 Sep;28(9):829-839.
213. DeFail AJ, Chu CR, Izzo N, Marra KG. Controlled release of bioactive TGF-beta 1 from microspheres embedded within biodegradable hydrogels. *Biomaterials* 2006 Mar;27(8):1579-1585.
214. Zhou S, Eid K, Glowacki J. Cooperation between TGF-beta and Wnt pathways during chondrocyte and adipocyte differentiation of human marrow stromal cells. *J Bone Miner Res* 2004 Mar;19(3):463-470.
215. Tuli R, Tuli S, Nandi S, Huang X, Manner PA, Hozack WJ, et al. Transforming growth factor-beta-mediated chondrogenesis of human mesenchymal progenitor cells involves N-cadherin and mitogen-activated protein kinase and Wnt signaling cross-talk. *The Journal of biological chemistry* 2003 Oct 17;278(42):41227-41236.
216. Jakob M, Demarteau O, Schafer D, Hintermann B, Dick W, Heberer M, et al. Specific growth factors during the expansion and redifferentiation of adult human articular chondrocytes enhance chondrogenesis and cartilaginous tissue formation in vitro. *Journal of cellular biochemistry* 2001 Mar 26;81(2):368-377.

217. Massague J, Like B. Cellular receptors for type beta transforming growth factor. Ligand binding and affinity labeling in human and rodent cell lines. *The Journal of biological chemistry* 1985 Mar 10;260(5):2636-2645.
218. Shasha N, Aubin PP, Cheah HK, Davis AM, Agnidis Z, Gross AE. Long-term clinical experience with fresh osteochondral allografts for articular knee defects in high demand patients. *Cell Tissue Bank* 2002;3(3):175-182.
219. Gross AE, Shasha N, Aubin P. Long-term followup of the use of fresh osteochondral allografts for posttraumatic knee defects. *Clinical orthopaedics and related research* 2005 Jun(435):79-87.
220. Allen RT, Robertson CM, Pennock AT, Bugbee WD, Harwood FL, Wong VW, et al. Analysis of stored osteochondral allografts at the time of surgical implantation. *The American journal of sports medicine* 2005 Oct;33(10):1479-1484.
221. Strong DM, Friedlaender GE, Tomford WW, Springfield DS, Shives TC, Burchardt H, et al. Immunologic responses in human recipients of osseous and osteochondral allografts. *Clinical orthopaedics and related research* 1996 May(326):107-114.
222. Sirlin CB, Brossmann J, Boutin RD, Pathria MN, Convery FR, Bugbee W, et al. Shell osteochondral allografts of the knee: comparison of mr imaging findings and immunologic responses. *Radiology* 2001 Apr;219(1):35-43.
223. Nordstrom DC, Santavirta S, Aho A, Heikkila J, Teppo AM, Konttinen YT. Immune responses to osteoarticular allografts of the knee--cytokine studies. *Archives of orthopaedic and trauma surgery* 1999;119(3-4):195-198.
224. Temenoff JS, Mikos AG. Injectable biodegradable materials for orthopedic tissue engineering. *Biomaterials* 2000 Dec;21(23):2405-2412.
225. Sittinger M, Bujia J, Minuth WW, Hammer C, Burmester GR. Engineering of cartilage tissue using bioresorbable polymer carriers in perfusion culture. *Biomaterials* 1994 May;15(6):451-456.
226. Nehrer S, Breinan HA, Ramappa A, Hsu HP, Minas T, Shortkroff S, et al. Chondrocyte-seeded collagen matrices implanted in a chondral defect in a canine model. *Biomaterials* 1998 Dec;19(24):2313-2328.
227. Lynn AK, Brooks RA, Bonfield W, Rushton N. Repair of defects in articular joints. Prospects for material-based solutions in tissue engineering. *J Bone Joint Surg Br* 2004 Nov;86(8):1093-1099.
228. Campoccia D, Doherty P, Radice M, Brun P, Abatangelo G, Williams DF. Semisynthetic resorbable materials from hyaluronan esterification. *Biomaterials* 1998 Dec;19(23):2101-2127.
229. Radin EL, Burr DB. Hypothesis: joints can heal. *Seminars in arthritis and rheumatism* 1984 Feb;13(3):293-302.
230. Kuettner KE, Pauli BU, Gall G, Memoli VA, Schenk RK. Synthesis of cartilage matrix by mammalian chondrocytes in vitro. I. Isolation, culture characteristics, and morphology. *The Journal of cell biology* 1982 Jun;93(3):743-750.
231. Kuettner KE, Memoli VA, Pauli BU, Wrobel NC, Thonar EJ, Daniel JC. Synthesis of cartilage matrix by mammalian chondrocytes in vitro. II. Maintenance of collagen and proteoglycan phenotype. *The Journal of cell biology* 1982 Jun;93(3):751-757.
232. Binette F, McQuaid DP, Haudenschield DR, Yaeger PC, McPherson JM, Tubo R. Expression of a stable articular cartilage phenotype without evidence of hypertrophy by adult human articular chondrocytes in vitro. *J Orthop Res* 1998 Mar;16(2):207-216.
233. Kruyt MC, de Bruijn JD, Yuan H, van Blitterswijk CA, Verbout AJ, Oner FC, et al. Optimization of bone tissue engineering in goats: a peroperative seeding method using cryopreserved cells and localized bone formation in calcium phosphate scaffolds. *Transplantation* 2004 Feb 15;77(3):359-365.
234. Solursh M. Formation of cartilage tissue in vitro. *Journal of cellular biochemistry* 1991 Mar;45(3):258-260.
235. Takagi M, Umetsu Y, Fujiwara M, Wakitani S. High inoculation cell density could accelerate the differentiation of human bone marrow mesenchymal stem cells to chondrocyte cells. *Journal of bioscience and bioengineering* 2007 Jan;103(1):98-100.

236. Seghatoleslami MR, Tuan RS. Cell density dependent regulation of AP-1 activity is important for chondrogenic differentiation of C3H10T1/2 mesenchymal cells. *Journal of cellular biochemistry* 2002;84(2):237-248.
237. Naumann A, Dennis JE, Aigner J, Coticchia J, Arnold J, Berghaus A, et al. Tissue engineering of autologous cartilage grafts in three-dimensional in vitro macroaggregate culture system. *Tissue Eng* 2004 Nov-Dec;10(11-12):1695-1706.
238. Denker AE, Haas AR, Nicoll SB, Tuan RS. Chondrogenic differentiation of murine C3H10T1/2 multipotential mesenchymal cells: I. Stimulation by bone morphogenetic protein-2 in high-density micromass cultures. *Differentiation; research in biological diversity* 1999 Jan;64(2):67-76.
239. Zhang W, Green C, Stott NS. Bone morphogenetic protein-2 modulation of chondrogenic differentiation in vitro involves gap junction-mediated intercellular communication. *Journal of cellular physiology* 2002 Nov;193(2):233-243.
240. Stokes DG, Liu G, Dharmavaram R, Hawkins D, Piera-Velazquez S, Jimenez SA. Regulation of type-II collagen gene expression during human chondrocyte de-differentiation and recovery of chondrocyte-specific phenotype in culture involves Sry-type high-mobility-group box (SOX) transcription factors. *The Biochemical journal* 2001 Dec 1;360(Pt 2):461-470.
241. Reginato AM, Iozzo RV, Jimenez SA. Formation of nodular structures resembling mature articular cartilage in long-term primary cultures of human fetal epiphyseal chondrocytes on a hydrogel substrate. *Arthritis and rheumatism* 1994 Sep;37(9):1338-1349.
242. Lombello CB, Malmonge SM, Wada ML. PolyHEMA and polyHEMA-poly(MMA-co-AA) as substrates for culturing Vero cells. *Journal of materials science* 2000 Sep;11(9):541-546.
243. Bujia J, Behrends U, Rotter N, Pitzke P, Wilmes E, Hammer C. Expression of ICAM-1 on intact cartilage and isolated chondrocytes. *In vitro cellular & developmental biology* 1996 Feb;32(2):116-122.
244. Yanamandra N, Kondraganti S, Gondi CS, Gujrati M, Olivero WC, Dinh DH, et al. Recombinant adeno-associated virus (rAAV) expressing TFPI-2 inhibits invasion, angiogenesis and tumor growth in a human glioblastoma cell line. *International journal of cancer* 2005 Jul 20;115(6):998-1005.
245. Kondraganti S, Gondi CS, McCutcheon I, Dinh DH, Gujrati M, Rao JS, et al. RNAi-mediated downregulation of urokinase plasminogen activator and its receptor in human meningioma cells inhibits tumor invasion and growth. *International journal of oncology* 2006 Jun;28(6):1353-1360.
246. Sporn MB, Roberts AB. Transforming growth factor-beta: recent progress and new challenges. *The Journal of cell biology* 1992 Dec;119(5):1017-1021.
247. Shea CM, Edgar CM, Einhorn TA, Gerstenfeld LC. BMP treatment of C3H10T1/2 mesenchymal stem cells induces both chondrogenesis and osteogenesis. *Journal of cellular biochemistry* 2003 Dec 15;90(6):1112-1127.
248. Reddi AH. Morphogenesis and tissue engineering of bone and cartilage: inductive signals, stem cells, and biomimetic biomaterials. *Tissue Eng* 2000 Aug;6(4):351-359.
249. Asahina I, Sampath TK, Hauschka PV. Human osteogenic protein-1 induces chondroblastic, osteoblastic, and/or adipocytic differentiation of clonal murine target cells. *Experimental cell research* 1996 Jan 10;222(1):38-47.
250. Yeong WY, Chua CK, Leong KF, Chandrasekaran M. Rapid prototyping in tissue engineering: challenges and potential. *Trends in biotechnology* 2004 Dec;22(12):643-652.
251. Hutmacher DW, Sitterling M, Risbud MV. Scaffold-based tissue engineering: rationale for computer-aided design and solid free-form fabrication systems. *Trends in biotechnology* 2004 Jul;22(7):354-362.
252. Hollister SJ. Porous scaffold design for tissue engineering. *Nature materials* 2005 Jul;4(7):518-524.
253. Vozzi G, Flaim C, Ahluwalia A, Bhatia S. Fabrication of PLGA scaffolds using soft lithography and microsyringe deposition. *Biomaterials* 2003 Jun;24(14):2533-2540.
254. Smay JE, Cesarano J, Tuttle BA, Lewis JA. Directed colloidal assembly of linear and annulate lead of zirconia titanate arrays. *J Am Ceram Soc* 2005;87(2):293-295.
255. Hutmacher DW. Scaffold design and fabrication technologies for engineering tissues--state of the art and future perspectives. *Journal of biomaterials science* 2001;12(1):107-124.

256. Giordano RA, Wu BM, Borland SW, Cima LG, Sachs EM, Cima MJ. Mechanical properties of dense polylactic acid structures fabricated by three-dimensional printing. *Journal of biomaterials science* 1996;8(1):63-75.
257. Antonov EN, Bagratashvili VN, Whitaker MJ, Barry JJ, Shakesheff KM, Konovalov AN, et al. Three-dimensional Bioactive and Biodegradable Scaffolds Fabricated by Surface-Selective Laser Sintering. *Adv Mater Deerfield* 2004 Dec 20;17(3):327-330.
258. Moroni L, de Wijn JR, van Blitterswijk CA. 3D fiber-deposited scaffolds for tissue engineering: influence of pores geometry and architecture on dynamic mechanical properties. *Biomaterials* 2006 Mar;27(7):974-985.
259. Lin CY, Kikuchi N, Hollister SJ. A novel method for biomaterial scaffold internal architecture design to match bone elastic properties with desired porosity. *Journal of biomechanics* 2004 May;37(5):623-636.
260. Lin AS, Barrows TH, Cartmell SH, Guldborg RE. Microarchitectural and mechanical characterization of oriented porous polymer scaffolds. *Biomaterials* 2003 Feb;24(3):481-489.
261. Hollister SJ, Maddox RD, Taboas JM. Optimal design and fabrication of scaffolds to mimic tissue properties and satisfy biological constraints. *Biomaterials* 2002 Oct;23(20):4095-4103.
262. Li JP, de Wijn JR, Van Blitterswijk CA, de Groot K. Porous Ti6Al4V scaffold directly fabricating by rapid prototyping: preparation and in vitro experiment. *Biomaterials* 2006 Mar;27(8):1223-1235.
263. Yan Y, Xiong Z, Hu Y, Wang S, Zhang R, Zhang C. Layered manufacturing of tissue engineering scaffolds via multi-nozzle deposition. *Biomaterials* 2003;23(24):4739-4751.
264. Smith CM, Stone AL, Parkhill RL, R.L. S, Simpkins MW, Kachurin AM. Three-dimensional bioassembly tool for generating viable tissue-engineered constructs. *Tissue Eng* 2004;Sep-Oct;10(9-10):1566-1576.
265. Fan H, Lu Y, Stump A, Reed ST, Baer T, Schunk R, et al. Rapid prototyping of patterned functional nanostructures. *Nature* 2000 May 4;405(6782):56-60.
266. Kino-Oka M, Maeda Y, Yamamoto T, Sugawara K, Taya M. A kinetic modeling of chondrocyte culture for manufacture of tissue-engineered cartilage. *Journal of bioscience and bioengineering* 2005 Mar;99(3):197-207.
267. Furukawa KS, Suenaga H, Toita K, Numata A, Tanaka J, Ushida T, et al. Rapid and large-scale formation of chondrocyte aggregates by rotational culture. *Cell transplantation* 2003;12(5):475-479.
268. Martin I, Dozin B, Quarto R, Cancedda R, Beltrame F. Computer-based technique for cell aggregation analysis and cell aggregation in in vitro chondrogenesis. *Cytometry* 1997 Jun 1;28(2):141-146.
269. Gilbert SF, editor. *Developmental Biology*: Sinauer Associates Inc, 2000.
270. Loty S, Forest N, Boulekbache H, Sautier JM. Cytochalasin D induces changes in cell shape and promotes in vitro chondrogenesis: a morphological study. *Biology of the cell / under the auspices of the European Cell Biology Organization* 1995;83(2-3):149-161.
271. Taylor G. Electrically driven jets. *Proc R Soc London* 1969:453-475.
272. Larrando L, Manley R. Electrostatic Fiber Spinning from Polymer Melts. I. Experimental Observations on Fiber Formation and Properties. *J Polym Sci: Pol Phys Ed* 1981;19:909-920.
273. Deitzel J, Kleinmeyer J, Harris D, Beck Tan N. The Effect of Processing Variables on the Morphology of Electrospun Nanofibers and Textiles. *Polymers* 2001;42:261-272.
274. Rutledge G, Li Y, Fridrikh S, Warner S, Kalayci V, Patra P. Electrostatic Spinning and Properties of Ultrafine Fibers. . National Textile Center: Annual Report 2001:1-10.
275. Kwon IK, Kidoaki S, Matsuda T. Electrospun nano- to microfiber fabrics made of biodegradable copolyesters: structural characteristics, mechanical properties and cell adhesion potential. *Biomaterials* 2005 Jun;26(18):3929-3939.
276. Boland ED, Coleman BD, Barnes CP, Simpson DG, Wnek GE, Bowlin GL. Electrospinning polydioxanone for biomedical applications. *Acta biomaterialia* 2005 Jan;1(1):115-123.
277. Stevens MM, George JH. Exploring and engineering the cell surface interface. *Science (New York, NY)* 2005;310(5751):1135-1138.

278. Moroni L, Licht R, de Boer J, de Wijn JR, van Blitterswijk CA. Fiber diameter and texture of electrospun PEOT/PBT scaffolds influence human mesenchymal stem cell proliferation and morphology, and the release of incorporated compounds. *Biomaterials* 2006 Oct;27(28):4911-4922.
279. Badami AS, Kreke MR, Thompson MS, Riffle JS, Goldstein AS. Effect of fiber diameter on spreading, proliferation and differentiation of osteoblastic cells on electrospun poly(lactic acid) substrates. *Biomaterials* 2006;27(4):596-606.
280. Beumer GJ, van Blitterswijk CA, Ponec M. Biocompatibility of a biodegradable matrix used as a skin substitute: an in vivo evaluation. *Journal of biomedical materials research* 1994 May;28(5):545-552.
281. Beumer GJ, van Blitterswijk CA, Ponec M. Degradative behaviour of polymeric matrices in (sub)dermal and muscle tissue of the rat: a quantitative study. *Biomaterials* 1994 Jun;15(7):551-559.
282. Bakker D, van Blitterswijk CA, Hesseling SC, Grote JJ. Effect of implantation site on phagocyte/polymer interaction and fibrous capsule formation. *Biomaterials* 1988 Jan;9(1):14-23.
283. Van Blitterswijk CA, van den Brink J, Leenders H, Bakker D. The Effect of PEO Ratio on Degradation, calcification and Bone Bonding of PEO/PBT copolymer (Polyactive). *Cell and Mater* 1993;3:23-26.
284. Bulstra SK, Geesink RG, Bakker D, Bulstra TH, Bouwmeester SJ, van der Linden AJ. Femoral canal occlusion in total hip replacement using a resorbable and flexible cement restrictor. *J Bone Joint Surg Br* 1996 Nov;78(6):892-898.
285. Mensik I, Lamme EN, Riesle J, Brychta P. Effectiveness and safety of the PEOT/PBT copolymer scaffold as dermal substitute in scar reconstruction wounds (feasibility trial). *Cell Tissue Bank* 2002;3(4):245-253.
286. Landers R, Hubner U, Schmelzeisen R, Mulhaupt R. Rapid prototyping of scaffolds derived from thermoreversible hydrogels and tailored for applications in tissue engineering. *Biomaterials* 2002 Dec;23(23):4437-4447.
287. Rao RB, Krafcik KL, Morales AM, Lewis JA. Microfabricated deposition nozzles for direct-write assembly of three-dimensional periodic structures *Adv Mater* 2005;17(3):289-+.
288. Lewis JA, Gratson GM. Direct writing in three dimensions. *Materials today* 2004;7/8:32-39.
289. Yoshimoto H, Shin YM, Terai H, Vacanti JP. A biodegradable nanofiber scaffold by electrospinning and its potential for bone tissue engineering. *Biomaterials* 2003 May;24(12):2077-2082.
290. Min BM, Lee G, Kim SH, Nam YS, Lee TS, Park WH. Electrospinning of silk fibron nanofibers and its effect on the adhesion and spreading of normal human keratinocytes and fibroblasts in vitro. *Biomaterials* 2004;25(7-8):1289-1297.
291. Bognitzki M, Czado W, Frese T, Schaper A, Hellwig M, Steinhart M, et al. Nanostructured Fibers via Electrospinning. *Adv Mater* 2001;13(1):70-72.
292. Larrondo L, Manley R. Electrostatic Fiber Spinning from Polymer Melts. II. Examination of the Flow Field in an Electrically Driven Jet. *J Polym Sci: Pol Phys Ed* 1981;19:921-932.
293. Miot S, Woodfield T, Daniels AU, Suetterlin R, Peterschmitt I, Heberer M, et al. Effects of scaffold composition and architecture on human nasal chondrocyte redifferentiation and cartilaginous matrix deposition. *Biomaterials* 2005 May;26(15):2479-2489.
294. Mahmood TA, de Jong R, Riesle J, Langer R, van Blitterswijk CA. Adhesion-mediated signal transduction in human articular chondrocytes: the influence of biomaterial chemistry and tenascin-C. *Experimental cell research* 2004 Dec 10;301(2):179-188.
295. Barry JJ, Gidda HS, Scotchford CA, Howdle SM. Porous methacrylate scaffolds: supercritical fluid fabrication and in vitro chondrocyte responses. *Biomaterials* 2004 Aug;25(17):3559-3568.
296. Li C, Vepari C, Jin HJ, Kim HJ, Kaplan DL. Electrospun silk-BMP-2 scaffolds for bone tissue engineering. *Biomaterials* 2006 Jun;27(16):3115-3124.
297. Jiang H, Hu Y, Li Y, Zhao P, Zhu K, Chen W. A facile technique to prepare biodegradable coaxial electrospun nanofibers for controlled release of bioactive agents. *J Control Release* 2005 Nov 28;108(2-3):237-243.
298. Langer R. Tissue engineering. *Mol Ther* 2000 Jan;1(1):12-15.

299. Wang X, Grogan SP, Rieser F, Winkelmann V, Maquet V, Berge ML, et al. Tissue engineering of biphasic cartilage constructs using various biodegradable scaffolds: an in vitro study. *Biomaterials* 2004 Aug;25(17):3681-3688.
300. Solchaga LA, Dennis JE, Goldberg VM, Caplan AI. Hyaluronic acid-based polymers as cell carriers for tissue-engineered repair of bone and cartilage. *J Orthop Res* 1999 Mar;17(2):205-213.
301. Pieper JS, van der Kraan PM, Hafmans T, Kamp J, Buma P, van Susante JL, et al. Crosslinked type II collagen matrices: preparation, characterization, and potential for cartilage engineering. *Biomaterials* 2002 Aug;23(15):3183-3192.
302. Liu X, Ma PX. Polymeric scaffolds for bone tissue engineering. *Annals of biomedical engineering* 2004 Mar;32(3):477-486.
303. Radder AM, Leenders H, van Blitterswijk CA. Bone-bonding behaviour of polyethylene oxide)-polybutylene terephthalatecopolymer coatings and bulk implants: a comparative study. *Biomaterials* 1995 May;16(7):507-513.
304. Yuan H, Van Den Doel M, Li S, Van Blitterswijk CA, De Groot K, De Bruijn JD. A comparison of the osteoinductive potential of two calcium phosphate ceramics implanted intramuscularly in goats. *Journal of materials science* 2002 Dec;13(12):1271-1275.
305. Habibovic P, Yuan H, van den Doel M, Sees TM, van Blitterswijk CA, de Groot K. Relevance of osteoinductive biomaterials in critical-sized orthotopic defect. *J Orthop Res* 2006 May;24(5):867-876.
306. Voigt W, editor. *Lehrbuch der Kristallphysik*. Leipzig: B.G. Teubner, 1910.
307. Reuss A. *Zeitschrift fuer Angewandte Mathematik und Mechanik* 1929;9:49-58.
308. Habibovic P, Yuan H, Van der Valk CM, Meijer GJ, Van Blitterswijk C, De Groot K. 3D microenvironment essential element for osteoinduction by biomaterials. *Biomaterials* 2005;26(17):3565-3575.
309. Gutierrez AP, Canovas MF. The modulus of elasticity of high performance concrete. *materials and structures* 1995;28:559-568.
310. Gere JM, Timoshenko SP, editors. *Mechanics of Materials*. Third Edition. Boston: PWS-KENT Publishing company, 1990.
311. Athanasiou KA, Zhu C, Lanctot DR, Agrawal CM, Wang X. Fundamentals of biomechanics in tissue engineering of bone. *Tissue Eng* 2000 Aug;6(4):361-381.
312. Habibovic P, Sees TM, van den Doel MA, van Blitterswijk CA, de Groot K. Osteoinduction by biomaterials--physicochemical and structural influences. *Journal of biomedical materials research* 2006 Jun 15;77(4):747-762.
313. Wang DW, Fermor B, Gimble JM, Awad HA, Guilak F. Influence of oxygen on the proliferation and metabolism of adipose derived adult stem cells. *Journal of cellular physiology* 2005 Jul;204(1):184-191.
314. von der Mark K, Conrad G. Cartilage cell differentiation: review. *Clinical orthopaedics and related research* 1979 Mar-Apr(139):185-205.
315. Murphy CL, Sambanis A. Effect of oxygen tension and alginate encapsulation on restoration of the differentiated phenotype of passaged chondrocytes. *Tissue Eng* 2001 Dec;7(6):791-803.
316. Hendriks JAA, Moroni L, Riesle J, De Wijn JR, Van Blitterswijk CA. 3D Fiber-deposited scaffolds with enhanced cell entrapment capacity and matching physico-chemical properties favor cartilage regeneration. manuscript in preparation.
317. Sokoloff L. Elasticity of Articular Cartilage: Effect of Ions and Viscous Solutions. *Science* (New York, NY) 1963 Sep 13;141:1055-1057.
318. Roosendaal G, Vianen ME, van den Berg HM, Lafeber FP, Bijlsma JW. Cartilage damage as a result of hemarthrosis in a human in vitro model. *The Journal of rheumatology* 1997 Jul;24(7):1350-1354.
319. Roosendaal G, Vianen ME, Marx JJ, van den Berg HM, Lafeber FP, Bijlsma JW. Blood-induced joint damage: a human in vitro study. *Arthritis and rheumatism* 1999 May;42(5):1025-1032.
320. Hooiveld MJ, Roosendaal G, Vianen ME, van den Berg HM, Bijlsma JW, Lafeber FP. Immature articular cartilage is more susceptible to blood-induced damage than mature articular cartilage: an in vivo animal study. *Arthritis and rheumatism* 2003 Feb;48(2):396-403.

321. Hooiveld MJ, Roosendaal G, van den Berg HM, Bijlsma JW, Lafeber FP. Haemoglobin-derived iron-dependent hydroxyl radical formation in blood-induced joint damage: an in vitro study. *Rheumatology (Oxford, England)* 2003 Jun;42(6):784-790.
322. Hooiveld MJ, Roosendaal G, Jacobs KM, Vianen ME, van den Berg HM, Bijlsma JW, et al. Initiation of degenerative joint damage by experimental bleeding combined with loading of the joint: a possible mechanism of hemophilic arthropathy. *Arthritis and rheumatism* 2004 Jun;50(6):2024-2031.
323. Hooiveld M, Roosendaal G, Wenting M, van den Berg M, Bijlsma J, Lafeber F. Short-term exposure of cartilage to blood results in chondrocyte apoptosis. *The American journal of pathology* 2003 Mar;162(3):943-951.
324. Jansen NW, Roosendaal G, Bijlsma JW, Degroot J, Lafeber FP. Exposure of human cartilage tissue to low concentrations of blood for a short period of time leads to prolonged cartilage damage: an in vitro study. *Arthritis and rheumatism* 2007 Jan;56(1):199-207.
325. Jansen EJP, Kruijer, R. Repair of articular cartilage lesion with PolyActive 1000PEOT70PBT30 and 300PEOT55PBT45 in rabbits: with and without allogenic cells. ICRS. Toronto, Canada, 2002.
326. Felszeghy S, Hyttinen M, Tammi R, Tammi M, Modis L. Quantitative image analysis of hyaluronan expression in human tooth germs. *European journal of oral sciences* 2000 Aug;108(4):320-326.
327. van Loon JA. Biocompatibility testing of degradable polymers. Leiden: Rijksuniversiteit Leiden; 1995.
328. Lamme EN, Druce D, Pieper J, May PS, Kaim P, Jacobsen F, et al. Long-term Evaluation of Porous PEOT/PBT Implants for Soft Tissue Augmentation. *J Biomater Appl* 2007 May 10.
329. Meijer GJ, van Dooren A, Gaillard ML, Dalmeijer R, de Putter C, Koole R, et al. Polyactive as a bone-filler in a beagle dog model. *International journal of oral and maxillofacial surgery* 1996 Jun;25(3):210-216.
330. Kuijjer R, Bouwmeester SJ, Drees MM, Surtel DA, Terwindt-Rouwenhorst EA, Van Der Linden AJ, et al. The polymer Polyactive as a bone-filling substance: an experimental study in rabbits. *Journal of materials science* 1998 Aug;9(8):449-455.
331. Davies JE, editor. *Bone Engineering*. Toronto, 2000.
332. Miot S, Scandiucci de Freitas P, Wirz D, Daniels AU, Sims TJ, Hollander AP, et al. Cartilage tissue engineering by expanded goat articular chondrocytes. *J Orthop Res* 2006 May;24(5):1078-1085.
333. Meijer GJ, Radder A, Dalmeijer R, de Putter C, Van Blitterswijk CA. Observations of the bone activity adjacent to unloaded dental implants coated with Polyactive or HA. *Journal of oral rehabilitation* 1995 Mar;22(3):167-174.
334. Li P, Bakker D, van Blitterswijk CA. The bone-bonding polymer Polyactive 80/20 induces hydroxycarbonate apatite formation in vitro. *Journal of biomedical materials research* 1997 Jan;34(1):79-86.
335. Jackson DW, Lator PA, Aberman HM, Simon TM. Spontaneous repair of full-thickness defects of articular cartilage in a goat model. A preliminary study. *The Journal of bone and joint surgery* 2001 Jan;83-A(1):53-64.
336. Guettler JH, Demetropoulos CK, Yang KH, Jurist KA. Dynamic evaluation of contact pressure and the effects of graft harvest with subsequent lateral release at osteochondral donor sites in the knee. *Arthroscopy* 2005 Jun;21(6):715-720.
337. Guettler JH, Demetropoulos CK, Yang KH, Jurist KA. Osteochondral defects in the human knee: influence of defect size on cartilage rim stress and load redistribution to surrounding cartilage. *The American journal of sports medicine* 2004 Sep;32(6):1451-1458.
338. Garretson RB, 3rd, Katolik LI, Verma N, Beck PR, Bach BR, Cole BJ. Contact pressure at osteochondral donor sites in the patellofemoral joint. *The American journal of sports medicine* 2004 Jun;32(4):967-974.
339. Meijer GJ, de Bruijn JD, Koole R, van Blitterswijk CA. Cell-based bone tissue engineering. *PLoS medicine* 2007 Feb;4(2):e9.
340. Siddappa R, Fernandes H, Liu J, Blitterswijk CA, de Boer J. The Response of Human Mesenchymal Stem Cells to Osteogenic Signals

- and its Impact on Bone Tissue Engineering. *Current stem cell Research & Therapy* 2007;2.
341. Siddappa R, Licht R, van Blitterswijk C, de Boer J. Donor variation and loss of multipotency during in vitro expansion of human mesenchymal stem cells for bone tissue engineering. *J Orthop Res* 2007 Aug;25(8):1029-1041.
342. Phinney DG, Kopen G, Righter W, Webster S, Tremain N, Prockop DJ. Donor variation in the growth properties and osteogenic potential of human marrow stromal cells. *Journal of cellular biochemistry* 1999 Dec 1;75(3):424-436.
343. Mendes SC, Tibbe JM, Veenhof M, Both S, Oner FC, van Blitterswijk CA, et al. Relation between in vitro and in vivo osteogenic potential of cultured human bone marrow stromal cells. *Journal of materials science* 2004 Oct;15(10):1123-1128.
344. Bertram H, Mayer H, Schliephake H. Effect of donor characteristics, technique of harvesting and in vitro processing on culturing of human marrow stroma cells for tissue engineered growth of bone. *Clinical oral implants research* 2005 Oct;16(5):524-531.
345. pictures for the front cover and tabs were obtained and modified from <http://www.stephenmaclellan.com/photographs/other.htm>,
<http://www.glaucusorg.uk/Moonjell.htm>;
<http://www.cepolina.com/freephoto/vj/jellyfish.orange2-animalsea.htm>;
<http://www.kulturpixel.de/artikel/29SkarinaBibelWeissrusslandOstslawischMilich> BibliothekLuther
<http://www.kmm.nl/>

Summary

Tissue engineering (TE) is one of the most promising strategies to replace damaged or lost tissue. It may involve the transplantation of cells seeded on an appropriate scaffold. Numerous studies have been performed on bone and cartilage TE, respectively. However, osteochondral TE is not simply combining engineered cartilage and bone to replace diseased osteochondral parts in the body. This thesis identifies critical steps to be taken to develop osteochondral constructs.

One of the most significant steps is seeding cells efficiently and effectively.

Bone marrow is a source for mesenchymal stem cells (MSCs) which can be differentiated into bone and cartilage, respectively. The application of one single cell type with this multipotent characteristic is a major advantage for osteochondral TE. Seeded onto osteoinductive materials, MSCs differentiate into the osseous lineage. The major drawback lays, however, in the use of MSCs for the chondral part. Chondrogenic differentiation of MSCs requires serum-free medium containing transforming growth factor $\beta 1$ (TGF $\beta 1$). However, proteins in the serum are essential for cellular attachment. The serum-free condition of cell differentiation is therefore associated with the lack of cell attachment on the scaffold. Chapter 1 addresses this issue. The use of different scaffold compositions and the application of different seeding strategies was evaluated to increase cell seeding efficiency and to allow cell differentiation. Different copolymer compositions (polyethylene oxide) (PEOT) / polybutylene terephthalate) (PBT)) could not demonstrate an improved effect on cell attachment, while different seeding strategies were more successful. The incorporation of a single cell suspension cells into a hydrogel and the aggregation of single cells prior to the seeding have been shown to be most effective in terms of loaded cell number and generated cartilage.

Despite the fact that successful strategies have been identified to improve cell seeding, the majority of generated tissue is not hyaline but fibrous cartilage of minor quality. To allow reconstruction of clinical defects it is crucial to increase the quantity and quality of cartilage.

One possibility to increase the amount of generated cartilage is to release growth factors such as TGF $\beta 1$ from the scaffolds.. To prepare porous scaffolds releasing proteins, a novel technique is coating prefabricated PEOT/PBT scaffolds with protein containing emulsion. This advanced technology and its application in cartilage TE is described in chapter 2. The results showed a successfully tailored release of bioactive TGF $\beta 1$ *in vitro* from 10 to 40 days. This was accomplished by varying copolymer compositions or by increasing the succinate substitution. In the presence of released TGF $\beta 1$ MSCs differentiated into the chondrogenic lineage. The relevance of TGF $\beta 1$ releasing scaffolds for cartilage TE has been further investigated by comparing two TGF $\beta 1$ releasing profiles with instant and repeated supplementation of the same total amount of TGF $\beta 1$ (chapter 3). The results showed that fast and instant release was more effective than the sustained delivery of TGF $\beta 1$ (either released or supplemented). This outcome had consequences for the further development of osteochondral constructs. The generally accepted protocol to differentiate MSCs into the chondrogenic lineage describes an incubation period of 21 days in TGF $\beta 1$ containing serum-free medium. In contrast, the results of chapter 3 raised the hypothesis that cartilage generation can be achieved by inducing MSCs with a bolus administration of TGF $\beta 1$ and implanting them directly after the induction.

Chapter 4 deals with this theory and describes the induction of MSCs for a short period of 4hrs in TGF $\beta 1$ containing chondrogenic differentiation medium. 4hrs led to the formation of stable aggregates of MSCs, however, this short period was not sufficient to induce chondrogenic differentiation. After an additional cultivation period of 20hrs in TGF

β 1 containing medium cells generated cartilage like tissue. In addition, our results suggested that an optimal growth factor concentration is between 10 and 70ng/ml TGF β 1. Advantages of this technique include a fast and efficient cell incorporation due to the formation of aggregates and a cost and time efficient cell differentiation.

The application of scaffold materials and scaffold architecture is crucial for successful osteochondral TE. Scaffolds need to provide niches for chondrogenic and osseous differentiation, respectively, while at the same time withstand mechanical forces. When a three dimensional fiber deposition technique is used to produce scaffolds with properties matching cartilage, the resulting pore size and porosity are large in relation to the cell size. In such an open structure, the cell seeding efficiency is very low. In chapter 5 we investigated the possibility to increase entrapment and differentiation of cells by adapting the scaffold design. Microfibrillar structures have been integrated within the macrofibers of porous three dimensional 300/55/45 scaffolds using electrospinning. The results showed a significantly higher cell number and increased proliferation and cartilaginous matrix production as compared to scaffolds without microfibers. Selective attachment and spreading of MSCs were observed on the electrospun network, whereas scaffolds without microfibers remained empty. Different scaffold fabrication techniques can be combined to realize material properties in terms of matching mechanical properties of the desired tissue, increasing cell seeding and supporting cell differentiation. Going one step further, it can be adopted to assemble osteochondral constructs composed of polymers and ceramics, which is described in chapter 6.

The photolithographic technology was applied to produce porous, three dimensional biphasic calcium phosphate particles of tailor-made architecture. These particles were integrated into the pores of a three dimensional fiber-deposited osteochondral matrix composed of PEOT/PBT 1000/70/30 for the osseous part and PEOT/PBT 300/55/45 for the chondral part. Results from previous studies were adopted to implement respective seeding of undifferentiated MSCs into the osseous part and chondrogenic MSCs into the chondral part. These osteochondral constructs were implanted subcutaneous in the back of nude mice and after 4 weeks analysis showed cartilage tissue generation in the chondral part and bone tissue in the osseous part. The applied technologies facilitate efficient cell entrapment, cartilage generation and production of integrated osteochondral constructs and offer great potential for clinical practice.

The final relevant step is the step toward the clinic. Although the application of cell-based TE constructs in an osteochondral environment is not developed in such an extent that clinical trials could have been performed, the safety of the scaffold material and the handling of the implants could be demonstrated in a clinical feasibility study. Its results are described in the last chapter (chapter 7). This clinical trial demonstrates the safety, long-term biocompatibility and osteoconductivity of porous PEOT/PBT implants. In addition, the ease of arthroscopic scaffold insertion, the congruent surface tissue repair of predominantly fibrocartilagenous nature, and the absence of intraarticular adverse events indicates its suitability for the filling of donor sites during mosaicplasty to prevent postoperative bleeding and donor site morbidity.

Samenvatting

Tissue engineering (TE) is één van de meest belovende strategieën om beschadigd of verloren weefsel te vervangen. Transplantatie van cellen in combinatie met een geschikt dragermateriaal is één van de mogelijke toepassingen. Vele studies zijn verricht met betrekking tot bot en kraakbeen TE. TE voor de vervanging van beschadigde osteochondrale delen is echter niet het simpele resultaat van het samenvoegen van kraakbeen en bot. Dit proefschrift identificeert de benodigde kritische stappen om osteochondrale constructen te ontwikkelen.

Eén van de meest kritische stappen is het efficiënt zaaien van de cellen op het dragermateriaal. Beenmerg is een bron voor mesenchymale stamcellen (MSCs) die getransformeerd kunnen worden in respectievelijk botcellen en kraakbeencellen. Het gebruik van één multipotentieel celtype is een groot voordeel voor osteochondrale TE. Eenmaal aangebracht op osteoinductieve dragermaterialen kunnen de MSCs differentiëren in botcellen. De moeilijkheid ligt echter in het gebruik van MSCs voor het creëren van het kraakbeen-deel. Het differentiëren van MSCs in kraakbeencellen vereist serum-vrij medium met toegevoegd transforming growth factor $\beta 1$ (TGF $\beta 1$). De proteïnen in serum zijn echter essentieel voor cel adhesie. Serum-vrije condities voor cel differentiatie zijn daarom geassocieerd met de afwezigheid van cel hechting aan het dragermateriaal. Hoofdstuk 1 behandelt dit onderwerp. Verschillende dragermateriaal composities en zaaimethoden zijn geëvalueerd om de zaai efficiëntie te vergroten en tegelijkertijd cel differentiatie toe te staan. Waar de evaluatie van diverse co-polymeer composities polyethylene oxide terephthalate (PEOT) / polybutylene terephthalate (PBT)) geen effect op cel hechting heeft aangetoond, heeft het testen van verschillende zaaimethoden dit wel. De incorporatie van een celsuspensie in een hydrogel en aggregatie van cellen voor het zaai proces zijn het meest efficiënt gebleken met betrekking tot het aantal cellen op het dragermateriaal en het proces van kraakbeen formatie.

Ondanks de succesvolle strategieën voor het zaaien van cellen is het merendeel van het gevormde kraakbeen niet hyaline maar fibreus en dus van mindere kwaliteit voor deze toepassing. Voor een goede klinische toepassing is het cruciaal om de kwantiteit en kwaliteit van het gevormde kraakbeen te verbeteren. Een mogelijkheid om de hoeveelheid gevormd kraakbeen te vergroten is het gebruik van dragermaterialen waaruit groeifactoren zoals TGF $\beta 1$ vrijkomen. Een nieuwe techniek voor het fabriceren van proteïne afgevend poreuze dragermaterialen is het bedekken van PEOT/PBT materialen met een proteïne emulsie. Deze geavanceerde technologie en de toepasbaarheid voor kraakbeen TE is beschreven in hoofdstuk 2. De resultaten hebben een gecontroleerde afgifte van het bioactieve TGF $\beta 1$ tussen 10 en 40 dagen *in vitro* aangetoond. Dit was bereikt door de co-polymeer compositie te variëren en door de succinaat substitutie te vergroten. In de aanwezigheid van deze TGF $\beta 1$ differentieerden de MSCs in kraakbeencellen.

De relevantie van TGF $\beta 1$ afgevend dragermaterialen voor kraakbeen TE is verder bestudeerd door twee afgifte profielen, onmiddellijke en verdeelde afgifte met dezelfde totale hoeveelheid afgegeven TGF $\beta 1$, te vergelijken (hoofdstuk 3). De resultaten hebben uitgewezen dat een snelle en totale afgifte efficiënter is dan een geleidelijke afgifte van TGF $\beta 1$. Dit resultaat had consequenties voor de verdere ontwikkeling van osteochondrale constructen. Het algemeen geaccepteerde protocol om MSCs te differentiëren in kraakbeencellen schrijft een incubatie periode van 21 dagen in TGF $\beta 1$ gesupplementeerd medium (chondrogeen medium) voor. In tegenstelling hebben de resultaten van hoofdstuk 3 de hypothese opgeleverd dat kraakbeen generatie geïnitieerd kan worden door MSCs direct te implanteren na inductie d.m.v. een bolus administratie van TGF $\beta 1$.

In hoofdstuk 4 komt deze theorie aan bod en is de inductie van MSCs voor een korte periode van 4 uren in chondrogeen differentiatie medium beschreven. 4 uur stimulatie resulteerde in de formatie van stabiele aggregaten van MSCs. Echter, deze korte periode was niet voldoende om chondrogene differentiatie te induceren. Na een additionele cultivatie periode van 20 uur in

chondrogeen medium waren de cellen in staat om kraakbeenachtig weefsel te vormen. Bovendien suggereren de resultaten dat de optimale groeifactor concentratie tussen de 10 en 70ng/ml TGF β 1 ligt. De voordelen van deze technologie includeren een snelle en efficiënte cel incorporatie door de formatie van aggregaten en een kostbesparende en tijdsefficiënte cel differentiatie.

Het gebruik van een dragermateriaal met een geschikte architectuur is cruciaal voor succesvol kraakbeen TE. De materialen moeten een niche voor respectievelijk chondrogene en osteogene differentiatie verschaffen en tegelijkertijd mechanische krachten weerstaan. Wanneer een 3-dimensionale vezel depositie techniek (plotten) wordt gebruikt om dragermaterialen te fabriceren met eigenschappen die vergelijkbaar zijn met kraakbeen, resulteert dit in een porie grootte en poreusiteit die groot is in verhouding tot een cel. In een dergelijke open structuur is de zaai efficiëntie erg laag. In hoofdstuk 5 is het effect van dragermateriaal ontwerp op de mogelijkheid om cellen te verstrikken in het materiaal en cel differentiatie geëvalueerd. Micro-fibrilaire structuren waren geïntegreerd met de macro-vezels van poreuze 3-dimensionale 300/55/45 materialen d.m.v. electrospinning. De resultaten met dit materiaal toonden een significant hoger aantal cellen en een verhoogde proliferatie en kraakbeen matrix productie in vergelijking tot materialen zonder micro-vezels. Selectieve hechting en spreiding van MSCs waren zichtbaar op het netwerk van microvezels, terwijl de dragermaterialen zonder microvezels geen celhechting vertoonden. Verschillende fabricatie technieken van dragermaterialen kunnen dus worden gecombineerd om geschikte eigenschappen te realiseren m.b.t. de mechanische eigenschappen van het te regenereren weefsel, zaai efficiëntie en cel differentiatie.

Een stap verder is het samenstellen van osteochondrale constructen uit polymeren en keramieken. De toepassing van verschillende productie technieken om dit te bereiken is beschreven in hoofdstuk 6. PEOT/PBT polymeren met respectievelijk eigenschappen voor kraakbeen en bot waren geplot, waarbij voor grotere poriën in het botdeel was gekozen. Vervolgens waren 3-dimensionale osteoinductieve calciumfosfaat partikels, geproduceerd d.m.v. een fotolithografische techniek, geïntegreerd in deze poriën. De bevindingen uit vorige studies zijn toegepast om ongedifferentieerde MSCs in het bot-deel en chondrogeen gedifferentieerde MSCs in het kraakbeen-deel te zaaien. De osteochondrale constructen zijn vervolgens subcutaan geïmplanteerd in de rug van naakte muizen en de resultaten na 4 weken implantatie hebben kraakbeen weefsel in het kraakbeen-deel en botweefsel in het bot-deel aangetoond. De toegepaste technologie heeft geresulteerd in een efficiënte cel zaaing, kraakbeen formatie en geïntegreerde osteochondrale constructen en biedt groot perspectief voor gebruik in de kliniek.

De laatste stap is de stap naar de kliniek. Ondanks dat de ontwikkeling van op-cellen-gebaseerde osteochondrale TE nog niet ver genoeg is gevorderd om in klinische studies te worden getest, is de veiligheid en de hanteerbaarheid van het dragermateriaal aangetoond in een klinische studie. Deze resultaten zijn beschreven in het laatste hoofdstuk (hoofdstuk 7). De klinische studie toont de veiligheid, lange-termijn biocompatibiliteit en osteoconductiviteit van poreuze PEOT/PBT implantaten. Bijkomend zijn het gemak van het arthroscopische inbrengen van het materiaal, de integratie van het geregenereerde weefsel bestaande uit hoofdzakelijk fibreus kraakbeen en de afwezigheid van ongewenste intra-articulaire effecten aangetoond. Dit demonstreert de toepasbaarheid van deze technologie voor het vullen van defecten die ontstaan zijn na het uitnemen van autoloog donor materiaal tijdens een mosaicplasty procedure en voorkomt zodoende postoperatieve bloedingen en morbiditeit.

Zusammenfassung

Gewebezüchtung (engl: Tissue engineering, TE) ist eine der vielversprechendsten Strategien, um geschädigtes und zerstörtes Gewebe zu ersetzen. Die Transplantation von geeigneten Trägermaterialien mit Zellen ist eine der möglichen Anwendungen. Viele Studien über Knochen- und Knorpelzüchtungen sind veröffentlicht. Die Entwicklung eines Gewebeersatzes für Knochen-Knorpel-Defekte (osteocondrale Defekte) ist jedoch nicht so einfach, dass beide Züchtungen lediglich miteinander kombiniert werden könnten. Diese Doktorarbeit identifiziert die nötigen Schritte, um osteocondralen Ersatz zu entwickeln. Einer der kritischsten Schritte dabei ist das effiziente Besiedeln des Trägermaterials mit Zellen.

Knochenmark ist eine Bezugsquelle für mesenchymale Stammzellen (engl: mesenchymal stem cells, MSCs), welche zu Knochen- oder Knorpelzellen differenzieren können; sie sind multipotent. Die Verwendung einer multipotenten Zellart ist ein grosser Vorteil für osteocondrales TE. Calciumphosphathaltige Trägermaterialien werden für den Knochenanteil genutzt. Sie unterstützen das Anheften von Zellen und sind osteoinduktiv, d.h. die Differenzierung von besiedelten MSCs zu Knochenzellen fördern. Schwierig dahingegen ist der Gebrauch von MSCs für den Knorpelteil. Die Differenzierung zu Knorpelzellen (chondrogene Differenzierung) ist in serumfreiem Kulturmedium mit zugefügtem Wachstumsfaktor transforming growth factor β 1 (TGF β 1) möglich. Allerdings sind die im Serum enthaltenden Proteine essentiell für das Haften von Zellen (Adhäsion). Die serumfreien Bedingungen für chondrogene Zelldifferenzierung wirken daher der Zelladhäsion entgegen, welche eine der Grundvoraussetzungen für TE ist.

Kapitel 1 behandelt dieses Thema. Um die Adhäsion der Zellen bei gleichzeitiger Differenzierung effizient zu unterstützen, wurden verschiedene Besiedlungsmethoden an unterschiedlichen Trägermaterialien getestet. Die Verteilung von Poly(ethylene oxide) (PEOT) und Poly(butylene terephthalate) (PBT), durch die sich die Trägermaterialien unterscheiden, hatte keinen Einfluss auf die Zelladhäsion. Die Anwendung von verschiedenartigen Besiedlungsmethoden war jedoch wirksam. Hinsichtlich der Zellzahl und der Zelldifferenzierung zeigte sich, dass die Methoden am effektivsten waren, bei denen einzelne Zellen in ein Gel eingeschlossen wurden (Incorporation) oder bei denen einzelne Zellen vor dem Besiedeln angehäuft wurden (Aggregation). Trotz dieser erfolgreichen Methoden ist der überwiegende Teil des gezüchteten Gewebes kein hochwertiger Gelenkknorpel, sondern fibröser Knorpel von minderwertiger Qualität. Desweiteren ist neben der Qualität auch die Quantität ausschlaggebend, um TE in der klinischen Praxis anwenden zu können. Eine Möglichkeit, um die Menge des gezüchteten Knorpels zu erhöhen, ist der Einsatz von Trägermaterialien, die chondrogene Wachstumsfaktoren freisetzen. Ein neues Verfahren für die Herstellung von porösen, Protein freisetzenden Materialien ist das Beschichten der PEOT/PBT-Copolymeren mit einer Proteinemulsion. Dieses fortgeschrittene Verfahren und dessen Anwendbarkeit in der Knorpelzüchtung sind im Kapitel 2 beschrieben. Die Ergebnisse zeigten, dass biologisch aktives TGF β 1 von 10 bis 40 Tagen kontrolliert abgegeben werden kann. Dies wurde durch Variation der Polymerzusammensetzung und durch erhöhte Succinatsubstitution erzielt. Durch das freigesetzte TGF β 1 differenzierten die MSCs zu Knorpelzellen.

Die Bedeutung von TGF β 1 freisetzenden Trägern in Bezug auf Knorpel-TE wurde weiter evaluiert, indem zwei Freisetzungsprofile miteinander verglichen wurden: sofortige und langsam verteilte Freisetzung der Gesamtmenge TGF β 1 (Kapitel 3). Der Vergleich wies aus, dass bezüglich der Knorpelbildung die sofortige, schnelle

Freisetzung gegenüber einer langsamen, verteilten Freigabe effizienter ist. Diese Feststellung hatte Folgen für die weitere Entwicklung von osteochondralem Gewebeersatz.

Das allgemein anerkannte Standardprotokoll zur chondrogenen Differenzierung schreibt die Inkubation von MSCs in TGF β 1-haltigem Kulturmedium für 21 Tagen vor. Demgegenüber geben die Resultate von Kapitel 3 Anlass zur Hypothese, dass Knorpelbildung *in vivo* induziert werden kann, indem man MSCs kurz mit einer hohen Konzentration TGF β 1 inkubiert und direkt danach implantiert.

Kapitel 4 befasst sich mit dieser Hypothese: Die Inkubation von MSCs in TGF β 1-haltigem Kulturmedium für 4 Stunden ist beschrieben. Eine Einwirkzeit von 4 Stunden resultierte in die Formation von stabilen Zellaggregaten, konnte jedoch chondrogene Differenzierung nicht induzieren. Die Bildung von Knorpel konnte erst nach einer Inkubationsperiode von 20 zusätzlichen Stunden nachgewiesen werden. Die optimale Konzentration von TGF β 1 lag zwischen 10 und 70ng/ml. Vorteile dieses neuen Protokolles umfassen eine schnelle und effiziente Besiedlung durch Aggregation der Zellen sowie Zeit und Geld sparende Zelldifferenzierung.

Für erfolgreiches Knorpel-TE ist auch die Architektur des Trägermaterials ausschlaggebend. Die Zellträger sollten passende Nischen für entweder Knorpel- oder Knochenbildung bieten und gleichzeitig mechanischen Kräften widerstehen. Eine Polymerfaser-Drucktechnik wird verwendet, um mit gerichteten Fasern dreidimensionale Materialien herzustellen (engl: 3D fiber deposited, plotten). Die Faserdicke und der Abstand zwischen zwei geplotteten Fasern (= Porengrösse) können so manipuliert werden, dass Gerüste mit spezifischen mechanischen Eigenschaften produziert werden können. Die eingestellte Porengrösse, die zu knorpelähnlichen Eigenschaften des Materials führt, steht jedoch zu keinem Verhältnis mit der Grösse von Zellen. Dadurch ist die Zellzahl nach Besiedlung von geplotteten Trägern sehr niedrig. Der fünfte Teil der Dissertation beschreibt Möglichkeiten, die Zellzahl trotz grosser Poren zu erhöhen und gleichzeitig Zelldifferenzierung zu gewährleisten. Mit Hilfe von Elektrospinning werden Mikrofasern zwischen die geplotteten Fasern von 3D-Trägern gebracht. Im Vergleich zu geplotteten, Mikrofasern-freien Trägern konnten dadurch signifikant grössere Mengen Zellen gesiedelt werden, wobei sich die MSCs gezielt an die Mikrofasern hefteten. Desweiteren waren die Proliferation der Zellen sowie die Knorpelbildung erhöht. Verschiedene Techniken wie Plotten und Elektrospinning können also miteinander kombiniert werden, um Trägermaterialien mit hoher Zellaffinität, mechanischen Merkmalen von Knorpel und Differenzierung unterstützenden Eigenschaften herzustellen. Die Kombination von unterschiedlich hergestellten Materialien und der Aufbau von osteochondralen Gerüsten ergibt den folgenden, logischen Schritt und wird im nächsten Kapitel (Kapitel 6) vorgestellt.

PEOT/PBT-Polymere mit Knorpel bzw. Knochen entsprechenden Eigenschaften wurden geplottet, wobei die Poren für den Knochenteil grösser gewählt wurden. Osteoinduktive Calciumphosphate wurden mit Hilfe von Fotolithografie passend dreidimensional geformt und in diese Poren eingeschlossen. Die Informationen der vorangegangenden Studien wurden angewandt, um effizientes Siedeln von MSCs im Knorpel bzw. Knochenteil und die entsprechende Differenzierung zu Knorpel- bzw. Knochen zu erreichen. Nach Implantation in immundefiziente Mäuse enthielten die osteochondralen Konstrukte Knorpel im Knorpelteil und Knochen im Knochenteil. Dadurch ist diese Technologie für den klinischen Gebrauch sehr vielversprechend.

Einer der letzten Schritte ist der Schritt in die Klinik. Auch wenn die Gewebezüchtung mit Zellen für eine therapeutische Anwendung noch nicht reif genug ist, konnte man schon die Sicherheit und einfache Handhabung der Trägermaterialien in einer klinischen Studie nachweisen. In Kapitel 7 sind die Ergebnisse dieser Studie beschrieben.

Osteochondrale Zylinder wurden aus gesunden Teilen des Knies in Defekte der gewichtstragenden Regionen transplantiert (= Mosaikplastik). Durch das Offenlassen der Entnahmestellen können Blutungen in die Gelenke hinein und Schäden an der Entnahmestelle (= Morbidität) auftreten. In dieser Studie wurden die Entnahmestellen mit PEOT/PBT-Zylindern aufgefüllt. Die Untersuchungen wiesen nach, dass die PEOT/PBT-Implantate sicher, biokompatibel und osteokonduktiv waren, d.h. eine „Leitschiene“ für regenerierenden Knochen darstellten. Der gebildete Knorpel bildete eine glatte Oberfläche, war sehr gut in die Umgebung integriert und es wurden keine ernsthaften Nebeneffekte festgestellt. Dass das Implantieren dieser Materialien arthroskopisch möglich ist, bietet einen zusätzlichen Vorteil und bringt den Beweis, dass die Technologie für das Auffüllen von Defekten gebraucht werden kann und Morbidität verhindert.

Curriculum Vitae



Doreen Hamann was born on November 27th, 1978 in Parchim, Germany.

In 1997 she graduated from secondary school (Gymnasium) in 1997 and started her Biology study at the University Rostock, Germany. After obtaining her intermediate diploma in 1999, she specialized in Human Biology at the EMA University Greifswald, Germany. Her focus was on functional morphology, pharmacology and biochemistry. She performed internships at the Neuroembryonic Research Laboratory of the Department

of Anatomy (University of Rostock, Germany) and at the Tissue Engineering Laboratory, Department of Plastic and Hand Surgery in Freiburg, Germany. In 2001 she was awarded the Leonardo Da Vinci grant from the European Community and Association for Science, Training and Technology and completed a masters thesis entitled "*Human bone marrow-derived mesenchymal stem cells: optimization of chondrogenic differentiation*" under the supervision of Dr. J. Riesle at IsoTis B.V., a medical technology company in Bilthoven, The Netherlands.

After receiving a Master of Science in Human Biology in 2003 from the Faculty of Mathematics and Science at the EMA University, she accepted a PhD position in the group of Prof. C.A. van Blitterswijk at IsoTis B.V. in collaboration with the Institute for Biomedical Technology (University of Twente, Enschede, The Netherlands). The results of her research are described in this thesis.

Since September 2007 she has been working at genae associates in Antwerp, Belgium.

List of publications

Doreen Hamann, Lorenzo Moroni, Clemens van Blitterswijk. Comparison of seeding methods as the critical factor for cartilage tissue engineering utilizing mesenchymal stem cells on 3D fiber-deposited scaffolds. *In preparation*

Jerome Sohier, Mireille Koenders, **Doreen Hamann**, Clemens van Blitterswijk, Klaas de Groot, Jeroen Bezemer. Tailored release of TGF beta 1 from porous scaffolds and potential for cartilage tissue engineering. *Int J Pharm.* 2007 Mar 6;332(1-2):80-9. *Epub 2006 Sep 29.*

Jerome Sohier, **Doreen Hamann**, Ramakrishnaia Siddappa, Clemens van Blitterswijk, Klaas de Groot, Jeroen Bezemer. TGF beta 1 released from porous scaffolds: influence of delivery rates on cartilage formation. *Submitted*

Doreen Hamann, Jerome Sohier, Clemens van Blitterswijk. A novel approach to improve seeding efficiency and chondrogenic differentiation of mesenchymal stem cells for tissue engineering applications. *In preparation*

Lorenzo Moroni, Roka Schotel, **Doreen Hamann**, Joost de Wijn, Clemens van Blitterswijk. 3D fiber deposited electrospun integrated scaffolds enhance cartilage tissue formation. *Submitted*

Doreen Hamann¹ and Lorenzo Moroni¹, Luca Paoluzzi², Clemens van Blitterswijk¹. Biomaterial Assembly through Rapid Prototyping for osteochondral tissue engineering. *Submitted*

Doreen Hamann and Lajos Bartha, Jeroen Pieper, Fabienne Péters, Jens Riesle, Andras Vajda, Pal Kaposi Novak, Laszlo Rudolf Hangody, Gabor Vasarhelyi, Clemens van Blitterswijk, Joost de Wijn, Annamaria Kenyeres, Laszlo Modis, Laszlo Hangody. A clinical feasibility study to evaluate the safety and efficacy of PEOT/PBT implants for human donor site filling during mosaicplasty. *Submitted*

Doreen Hamann, Clemens van Blitterswijk. A new approach to improve seeding efficiency and chondrogenic differentiation using stem cells in osteochondral tissue engineering.

15th Conference of the Dutch Society for Biomaterials and Tissue Engineering, Lunteren, The Netherlands, Dec. 2006

Doreen Hamann, Lorenzo Moroni, Luca Paoluzzi and Clemens van Blitterswijk .Osteochondral Tissue Engineering. *Regenerate World Congress on Tissue Engineering and Regenerative Medicine, Pittsburgh, PS, USA, Apr. 2006*

Doreen Hamann, Lorenzo Moroni, Luka Paoluzzi and Clemens van Blitterswijk. Osteochondral tissue engineering based on mesenchymal stem cells loaded on triphasic prototyped scaffolds. *ICRS 6th symposium, San Diego, C, USA, Jan. 2006*

Doreen Hamann, Clemens van Blitterswijk. Effect of fibronectin on cell attachment and chondrogenic differentiation of mesenchymal stem cells. *Dutch annual conference on Biomedical engineering, Papendal, The Netherlands, Oct. 2004*